Layered Modeling and Simulation of Complex Biotechnological Processes

- Optimizing Rhamnolipid Production by *Pseudomonas aeruginosa* during Cultivation in a Bioreactor -

zur Erlangung des akademischen Grades eines
DOKTORS DER INGENIEURWISSENSCHAFTEN (Dr.-Ing.)

von der Fakultät für Chemieingenieurwesen und Verfahrenstechnik
des Karlsruher Instituts für Technologie (KIT)

genehmigte
DISSERTATION

von
Dipl.-Ing. Marius Henkel
aus Lauterbach, Hessen

Referent: Prof. Dr. rer. nat. Christoph Syldatk
Korreferent: Prof. Dr.-Ing. Rudolf Hausmann

Tag der mündlichen Prüfung: 21. November 2014

The important thing is not to stop questioning.
Curiosity has its own reason for existing.

Albert Einstein

Acknowledgements

I would like to express my sincerest gratitude to the following people for their continuous support and guidance throughout my work:

Prof. Dr. rer. nat. Christoph Syldatk for giving me the opportunity to perform the work for this thesis in his group, for his guidance, support and helpful comments, allowing for academic freedom whenever possible, and for entrusting me with the undergraduate practical training in bioprocess engineering, which helped me gain first experience in teaching.

Prof. Dr.-Ing. Rudolf Hausmann for his supervision as my mentor and letting me join his team in rhamnolipid research, for his motivating and patient personality, his constant guidance and helpful pieces of advice at the right moment.

Friends, colleagues and former colleagues at the Technical Biology, thank you all for the friendly and supporting atmosphere in the institute: M. Sc. Janina Beuker, M. Sc. Martin Pöhnlein, Dipl.-Biotechnol. Johannes Kügler, Dr.-Ing. Markus Michael Müller, M. Sc. Judit Willenbacher, Harald Gotzmann, Werner Mandel, Desiree Westermann, M. Sc. Sarah Dold, M. Sc. Christin Slomka, Dipl.-Biol. (t.o.) Julia Stolarow, Dr.-Ing. Berna Gerçe, Dr.-Ing. Barbara Hörmann, Dr.-Ing. Ines Schulze, Laura Krämer, Dr. rer. nat. Markus Andre, Dr. rer. nat. Mareike Perzborn, Dipl.-Ing. Melanie Gerlitzki, Dipl.-Ing. Florian Oswald, Dr.-Ing. Ulrike Engel, Dr.-Ing. Katrin Ochsenreither.

All the students who contributed to the development of this work, either by working on a student project or thesis or by contributing as research assistants to the enormous amount of measurements, and last but not least for giving me the opportunity to teach: B. Sc. André Tschöpe, B. Sc. Vera Colditz, Dipl.-Ing. Jens Nörtershäuser, Dipl.-Ing. Johanna Stegmann, B. Sc. Didem Ertaş, B. Sc. Gang Wang, B. Sc. Marcel Loewert.

Dr. rer. nat. Anke Neumann and Dr. rer. nat. Jens Rudat, thank you for your helpful comments and input, and just the right amount of necessary critique during our meetings and seminars - it was much appreciated.

Dipl.-Ing. Michaela Zwick and Sandra Baumann, thank you for being such a big help in the last years and for keeping everything running smoothly!

Siegfried Almstedt, our master mechanic, for excellent assistance with the maintenance of the bioreactors as well as crafting several custom-designed parts for me and our group.

Academic partners and project coworkers, thank you for three productive years of rhamnolipid research: Dipl.-Biol. Anke Schmidberger, Dr.-Ing. Christian Kühnert, Dipl.-Ing. Markus Vogelbacher, Dr.-Ing. Thomas Bernard and Dr. rer. nat. Thomas Schwartz

The Baden-Württemberg Stiftung for funding the project as part of the environmental technology research program.

Preamble

Parts of this thesis are based on peer-reviewed research articles and reviews published accompanying the work performed for this dissertation between March 2011 and April 2014. Text taken or adapted from previously published work is indicated with full reference provided for the published material. The text is identical in content, however, layout, citation style and fomatting of the reference lists have been adjusted for a uniform presentation within this thesis.

A list of published work associated with this thesis, including selected conference talks and posters, is available on the next pages.

Chapters based on previously published material

Chapter 3 is based on a review article, which provides a general introduction to biosurfactants and the theoretical background. In addition, the necessary calculations of yields required for the course of modeling described in subsequent chapters of this thesis are presented. Published as:
Henkel et al., Process Biochemistry 2012, 47(8), pp. 1207-1219

Chapters 4 is based on a research paper, which provides a mathematical description for the cell-density dependent regulation of rhamnolipid production during cultivation in a bioreactor. Published as:
Henkel et al., Applied Microbiology and Biotechnology 2013, 97(17), pp. 7607-7616

Chapters 5 is based on a research paper, which contains a complex process model to describe rhamnolipid production during batch cultivations in a bioreactor. Published as:
Henkel et al., Applied Microbiology and Biotechnology 2014, 98(16), pp. 7013–7025

Publications related to this thesis

Original Research Paper

Henkel M, Schmidberger A, Kühnert C, Beuker J, Bernard T, Schwartz T, Syldatk C and Hausmann R
Kinetic modeling of the time course of *N*-butyryl-homoserine lactone concentration during batch cultivations of *Pseudomonas aeruginosa* PAO1
Applied Microbiology and Biotechnology 2013, 97(17), pp. 7607-7616

Schmidberger A, Henkel M, Hausmann R and Schwartz T
Expression of genes involved in rhamnolipid synthesis in *Pseudomonas aeruginosa* PAO1 in a bioreactor cultivation
Applied Microbiology and Biotechnology 2013, 97(13), pp. 5779-5791

Henkel M, Schmidberger A, Vogelbacher M, Kühnert C, Beuker J, Bernard T, Schwartz T, Syldatk C and Hausmann R
Kinetic modeling of rhamnolipid production by *Pseudomonas aeruginosa* PAO1 including cell density-dependent regulation
Applied Microbiology and Biotechnology 2014, 98(16), pp. 7013–7025

Schmidberger A, Henkel M, Hausmann R and Schwartz T
Influence of ferric iron on gene expression and rhamnolipid synthesis during batch cultivation of *Pseudomonas aeruginosa* PAO1
Applied Microbiology and Biotechnology 2014, 98(15), pp. 6725–6737

Kügler JH, Muhle-Goll C, Kraft A, Heinzler R, Henkel M, Wray V, Luy B, Brenner-Weiss G, Lang S, Syldatk C and Hausmann R
Trehalose lipid biosurfactants produced by the actinomycetes *Tsukamurella spumae* and *T. pseudospumae*
Applied Microbiology and Biotechnology 2014, available online since August 5, 2014

Reviews & Book Chapters

Henkel M, Müller MM, Kügler JH, Lovaglio RB, Contiero J, Syldatk C and Hausmann R
Rhamnolipids as biosurfactants from renewable resources: Concepts for next-generation rhamnolipid production
Process Biochemistry 2012, 47(8), pp. 1207-1219

Müller MM, Kügler JH, Henkel M, Gerlitzki M, Hörmann B, Pöhnlein M, Syldatk C and Hausmann R
Rhamnolipids - Next generation surfactants?
Journal of Biotechnology 2012, 162(4), pp. 366-380

Henkel M, Syldatk C and Hausmann R
The prospects for the production of rhamnolipids on renewable resources
In: Kosaric N & Sukan FV (ed.) Biosurfactants: Production and Applications, second edition. *Surfactant Science*. Taylor & Francis. ISBN 978-1-4665-9669-6. In press.

Selected Conference Talks

Henkel M, Schmidberger A, Kühnert C, Müller MM, Schwartz T, Bernard T, Syldatk C and Hausmann R
Modellbasierte Optimierung der biotechnologischen Produktion von Rhamnolipiden mit *Pseudomonas aeruginosa*
DECHEMA group meeting (Messen und Regeln in der Biotechnologie), 'Mess- und Regelungskonzepte in der Lebensmittel- und Umweltbiotechnologie', 18.10.2011, Gerlingen

Henkel M, Schmidberger A, Kühnert C, Beuker J, Schwartz T, Bernard T, Syldatk C and Hausmann R
Strategies for optimized biotechnological production of rhamnolipids: Green surfactants based on renewable resources
Forum Life Science, International congress at the Technische Universität München, 13.-14.03.2013, München-Garching

Henkel M, Schmidberger A, Kühnert C, Beuker J, Schwartz T, Bernard T, Syldatk C and Hausmann R
A model for rhamnolipid production with *Pseudomonas aeruginosa*: Development of optimized biotechnological processes
DECHEMA international conference 'Biosurfactants - Challenges and perspectives', 16.-17.05.2013, Frankfurt am Main

Selected Poster Presentations

Henkel M, Schmidberger A, Kühnert C, Schwartz T, Bernard T, Syldatk C and Hausmann R
Modellierung und Optimierung der biotechnologischen Produktion von Rhamnolipiden mit *Pseudomonas aeruginosa*
GVC/DECHEMA conference 'Biopharmazeutische Produktion', 14.05.-16.05.2012, Freiburg. Awarded with the best-poster award

Henkel M, Kügler JH, Syldatk C and Hausmann R
Biosurfactants from renewable resources: concepts for next-generation rhamnolipid production
DECHEMA international conference 'Industrial use of renewable raw-materials', 14.02.-15.02.2012, Frankfurt

Henkel M, Kühnert C, Schmidberger A, Vogelbacher M, Schwartz T, Bernard T, Syldatk C and Hausmann R
Modellgestützte Analyse und Optimierung zur biotechnologischen Produktion von Rhamnolipiden
DECHEMA group meeting (Messen und Regeln in der Biotechnologie), 'Von der Datenflut zum Erkenntnisgewinn', 29.10.2013, Frankfurt am Main

Abstract

Biological systems generally consist of several subunits which are interconnected by complex mechanisms. The behavior of the system is often difficult to assess by basic observations, mostly due to the presence of nonlinear elements such as feedback or feedforward cascades of biochemical reactions or regulatory networks. Modeling approaches for the description of a complex bioprocess in a bioreactor can principally be assigned to three layers, each representing a different perspective and level of detail: the process layer, the metabolic layer and the genetic layer. For many complex bioprocesses, modeling approaches include only part of the available knowledge, even though combining information from all layers could benefit the overall understanding of the system. One example for such complex bioprocesses is the biotechnological production of rhamnolipid biosurfactants, where knowledge from different layers has not yet been combined in a single modeling approach up to today.

Rhamnolipids are microbial glycolipids mainly known from *Pseudomonas aeruginosa* produced during cultivation on different substrates like vegetable oils, sugars, glycerol or hydrocarbons. The advantages assigned to rhamnolipids have been demonstrated very conclusively in the past, and the potential for rhamnolipids replacing conventional surfactants in numerous applications has been demonstrated. However, besides costs for downstream processing of rhamnolipids, relatively high raw-material prices and low productivities currently restrict the overall applicability and detain an economical production of rhamnolipids on an industrial large scale. Therefore, rhamnolipids still do not find widespread application, and process optimization is restricted to heuristic approaches, since for the most part, quantitative descriptions of the process were not available. In addition, increasing interest in finding and developing alternative non-pathogenic strains led to the development of several non-*P. aeruginosa* host strains intended for the heterologous production of rhamnolipids. However, achieved yields and final product concentrations with these alternative strains can by far not compete with the productivity of wild-type *P. aeruginosa*. Therefore, one pragmatic approach for enhanced rhamnolipid formation is the optimization of a process for rhamnolipid production using wild-type strains with comparably high product yields.

In this thesis, a model for the regulation of rhamnolipid production and data obtai-

ned from metabolic balancing were combined with a process model on a bioreactor scale. The model was used to derive an optimized process control stategy for enhanced rhamnolipid formation, which was evaluated experimentally. A well-investigated platform process and wild-type strain with comparably high yields, *P. aeruginosa* PAO1 cultivated with sunflower oil and nitrate, was chosen for this task.

Chapter 2 "Mathematical description of biological processes" gives a general overview of different concepts and strategies for the development of a mathematical model, and how these may be used as tools for bioprocess engineering. In addition to a classification of different modeling approaches, existing work on modeling rhamnolipid production and quorum sensing is described and discussed. Furthermore, it is proposed that modeling approaches for complex bioprocesses may be assigned to three layers: the process layer, the metabolic layer and the genetic layer.
Chapter 3 "Rhamnolipids: Biosurfactants based on renewable resources" gives an introduction to biosurfactants and rhamnolipids including structure & properties, biosynthetic pathways, genetic regulation & quorum sensing, biotechnological production, areas of application as well as a short economical analysis. Furthermore, balancing of the metabolic interconversions starting from different substrates and leading to rhamnolipid precursor formation is described. The theoretical yields calculated from the metabolic expressions were implemented in the process model in the following course of this thesis.
Chapter 4 "Kinetic modeling of *N*-butyryl-homoserine lactone levels" is focused on the regulation of rhamnolipid production during cultivation in a bioreactor. The production of rhamnolipid biosurfactants by *Pseudomonas aeruginosa* is under complex control of a quorum sensing dependent regulatory network. Quorum sensing affects the regulation of more than 300 genes in *Pseudomonas aeruginosa*, influencing growth, biofilm formation and the biosynthesis of several products. A mathematical description of a cell-density based model for *N*-butyryl-homoserine lactone (C_4-HSL) was developed including production and degradation kinetics which provides a quantitative expression for quorum sensing. In this system, expression of the rhamnolipid biosynthesis genes *rhlAB* is directly coupled to the C_4-HSL concentration via the *rhl* system. 3-oxo-dodecanoyl-homoserine lactone (3o-C_{12}-HSL) displayed a lipophilic character and accumulated in the hydrophobic phase. Production of C_4-HSL was found to be proportional to biomass concentration rather than influenced by autoinduction mechanisms. Rhamnolipid production rates, as determined experimentally, were shown to correlate linearly with the concentration of autoinducer C_4-HSL. Additionally, degradation of C_4-HSL has been found to occur in the aqueous supernatant of the culture by yet unknown extracellular mechanisms, thereby contributing to the comlex mechanisms of counteracting buildup of autoinducer molecules, which is commonly referred to as 'quorum quenching'. Similar to mechanisms of degradation

known for other HSL autoinducer molecules, a putative, extracellular protein with C_4-HSL degrading activity was assumed (putative C_4-HSL acylase). These findings were used to derive a simple model, which is based on data for catalytic efficiency of HSL-acylases extracted from literature ($k_{\mathrm{cat}}/K_{\mathrm{m}}$), experimentally determined basal C_4-HSL production rates ($q^{\mathrm{basal}}_{C_4\text{-HSL}}$), and two fitted parameters which describe the formation of the putative acylase and is therefore comparatively simple.
Chapter 5 "Modeling the production of rhamnolipids in a bioreactor" is focused on the description of the time-course of batch cultivations by a process model. To systematically establish a knowledge-based process for rhamnolipid production, a deeper understanding of the time-course and coupling of process variables is required. By combining reaction kinetics, stoichiometry and experimental data, a process model for rhamnolipid production with *P. aeruginosa* PAO1 on sunflower oil was developed as a system of coupled ordinary differential equations (ODEs). In addition, cell-density based quorum sensing dynamics were included in the model. The model comprises a total of 36 parameters, 14 of which are yield coefficients and 7 of which are substrate affinity and inhibition constants. Of all 36 parameters, 30 were derived from dedicated experimental results, literature, and databases and 6 of them were used as fitting parameters. The model is able to describe data on biomass growth, substrates and products obtained from a reference batch process and other validation scenarios. Furthermore, the model comprises a partial model for the complex process of degradation of triglycerides by lipases. One of the main factors exhibiting a negative effect on growth in the investigated batch process is the accumulation of fatty acids in the culture broth due to an excess of sunflower oil. The negative effect of fatty acids on growth was quantified and implemented in the model equations.
Chapter 6 "Application of the model: an optimized fed-batch process" summarizes the application of the process model to investigate and develop fed-batch strategies for enhanced rhamnolipid formation. The process model was used to calculate a sunflower oil feeding strategy leading to significantly lower fatty acid concentrations in simulations. Indirectly, the negative effect of fatty acids on the growth rate is linked to rhamnolipid production via the formation of biomass and the biomass-specific build-up of C_4-HSL signaling molecules. The proposed feeding strategy was investigated experimentally. An increase in final rhamnolipid concentration of approx. 20% with approx. 80% increased yield as compared to the previous process in batch mode of operation was determined.

By reaching this level of complexity related to modeling of a process for rhamnolipid production, this thesis provides a missing piece in a puzzle for knowledge-based strategies for enhanced rhamnolipid formation. It is shown that existing production processes have much potential for optimization, which may ultimately lead to a point where large-scale production of rhamnolipids becomes economically feasible.

In this thesis, a process for the production of rhamnolipids in a bioreactor was successfully modeled by combining a process model with information obtained from metabolism and regulation on a genetic scale. It was furthermore shown that a multi-layer modeling approach may also benefit the understanding of the process, e.g. as it was shown for the description of a putative C_4-HSL specific acylase or the quantification of the negative effect of fatty acids on rhamnolipid formation. The developed methods may provide a framework in the future for model-based optimization of complex bioprocesses.

Zusammenfassung

Biologische Systeme bestehen in der Regel aus einer Vielzahl verschiedener Untereinheiten, welche mittels komplexer Mechanismen verknüpft sind. Somit ist es oft nicht möglich, das Systemverhalten durch einfache Untersuchungen oder Beobachtungen abzuschätzen. Dies ist zum Teil durch die Anwesenheit nichtlinearer Strukturelemente, wie zum Beispiel Rückkopplungen in biochemischen Reaktionen oder regulatorischen Netzwerken, begründet. Modellierungsansätze, welche einen komplexen Prozess in einem Bioreaktor beschreiben, können grundsätzlich drei Ebenen zugeordnet werden: der Prozessebene, der metabolischen Ebene und der genetischen Ebene. In vielen Modellen für komplexe Bioprozesse wird nur ein geringer Teil des vorhandenen Wissens über den Prozess zur Modellentwicklung verwendet, obwohl Wissen aus anderen Ebenen zum Prozessverständnis beitragen könnte. Ein Beispiel für einen solchen komplexen Bioprozess ist die biotechnologische Herstellung von Rhamnolipid Biotensiden, für den bisher noch kein Modellierungsansatz mit Kombination verschiedener Modellierungsebenen existiert.
Rhamnolipide sind mikrobielle Glykolipide, die von dem Bakterium *Pseudomonas aeruginosa* produziert werden, und auf Basis nachwachsender Rohstoffe, wie z.B. Pflanzenöle oder Zucker, hergestellt werden können. Die vorteilhaften Eigenschaften von Rhamnolipiden wurden in der Vergangenheit an mehreren verschiedenen Beispielen demonstriert. Somit haben Rhamnolipide das Potenzial, herkömmliche Tenside in verschiedenen Anwendungen zu ersetzen. Ein Grund dafür, dass sich biotechnologisch hergestellte Rhamnolipide bisher auf dem Markt gegenüber synthetischen Tensiden noch nicht durchsetzen konnten, sind relativ geringe Produktausbeuten. Bisherige Methoden der Prozessentwicklung basieren hauptsächlich auf heuristischen Ansätzen, da kinetische und qualitative Modellbeschreibungen des Prozesses meist nicht bekannt sind. Weiterhin wurden nicht pathogene Stämme für die heterologe Produktion von Rhamnolipiden entwickelt. Die mit diesen Stämmen erreichten Ausbeuten und maximalen Produktkonzentrationen können allerdings nicht mit denen konkurrieren, welche mit Wildtyp Stämmen von *P. aeruginosa* erreicht werden können. Ein pragmatischer Ansatz für eine effizientere Rhamnolipidproduktion ist somit eine Optimierung eines Prozesses basierend auf Wildtyp Stämmen mit vergleichsweise hohen Ausbeuten.

Im Rahmen dieser Arbeit wurde ein Modell für die Regulation der Rhamnolipidbildung mit Daten aus metabolischen Bilanzierungen und einem Prozessmodell mit Sonnenblumenöl als Kohlenstoffquelle verknüpft. Das Model wurde dazu verwendet, eine optimierte Prozessführungsstrategie zu entwickeln und zu untersuchen, welche zu erhöhten Rhamnolipidkonzentrationen führte. Für diese Arbeit wurde ein Prozess zur Kultivierung von *P. aeruginosa* PAO1 mit Sonnenblumenöl und Nitrat als Nährstoffquellen verwendet, ein in der Vergangenheit als Plattform etabliertes System zur Rhamnolipidproduktion.

Kapitel 2 „Mathematical description of biological processes“ enthält eine Übersicht über verschiedene Konzepte und Strategien zur Entwicklung mathematischer Modelle, und wie diese als Werkzeuge für die Bioprozesstechnik genutzt werden können. Zusätzlich zu einer Klassifizierung verschiedener Modellierungsansätze werden existierende Modelle für die Bildung von Rhamnolipiden und Quorum Sensing beschrieben und diskutiert. Weiterhin werden verschiedene Ebenen von Modellierungsansätzen vorgestellt: die Prozessebene, die metabolische Ebene und die genetische Ebene.
Kapitel 3 „Rhamnolipids: Biosurfactants based on renewable resources“ beinhaltet eine Übersicht über mikrobielle Biotenside und Rhamnolipide sowie deren Struktur und Eigenschaften, Biosynthesewege, genetische Regulationsmechanismen und Quorum Sensing. Zusätzlich werden Verfahren zur biotechnologischen Herstellung, mögliche Anwendungsgebiete sowie eine kurze Übersicht über die Wirtschaftlichkeit und theoretische Ausbeuten erläutert und diskutiert. Weiterhin wurden mittels metabolischer Bilanzierung der Abbau verschiedener Substrate und Bildung von Vorstufen der Rhamnolipidsynthese anhand der Stoffwechselwege von *P. aeruginosa* beschrieben. Die daraus berechneten theoretischen Ausbeuten wurden im folgenden Verlauf dieser Arbeit im Prozessmodell implementiert.
Kapitel 4 „Kinetic modeling of *N*-butyryl-homoserine lactone levels“ thematisiert die komplexen Regulationsmechanismen der Rhamnolipidbildung. Die Regulation der Rhamnolipidbildung erfolgt in *P. aeruginosa* durch ein komplexes, zelldichteabhängiges Quorum Sensing Netzwerk. In *P. aeruginosa* unterliegen mehr als 300 Gene den Regulationsmechnismen des Quorum Sensing Netzwerks, welches unter anderem Wachstum, Biofilmbildung und die Biosynthese verschiedener Produkte beeinflusst. Mittels eines zelldichteabhängigen Modells für *N*-butyryl-Homoserin Lacton (C_4-HSL), welches eine Produktions- und Abbaukinetik beeinhaltet, wurde eine quantitative Beschreibung für Quorum Sensing während der Kultivierung entwickelt. In der Struktur des Modells ist die Expression der Rhamnolipid Biosynthesegene *rhlAB* direkt an die Konzentration von C_4-HSL über das *rhl* System gekoppelt. Im Verlauf der Kultivierung zeigte 3-oxo-dodecanoyl-Homoserin Lacton (3o-C_{12}-HSL) stark lipophile Eigenschaften und akkumulierte in der hydrophoben Ölphase. Experimentell bestimmte C_4-HSL Produktionsraten folgten der Biomassekonzentration

proportional anstatt einem Feedback durch Autoinduktion zu unterliegen. Rhamnolipid Bildungsraten korrelierten über den gesamten Verlauf der Kultivierung linear mit den gemessenen C_4-HSL Konzentrationen. Die höchste Abbaurate von C_4-HSL konnte im wässrigen Kulturüberstand, durch einen bisher unbekannten Mechanismus, nachgewiesen werden. Damit konnte ein Effekt erfasst werden, welcher an komplexen, unter dem Begriff 'Quorum Quenching' zusammengefassten, Mechanismen beteiligt ist, die spezifisch der Akkumulation von HSL Signalmolekülen im Kulturmedium entgegenwirken. Die experimentellen Ergebnisse wurden dazu verwendet, ein einfaches Modell für C_4-HSL zu entwickeln, welches Mechanismen zum Abbau von C_4-HSL in Form eines extrazellulären Proteins beinhaltet (putative C_4-HSL spezifische Acylase). Die kinetischen Parameter des Modells wurden sowohl Literaturdaten entnommen (katalytische Effizienz, $k_{\mathrm{cat}}/K_{\mathrm{m}}$) als auch experimentell bestimmt (basale C_4-HSL Bildungsrate, $q^{\mathrm{basal}}_{\mathrm{C_4\text{-}HSL}}$). Bildungs- und Abbaurate der putativen C_4-HSL spezifischen Acylase wurden mit Hilfe des Modells angepasst.

Kapitel 5 „Modeling the production of rhamnolipids in a bioreactor" beinhaltet Arbeiten zur Beschreibung des Verlaufs der Kultivierung durch ein Prozessmodell. Für die zielgerichtete Entwicklung eines wissensbasierten Prozesses mit optimierter Rhamnolipidbildung ist ein tieferes Verständnis der Kopplung der Prozessgrößen nötig. Durch Kombination von Reaktionskinetiken, stöchiometrischen Beziehungen und experimentellen Daten wurde ein Prozessmodell bestehend aus gewöhnlichen Differentialgleichungen (ODEs) für die Kultivierung von *P. aeruginosa* PAO1 im Bioreaktor mit Sonnenblumenöl entwickelt. Weiterhin wurden zelldichteabhängige Quorum Sensing Regulationsmechanismen im Modell implementiert. Das Prozessmodell beinhaltet 36 Parameter, darunter 14 Ausbeutekoeffizienten und 7 Substrataffinitäts- und Inhibierungskonstanten. Von allen 36 Parametern wurden 30 Parameter aus experimentellen Daten abgeleitet, aus Literaturdaten extrahiert oder aus Datenbanken entnommen und 6 Parameter mit Hilfe des Modells angepasst. Das Modell beschreibt experimentelle Daten von Biomassewachstum, Substratverbrauch und Produktbildung in einem Referenz Batch Verfahren sowie anderen Validierungsszenarien. Weiterhin beinhaltet das Prozessmodell ein vereinfachtes Teilmodell für den komplexen Mechanismus des Abbaus von Triglyceriden durch Lipasen im Kulturüberstand. Einer der Faktoren, welcher das Wachstum der Mikroorganismen im untersuchten Batch Prozess negativ beeinflusst ist die dadurch resultierende Akkumulation von Fettsäuren im Kulturmedium durch einen Überschuss an Sonnenblumenöl. Dieser negative Effekt der Fettsäuren auf das Wachstum wurde quantitativ erfasst und durch die Modellgleichungen abgebildet.

Kapitel 6 „Application of the model: an optimized fed-batch process" fasst die Anwendung des Prozessmodells zusammen und gibt eine Übersicht über die Untersuchung und Entwicklung von Fed-Batch Strategien für gesteigerte Rhamnolipid-

bildung. Das Prozessmodell wurde dazu verwendet, eine Zufütterungsstrategie von Sonnenblumenöl zu berechnen, welche zu signifikant niedrigeren Fettsäurekonzentrationen im Verlauf der Kultivierung führt. Es wurde eine gesteigerte Rhamnolipidbildungsrate postuliert, begründet durch eine niedrigere Konzentration an Fettsäuren, wodurch der negative Effekt auf die Wachstumsrate reduziert wird. Die Wachstumsrate ist im Prozessmodell indirekt über den biomassespezifischen Aufbau von C_4-HSL mit der Rhamnolipidbildungsrate verknüpft. Die berechnete Zufütterungsstrategie wurde experimentell untersucht, und es konnte eine um etwa 20% gesteigerte Endkonzentration an Rhamnolipiden sowie eine um etwa 80% verbesserte Ausbeute im Vergleich zum Referenz Batch Prozess erzielt werden.

Das erreichte Level an Komplexität der Modellierung des Prozesses zur Rhamnolipidbildung sowie die gewonnenen Erkenntnisse stellen einen wichtigen Baustein zur Entwicklung wissensbasierter Strategien für optimierte Rhamnolipidbildung dar. Es konnte zudem gezeigt werden, dass bestehende Prozesse zur Produktion von Rhamnolipiden ein hohes Optimierungspotenzial haben, und in Zukunft die Basis für eine ökonomische und nachhaltige Produktion mikrobieller Rhamnolipide aus erneuerbaren Rohstoffen durch *P. aeruginosa* bilden könnten. Im Rahmen dieser Arbeit wurde ein komplexer Bioprozess zur Herstellung von Rhamnolipiden in einem Bioreaktor erfolgreich durch Kombination eines Prozessmodells mit metabolischen und regulatorischen Ansätzen beschrieben. Weiterhin konnte gezeigt werden, dass ein Modellierungsansatz mit Elementen auf mehreren Ebenen zum Prozessverständnis beitragen kann, wie zum Beispiel an der putativen C_4-HSL spezifischen Acylase oder der Beschreibung des negativen Effekts von Fettsäuren auf die Rhamnolipidbildung deutlich wird. Die entwickelten Methoden könnten in Zukunft als Konzept für eine modellbasierte Optimierung anderer komplexer Bioprozesse dienen.

Table of contents

Appendix

1. Introduction

Biological systems generally consist of several subunits which are interconnected by complex mechanisms. The behavior of the system is often difficult to assess by basic observations, mostly due to the presence of nonlinear elements such as feedback or feedforward cascades of biochemical reactions or regulatory networks. Modeling approaches for the description of a complex bioprocess in a bioreactor can principally be assigned to three layers, each representing a different perspective and level of detail: the process layer, the metabolic layer and the genetic layer. For many complex bioprocesses, modeling approaches include only part of the available knowledge, even though combining information from all layers could benefit the overall understanding of the system. One example for such complex bioprocesses is the biotechnological production of rhamnolipid biosurfactants. Surfactants are an important class of molecules used in various industrial applications as well as for everyday household requirements. These applications range from cleaning (e.g. as household detergents) to the food industry (usually as emulsifiers or stabilizers), enhanced oil recovery (EOR) or the pharmaceutical sector [Desai and Banat 1997]. As amphiphilic molecules, surfactants are used to facilitate the production of foam, emulsions and dispersions. Originally, surfactants were produced from renewable resources like plant oil or animal fat. Today, however, many of the surfactants available on the market are derived from petrochemical sources [Van Bogaert *et al.* 2007].
Within the last decades, environmental concerns and consumers perception with respect to the environmental impact of household products led to an increased interest in bio-based chemicals and sustainable production processes. Many surfactants used today display partial or slow biodegradability, and therefore their disposal contributes to impact on the environment. Besides synthesis from petrochemical sources, surfactants may also be obtained by exploiting renewable feedstocks [Kosaric 1992, Lang 2002]. This is currently performed followi-

ng two different strategies for the production of biosurfactants: the chemical synthesis of surfactants from renewable resources and the biotechnological production yielding microbial biosurfactants. One example for microbial biosurfactants are rhamnolipids, surface-active glycolipids known to be produced by *Pseudomonas aeruginosa*. Rhamnolipids are generally reported to display a much better biodegradability along with lower toxicity than chemically synthesized surfactants [Rahman *et al.* 2002, Develter *et al.* 2007]. By using many different renewable substrates as sources of carbon and energy, such as plant- or vegetable oils or sugars, rhamnolipids can be produced biotechnologically [Kosaric 1992, Lang 2002]. Besides favorable physico-chemical properties [Banat 1995], rhamnolipids have been reported to show anti-microbial and anti-fungal properties, which may be suitable for application as an active ingredient in medical products or crop science [Varnier *et al.* 2009].

The high potential of rhamnolipids has been demonstrated and discussed on various occasions, however, today, rhamnolipids still do not find widespread application. Potential reasons for this may be the use of high-priced substrates, relatively low product yields during the processes and expensive downstream-processing, which lead to rhamnolipid synthesis not being economically competitive for the most part, as opposed to synthetic surfactants derived from petrochemical sources. Therefore, the application of rhamnolipids is restricted to specialized applications, and rhamnolipids are currently not being produced on an industrial large scale.

In addition to these obstacles, while aiming for an efficient production process, the formation of rhamnolipids by *P. aeruginosa* is under control of a highly complex cell density-dependent regulatory network [Soberón-Chávez *et al.* 2005b]. While the molecular basis of quorum sensing in *P. aeruginosa* was subject to extensive research in the past, little is known about the dynamics and kinetics of these regulatory events during cultivation in a bioreactor. In addition, due to a lack of understanding regarding the interconnection of these regulatory events, a mathematical description which could serve as a platform for studying quorum sensing, using the example of rhamnolipid formation, was yet to be developed.

Research Proposal

Today, existing processes and strategies for rhamnolipid production are mainly based on heuristic approaches. Current research related to optimized rhamnolipid production is mainly focused on the optimization of growth medium components by employing techniques such as response surface methodology. Besides studies on optimized growth conditions, increasing interest in finding and developing alternative non-pathogenic strains led to the development of several non-*P. aeruginosa* host strains intended for the heterologous production of rhamnolipids [Cha *et al.* 2008, Wittgens *et al.* 2011]. However, achieved yields and final product concentrations with these alternative strains can by far not compete with the productivity of wild-type *P. aeruginosa* [Ochsner *et al.* 1995]. Therefore, one pragmatic approach for enhanced rhamnolipid formation is the optimization of a process for rhamnolipid production using high yield wild-type strains.

To derive knowledge-driven strategies for optimized product formation, further quantitative understanding of the process and interrelation of process variables are a prerequisite. A suitable and well-investigated platform process and strain with comparably high yields, *P. aeruginosa* PAO1 cultivated with sunflower oil and nitrate [Müller *et al.* 2010], was chosen for this task.

This biological process provides an ideal platform for these investigations, since the genome of the applied strain PAO1 is fully sequenced and annotated. Since rhamnolipid production is under control of a complex cell-density dependent regulatory quorum sensing network [Soberón-Chávez *et al.* 2005b], a mathematical representation of the genetic layer is a prerequisite for an accurate simulation of product formation.

As the sole source of carbon sunflower oil consists of two utilizable carbon sources, fatty acids and glycerol, which are only accessible by the microorganisms upon previous extracellular enzymatic cleavage by lipases, the chosen process also provides a challenge on the metabolic layer. The intention of this work was to develop and validate a process model for rhamnolipid production by including knowledge on cell-density dependent regulation and insight on metabolism and yields. The potential of this model was demonstrated by predicting the time-course of process variables in several validation experiments, as well as the prediction and investigation of an optimized feeding strategy.

This thesis is composed of the following contents

- Classification and description of existing modeling approaches to describe rhamnolipid production and quorum sensing including the required theoretical background of modeling of biological processes. **(Chapter 2)**
- Calcluations of theoretical maximum yields for rhamnolipid product formation, related *de novo* synthesis of precursors as well as metabolic pathways of substrate utilization in *P. aeruginosa* PAO1 **(Chapter 3)**
- Establishing a suitable analytical method for extracellular autoinducer molecules and identification of the time-course during the reference cultivation **(Chapter 4)**
- Development of a quantitative kinetic model for the time-course of *N*-butyryl-homoserine lactone during batch cultivation **(Chapter 4)**
- Identification and calculation of relevant kinetic parameters for the mathematical description of the cultivation **(Chapter 5)**
- Development of a model for rhamnolipid production on a process level by including the knowledge gained from the described investigations on the process layer, metabolic layer and genetic layer **(Chapter 5)**
- Investigation and validation of a model-derived fed-batch strategy for enhanced rhamnolipid production **(Chapter 6)**
- The evaluation of the model as a tool to predict novel process control strategies along with reparameterization according to novel data obtained from the fed-batch experiment **(Chapter 6)**

References for Chapter 1

[Banat 1995] Banat, I. M. (1995). Biosurfactants production and possible uses in microbial enhanced oil-recovery and oil pollution remediation - a review. *Bioresource Technology*, 51(1), pp. 1–12.

[Cha *et al.* 2008] Cha, M., Lee, N., Kim, M., and Lee, S. (2008). Heterologous production of *Pseudomonas aeruginosa* EMS1 biosurfactant in *Pseudomonas putida*. *Bioresource Technology*, 99(7), pp. 2192–2199.

[Desai and Banat 1997] Desai, J. D. and Banat, I. M. (1997). Microbial production of surfactants and their commercial potential. *Microbiology and Molecular Biology Reviews*, 61(1), pp. 47–64.

[Develter *et al.* 2007] Develter, D., Walcarius, B., and Fleurackers, S. (2007). Biosurfactants in cleaning and cosmetics. Third International Conference on Renewable Resources & Biorefineries (RRB), June 4 - 6, 2007, Ghent, Belgium. Available online under http://www.rrbconference.com/rrb3-2007.

[Kosaric 1992] Kosaric, N. (1992). Biosurfactants in industry. *Pure And Applied Chemistry*, 64(11), pp. 1731–1737.

[Lang 2002] Lang, S. (2002). Biological amphiphiles (microbial biosurfactants). *Current Opinion in Colloid & Interface Science*, 7(1-2), pp. 12–20.

[Müller *et al.* 2010] Müller, M., Hörmann, B., Syldatk, C., and Hausmann, R. (2010). *Pseudomonas aeruginosa* PAO1 as a model for rhamnolipid production in bioreactor systems. *Applied Microbiology and Biotechnology*, 87(1), pp. 167–174.

[Ochsner *et al.* 1995] Ochsner, U. A., Reiser, J., Fiechter, A., and Witholt, B. (1995). Production of *Pseudomonas aeruginosa* rhamnolipid biosurfactants in heterologous hosts. *Applied and Environmental Microbiology*, 61(9), pp. 3503–3506.

[Rahman *et al.* 2002] Rahman, K. S. M., Banat, I. M., Thahira, J., Thayumanavan, T., and Lakshmanaperumalsamy, P. (2002). Bioremediation of gasoline contaminated soil by a bacterial consortium amended with poultry litter, coir pith and rhamnolipid biosurfactant. *Bioresource Technology*, 81(1), pp. 25–32.

[Soberón-Chávez *et al.* 2005] Soberón-Chávez, G., Lépine, F., and Déziel, E. (2005). Production of rhamnolipids by *Pseudomonas aeruginosa*. *Applied Microbiology and Biotechnology*, 68(6), pp. 718–725.

[Van Bogaert *et al.* 2007] Van Bogaert, I. N. A., Saerens, K., De Muynck, C., Develter, D., Soetaert, W., and Vandamme, E. J. (2007). Microbial production and application of sophorolipids. *Applied Microbiology and Biotechnology*, 76(1), pp. 23–34.

[Varnier *et al.* 2009] Varnier, A. L., Sanchez, L., Vatsa, P., Boudesocque, L., Garcia-Brugger, A., Rabenoelina, F., Sorokin, A., Renault, J. H., Kauffmann, S., Pugin, A., Clement, C., Baillieul, F., and Dorey, S. (2009). Bacterial rhamnolipids are novel MAMPs conferring resistance to *Botrytis cinerea* in grapevine. *Plant Cell and Environment*, 32(2), pp. 178–193.

[Wittgens *et al.* 2011] Wittgens, A., Tiso, T., Arndt, T. T., Wenk, P., Hemmerich, J., Muller, C., Wichmann, R., Kupper, B., Zwick, M., Wilhelm, S., Hausmann, R., Syldatk, C., Rosenau, F., and Blank, L. M. (2011). Growth independent rhamnolipid production from glucose using the non-pathogenic *Pseudomonas putida* KT2440. *Microbial Cell Factories*, 10(1).

2. Mathematical description of biological processes

This chapter includes a summary of theoretical background on modeling and simulation of biological processes. Furthermore, existing modeling approaches of rhamnolipid production and quorum sensing are described and classified. It is proposed that modeling approaches for complex bioprocesses may be assigned to three layers: the process layer, the metabolic layer and the genetic layer.

2.1 Modeling as a tool for bioprocess engineering

Biological systems are typically composed of several subunits with complex interconnections. As such, the behavior of the system is often difficult to assess by basic observations. This is mainly due to the fact that many of the interconnections are of nonlinear architecture, such as feedforward cascades of biochemical reactions. Therefore, depending on the complexity of the investigated system, it may be difficult to work back from an input signal of the system to an output simply by conclusions drawn from observation or model structure.

> Even the simplest living cell is a system of such forbidding complexity that any mathematical description of it is an extremely modest approximation
>
> [Bailey 1998]

The starting point for most modeling approaches is a biological experiment resulting in a specific experimental outcome or an observation associated with the experiment. To develop a successful model of a biological process, this experimental outcome or observation needs to be described by mathematical means. Modeling of complex systems is typically applied to provide a platform for implementing available knowledge on the system. Once this platform is established, the existing model structure may be subjected to system analysis, e.g. studies on stability. Furthermore, the model may then be used for many different applications, such as the optimization of a biotechnological process by improving substrate consumption or product yields.

2.1.1 Modeling in industrial applications

In industrial applications, modeling is applied to existing processes with the intention of developing an optimized outcome (e.g. as process control strategies), as a tool to assess and establish novel processes, to unveil potentially hidden interactions which may be used for optimization purposes or as a tool for advanced process control (e.g. controlled addition of substrate for a bioprocess). Potential applications and intentions of modeling approaches of biological systems are summarized in Tab. 2.1. While industrial applications are mainly product-oriented, and therefore focus on enhanced yields or the potential of novel processes (e.g. subtrate-to-product ratio), modeling may furthermore be used as a tool for fundamental research (e.g. to unveil hidden interactions in metabolic or genetic networks).
Furthermore, modeling may also be applied as a tool for quality control (Tab. 2.1). One major point when assessing the outcome of industrial processes is consistent product quality. While a certain degree of robustness and reproducibility of the

process are a prerequisite for this, specialized tools may be applied to assess and maintain product quality. The assessment and control of product quality according to the stability of (internal) process parameters is referred to as Quality by Design.

Table 2.1: Potential application and intention of modeling approaches of biological systems.

Application	**Example**
Optimizing existing processes	Enhancing product yield / reducing waste
	Development of fed-batch strategies
Establishing novel processes	Defining operating points
	Assessing the potential of processes
Research	Unveiling potentially hidden interactions
	Quantifying inaccessible interactions
Quality control	Process analytical technology (PAT)
	Development of Soft sensors

In the last decade, the United States Food and Drug Administration (FDA) has released a regulatory framework to design, control and assess the quality of pharmaceutical manufacturing processes, which is known as Process Analytical Technology (PAT). Through the identification and measurement of critical process parameters, PAT is intended as a method to obtain a better understanding of processes, preferably in real-time [Hinz 2006]. The main idea of PAT is to provide an incentive to the pharmaceutical industry to improve production processes. By obtaining a deeper understanding of a process, potentially waste and overall costs may be reduced. In addition, a better understanding of the process will also allow for a much easier detection of batch variability used for applications in quality control [Hinz 2006]. Besides the availability of specialized hardware including sensors such as near-infrared spectroscopy (NIRS) to monitor a process, typically modeling is required to account for internal state variables or parameters that are otherwise difficult or impossible to measure.

2.1.1.1 Soft sensors

The expression 'soft sensor' describes software which processes input data from hardware sensors to derive new quantities which are either difficult or impossible to measure. It should be noted however, that since all measured data processed by the soft sensor includes measurement errors, the output of a soft sensor is typically referred to as *estimated* rather than *measured* [Stephanopoulos and San 1984]. A soft sensor typically consists of a hardware sensor and an estimation module (Fig. 2.1). Using measured state variables X, an estimation module calculates the desired quantities X_{est} from measured data and a model [Luttmann *et al.* 2012]. The model is used to draw the connection between measured data and the quantities in

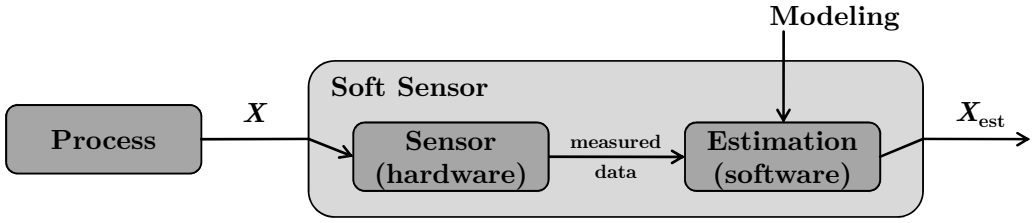

Figure 2.1: General principle of a soft sensor based on a process model. State variables X are measured by a hardware sensor, and an estimated output X_{est} is generated using a software estimator based on process modeling [Chéruy 1997].

question. Many different approaches may be used to develop models for this purpose. The most prominent examples are the application of artificial neural networks (ANN) or metabolic networks including a stoichiometric description of the reactions [de Assis and Filho 2000].

2.2 Towards a model for rhamnolipid production

Processes and strategies for rhamnolipid production are currently mainly based on heuristic approaches. Research related to optimized rhamnolipid production is mainly focused on the optimization of growth medium components by employing techniques such as response surface methodology (e.g., [Eswari *et al.* 2013, Luo *et al.* 2013]). Wild type high-producing strains of *P. aeruginosa* provide a solid basis for the optimization of rhamnolipid production, due to the ability to produce rhamnolipids in comparably high yields [Müller *et al.* 2010]. By exploiting the full potential of these strains, these levels may be further enhanced. For the knowledge-based development of an optimized process, further quantitative understanding of the process and interrelation of process variables are a prerequisite.

The production of rhamnolipids by *P. aeruginosa* is under control of a complex cell-density dependent quorum sensing regulatory network. One important signaling molecule involved in quorum sensing controlled regulatory circuits is *N*-butyryl-homoserine lactone (C_4-HSL), which is furthermore an important effector of rhamnolipid formation [Soberón-Chávez *et al.* 2005b]. A detailed description of quorum sensing mechanisms and regulation of rhamnolipid production in *P. aeruginosa* is provided in Chapter 3. To establish a conclusive approach to account for regulation of rhamnolipid formation, kinetic data on cell-density dependent quorum sensing needs to be included in a model for the bioprocess. Due to its complex structure with two direct feedback mechanisms and additional activation and quenching mechanisms, several simplifications of the model structure may be required.

A mathematical expression for the *rhl*-subsystem involved in quorum sensing has been developed in the past [Chen *et al.* 2004], by modeling the formation and dissociation of the C_4-HSL/RhlR complex in *P. aeruginosa* PAO1. However, no connec-

tion to process variables, e.g., biomass concentration, was established in that study. The development of a kinetic model for the time course of C_4-HSL concentration, which is based on growth and cell concentration, is described in detail in Chapter 4. De Lima *et al.* developed a model of rhamnolipid production in the past by using an expression proportional to biomass growth for all product formation and substrate consumption rates [DE LIMA *et al.* 2009]. This has the major advantage of the model being comparably simple, since only one parameter is required for every simulated product or substrate, respectively. However, this approach is usually accompanied by a major disadvantage of the inaccuracy and inability to describe certain biological phenomena, such as above mentioned regulatory effects on rhamnolipid formation. The model is based on a predetermined time-course for biomass concentration, instead of biological mechanisms or assumptions. This is discussed in further detail in Chapter 5.

The following sections provide on overview on the classification of models and provide examples of existing work on modeling of rhamnolipid production and cell-density dependent quorum sensing regulation.

2.3 Classification of modeling approaches

2.3.1 System, boundaries & model

A system is typically defined as a number of components that are interacting with each other. As a first step of a modeling approach, it is most important to define the boundaries of the system which separate the system from its surroundings [WIECHERT 2002]. Theoretically, the boundaries can be chosen freely, thereby encompassing any part or subunits of larger systems. However, in general, due to practicality and simplicity, boundaries are set to define systems where most changes and conversions occur inside the system rather than in the surroundings.
Basically, a system can be described by three properties: input variables u, state variables x and output variables. While input variables interfere with the system from the surroundings, state variables are typical physico-chemical properties such as concentrations which define the state of the system. Output variables are, by themselves or combined with other state variables, measureable parts of the system and are therefore accessible from outside of the system. When the boundaries of the system are set, a mathematical model is used to describe the interrelation and connection between input variables and state variables using mathematical equations. Strategies for developing mathematical models vary depending on the complexity of the system, the purpose of the model and the intended model application and structure (see also section 2.3.2). For complex systems, the development of the equations may be performed using computer aided modeling approaches (also

known as data-driven modeling). This in turn demonstrates the need for structured or normalized and easily accessible data [Wiechert 2002].
Models for quorum sensing regulatory systems have been developed with varying complexities, ranging from a description of the inner regulatory system without external effectors [Chen *et al.* 2004, Viretta and Fussenegger 2004] to a holistic view of the regulatory network, which includes interplay between different regulatory systems and diffusion/secretion of signaling molecules by the bacterial cells, which requires for an adjustment of system boundaries as opposed to an intracellular model on a molecular level, e.g. the formation and degradation of mRNA [Dockery and Keener 2000].

2.3.2 Classification of mathematical models

Choosing a suitable approach is crucial for the success of a modeling project. This approach is typically chosen according to the desired application and intention, which range from improving existing processes and the setup or assessment of novel processes to applications in research. In the following sections, a general classification of different models, which differ in their mathematical structure, is provided (see also Tab. 2.2).

2.3.2.1 Deterministic versus stochastic modeling

Deterministic modeling is based on physico-chemical conversions and uses balancing equations of state variables. A balancing equation describes the effects of input or conversion on one state variable, and is typically expressed as a differential equation (DE). In general, deterministic modeling is the most common class of describing a system by mathematical means. Deterministic modeling may be applied to describe a process at different levels, ranging from a (bio-)reactor process model to biochemical reactions inside a cell. The complexity of the model is chosen according to the desired application, and may include a structured description of individual subunits (see also section 2.3.2.4) or a segregated or non-segregated description of, e.g., a cell population (see also section 2.3.2.3). Due to comparably high concentrations of each individual component, the reaction rates are typically assumed to be only dependent on the concentration of the components involved.
As opposed to deterministic modeling, a stochastic model may be required if the amount of one or more components interacting with each other is lower, and therefore the reaction becomes a stochastic process rather than influenced solely by available concentrations. Stochastic modeling assigns probabilities to individual processes or reactions and individual components of the system. A probability $P_{\mathrm{n}}(t)$ is calculated for each component x inside the system to be present in quantity n at a given time t. This temporal distribution may be interpreted as a series of individual

experiments with different outcome. It is obvious that this may become a significantly more difficult process for complex systems with multiple components. This has been successfully applied to describe a regulatory model for small RNAs in the past [Baker *et al.* 2012], which is one example for applying stochastic modeling. Furthermore, a stochastic model for quorum sensing in *Agrobacterium tumefaciens* was developed and investigated in the past [Goryachev *et al.* 2005]. The authors hypothesized, based on the model, that quorum sensing in *A. tumefaciens* may act as a detector for biofilm formation, since much higher concentrations of signaling molecules are reached in biofilms with a tight accumulation of cells, as opposed to planctonic cells.

2.3.2.2 Discrete versus continuous modeling

Besides the continuous simulation of each state variable over time, it is also possible to model the course of variables in discrete time. Since the kinetic bahavior of a system is mostly unknown, but the general model structure is available through biological knowledge, it may be favorable to focus on qualitative properties, which is a typical application for discrete models. This may be especially useful if variables with discrete states are investigated, such as a genetic switch, and therefore, state variables are assigned discrete values. Discrete models can be easily developed from logical graph/interaction networks, which assign each component an activating or inhibiting property. Besides the modeling in continuous time, spatial models may be developed if required to account for concentration gradients, e.g. diffusion of metabolites inside or outside of a cell along an additional dimension z. An approach using discrete modeling has been used to describe the formation of periodic patterns of gene expression in epithelial cells in the past [Simakov and Pismen 2013].

2.3.2.3 Segregated versus non-segregated modeling

In most biotechnological models, differences between individual cells were not accounted for, and instead, the cell population in the system was assumed to be composed of average cells, which is referred to as a non-segregated model. Segregated models however account for an inhomogeneous distribution among a population of cells, mathematically described by equations typically referred to as population balance equations (PBEs). One simple example for segregated models is to include a size-distribution, which accounts for changes in cell volume due to growth or cell cycle progression. As opposed to non-segregated models, segregated models require additional equations to describe changes and conversions of these inhomogeneous populations. Since these segregated approaches as described above include a distribution of different properties over time, they are also referred to as statistical models. A segregated model has been applied to describe plasmid propagation in

Table 2.2: General classification of models and typical examples for biotechnological applications.

deterministic modeling in bioreactor scale	**stochastic** formation of transcription factor complexes
discrete genetic switches	**continuous** diffusion models
segregated size-distribution of cells	**non-segregated** homogenous cell culture
structured metabolic models	**unstructured** simplified descriptions of biological subunits

recombinant organisms in the past [Seo and Bailey 1985].
Even though most models for cell density dependent regulatory mechanisms assume a homogenous cell population, the interplay between cells producing and the cells affected by quorum sensing signaling molecules and cells which are not participating in the signaling process, so-called cheater cells, have also been investigated [Melke *et al.* 2010].

2.3.2.4 Structured versus unstructured modeling

The required complexity of models and model subunits is predefined by the intended application. In most biotechnological models, unstructured approaches are used to describe the cell population, resulting in biomass being described by only one state variable (so called black box model). However, structured modeling may be applied to account for individual components of the cells, e.g., metabolites or protein expression and turnover. The resulting description of the processes inside the cell convert the previously black box model of biomass into a so called white box model. White box models of cell populations typically include descriptions of physiological or metabolic processes, e.g., diffusion rates or metabolic distributions. However, the term black box or white box, respectively, is not restricted to biomass, and may also be used to describe the level of detail regarding subunits in a system. Examples for structured approaches include a dynamic model for *Saccharomyces cerevisiae* [Theobald *et al.* 1997] which was used to perform studies on the intracellular dynamics of pathways, such as the pentose phosphate pathway (PPP) [Buziol *et al.* 2002].
Due to the fact that a modeling approach for quorum sensing regulation includes both intracellular genetic mechanisms as well as extracellular state variables, these models are typically of structured architecture. One example for this is a study of diffusion and uptake of the autoinducer molecules, which is of interest when gradi-

ents of autoinducer molecules are present, e.g., due to a local accumulation of cells, such as in biofilms [Anguige *et al.* 2006].

2.4 Model development

In general, there are two different approaches for the development of a mathematical model: data-driven modeling (sometimes also referred to as knowledge-based or top-down modeling) and first-principles modeling (also known as bottom-up modeling). The mathematical description of a complex system is not necessarily restricted to one single approach, and may instead be developed as a combination of both, e.g. as individual partial models being combined to a more complex system. Strategies for the development of mathematical models for bioprocess have been extensively reviewed in the past, e.g., [Schügerl 2001, Wiechert 2002].

Data-driven modeling is focused on the availability of experimental sets of data, which are then used to deduce a model structure by analysing and interpreting the data. Data used for this method of model development may include gene expression data (e.g. DNA microarray data), proteomics or metabolomics. First-principles modeling focuses on smaller subsystems and includes biological knowledge for the development of a mathematical model, without including assumptions obtained from empirical modeling or data-based fitting parameters. After the model for the subsystem has been verified, it may be combined with others to larger units. The inclusion of structures related to control engineering is also an important part of the development of models for biological processes, since many mechanisms rely in their function on the presence of feedback loops. The process of model development may be regarded as an iterative process, meaning that as further information becomes available, e.g. due to experiments or analysis of model structure or dynamics, the model is adjusted and refined. Sometimes, this may even lead to changes in model structure due to novel insight into the system [Wiechert 2002]. As a first step, it is generally favorable to define the intention of the modeling and the expected outcome as precisely as possible. Following this step, the boundaries of the system need to be defined. Next, the state variables which are to be included in the model and relevant inputs are specified. The state variables are extensive properties, meaning that they are proportional to the amount of material in the system. Therefore, corresponding mass balance equations can be constructed for the chosen state variables. These model equations are then mostly solved numerically using appropriate software tools. In general, the model obtained is only a rough estimation of the system, and is therefore refined in consecutive steps. These steps include the investigation or validation of model structure and parameter identification. In an interative process, the results may then lead to further experiments becoming necessary to validate the novel structure or kinetic parameters. This general strategy for experimental design

and model development is further discussed in Chapter 5, where the development of the process model for rhamnolipid production is presented.

2.4.1 Data-driven modeling

Data-driven modeling focuses on the combination of data from different sources to deduce the structure of a network. This approach is effective in uncovering hidden interactions and connections of measured variables, since it usually includes large sets of data. Therefore, in contrast to first-principles modeling, the interrelation of different species is not required to be known to derive a model. Using measurement data, data-driven modeling is able to provide information about the quantitative connection of species. This technique is also commonly referred to as 'Reverse Engineering', since information is used to reconstruct the system. Several different data-driven methods for modeling have been extensively discussed and reviewed in the past [Karim *et al.* 2003, Gunther *et al.* 2009].
If the amount of data available is high (e.g. DNA microarray data), it needs to be reduced to obtain useable information. This may be performed by clustering of elements (e.g. genes) with an identical dynamic behavior (e.g. gene expression profile). A potential correlation of these elements may then be investigated in further detail. If the amount of data however is limited, the identification of interactions is typically performed differently. By assuming that either all elements are connected or none of the elements are connected, it is possible to identify and separate connected from non-connected elements when trying to describe data and adding or removing connections. The systematic extraction and evaluation of data aimed at identifying novel structures or interactions by computational tools is also known as data mining. In recent years, the term data mining has also been applied to any kind of data processing on a large scale.

2.4.2 First-principles modeling

A first-principles model is typically developed including only the current level of established science, without making any assumptions derived from empirical models or quantitative data. They are generally based on mass balancing and elemental balancing. One example for a first-principles model is a physiological model of cell metabolism, which includes only information on stoichiometric substrate and metabolite conversions.
Most logical systems are examples for first-principles modeling approaches, which represent effects (positive or negative) of individual parts of a network on each other. The structure of the model is initially developed without any quantitative data, parameters or empirical assumptions. Biochemical networks or regulatory networks involved in signal transduction processes typically lack quantitative information which

is required for the parameterization of dynamic models [Klamt 2006]. If this is the case, logical systems may be applied to provide a first qualitative overview of the system structure. In some cases, when monotonic logic can be assumed, this overview maybe already be used to derive information in the dynamic behavior of the system.

2.5 Layers of modeling

The modeling required to describe a complex process in a bioreactor can be assigned to three layers, each representing a different perspective and level of detail: the process layer, the metabolic layer and the genetic layer (Fig. 2.2) [1].
The process layer is typically represented by a system of coupled differential equations (DE), and describes dependencies and conversion of the state variables (e.g. biomass concentration and substrate concentration) by yield coefficients and specific rates (e.g. substrate consumption rate or product formation rate). Depending on the intended application, the model derived from the process layer may be sufficiently detailed. However, the process model may be further refined by including knowledge from the metabolic or genetic layer.
The metabolic layer includes a model for substrate conversion, flux distributions or enzyme kinetics. While the model for the process layer is typically based on differential equations, metabolic models are usually composed of systems of linear equations, either by defining the boundaries of a physiological white box model (including enzymatic conversion within the metabolic network) or by assuming a black box with input and output variables. While the white box approach gives detailed information about the metabolic state of the microorganisms which can be integrated in the process model, a metabolic black box model may be used to obtain yield coefficients for substrate conversion instead.
The genetic layer includes and processes information on genetic regulation by transcription factors or extracellular stimuli such as inducers of gene expression or quorum sensing signaling molecules. The genetic layer of modeling can not be assigned a general structure or setup, since the methods to develop a regulatory model typically range from logical graph/interaction networks to dynamic models including the formation of a transcription factor complex. The intention of the genetic layer of modeling is typically to obtain information on induction or repression, which may then be integrated in the metabolic or the process layer (e.g. as modified rates for substrate uptake or product formation).

[1] This terminology is originally known from computer science to classify different perspectives of a network regarding the transfer of information and conversion of signals by partitioning the system according to the 7 layers of the Open Systems Interconnection model (OSI) [Zimmermann 1980]

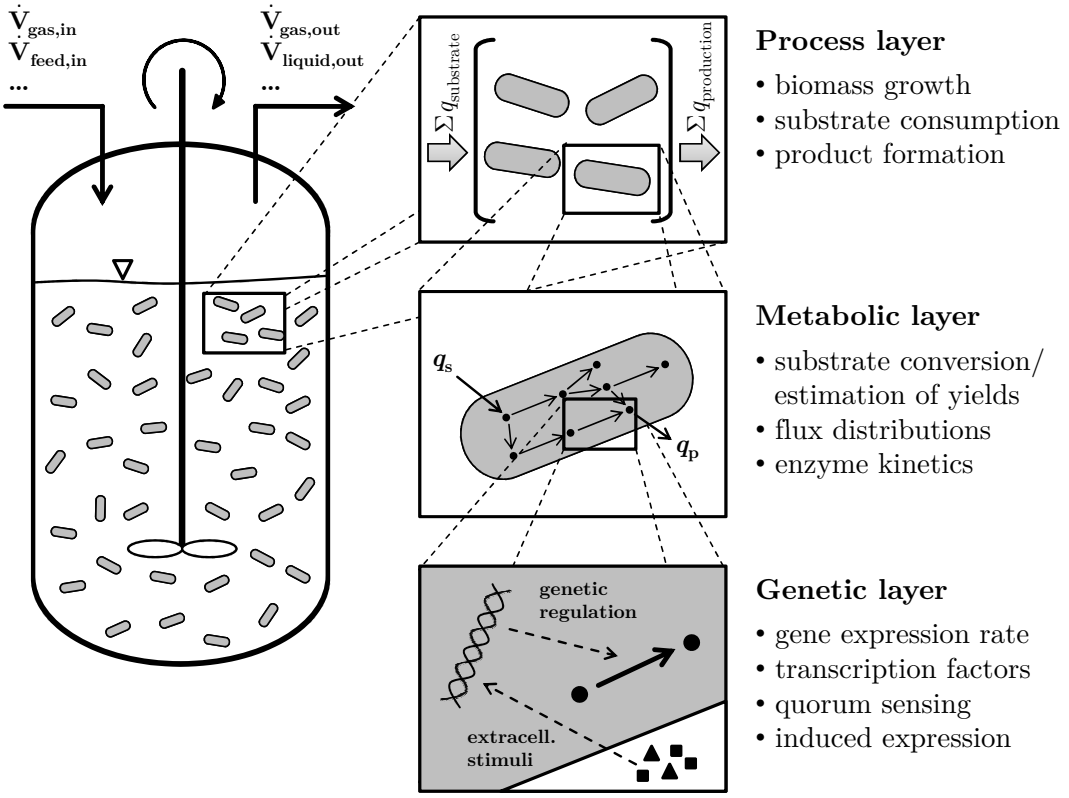

Figure 2.2: Different layers of modeling for a process in a bioreactor.

In the following sections, the different layers are discussed in further detail. They are closely connected (see also section 2.5.2.1), which is adressed providing chosen examples. Special consideration is given to the integration and combination of models or information obtained through modeling from different layers.

2.5.1 Modeling: Process layer

The process model provides a description of the process on a bioreactor scale. Typically, differential equations are used to model the time course of relevant chosen state variables. Substrate conversions are described by yields and production rates, either determined experimentally, estimated or obtained by other means such as balancing equations on the metabolic layer. Furthermore, the bioreactor model may be used as a platform for refining the model structure, e.g. if new information on the metabolism of genetic regulation becomes available. The level of detail for the process model is generally defined by its intended application. For example, in many cases, by-product formation may be neglected. This is of little relevance for most purposes of modeling, however, for specific optimization approaches, e.g. the optimization of carbon yield, it may no longer be neglected and the model needs to be expanded. The general concept, which is commonly followed, is to keep the model as detailed as necessary while at the same time, minimizing the level of detail as much as possible. This is favorable for applications of optimization, since the amount of parameters

greatly influences the required computation time. Typically, several simplifications are applied to the model, which are also intended to reduce the complexity of the model and overall parameters. Common assumptions for cultivations in a bioreactor are: ideal mixing, constant volume (for a batch process) or absence of limitation by certain substrates (e.g. oxygen supply).
In this thesis, a process model was developed for a complex bioprocess: the cell-density dependent production of rhamnolipids under control of a complex quorum sensing regulatory network during cultivation on sunflower oil as a sole source of carbon. A detailed description on the development of the model is presented in Chapter 5.

2.5.1.1 Growth kinetics

Growth kinetics describe the connection between specific growth rate and concentration of a limiting substrate. As such, the mathematical description of growth kinetics is an important part of a model for a bioprocess using growing cells. By far, the most prevalent model is the comparably simple MONOD kinetic, which was first described in 1949 to provide an empiric model describing data on growth of microorganisms [Monod 1949]. The MONOD equation is similar to the MICHAELIS-MENTEN equation for the reaction rate of an enzyme depending on substrate concentration [Michaelis and Menten 1913] (see also 2.5.2.1). This may be explained due to the fact that living cells rely on enzymatic processes for the conversion of substrates, resulting in cellular growth, and therefore, are subject to the same product limitations. In contrast to the MICHAELIS-MENTEN equation, which is based on assumptions regarding the reaction mechanisms (e.g. reversible binding, presence of only one substrate), the MONOD kinetic is based solely on empirical observations [Monod 1949]. More complex models for growth kinetics cover additional effects such as product or substrate inhibition.
Even though the MONOD model is a comparably old model in modern biotechnology, it is still by far the most widely used method to describe substrate limitation. Over time, several modifications have been made to the MONOD equation to provide a better fitting of experimental data (Tab. 2.3). However, these models are still only based on empirical observations. One exception is the TEISSIER equation, which is not based on the MONOD model, however, it is not based on biological principles either [Teissier 1936].
Choosing a suitable growth kinetic is crucial when substrate inhibition and limitation or inhibition due to (by-)product is an issue in the intended application of the model. The choice of a kinetic to describe growth in presence of two different substrates is discussed in further detail in Chapter 5 using the investigated process for rhamnolipid production.

Table 2.3: Chosen different approaches to describe the specific growth rate depending on the substrate availability.

Name	Equation	Reference
MONOD	$\mu = \mu_{max} \cdot \frac{S}{K_S+S}$	[Monod 1949]
multi-sub. MONOD	$\mu = \mu_{max} \cdot \frac{S_1}{K_{S,1}+S_1} \cdot \frac{S_2}{K_{S,2}+S_2}$	[Bader 1978]
ANDREWS	$\mu = \mu_{max} \cdot \frac{S}{K_S+S+\frac{S^2}{K_i}}$	[Andrews 1968]
MOSER	$\mu = \mu_{max} \cdot \frac{S^n}{K_S+S^n}$	[Moser 1957]
CONTOIS	$\mu = \mu_{max} \cdot \frac{S}{B \cdot X+S}$	[Contois 1959]
TESSIER	$\mu = \mu_{max} \cdot (1 - e^{(\frac{-S}{K_S})})$	[Teissier 1936]

2.5.2 Modeling: Metabolic layer

The metabolic layer generally includes models for substrate uptake and conversion on a cellular level. Metabolic models typically describe stoichiometric conversion between various metabolites, and as such, they are described by systems of linear equations. Therefore, they are comparatively simple in calculation by computational methods, and additional process data (e.g. generated CO_2) is easily integrated. However, since mostly the network is assumed to be in a steady state, dynamic information on the system, such as transient changes in certain metabolite concentrations is lost during the investigation. When a metabolic model is intended for use with a process model, the metabolic model is typically used to provide information about substrate uptake and product formation in form of specific rates. The complexity of the system investigated by modeling within the metabolic layer varies greatly depending on the purpose of the approach.

A straightforward approach for the description of metabolic processes may be obtained by assuming a metabolic black box. A black box is a mathematical representation of an object, which is only characterized by its input and corresponding output (Fig. 2.3). The output is generated from the input without any knowledge on the internal conversions by mathematical means. For many biological systems, depending on the intended application of the model, the description of the metabolic layer by a black box is typically a simple and pragmatic approach. When internal conversion of substrates are of no interest for the general modeling approach, a black box design is usually favored to a more complex metabolic network, since less data is required for its generation.

Modeling approaches which include a detailed description of the biochemical network and conversions in the microorganisms are commonly referred to as 'white box' models. White box models require for detailed knowledge on the process, which describes all extracellular substrate uptake rates as well as all intracellular conversion

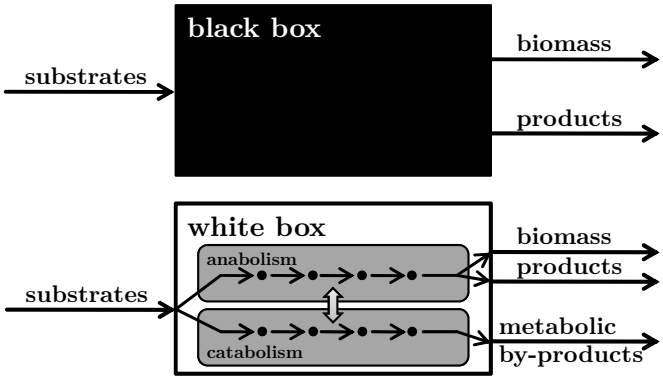

Figure 2.3: Comparison of black box and white box approaches for metabolic modeling.

rates. As a basis for developing such complex models, typically a large amount of experimental data is required, which may be obtained by metabolic flux balance analysis and metabolic databases, which contain the structure of the biochemical network as well as kinetic parameters. Metabolic flux analysis is a method to investigate production and consumption rates of individual metabolites in biological systems. While metabolic flux analysis is a powerful tool for finding bootlenecks in metabolic networks to indentify targets for metabolic strain engineering, it is also an important source of data to create metabolic models or supplementing existing models with metabolic insights. Most commonly, metabolic flux distributions are described by stoichiometric conversions between different metabolites by linear equation systems. This technique has been used for the optimization of rhamnolipid production in the past [Eswari *et al.* 2013].
As part of this thesis, both a black box and a white box approach were used to model the metabolic layer. A white box logical network for biochemical conversions was created from online databases and available knowledge on product formation, and used to calculate maximum theoretical yields for substrate conversion and product formation to be included in the process model. The final implementation of substrate conversion in the process model was performed assuming a black box model to reduce the amount of free parameters in the model.

2.5.2.1 Enzyme kinetics

Enzyme kinetics provide the basis for most metabolic models. They describe the connection between reaction rate and concentration of a substrate. The most prominent model is the MICHAELIS-MENTEN equation, which was first described in 1913 to describe the reaction rate of an enzyme [Michaelis and Menten 1913]. The model is based on a mathematical description of the mechanisms of reversible formation of an enzyme-substrate-complex, which then releases the product and the

Table 2.4: Chosen different approaches to describe enzymatic reaction rate depending on the substrate concentration.

Name	Equation	Reference
MICHAELIS-MENTEN	$v = v_{max} \cdot \frac{S}{K_m+S}$	[Michaelis and Menten 1913]
Presence of inhibitor	$v = v_{max} \cdot (1 - \frac{I}{K_i+I})$	[Walsh *et al.* 2007]
Intermediate complex	$v_0 = k_{cat} \cdot \frac{S \cdot E_0}{K_m+S}$	[Walsh *et al.* 2007]

complex dissociates. The model may be further enhanced to include the effect of inhibitors or other modifications (Tab. 2.4).

The substrate concentration calculated from the process model may be used to calculate specific substrate uptake rates. Using these specific uptake rates, the system of linear equations is used to calculate the remaining substrate conversions. One example for this approach has been described by Doyle and coworkers, who calculated maximum uptake and production rates from extracellular concentrations [Mahadevan *et al.* 2002]. This provides one example how kinetics may be used to connect the process layer and the metabolic layer.
As part of this thesis, enzyme kinetics have been included on several layers: to calculate the cleaving of sunflower oil into fatty acids and glycerol on the process layer, to describe the conversion of the product mono-rhamnolipid to di-rhamnolipid on the metabolic layer and to calculate the enzymatic degradation of C_4-homoserine lactone autoinducer molecules on the genetic layer (Chapters 4 & 5).

2.5.3 Modeling: Genetic layer

In cellular systems, activities and concentrations of enzymes are typically controlled by tight regulatory mechanisms. This regulatory mechanisms include transcription factor binding to DNA, which enhances or inhibits transcription. Besides this regulation at the genetic level, there are posttranscriptional modifications affecting protein activity, which are not further discussed here. Many different models describing regulatory effects have been described in the past, and these models are not uniform in structure. Investigated approaches include linear weight modeling, linear and nonlinear ordinary differential equations as well as graph-theoretic or hierarchical models. While deterministic and continuous models are generally applied to model biological processes, a stochastic model has also been described to calculate the effects of small RNAs in the past [Baker *et al.* 2012] as well as a discrete model, which has been applied to investigate gene expression patterns [Simakov and Pismen 2013]. More complex regulatory models may also include transcription and translation, and are therefore able to describe genetic regulation on a deeper level (e.g. including mRNA concentration and stability into the model). This is typically described by a complex

system of differential equations. Covert and Palsson combined a gene regulatory network with a metabolic flux balance analysis to study the central metabolism in *E. coli* [Covert and Palsson 2002]. The regulatory model was composed of logical rules, which could efficiently be used to predict phenotypes of several growth experiments.

Potential application for regulatory models are the description of effects of transcription factor complexes, which form only upon induction by a certain stimulus. Besides these biological mechanisms which can be regarded as stand-alone units of genetic regulation, there are other mechanisms which are tied into other cellular processes, such as growth of the microorganisms. These processes are influenced both by the dynamics of the bioprocess described in the process layer, but also by their own dynamics. One example for this is the cell-density dependent expression of genes under control of a quorum sensing network, as described in previous sections.

In this thesis, a model for the concentration of an extracellular quorum sensing signaling molecule was developed, which includes biomass data from the process layer to calculate specific product formation rate via a correlation of gene expression and an enzyme responsible for product formation. A detailed description on the development of the model is presented in Chapter 4.

2.5.4 Combining different layers of modeling

Existing models for biotechnological processes typically only include information from one layer of modeling and therefore, most knowledge on the process, which could benefit the overall understanding of the system, is not integrated in the model. As a working approach, many studies on improving a biological system focus on the process layer. Even though the composition of the metabolic network is known for many microorganisms, metabolic flux analysis is mainly performed as an analytical tool for determining target genes for strain engineering. Since most of the metabolic data is available digitally, more information could potentially be included in the model. In many cases, models for rhamnolipid production include a predetermined time-course of biomass formation, such as the interpolation of experimental data by a logistic function for growth [de Lima *et al.* 2009]. This may be favorable in some cases due to simplicity, however, when complex interactions, such as cell-density dependent quorum sensing regulation are to be studied, this approach of predetermined biomass formation may no longer be feasible.

In this thesis, approaches from different layers are investigated and combined using the example of a complex bioprocess, the formation of rhamnolipids by *P. aeruginosa*, with a strongly regulated product formation and extracellular enzymatic conversion of carbon substrate (Chapters 4 & 5). The model created from combining the different approaches was then used to predict a process control strategy with

increased productivity, which was furthermore verified experimentally to provide a proof of concept (Chapter 6).

References for Chapter 2

[Andrews 1968] Andrews, J. F. (1968). A mathematical model for the continuous culture of microorganisms utilizing inhibitory substrate. *Biotechnology and Bioengineering*, 10(6), pp. 707–724.

[Anguige *et al.* 2006] Anguige, K., King, J. R., and Ward, J. P. (2006). A multi-phase mathematical model of quorum sensing in a maturing *Pseudomonas aeruginosa* biofilm. *Mathematical Biosciences*, 203(2), pp. 240–276.

[de Assis and Filho 2000] de Assis, A. J. and Filho, R. M. (2000). Soft sensors development for on-line bioreactor state estimation. *Computers & Chemical Engineering*, 24(2), pp. 1099–1103.

[Bader 1978] Bader, F. G. (1978). Analysis of double-substrate limited growth. *Biotechnology and Bioengineering*, 20(2), pp. 183–202.

[Bailey 1998] Bailey, J. E. (1998). Mathematical modeling and analysis in biochemical engineering: past accomplishments and future opportunities. *Biotechnology Progress*, 14(1), pp. 8–20.

[Baker *et al.* 2012] Baker, C., Jia, T., and Kulkarni, R. V. (2012). Stochastic modeling of regulation of gene expression by multiple small RNAs. *Physical review E, statistical, nonlinear, and soft matter physics*, 85(6).

[Buziol *et al.* 2002] Buziol, S., Becker, J., Baumeister, A., Jung, S., Mauch, K., Reuss, M., and Boles, E. (2002). Determination of in-vivo kinetics of the starvation-induced Hxt5 glucose transporter of *Saccharomyces cerevisiae*. *FEMS Yeast Research*, 2(1), pp. 283–291.

[Chen *et al.* 2004] Chen, F., Chen, C. C., Riadi, L., and Ju, L. K. (2004). Modeling *rhl* quorum sensing regulation on rhamnolipid production by *Pseudomonas aeruginosa*. *Biotechnology Progress*, 20(5), pp. 1325–1331.

[Chéruy 1997] Chéruy, A. (1997). Software sensors in bioprocess engineering. *Journal of Biotechnology*, 52(3), pp. 193–199.

[Contois 1959] Contois, D. E. (1959). Kinetics of bacterial growth: relationship between population density and specific growth rate of continuous cultures. *Journal of General Microbiology*, 21, pp. 40–50.

[Covert and Palsson 2002] Covert, M. W. and Palsson, B. O. (2002). Transcriptional regulation in constraints-based metabolic models of *Escherichia coli*. *Journal of Biological Chemistry*, 277(1), pp. 28058–28064.

[Dockery and Keener 2000] Dockery, J. D. and Keener, J. P. (2000). A mathematical model for quorum sensing in *Pseudomonas aeruginosa*. *Bulletin of Mathematical Biology*, 00, pp. 1–22.

[Eswari *et al.* 2013] Eswari, J. S., Anand, M., and Venkateswarlu, C. (2013). Optimum culture medium composition for rhamnolipid production by *Pseudomonas aeruginosa* AT10 using a novel multi-objective optimization method. *Journal of Chemical Technology and Biotechnology*, 88(2), pp. 271–279.

[Goryachev *et al.* 2005] Goryachev, A. B., Toh, D. J., Wee, K. B., Lee, T., Zhang, H. B., and Zhang, L. H. (2005). Transition to quorum sensing in an *Agrobacterium* population: A stochastic model. *PLoS Computational Biology*, 1(4), pp. 265–275.

[Gunther *et al.* 2009] Gunther, J. C., Baclaski, J., Seborg, D. E., and Conner, J. S. (2009). Pattern matching in batch bioprocesses - Comparisons across multiple products and operating conditions. *Computers and Chemical Engineering*, 33(1), pp. 88–96.

[Hinz 2006] Hinz, D. C. (2006). Process analytical technologies in the pharmaceutical industry: the FDA's PAT initiative. *Analytical and Bioanalytical Chemistry*, 384(5), pp. 1036–1042.

[Karim *et al.* 2003] Karim, M. N., Hodge, D., and Simon, L. (2003). Data-based modeling and analysis of bioprocesses: some real experiences. *Biotechnology Progress*, 9(5), pp. 1591–1605.

[Klamt 2006] Klamt, S. (2006). A methodology for the structural and functional analysis of signaling and regulatory networks. *BMC Bioinformatics*, 7(56).

[Luo *et al.* 2013] Luo, Z., Yuan, X. Z., Zhong, H., Zeng, G. M., Liu, Z. F., Ma, X. L., and Zhu, Y. . (2013). Optimizing rhamnolipid production by *Pseudomonas aeruginosa* ATCC 9027 grown on waste frying oil using response surface method and batch-fed fermentation. *Journal of Central South University*, 20(4), pp. 1015–1021.

[Luttmann *et al.* 2012] Luttmann, R., Bracewell, D. G., Cornelissen, G., Gernaey, K. V., Glassey, J., Hass, V. C., Kaiser, C., Preusse, C., Striedner, G., and Mandenius, C. F. (2012). Soft sensors in bioprocessing: a status report and recommendations. *Biotechnology Journal*, 7(8), pp. 1040–1048.

[Mahadevan *et al.* 2002] Mahadevan, E., Edwards, J. S., and Doyle, F. J. (2002). Dynamic flux balance analysis of diauxic growth in *Escherichia coli*. *Biophysical Journal*, 83(3), pp. 1331–1340.

[Melke *et al.* 2010] Melke, P., Sahlin, P., Levchenko, A., and Jonsson, H. (2010). A cell-based model for quorum sensing in heterogeneous bacterial colonies. *PLoS Computational Biology*, 6(6).

[Michaelis and Menten 1913] Michaelis, L. and Menten, M. L. (1913). Die Kinetik der Invertinwirkung. *Biochemische Zeitschrift*, 49(1), pp. 333–369.

[Müller *et al.* 2010] Müller, M., Hörmann, B., Syldatk, C., and Hausmann, R. (2010). *Pseudomonas aeruginosa* PAO1 as a model for rhamnolipid production in bioreactor systems. *Applied Microbiology and Biotechnology*, 87(1), pp. 167–174.

[Monod 1949] Monod, J. (1949). The growth of bacterial cultures. *Annual Review of Microbiology*, 3(1), pp. 371–394.

[Moser 1957] Moser, H. (1957). Structure and dynamics of bacterial populations maintained in the chemostat. *Cold Spring Harbor Symposia on Quantitative Biology*, 22, pp. 121–137.

[Schügerl 2001] Schügerl, K. (2001). Progress in monitoring, modeling and control of bioprocesses during the last 20 years. *Journal of Biotechnology*, 85(2), pp. 149–173.

[Seo and Bailey 1985] Seo, J. H. and Bailey, J. E. (1985). A segregated model for plasmid content and product synthesis in unstable binary fission recombinant organisms. *Biotechnology and Bioengineering*, 27(2), pp. 156–166.

[Simakov and Pismen 2013] Simakov, D. S. and Pismen, L. M. (2013). Discrete model of periodic pattern formation through a combined autocrine-juxtacrine cell signaling. *Physical Biology*, 10(4).

[Soberón-Chávez *et al.* 2005] Soberón-Chávez, G., Lépine, F., and Déziel, E. (2005). Production of rhamnolipids by *Pseudomonas aeruginosa*. *Applied Microbiology and Biotechnology*, 68(6), pp. 718–725.

[Stephanopoulos and San 1984] Stephanopoulos, G. and San, K. Y. (1984). Studies on on-line bioreactor identification. I. Theory. *Biotechnology and Bioengineering*, 26(10), pp. 1176–1188.

[Teissier 1936] Teissier, G. (1936). Les lois quantitatives de la croissance. *Annales de Physiologie et de Physiochimie Biologique*, 12, pp. 527–573.

[Theobald *et al.* 1997] Theobald, U., Mailinger, W., Baltes, M., Rizzi, M., and Reuss, M. (1997). In-vivo analysis of metabolic dynamics in *Saccharomyces cerevisiae*: I. Experimental observation. *Biotechnology and Bioengineering*, 55(1), pp. 305–316.

[Viretta and Fussenegger 2004] Viretta, A. and Fussenegger, M. (2004). Modeling the quorum sensing regulatory network of human-pathogenic *Pseudomonas aeruginosa*. *Biotechnology Progress*, 20, pp. 670–678.

[Walsh *et al.* 2007] Walsh, R., Martin, E., and Darvesh, S. (2007). A versatile equation to describe reversible enzyme inhibition and activation kinetics: modeling β-galactosidase and butyrylcholinesterase. *Biochimica et Biophysica Acta*, 1770(5), pp. 733–746.

[Wiechert 2002] Wiechert, W. (2002). Modeling and simulation: tools for metabolic engineering. *Journal of Biotechnology*, 94(1), pp. 37–63.

[Zimmermann 1980] Zimmermann, H. (1980). OSI reference model - the ISO model of architecture for open systems interconnection. *IEEE Transactions on Communications*, 28(4), pp. 425–432.

3. Rhamnolipids: Biosurfactants based on renewable resources

This chapter is partly based on the publication

Rhamnolipids as biosurfactants from renewable resources: Concepts for next-generation rhamnolipid production

Marius Henkel[a], *Markus M. Müller*[a], *Johannes H. Kügler*[a], *Roberta B. Lovaglio*[b], *Jonas Contiero*[b], *Christoph Syldatk*[a] *and Rudolf Hausmann*[c]

[a]Institute of Process Engineering in Life Sciences, Section II: Technical Biology, Karlsruhe Institute of Technology (KIT), Karlsruhe, Germany [b]Institute of Biological Sciences, Department of Biochemistry and Microbiology, Universidade Estadual Paulista (UNESP), Rio Claro, SP, Brazil [c]Institute of Food Science and Biotechnology, Section Bioprocess Engineering, University of Hohenheim, Stuttgart, Germany

---

The final publication is available at sciencedirect.com

Bibliographic details

published August 2012, Volume 47, Issue 8, pp 1207-1219
Process Biochemistry (Elsevier Applied Science)

Print ISSN 1359-5113 - Online ISSN 1873-3298
DOI: 10.1016/j.procbio.2012.04.018

Authors' contributions to this publication

Marius Henkel collected and evaluated the data from literature, performed the metabolic balancing, obtained pricing information for the economic analysis and wrote the manuscript.

Markus M. Müller assisted with metabolic calculations, provided input for the design of the study and proof-read the manuscript.

Johannes H. Kügler, Roberta B. Lovaglio and Jonas Contiero contributed to scientific discussions and proof-read the manuscript.

Christoph Syldatk supervised the project, proof-read the manuscript and contributed to scientific discussions.

Rudolf Hausmann supervised the project, proof-read the manuscript and provided input for the design of the study.

3.1 Introduction

In the recent past, increasing environmental concerns of consumers led to a resurrection of industrial interest in bio-based chemicals, and notably surfactants. Surfactants are an important class of amphiphilic molecules, which lower the surface tension between two phases by accumulating at the interface. With a total worldwide production of over 15 million tons per year [Van Bogaert *et al.* 2007], surfactants find their application in many different fields ranging from cleaning to applications in food-processing (usually as emulsifiers), enhanced oil recovery (EOR) or the pharmaceutical sector. Due to their amphiphilic nature, these surface-active molecules facilitate the production of foam, emulsions and dispersions. Originally, surfactants were exclusively produced from renewable resources like plant oils or animal fat, however, the majority of available surfactants today is derived from petro-chemical sources [Van Bogaert *et al.* 2007]. Most surfactants used today are only partially or slowly biodegradable, and as such, they contribute to environmental pollution. Additionally, production of 'ordinary' surfactants depletes the world's non-renewable petrochemical resources. To address this issue, the production of surfactant molecules should be achieved by utilizing renewable substrates. One approach is the biotechnological production of microbial surfactants. These biologically produced molecules are generally reported to have less impact on the environment than conventional surfactants, since they are usually much better biodegradable and show less toxicity than synthetic surfactants. Some of these microbial surfactants also show excellent physico-chemical properties and hold several advantages over synthetic surfactants, like constant effectiveness over a wider range of pH and temperature [Oliveira *et al.* 2008]. One group among these promising biosurfactants are rhamnolipids, surface-active glycolipids mainly known from *Pseudomonas aeruginosa*. In the last years, biosurfactants gained more and more attention, since sustainable production processes became more appreciable, and they show the potential to replace synthetic surfactants. However, the application of biotechnologically produced surfactants is mainly restricted to certain areas, since production processes are for the most part not economically competitive with synthetic surfactants derived from petrochemical sources. This can be explained mainly due to the use of high-priced substrates, relatively low product-yields and expensive downstream-processing.

3.2 Biosurfactants

To distinguish surfactants which are dependent on petro-chemical sources from those which do not originate from petro-chemical sources, the term 'biosurfactant' was introduced. The classification 'biosurfactant' however, is used freely in the scientific community for either surfactants derived from renewable resources by chemical

Table 3.1: Classification of microbial biosurfactants. Modified and summarized according to [Lang and Trowitzsch-Kienast 2002].

Classification	**Example**	**Organism**
Glycolipids	Mannosylerythritol lipids	*Pseudozyma sp.*
	Sophorolipids	*Candida bombicola*
	Rhamnolipids	*Pseudomonas aeruginosa*
	Trehalose Lipids	*Rhodococcus sp.*
Lipopeptides / Lipoaminoacids	Surfactin	*Bacillus subtilis*
	Serrawettin	*Serratia marcescens*
	Lichenysin G	*Bacillus licheniformis*
Polymers	Carbohydrate/protein (Liposan)	*Yarrowia lipolytica*
	Lipopolysaccharides (Emulsan)	*Acinetobacter calcoaceticus*
Phospholipids / Glycerides / fatty acids	Phosphatidylcholin	*Gluconobacter cerinus*
	mono-/di-glycerides	*Clostridium pasteurianum*

means (e.g. transesterification to produce alkyl polyglycosides, APGs) or for biomolecules with surfactant-like properties produced by microorganisms. Other bio-based surfactants are methyl-sulfonates of fatty acid methyl esters (FAME), which are obtained by transesterification of fats. Regular soap can also be seen as a bio-based surfactant, since it is usually derived from plant or animal fat via saponification. The term 'biosurfactant', as used within this thesis, refers exclusively to surfactants from microbial origin. There are several microorganisms known to produce surface active molecules. Biosurfactants are a structurally diverse group of molecules. The group comprises simple molecules like fatty acids and phospholipids as well as glycolipids, lipopeptides and high molecular weight polymers like lipopolysaccharides (Tab. 3.1).

Glycolipids, which represent the most prominent group among biosurfactants, are low-molecular weight biosurfactants, which consist of mono- or oligosaccharides (glucose, mannose, galactose, rhamnose) and one or more saturated or unsaturated fatty acids, hydroxy-fatty acids or fatty alcohols. Some of the best-studied industrially relevant biosurfactants belong to the group of glycolipids (e.g. sophorolipids, trehaloselipids, mannosylerythritol-lipids (MEL) and rhamnolipids). Biosurfactants display a broad range of physico-chemical properties, and some of them, especially glycolipids [Develter *et al.* 2007], also have excellent surfactant/emulsifier properties. Biosurfactants are reported to display very low toxicity, while some of them retain antibacterial/antimycotical properties. Biosurfactants can be produced using renewable feedstocks and are completely biodegradeable

[Banat *et al.* 2000, Desai and Banat 1997, Kosaric 1992, Lang 2002]. Biosurfactants may fulfill additional functions other than reducing surface tension for enhanced uptake of hydrophobic substrates. These 'additional benefits' (e.g. antibiotic or antimycotic properties) will potentially make the application of biosurfactants in certain areas (e.g. in the medical field) even more promising and may open up new possibilities for industrial application compared to synthetic surfactants.

3.3 Rhamnolipids

Rhamnolipids are intensively studied microbial surfactants and belong to the group of glycolipids. Rhamnolipids contain one or two L-rhamnose units linked to one or two β-hydroxy fatty acids (Fig. 3.1) and are mainly known to be produced by *Pseudomonas aeruginosa*. Rhamnolipids were first described in 1946 as 'oily glycolipids' [Bergström *et al.* 1946]. The first steps in research on the chemical structure of rhamnolipids could identify L-rhamnose and β-hydroxydecanoic acid as subunits [Bergström *et al.* 1946, Hauser and Karnovsky 1954, Jarvis and Johnson 1949]. The exact chemical structure was unveiled in subsequent studies [Jarvis and Johnson 1949, Edwards and Hayashi 1965]. In the last decades, intensive research on various fields regarding rhamnolipid production has been conducted. Many research groups have dedicated their work to identifying genes related to the synthesis of rhamnolipids [Ochsner *et al.* 1994, Rahim *et al.* 2000, Rahim *et al.* 2001, Rehm *et al.* 2001, Zhu and Rock 2008] and provided insight into biosynthetic pathways [Rehm *et al.* 2001, Zhu and Rock 2008, Burger *et al.* 1963, Déziel *et al.* 2003, Hauser and Karnovsky 1957, Hauser and Karnovsky 1958]. Several different research groups focused on identifying genes and mechanisms responsible for the regulation of the production of rhamnolipids [Ochsner *et al.* 1994, Pearson *et al.* 1997, Pesci and Iglewski 1997]. Research has also been performed on detection and quantification of rhamnolipids [Déziel *et al.* 2000, Gartshore *et al.* 2000, Heyd *et al.* 2008, Mata-Sandoval *et al.* 1999, Rendell *et al.* 1990, Schenk *et al.* 1995, Siegmund and Wagner 1991]. Additionally, downstream-processing of rhamnolipids has also been investigated [Walter *et al.* 2010], since most procedures used for recovering rhamnolipids constitute a relevant proportion of the overall production process [Mulligan and Gibbs 1993]. Besides rhamnolipids from *P. aeruginosa*, *Burkholderia plantarii* is known to produce an unusual rhamnolipid containing three β-hydroxy-fatty acids [Andrä *et al.* 2006]. The length of the hydroxy-fatty acids ranges from 8 to 16 carbons, while β-hydroxydecanoic acid is the predominant species in *P. aeruginosa* [Déziel *et al.* 2000] and β-hydroxytetradecanoic acid has been found in rhamnolipids from *Burkholderia sp.* [Hörmann *et al.* 2010].

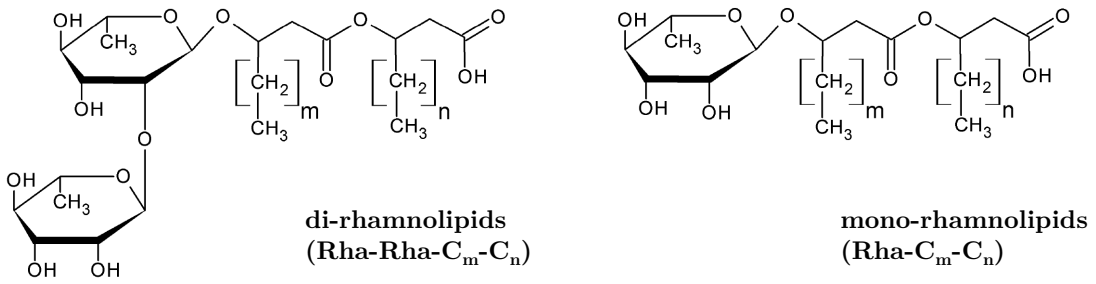

Figure 3.1: General structure of mono-rhamnolipids and di-rhamnolipids (m, n = 4 - 8) [Jarvis and Johnson 1949, Edwards and Hayashi 1965].

Rhamnolipids are produced by *P. aeruginosa* as a mixture of different congeners, with the predominant molecules being Rha-C_{10}-C_{10} (RL-1) and Rha-Rha-C_{10}-C_{10} (RL-3). Abdel-Mawgoud et al. reviewed the structural diversity of rhamnolipids [Abdel-Mawgoud *et al.* 2010]. The product spectrum of rhamnolipids produced by *P. aeruginosa* is highly dependent on the strain, which can be shown by comparison of different strains under identical conditions [Müller *et al.* 2011]. Rhamnolipids may fulfill different physiological functions, which were summarized as [Soberón-Chávez *et al.* 2005b]: Uptake of hydrophobic molecules for efficient degradation due to their surface-active properties, as means of competing with other microorganism due to their wide range of antimicrobial activity, attachement and contact to hydrophobic surfaces and as a virulence factor which facilitates intrusion into tissue due to their haemolytic activity, e.g. in the lung [Van Delden and Iglewski 1998]. In contrast to other biosurfactants, rhamnolipids display relatively high surface activities, and can be produced in relatively high yields and short times. Rhamnolipids reduce the surface tension of water from 72 - 31 mN/m [Syldatk *et al.* 1985b]. The critical micellar concentration (CMC), the concentration at which the formation of micelles starts, was determined to be between 20 - 225 mg/L in water [Syldatk *et al.* 1985b, Dubeau *et al.* 2009]. In the past, the biodegradability of rhamnolipids and sophorolipids was compared to synthetic surfactants Triton-X-100 and linear alkylbenzene sulphonates (LAS) [Develter *et al.* 2007]. It was shown that the synthetic surfactants, in all examination scenarios, were only partially degraded, while the biosurfactants were almost completely degraded. Additionally, they investigated the aquatoxicity of rhamnolipids and sophorolipids, which were, according to their EC_{50} values of 20 - 77 mg/L, about 12-times lower than synthetic surfactants.

3.4 Potential applications for biosurfactants

The total worldwide production of surfactants was over 10 Mt in the year 2007 [Van Bogaert *et al.* 2007]. The biggest market-value is achieved in the sector of

detergents for cleaning purposes (which attributes for up to 50 % of surfactant production) with a total of about 60 billion USD in the year 2004 [Scheibel 2004]. Establishing production processes of new surfactant molecules relying on renewable resources, independent of petro-chemical resources and effective at lower temperatures and concentrations would have positive effects on net energy consumption and might reduce CO_2 emission levels. Biosurfactants are already being made available to the end-user in the form of household detergents (e.g. Ecover Ltd., Malle, Belgium), and several other potential applications for biosurfactants in general have been discussed in the past (for reviews on application of biosurfactants see [Banat *et al.* 2000, Desai and Banat 1997, Kitamoto *et al.* 2002, Makkar and Cameotra 2002, Singh *et al.* 2007, Pornsunthorntawee *et al.* 2010]). In the following section, a short overview of potential applications of rhamnolipids is given. Rhamnolipids may potentially be used for bioremediation of contaminated soil by improving degradation of hydrocarbons by enhancing their bioavailability to degrading microorganisms [Kitamoto *et al.* 2002, Rahman *et al.* 2003, Paria 2008]. It has been demonstrated that in this case, biosurfactants display several advantages compared to synthetic surfactants, since biosurfactants can perform much better under atypical temperatures, pH and salinity [Banat 1995, Mulligan 2005, Van Hamme *et al.* 2003]. It has been demonstrated that rhamnolipids may also be applied in the field of oil recovery in a process referred to as microbial enhanced oil recovery (MEOR)[Banat 1995, Van Hamme *et al.* 2003], where biosurfactant producing microorganisms are used for in-situ treatment of oil-containing sands or in ex-situ applications, e.g. by flooding the deposit area [Sen 2008]. The application of biosurfactants as environmentally-friendly pesticides may constitute another market for microbial surfactants. Due to their antimycotic properties [Varnier *et al.* 2009], rhamnolipids are already being applied in a formulation of a biofungicide (ZONIX, Jeneil Biosurfactant Company, Saukville, Wisconsin, USA). Rhamnolipids have also been the target of investigation for a potential use in household detergents and cosmetics [Brown 1991, Klekner and Kosaric 1993]. Nitschke and Costa [Nitschke and Costa 2007] and Velikonja and Kosaric [Velikonja and Kosaric 1993] summarized potential applications of rhamnolipids in food. Rhamnolipids may be used to enhance stability and texture of different baked goods [Van Haesendonck and Vanzeveren 2006] or serve as a source of rhamnose for the synthesis of flavors [Trummler *et al.* 2003]. However, by now, none of the known biosurfactants have been approved as an additive for food. Microbial biosurfactants may potentially be used as active ingredients in pharmaceuticals (antimycotics, antibiotics) or for the anti-adhesive treatment of infusion sets. Considering the increasing amount of pathogens resistant to antibiotics, biosurfactants with antimicrobial activity (especially lipopeptides) may become more popular as drugs of

Table 3.2: Selected patented potential applications for rhamnolipids. Potential utilizations in different fields of application are presented along with chosen patents. Search for patents was conducted using *www.freepatentsonline.com* web service, accessed 02/2014 [Sumobrain-Solutions 2014].

Area of application	**Description**	**Patent no. (US)**
Bioremediation	Contaminated soil	5128262
Oil recovery	MEOR Additives	Appl. 20110067856 US 5866376
Pesticides	Biofungicide Pest control	US 5767090 Appl. US 20050266036
Detergents	Laundry detergent Surface cleaning	US 5520839 Appl. US 20080213194
Food additives	Bakery, dough texture Flavor (rhamnose synthesis)	Appl. US 20060233935 US 5550227
Medical sector	Autoimmune disease Wound healing	US 5466675 US 7262171
Cosmetics	Personal care	Appl. US 20080213194

last resort in the future [Landman *et al.* 2008, Seydlova and Svobodova 2008, Yuan and Tam 2008, Baltz *et al.* 2005, Eisenstein 2004]. An overview of patented potential applications for rhamnolipids is provided in Tab. 3.2, which demonstrates the high potential for rhamnolipids in different fields.

3.5 Rhamnolipid biosynthesis

The biosynthesis of rhamnolipids in *P. aeruginosa* is achieved by *de novo* synthesis of the precursors of the hydrophilic part, dTDP-L-rhamnose, and the hydrophobic part, 3-(3-hydroxyalkanoyloxy) alkanoic acid (HAA) [Hauser and Karnovsky 1957, Hauser and Karnovsky 1958, Burger *et al.* 1963]. The current understanding of rhamnolipid biosynthesis as well as relevant intermediates and byproducts is displayed in Fig. 3.2. The sugar moiety dTDP-L-rhamnose is synthesized from gluconeogenesis via *algC* and the *rmlBDAC* operon [Rahim *et al.* 2000]. The dependency of dTDP-L-rhamnose synthesis on *algC* demonstrates the interconnection of rhamnolipid biosynthesis and extracellular polysaccharide formation, since *algC* is also a key factor in alginate biosynthesis (Fig. 3.2). The hydrophobic moiety HAA is synthesized from β-hydroxyacyl-ACP via *rhlA*, which is initially obtained through fatty acid *de novo* synthesis linked to acyl carrier proteins (ACP).
The precursors dTDP-L-rhamnose and HAA are then linked by the rhamnosyltransferase RhlB yielding a mono-rhamnolipid molecule. A di-rhamnolipid may be formed

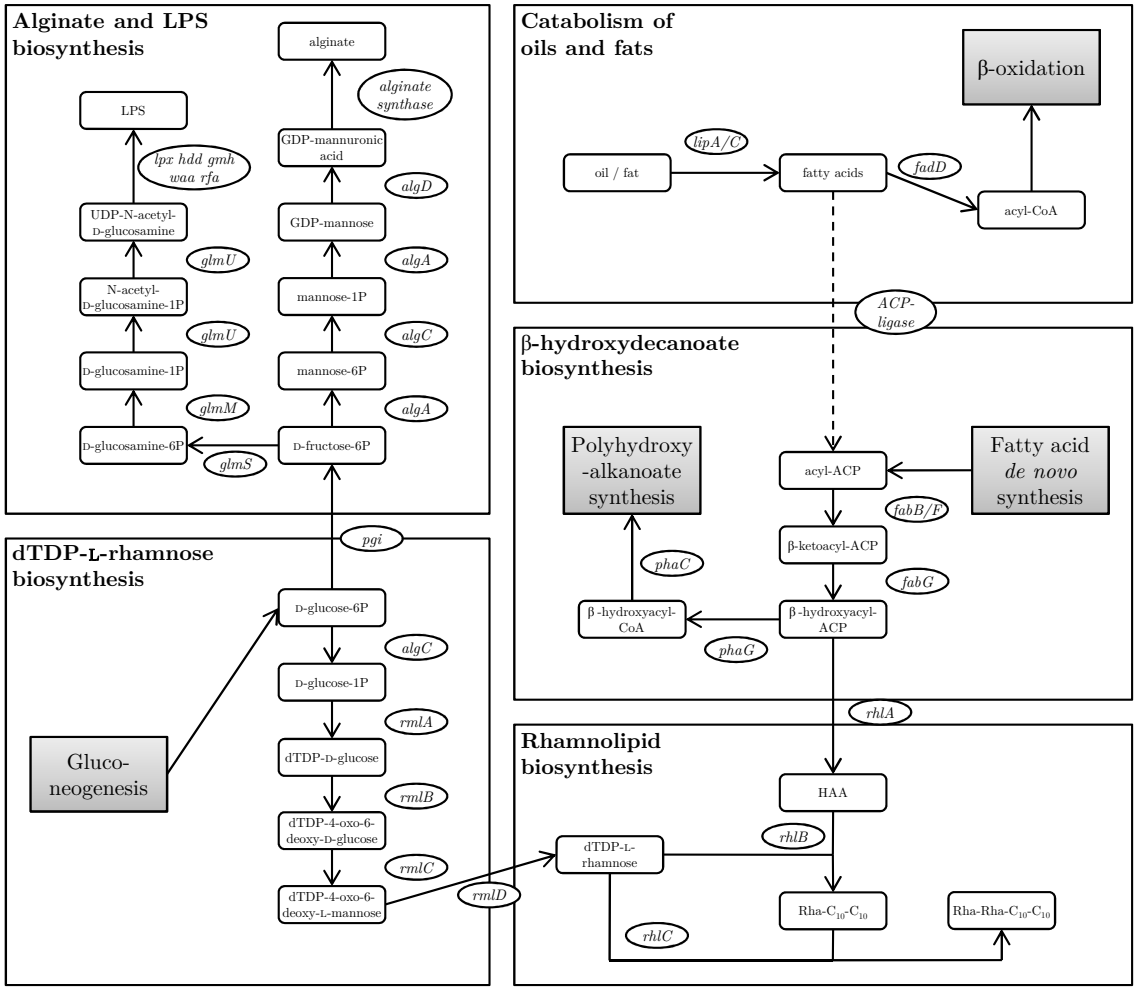

Figure 3.2: Schematic representation of the biosynthesis of rhamnolipids, rhamnolipid precursor molecules and potentially relevant byproducts associated with the production of rhamnolipids [Soberón-Chávez *et al.* 2005b]. Precursors, intermediates and products are represented by boxes. Arrows indicate enzymatic conversion, and respective genes are shown in ellipses. Abbreviations: HAA 3-(3-hydroxyalkanoyloxy)alkanoate; CoA coenzyme A; ACP acyl carrier protein.

from the mono-rhamnolipid and another dTDP-L-rhamnose by action of a second rhamnosyltransferase RhlC, which yields a di-rhamnolipid.

3.6 Control of rhamnolipid biosynthesis: a complex regulatory network

3.6.1 Quorum sensing

The term 'quorum sensing' refers to bacterial communication, which is mediated by small extracellular signaling molecules and a corresponding intracellular regulatory circuit. Quorum sensing was first described for *Vibrio fischeri* [Nealson and Hastings 1979], a gram-negative marine bacterium, which is responsible for luminescence in the light organs of certain marine fish, with which it

forms a symbiosis. Mechanisms required for luminescence in *V. fischeri* were found to be expressed at high cell densities only, conditions which can be typically found in light organs. Bacteria which communicate via quorum sensing secrete the signaling molecules to the surrounding medium.
These small signaling molecules are generally refered to as 'autoinducers' (AI), since they have the ability to have a positive effect on the expression of their corresponding synthetase, therefore inducing their own production. In gram-negative bacteria, two main categories of autoinducers have been identified, the so called autoinducers 1 (AI-1) homoserine lactones (HSL) and autoinducers 2 (AI-2) furanosyl borate diesters [Bassler *et al.* 1994]. Once a threshold has been reached, intracellular circuits induce the concerted expression of genes, such as genes responsible for the secretion of secondary metabolites, effect on swarming motility or the formation of extracellular matrix [Miller and Bassler 2001].
Quorum sensing in *Pseudomonas aeruginosa* is mediated by two HSL molecules, *N*-butyryl-homoserine lactone (C_4-HSL) and 3-oxo-dodecanoyl-homoserine lactone (3o-C_{12}-HSL). It affects the expression of more than 300 genes, which corresponds to approximately 6% of its genome, making quorum sensing on of the major effectors of gene expression on a cell level [Soberón-Chávez *et al.* 2005a]. Each autoinducer corresponds to an intracellular regulatory circuit, the *rhl* system (C_4-HSL) and the *las* system (3o-C_{12}-HSL), each with a receptor protein able to bind the AHL molecule (RhlR/LasR) and the corresponding autoinducer synthetase (RhlI/LasI) (Fig. 3.3).
Over the last years, the quorum sensing network as well as underlying regulatory mechanisms have been investigated in further detail, however, many aspects are not yet fully understood. Besides HSLs, another quorum sensing associated signaling system has been described in *P. aeruginosa*. This system is known as the Pseudomonas quinolone signal (PQS), which is mediated by 2-heptyl-3-hydroxy-4-quinolone [Pesci *et al.* 1999]. The PQS system has been increasingly in the focus of research in the recent past, however, the current understanding of its effect on the *rhl* and *las* system is still limited. Although the PQS system is linked to the HSL-based systems, the latter have been identified as the core of quorum sensing in *P. aeruginosa* [Williams and Camara 2009].

3.6.2 Regulation of rhamnolipid biosynthesis

The genes enconding for the RhlAB complex responsible for the formation of mono-rhamnolipid from its precursors (Fig. 3.2) are located on a single operon [Sullivan 1998]. Together with the gene for di-rhamnolipid synthesis, *rhlC*, the expression of *rhlAB* is under control of a complex cell-density dependent quorum sensing regulatory network. The complex of C_4-HSL bound to its soluble receptor,

RhlR, has been shown to be one of the major inducers and transcription factors for the *rhlAB* genes [Medina *et al.* 2003c].

In the past, several studies reported the induction of rhamnolipid formation to be mainly affected by environmental, nutritional and growth conditions, mediated by the sigma factors RpoN (σ^N) and RpoS (σ^S) [Medina *et al.* 2003a, Medina *et al.* 2003b, Rahim *et al.* 2001]. Even though the promoter region of *rhlR* contains a RpoN dependent site [Medina *et al.* 2003c], recent studies suggest that the availability of nitrogen in the culture broth may only play a secondary role regarding *rhlAB* expression.

Besides the complex and dynamic interactions of each partial system, other mechanisms have been identified which affect the quorum sensing system of gene expression, suggesting multiple hierarchic layers of control [Schuster and Greenberg 2006], each with its own dynamics.

In addition, several transcriptional and post-transcriptional mechanisms which affect the quorum sensing network in *P. aeruginosa* have been identified in the past. These include the regulatory proteins RsaL which is reported to be involved in quorum sensing homeostasis [Rampioni *et al.* 2006, Rampioni *et al.* 2007], or RsmA, a small RNA-binding protein which has a negative effect on quorum sensing as well as GacA, its antagonist [Heurlier *et al.* 2004]. Another multitarget repressor of quorum sensing activated genes, QscR, has been identified to act as a regulator homologue, however, with antagonistic mode of operation [Schuster and Greenberg 2006, Oinuma and Greenberg 2011].

In addition to these regulatory mechanisms, another layer of control over the quorum sensing system has been identified, which was termed 'quorum quenching'. Quorum quenching refers to the action of interfering with AHL signaling molecules and signal propagation, e.g., by cleavage of AHLs by acylases or lactonases [Hong *et al.* 2012, Lin *et al.* 2003, Sio *et al.* 2006], or by interfering with AHL receptor proteins [de Kievit and Iglewski 2000]. A total of 3 acylases able to degrade 3o-C_{12}-HSL have been identified in *P. aeruginosa*: HacB, QuiP and PvdQ [Wahjudi *et al.* 2011, Hong *et al.* 2012]. The activity of a putative C*4*-HSL specific acylase was suggested by experimental and simulation results to act as an antagonist of HSL-mediated signaling [Henkel *et al.* 2013], which is discussed in further detail in Chapter 4. PvdQ has also been shown to be involved in the regulation of iron uptake [Ochsner *et al.* 2002, Lamont and Martin 2003]. During cultivation on iron-limited media, the observed gene expression profile suggests a significant effect of iron on expression of *rhlAB* as well as several secondary regulatory genes [Schmidberger *et al.* 2014].

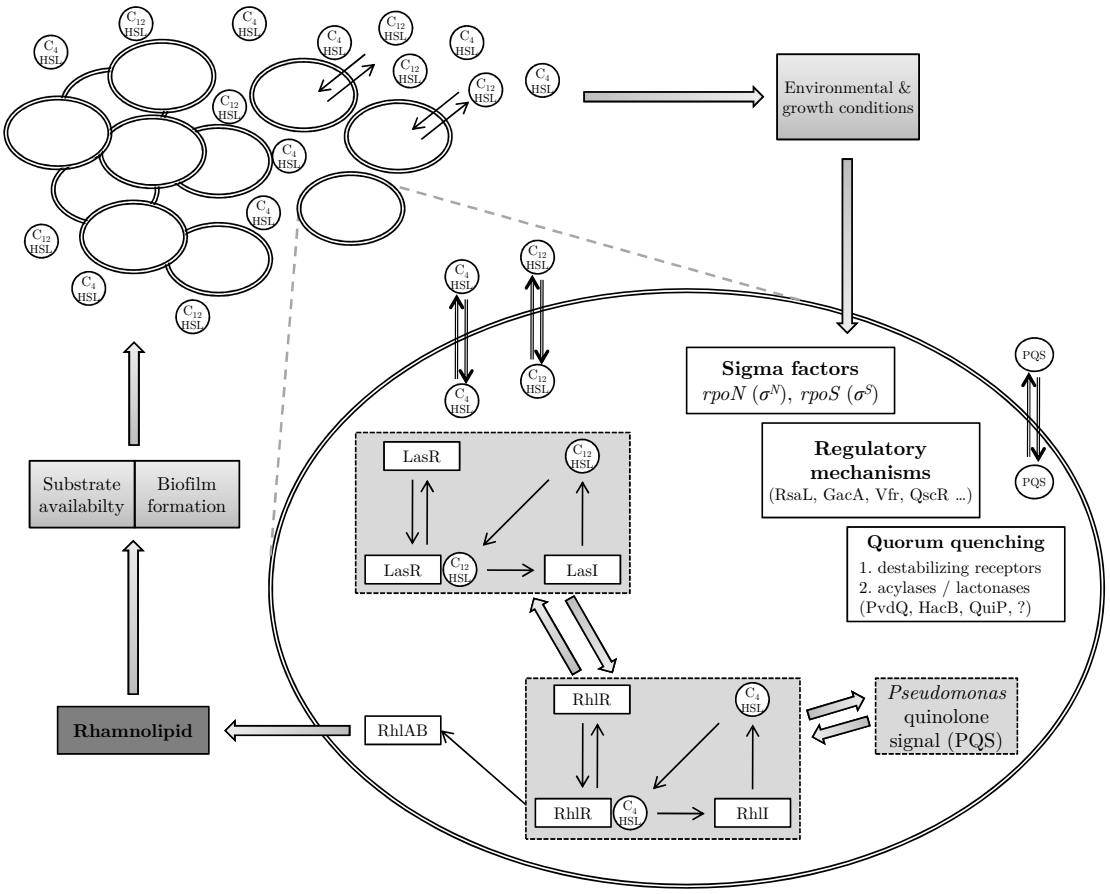

Figure 3.3: Simplified view on quorum sensing and other regulatory or metabolic mechanisms in *P. aeruginosa* involved in the regulation of rhamnolipid synthesis [Ochsner and Reiser 1995, Soberón-Chávez *et al.* 2005a].

3.7 Biotechnological production of rhamnolipids

There are several different microorganisms known to produce rhamnolipids, most of them belonging to the species *Pseudomonas aeruginosa*. However, by now, only a handful of species/strains are potentially relevant for industrial production processes, mainly due to vast differences in biosurfactant yields and maximum achievable concentrations. As a result, former industrial production processes for rhamnolipids (e.g. by Hoechst AG, Frankfurt-Hoechst, Germany) were carried out using *P. aeruginosa*. A maximum concentration of 112 g/L rhamnolipids has been reported in a fed-batch process on an industrial scale with soybean oil as a source of carbon [Giani *et al.* 1997]. However, in this patent held by former Hoechst AG (Frankfurt-Hoechst, Germany), critical details are missing, especially in terms of how the quantification of rhamnolipids has been performed. Therefore, up to today, these claims could not be verified. *P. aeruginosa* is well understood and relatively easy to cultivate. The synthesis of rhamnolipids by *P. aeruginosa* is well investigated, since they are key factors involved in virulence. In addition, the genome of the widely used strain PAO1 is fully sequenced and annotated. However, since *P. aeruginosa* is

opportunistically pathogen to humans (biosafety level S2) and therefore may pose a threat to immunodeficient persons, this bacterium would generally not be the first choice if it comes to large-scale industrial production, although this should be of no relevance for the purified product.

Many research groups have dedicated their work to finding alternative strains for the production of rhamnolipids. There are two main strategies which are investigated to bypass this problem: the production of rhamnolipids in non-pathogenic bacteria, by searching for alternative strains, and the heterologous production of rhamnolipids in non-pathogenic strains. Several attempts have been made for the heterologous production of rhamnolipids. In the past, rhamnolipid production in several host strains was compared by introducing the *rhlAB* operon (rhamnosyltransferase) [Ochsner *et al.* 1995]. Among the investigated species were *P. fluorescens*, *P. putida*, *E. coli* and *P. oleovorans*, with a highest rhamnolipid concentration of 60 mg/L reported for *P. putida* [Ochsner *et al.* 1995]. More recent work could demonstrate that, the availability of dTDP-L-rhamnose is restricting for the production of rhamnolipids in *E. coli* [Cabrera-Valladares *et al.* 2006]. However, studies on the heterologous production of rhamnolipids in *P. putida* exist, where it could be shown that rhamnolipid concentrations can be raised closer to levels observable for *P. aeruginosa*, with a maximum concentration of 7.2 g/L [Cha *et al.* 2008]. Even though the production of rhamnolipids in heterologous hosts has been quantified, only little is known on economics for alternative non-*P. aeruginosa* strains, in terms of maximum concentrations and yield. Alternative, non-pathogenic rhamnolipid-producing strains identified so far mainly belong to other species of *Pseudomonas* or *Burkholderia*. Even though much work has been performed on alternative strains in the last years, yields and maximum rhamnolipid concentrations known from wild type *P. aeruginosa* could by far not be reached in non-*P.aeruginosa* strains. An overview of different processes for rhamnolipid production along with relevant characteristics and parameters to determine efficiency is provided in Tab. 3.3. The most important cultivation strategies applied during rhamnolipid production can be summarized as [Lang and Wullbrandt 1999]:

- (Fed-)batch cultivations under growth-limiting conditions
- Continuous cultivation and production with free cells
- Semicontinuous production with immobilized cells (without nitrogen)
- Batch cultivations under resting cell conditions

Table 3.3: Biotechnological production of rhamnolipids: strains, substrates and relevant calculated characteristics for selected processes.

Substrate	**Strain/Organism**	$c_{\mathrm{RL\ max}}$ [g/L]	$t_{\mathrm{RL\ max}}$ [h]	$P_{\mathrm{v\ max}}$ [g_{RL}/(L·h)]	$Y_{\mathrm{P\|S}}$ [g_{RL}/g_S]	**Reference**
batch processes						
Sunflower oil	*P. aeruginosa* PAO1	39.0	90	0.43	0.23	[Müller *et al.* 2010]
Corn oil	*P. aeruginosa* UI29791	46	192	0.24	0.61	[Linhardt *et al.* 1989]
Soybean oil	*P. aeruginosa* DSM7107 DSM7108	78	167	0.47	0.62	[Giani *et al.* 1997]
Glycerol	*P. aeruginosa* DSM2874	8.5	168	0.05	0.21	[Syldatk *et al.* 1985a]
Glucose (immobilized cells)	*P. aeruginosa* DSM2874	4.5	168	0.03	0.11	[Syldatk *et al.* 1985b]
Glucose	*P. aeruginosa* S2	5.3	144	0.04	0.13	[Chen *et al.* 2007b]
fed-batch processes						
Soybean oil	*P. aeruginosa* DSM7108	95	264	0.44	0.69	[Giani *et al.* 1997]
Glucose	*P. aeruginosa* S2	6.1	195	0.03	0.15	[Chen *et al.* 2007b]
Oleic acid (resting cells)	*P. aeruginosa* DSM2874	45	321	0.14	0.23	[Trummler *et al.* 2003]
continuous processes						
Corn oil	*P. aeruginosa* DSM2659	18	D = 0.10	0.69	0.46	[Chen *et al.* 2007a]
Glucose	*P. aeruginosa* DSM2659	0.12	D = 0.14	0.13	0.05	[Chen *et al.* 2007a]

3.7.1 Substrates for the production of rhamnolipids

While there is a broad spectrum of substrates which have been employed for the production of rhamnolipids, ranging from petrochemical derived substances to substrates of natural origin, the most commonly used substrates are plant oils, sugars and glycerol. It has been shown that different waste substrates may also be used for the production of rhamnolipids, like fatty acids [Abalos *et al.* 2001], waste frying oil [Haba *et al.* 2000], olive oil production effluents [Mercade *et al.* 1993], whey wastes [Dubey and Juwarkar 2001] and soap stock [Benincasa *et al.* 2002]. In the future, these waste substrates may become more important, since they are usually less expensive and do not directly compete with food. Additionally, using waste substrates for biotechnological processes may also prove to be beneficial for the environment, since it may contribute to reducing the overall amount of waste generated.

Glycerol, as part of lipids, is very abundant in nature and many different organisms utilize glycerol as a carbon source. Glycerol is also a widely spread substrate used for production of rhamnolipids (e.g. [Syldatk *et al.* 1985a, Chen *et al.* 2007b]). The main sources of glycerol can be summarized as follows: glycerol can be chemically obtained from renewable resources, e.g. by basic hydrolysis (NaOH or KOH) of triglycerides of animal fat or vegetable oil. Glycerol is also a by-product of biodiesel production which is obtained by transesterification of vegetable oils (usually rapeseed oil or soybean oil) using methanol. Petrochemically, glycerol can also be produced by utilizing propene obtained from fossil sources (petroleum, natural gas, coal). Crude glycerol from biodiesel manufacturing has been successfully used as a substrate for the production of rhamnolipids [Walter *et al.* 2010, de Sousa *et al.* 2011]. By using glycerol for the production of rhamnolipids in batch operation, usually final rhamnolipid concentrations between 1.0 - 8.5 g/L can be obtained [Syldatk *et al.* 1985a, Santa Anna *et al.* 2002]. However, the substrate-to-product conversion rate is relatively low ($Y_{P|S}$ = 0.1 - 0.15), and the calculation of a maximum theoretical yield (Tab. 3.4) reveals that there is room for significant optimization.

Sugars, such as glucose have been used in many cases as a substrate for the production of rhamnolipids [Syldatk *et al.* 1985b, Makkar *et al.* 2011]. The food-processing industry also produces a variety of sugar-containing byproducts and waste-streams, most importantly generated by sugar processing plants and the dairy industry. However, since only few bacteria are able to metabolize galactose from the disaccharide lactose, the full potential may not be achievable without engineered strains. Wild type strains of *P. aeruginosa* are generally not able to utilize galactose as a substrate for growth (Tab. A.1 & Fig. A.1). The sugar and starch processing industry produces large amounts of carbohydrate-rich wastewater which may poten-

tially be utilized as a substrate for fermentation, which has been demonstrated for the industrial production of enzymes [Makkar and Cameotra 1997]. It is evident that these food and agro-industrial wastestreams could all serve as potential feedstocks for the production of rhamnolipids. Besides the fact that the application of sugar containing substrates (e.g. sucrose) for biotechnological processes results in a direct competition with food, pure sugar (e.g. glucose) is also comparably expensive (Tab. 3.4). Different sugars can be found in many industrial waste streams, however, many are not utilizable for biotechnological processes without pretreatment, and the concentration in the waste streams is often very low. This, in turn, results in higher costs for purification and/or transportation of the potential feedstocks. With glucose, final rhamnolipid concentrations (batch processes) of up to 4.5 g/L [Syldatk *et al.* 1985a] are reported. The average substrate-to-product conversion is lower than for glycerol ($Y_{P|S}$ = 0.06 - 0.11 g/g). However, the maximum theoretical yield (0.52 g/g, Tab. 3.4) reveals, that there is room for significant optimization.

Many different vegetable oils have been used in the past to produce rhamnolipids, e.g. sunflower, rapeseed, palm, fish, coconut, soybean and olive oil. The total annual production of oils and fats equals 3 Mt, 3/4 of which comes from plants and seeds [Nitschke *et al.* 2005]. Unrefined oil intended for use as an ingredient for food or to prepare food (e.g. deep-frying) typically undergoes a series of refinement steps to remove unwanted byproducts related to the oil extraction. These byproducts that can be found in crude oil are typically free fatty acids, pigments, sterols, hydrocarbons, protein fragments and other extracted material which contribute to its viscous and sticky consistency. These substances are removed mainly to make the oil longer-lasting and remove unwanted odor and taste. The recovered material during this process of refinement is referred to as soap stock. Today, the main applications for waste soap-stock are animal feed and production of soap. Soap-stock can serve as a cheap feedstock for biotechnological processes, since its average price is as low as about 10% of the price for refined oil [Nitschke *et al.* 2005]. It has been demonstrated that rhamnolipids are produced by *P. aeruginosa* while growing on sunflower oil soap stock as a sole carbon source, with a final rhamnolipid concentration of 15.9 g/L [Benincasa *et al.* 2002]. Furthermore soap-stocks from different vegetable oil industries (e.g. soybean, cottonseed, corn) have been investigated in the past regarding their potential to serve as a low-cost feedstock for the production of rhamnolipids, with a final concentration of 11.7 g/L and a yield of $Y_{X|S}$ = 0.75 g/g [Nitschke *et al.* 2010]. These findings led to the conclusion, that soap stock from different industries may be a suitable substrate for the production of rhamnolipids for high-value application (e.g. pharmaceuticals) [Zhu *et al.* 2007]. Large amounts of waste vegetable oils are produced mainly in the food industry (e.g. deep frying in potato/vegetable processing) and restaurants. It has been de-

monstrated that waste frying oil can be used for the production of rhamnolipids by *P. aeruginosa* [Haba *et al.* 2000]. In a different study, it was shown that by using waste soybean oil, similar rhamnolipid yields than with unused oil can be achieved [De Lima *et al.* 2007]. By now, plant and vegetable oils are the best substrate for the induction of rhamnolipid production with *P. aeruginosa*, and final concentrations and substrate-to-product conversion yields are generally higher than for non-hydrophobic substrates. However, most of the oils are in direct competition with food, and compared to other substrates, prices for plant oils are approximately in the same range. Fatty acids, on the other hand, may be obtained for roughly 1/3rd of the price (Tab. 3.4) in lower purities, usually referred to as rubber grade.

3.7.2 Comparison of substrates and metabolic yields

Theoretical maximum substrate conversion rates were calculated for the most important renewable substrates for rhamnolipid production based on ATP energy balancing applied to *P. aeruginosa* PAO1 metabolic pathways and are shown in Tab. 3.4 [Kanehisa and Goto 2000, Winsor *et al.* 2009] (details on calculation of ATP balancing can be found in Tab. A.1 - A.6 in the appendix). The energy balances for the substrate conversion yields are based on the assumption that substrate consumption will take place using the most favorable metabolic route, as depicted in Fig. A.1 (appendix). For maximum yields, it was assumed that the producing cells spend all the biochemical energy for the product formation [Erickson 1981, Andrews 1989]. When comparing observed substrate-to-product conversion rates to theoretical yields, it becomes evident that most processes run at about 20% efficiency and therefore, there is still a significant potential for optimization (Tab. 3.4). Furthermore, the price range between each individual feedstock is large, with glucose being approx. 3 times more expensive than rubber grade fatty acids. Compared with current market prices of 1–3 USD/kg of alkylpolyglycosides (APG), which are chemically synthesized from vegetable oil or sugars, it can be concluded that an optimization of the processes for rhamnolipid production will be necessary before it can compete with other surfactants from an economical perspective ([Alibaba Group 2014], accessed 02/2014). Another characteristic which varies between the different substrates is the space-time yield, presented as the specific volumetric productivity P_v in Tab. 3.3 & Tab. 3.4, which is several times higher when using a hydrophobic source of carbon, e.g. plant oils. Potential explanations and a hypothesis for this phenomenon, which is persitent throughout decades of rhamnolipid research, are discussed in further detail in Chapter 4.

Table 3.4: Experimental (Tab. 3.3) and maximum theoretical yields $Y_{P|S}$ and optimization potential for different substrates used for the production of rhamnolipids. Prices taken from [IndexMundi Portal 2014], accessed 02/2014. Details on the calculation of theoretical yields can be found in the appendix (Fig. A.1 and Tab. A.1 - A.6)

Substrate	**average** $Y_{P\|S}$ [g_{RL}/g_S]	**theoretical** $Y_{P\|S}$ [g_{RL}/g_S]	**Substrate costs [€/t]**	P_V [$g_{RL}/(L \cdot h)$]
Glucose	0.05 - 0.15	0.52	350 - 550	0.03 - 0.04
Glycerol	0.21	0.59	250 - 600	0.05
Triacylglycerides	0.20 - 0.45	1.25	550 - 700 (sunflower oil)	0.24 - 0.47
Fatty acids	0.23	1.26	300 - 500 (stearic acid)	0.14

References for Chapter 3

[Abalos *et al.* 2001] Abalos, A., Pinazo, A., Infante, M. R., Casals, M., Garcia, F., and Manresa, A. (2001). Physicochemical and antimicrobial properties of new rhamnolipids produced by *Pseudomonas aeruginosa* AT10 from soybean oil refinery wastes. *Langmuir*, 17(5), pp. 1367–1371.

[Abdel-Mawgoud *et al.* 2010] Abdel-Mawgoud, A. M., Lépine, F., and Déziel, E. (2010). Rhamnolipids: Diversity of structures, microbial origins, and roles. *Applied Microbiology and Biotechnology,*, 86(5), pp. 1323–1336.

[Alibaba Group 2014] Alibaba Group (2014). Alibaba global retail and wholesale trading platform. Available online under http://www.alibaba.com/, *accessed 02/2014*.

[Andrä *et al.* 2006] Andrä, J., Rademann, J., Howe, J., Koch, M. H. J., Heine, H., Zähringer, U., and Brandenburg, K. (2006). Endotoxin-like properties of a rhamnolipid exotoxin from *Burkholderia* (*Pseudomonas*) *plantarii*: Immune cell stimulation and biophysical characterization. *Biological Chemistry*, 387(3), pp. 301–310.

[Andrews 1989] Andrews, G. (1989). Estimating cell and product yields. *Biotechnology and Bioengineering*, 33(3), pp. 256–265.

[Baltz *et al.* 2005] Baltz, R. H., Miao, V., and Wrigley, S. K. (2005). Natural products to drugs: Daptomycin and related lipopeptide antibiotics. *Natural Product Reports*, 22(6), pp. 717–741.

[Banat 1995] Banat, I. M. (1995). Biosurfactants production and possible uses in microbial enhanced oil-recovery and oil pollution remediation - a review. *Bioresource Technology*, 51(1), pp. 1–12.

[Banat *et al.* 2000] Banat, I. M., Makkar, R. S., and Cameotra, S. S. (2000). Potential commercial applications of microbial surfactants. *Applied Microbiology and Biotechnology*, 53(5), pp. 495–508.

[Bassler *et al.* 1994] Bassler, B. L., Wright, M., and Silverman, M. (1994). Multiple signalling systems controlling expression of luminescence in *Vibrio harveyi*: sequence and function of genes encoding a second sensory pathway. *Molecular Microbiology*, 13(2), pp. 273–286.

[Benincasa *et al.* 2002] Benincasa, M., Contiero, J., Manresa, M. A., and Moraes, I. O. (2002). Rhamnolipid production by *Pseudomonas aeruginosa* LBI growing on soapstock as the sole carbon source. *Journal of Food Engineering*, 54(4), pp. 283–288.

[Bergström *et al.* 1946] Bergström, S., Theorell, H., and Davide, H. (1946). On a metabolic product of *Ps. pyocyanea*, pyolipic acid, active against *Mycobact. tuberculosis*. *Arkiv för Kemi, Mineralogi och Geologi*, 23 A(13), pp. 1–12.

[Brown 1991] Brown, M. J. (1991). Biosurfactants for cosmetic applications. *International Journal of Cosmetic Science*, 13(2), pp. 61–64.

[Burger *et al.* 1963] Burger, M., Glaser, L., and Burton, R. M. (1963). Enzymatic synthesis of a rhamnolipid by extracts of *Pseudomonas aeruginosa*. *Federation Proceedings*, 21(2), pp. 82–83.

[Cabrera-Valladares *et al.* 2006] Cabrera-Valladares, N., Richardson, A. P., Olvera, C., Trevino, L. G., Déziel, E., Lépine, F., and Soberón-Chávez, G. (2006). Monorhamnolipids and 3-(3-hydroxyalkanoyloxy)alkanoic acids (HAAs) production using *Escherichia coli* as a heterologous host. *Applied Microbiology and Biotechnology*, 73(1), pp. 187–194.

[Cha *et al.* 2008] Cha, M., Lee, N., Kim, M., and Lee, S. (2008). Heterologous production of *Pseudomonas aeruginosa* EMS1 biosurfactant in *Pseudomonas putida*. *Bioresource Technology*, 99(7), pp. 2192–2199.

[Chen *et al.* 2007a] Chen, S. Y., Lu, W. B., Wei, Y. H., Chen, W. M., and Chang, J. S. (2007a). Improved production of biosurfactant with newly isolated *Pseudomonas aeruginosa* S2. *Biotechnology Progress*, 23(3), pp. 661–666.

[Chen *et al.* 2007b] Chen, S. Y., Wei, Y. H., and Chang, J. S. (2007b). Repeated pH-stat fed-batch fermentation for rhamnolipid production with indigenous *Pseudomonas aeruginosa* S2. *Applied Microbiology and Biotechnology*, 76(1), pp. 67–74.

[De Lima *et al.* 2007] De Lima, C. J. B., Franca, F. P., Servulo, E. F. C., Resende, A. A., and Cardoso, V. L. (2007). Enhancement of rhamnolipid production in residual soybean oil by an isolated strain of *Pseudomonas aeruginosa*. *Applied Biochemistry and Biotechnology*, 137, pp. 463–470.

[Desai and Banat 1997] Desai, J. D. and Banat, I. M. (1997). Microbial production of surfactants and their commercial potential. *Microbiology and Molecular Biology Reviews*, 61(1), pp. 47–64.

[Develter *et al.* 2007] Develter, D., Walcarius, B., and Fleurackers, S. (2007). Biosurfactants in cleaning and cosmetics. Third International Conference on Renewable Resources & Biorefineries (RRB), June 4 - 6, 2007, Ghent, Belgium. Available online under http://www.rrbconference.com/rrb3-2007.

[Déziel *et al.* 2000] Déziel, E., Lépine, F., Milot, S., and Villemur, R. (2000). Mass spectrometry monitoring of rhamnolipids from a growing culture of *Pseudomonas aeruginosa* strain 57RP. *Biochimica et Biophysica Acta - Molecular and Cell Biology of Lipids*, 1485(2-3), pp. 145–152.

[Déziel *et al.* 2003] Déziel, E., Lépine, F., Milot, S., and Villemur, R. (2003). RhlA is required for the production of a novel biosurfactant promoting swarming motility in *Pseudomonas aeruginosa*: 3-(3-hydroxyalkanoyloxy)alkanoic acids (HAAs), the precursors of rhamnolipids. *Microbiology*, 149, pp. 2005–2013.

[Dubeau *et al.* 2009] Dubeau, D., Déziel, E., Woods, D. E., and Lépine, F. (2009). *Burkholderia thailandensis* harbors two identical *rhl* gene clusters responsible for the biosynthesis of rhamnolipids. *BMC Microbiology*, 9(263).

[Dubey and Juwarkar 2001] Dubey, K. and Juwarkar, A. (2001). Distillery and curd whey wastes as viable alternative sources for biosurfactant production. *World Journal of Microbiology & Biotechnology*, 17(1), pp. 61–69.

[Edwards and Hayashi 1965] Edwards, J. R. and Hayashi, J. A. (1965). Structure of a rhamnolipid from *Pseudomonas aeruginosa*. *Archives of Biochemistry and Biophysics*, 111(2), pp. 415–421.

[Eisenstein 2004] Eisenstein, B. I. (2004). Lipopeptides, focusing on daptomycin, for the treatment of gram-positive infections. *Expert Opinion on Investigational Drugs*, 13(9), pp. 1159–1169.

[Erickson 1981] Erickson, L. E. (1981). Energetic yields associated with hydrocarbon fermentations. *Biotechnology and Bioengineering*, 23(4), pp. 793–803.

[Gartshore *et al.* 2000] Gartshore, J., Lim, Y. C., and Cooper, D. G. (2000). Quantitative analysis of biosurfactants using Fourier Transform Infrared (FT-IR) spectroscopy. *Biotechnology Letters*, 22(2), pp. 169–172.

[Giani *et al.* 1997] Giani, C., Wullbrandt, D., Rothert, R., and Meiwes, J. (1997). *Pseudomonas aeruginosa* and its use in a process for the biotechnological preparation of L-Rhamnose. US patent 5658793, Hoechst Aktiengesellschaft, Frankfurt am Main, Germany.

[Haba *et al.* 2000] Haba, E., Espuny, M. J., Busquets, M., and Manresa, A. (2000). Screening and production of rhamnolipids by *Pseudomonas aeruginosa* 47T2 NCIB 40044 from waste frying oils. *Journal of Applied Microbiology*, 88, pp. 379–387.

[Hauser and Karnovsky 1954] Hauser, G. and Karnovsky, M. L. (1954). Studies on the production of glycolipide by *Pseudomonas aeruginosa*. *Journal of Bacteriology*, 68(6), pp. 645–654.

[Hauser and Karnovsky 1957] Hauser, G. and Karnovsky, M. L. (1957). Rhamnose and rhamnolipide biosynthesis by *Pseudomonas aeruginosa*. *Journal of Biological Chemistry*, 224(1), pp. 91–105.

[Hauser and Karnovsky 1958] Hauser, G. and Karnovsky, M. L. (1958). Studies on the biosynthesis of L-rhamnose. *Journal of Biological Chemistry*, 233(2), pp. 287–291.

[Henkel *et al.* 2013] Henkel, M., Schmidberger, A., Kühnert, C., Beuker, J., Bernard, T., Schwartz, T., Syldatk, C., and Hausmann, R. (2013). Kinetic modeling of the time course of *N*-butyryl-homoserine lactone concentration during batch cultivations of *Pseudomonas aeruginosa* PAO1. *Applied Microbiology and Biotechnology*, 97(17), pp. 7607–16.

[Heurlier *et al.* 2004] Heurlier, K., Williams, F., Heeb, S., Dormond, C., Pessi, G., Singer, D., Camara, M., Williams, P., and Haas, D. (2004). Positive control of swarming, rhamnolipid synthesis, and lipase production by the posttranscriptional RsmA/RsmZ system in *Pseudomonas aeruginosa* PAO1. *Journal of Bacteriology*, 186(10), pp. 2936–45.

[Heyd *et al.* 2008] Heyd, M., Kohnert, A., Tan, T. H., Nusser, M., Kirschhofer, F., Brenner-Weiss, G., Franzreb, M., and Berensmeier, S. (2008). Development and trends of biosurfactant analysis and purification using rhamnolipids as an example. *Analytical and Bioanalytical Chemistry*, 391(5), pp. 1579–1590.

[Hong *et al.* 2012] Hong, K. W., Koh, C. L., Sam, C. K., Yin, W. F., and Chan, K. G. (2012). Quorum quenching revisited - from signal decays to signalling confusion. *Sensors*, 12(4), pp. 4661–96.

[Hörmann *et al.* 2010] Hörmann, B., Müller, M. M., Syldatk, C., and Hausmann, R. (2010). Rhamnolipid production by *Burkholderia plantarii* DSM 9509(T). *European Journal of Lipid Science and Technology*, 112(6), pp. 674–680.

[IndexMundi Portal 2014] IndexMundi Portal (2014). Trade Statistics and Commodities Data. Available online under http://www.indexmundi.com/, *accessed 02/2014*.

[Jarvis and Johnson 1949] Jarvis, F. G. and Johnson, M. J. (1949). A glyco-lipide produced by *Pseudomonas aeruginosa*. *Journal of the American Chemical Society*, 71, pp. 4124–4126.

[Kanehisa and Goto 2000] Kanehisa, M. and Goto, S. (2000). KEGG: Kyoto Encyclopedia of Genes and Genomes. *Nucleic Acids Research*, 28(1), pp. 27–30.

[de Kievit and Iglewski 2000] de Kievit, T. R. and Iglewski, B. H. (2000). Bacterial quorum sensing in pathogenic relationships. *Infection and Immunity*, 68(9), pp. 4839–49.

[Kitamoto *et al.* 2002] Kitamoto, D., Isoda, H., and Nakahara, T. (2002). Functions and potential applications of glycolipid biosurfactants - from energy-saving materials to gene delivery carriers. *Journal of Bioscience and Bioengineering*, 94(3), pp. 187–201.

[Klekner and Kosaric 1993] Klekner, V. and Kosaric, N. (1993). Biosurfactants for cosmetics. In: Kosaric, N. (Ed.): *Biosurfactants: production - properties - applications*, Surfactant Science Series, pp. 373–390. New York: Marcel Dekker Inc.

[Kosaric 1992] Kosaric, N. (1992). Biosurfactants in industry. *Pure And Applied Chemistry*, 64(11), pp. 1731–1737.

[Lamont and Martin 2003] Lamont, I. L. and Martin, L. W. (2003). Identification and characterization of novel pyoverdine synthesis genes in *Pseudomonas aeruginosa*. *Microbiology*, 149(Pt 4), pp. 833–42.

[Landman *et al.* 2008] Landman, D., Georgescu, C., Martin, D. A., and Quale, J. (2008). Polymyxins revisited. *Clinical Microbiology Reviews*, 21(3), pp. 449–465.

[Lang 2002] Lang, S. (2002). Biological amphiphiles (microbial biosurfactants). *Current Opinion in Colloid & Interface Science*, 7(1-2), pp. 12–20.

[Lang and Trowitzsch-Kienast 2002] Lang, S. and Trowitzsch-Kienast, W. (2002). *Biotenside*. Stuttgart, Leipzig, Wiesbaden: Teubner.

[Lang and Wullbrandt 1999] Lang, S. and Wullbrandt, D. (1999). Rhamnose lipids - biosynthesis, microbial production and application potential. *Applied Microbiology and Biotechnology*, 51(1), pp. 22–32.

[Lin *et al.* 2003] Lin, Y. H., Xu, J. L., Hu, J., Wang, L. H., Ong, S. L., Leadbetter, J. R., and Zhang, L. H. (2003). Acyl-homoserine lactone acylase from *Ralstonia* strain XJ12B represents a novel and potent class of quorum-quenching enzymes. *Molecular Microbiology*, 47(3), pp. 849–60.

[Linhardt *et al.* 1989] Linhardt, R., Bakhit, R., Daniels, L., Mayerl, F., and Pickenhagen, W. (1989). Microbially produced rhamnolipid as a source of rhamnose. *Biotechnology and Bioengineering*, 33, pp. 365–368.

[Makkar and Cameotra 1997] Makkar, R. S. and Cameotra, S. S. (1997). Utilization of molasses for biosurfactant production by two *Bacillus* strains at thermophilic conditions. *Journal Of The American Oil Chemists Society*, 74(7), pp. 887–889.

[Makkar and Cameotra 2002] Makkar, R. S. and Cameotra, S. S. (2002). An update on the use of unconventional substrates for biosurfactant production and their new applications. *Applied Microbiology and Biotechnology*, 58(4), pp. 428–434.

[Makkar *et al.* 2011] Makkar, R. S., Cameotra, S. S., and Banat, I. M. (2011). Advances in utilization of renewable substrates for biosurfactant production. *AMB Express*, 1(5).

[Mata-Sandoval *et al.* 1999] Mata-Sandoval, J., Karns, J., and Torrents, A. (1999). High-performance liquid chromatography method for the characterization of rhamnolipid mixtures produced by *Pseudomonas aeruginosa* UG2 on corn oil. *Journal of Chromatography A*, 864, pp. 211 – 220.

[Medina *et al.* 2003a] Medina, G., Juarez, K., Diaz, R., and Soberon-Chavez, G. (2003a). Transcriptional regulation of *Pseudomonas aeruginosa* rhlR, encoding a quorum-sensing regulatory protein. *Microbiology*, 149(11), pp. 3073–81.

[Medina *et al.* 2003b] Medina, G., Juarez, K., and Soberon-Chavez, G. (2003b). The *Pseudomonas aeruginosa rhlAB* operon is not expressed during the logarithmic phase of growth even in the presence of its activator RhlR and the autoinducer *N*-butyryl-homoserine lactone. *Journal of Bacteriology*, 185(1), pp. 377–80.

[Medina *et al.* 2003c] Medina, G., Juarez, K., Valderrama, B., and Soberon-Chavez, G. (2003c). Mechanism of *Pseudomonas aeruginosa* RhlR transcriptional regulation of the *rhlAB* promoter. *Journal of Bacteriology*, 185(20), pp. 5976–83.

[Mercade *et al.* 1993] Mercade, M. E., Manresa, M. A., Robert, M., Espuny, M. J., Deandres, C., and Guinea, J. (1993). Olive oil mill effluent (OOME) - New substrate for biosurfactant production. *Bioresource Technology*, 43(1), pp. 1–6.

[Müller *et al.* 2011] Müller, M., Hörmann, B., Kugel, M., Syldatk, C., and Hausmann, R. (2011). Evaluation of rhamnolipid production capacity of *Pseudomonas aeruginosa* PAO1 in comparison to the rhamnolipid over-producer strains DSM 7108 and DSM 2874. *Applied Microbiology and Biotechnology*, 89, pp. 585–592.

[Müller *et al.* 2010] Müller, M., Hörmann, B., Syldatk, C., and Hausmann, R. (2010). *Pseudomonas aeruginosa* PAO1 as a model for rhamnolipid production in bioreactor systems. *Applied Microbiology and Biotechnology*, 87(1), pp. 167–174.

[Mulligan 2005] Mulligan, C. N. (2005). Environmental applications for biosurfactants. *Environmental Pollution*, 133(2), pp. 183–198.

[Mulligan and Gibbs 1993] Mulligan, C. N. and Gibbs, B. F. (1993). Factors influencing the economics of biosurfactants. In: Kosaric, N. (Ed.): *Biosurfactants: production - properties - applications*, Surfactant Science Series, pp. 329 – 371. New York: Marcel Dekker Inc.

[Nealson and Hastings 1979] Nealson, K. H. and Hastings, J. W. (1979). Bacterial bioluminescence: its control and ecological significance. *Microbiological Reviews*, 43(4), pp. 496–518.

[Nitschke and Costa 2007] Nitschke, M. and Costa, S. G. V. A. O. (2007). Biosurfactants in food industry. *Trends in Food Science & Technology*, 18(5), pp. 252–259.

[Nitschke *et al.* 2010] Nitschke, M., Costa, S. G. V. A. O., and Contiero, J. (2010). Structure and applications of a rhamnolipid surfactant produced in soybean oil waste. *Applied Biochemistry and Biotechnology*, 160(7), pp. 2066–2074.

[Nitschke *et al.* 2005] Nitschke, M., Costa, S. G. V. A. O., Haddad, R., Goncalves, L. A. G., Eberlin, M. N., and Contiero, J. (2005). Oil wastes as unconventional substrates for rhamnolipid biosurfactant production by *Pseudomonas aeruginosa* LBI. *Biotechnology Progress*, 21(5), pp. 1562–1566.

[Ochsner *et al.* 1994] Ochsner, U. A., Fiechter, A., and Reiser, J. (1994). Isolation, characterization, and expression in Escherichia coli of the *Pseudomonas aeruginosa rhlAB* genes encoding a rhamnosyltransferase involved in rhamnolipid biosurfactant synthesis. *Journal of Biological Chemistry*, 269(0), pp. 1–9.

[Ochsner and Reiser 1995] Ochsner, U. A. and Reiser, J. (1995). Autoinducer-mediated regulation of rhamnolipid biosurfactant synthesis in *Pseudomonas aeruginosa*. *Proceedings of the National Academy of Sciences USA*, 92, pp. 6424–6428.

[Ochsner *et al.* 1995] Ochsner, U. A., Reiser, J., Fiechter, A., and Witholt, B. (1995). Production of *Pseudomonas aeruginosa* rhamnolipid biosurfactants in heterologous hosts. *Applied and Environmental Microbiology*, 61(9), pp. 3503–3506.

[Ochsner *et al.* 2002] Ochsner, U. A., Wilderman, P. J., Vasil, A. I., and Vasil, M. L. (2002). GeneChip expression analysis of the iron starvation response in *Pseudomonas aeruginosa*: identification of novel pyoverdine biosynthesis genes. *Molecular Microbiology*, 45(5), pp. 1277–87.

[Oinuma and Greenberg 2011] Oinuma, K. and Greenberg, E. P. (2011). Acyl-homoserine lactone binding to and stability of the orphan *Pseudomonas aeruginosa* quorum-sensing signal receptor QscR. *Journal of Bacteriology*, 193(2), pp. 421–428.

[Oliveira *et al.* 2008] Oliveira, F. J. S., Vazquez, L., de Campos, N. P., and Franca, F. P. (2008). Production of rhamnolipids by a *Pseudomonas alcaligenes* strain. *Process Biochemistry*, 44(4), pp. 383–389.

[Paria 2008] Paria, S. (2008). Surfactant-enhanced remediation of organic contaminated soil and water. *Advances in Colloid and Interface Science*, 138(1), pp. 24–58.

[Pearson *et al.* 1997] Pearson, J. P., Pesci, E. C., and Iglewski, B. H. (1997). Roles of *Pseudomonas aeruginosa las* and *rhl* quorum-sensing systems in control of elastase and rhamnolipid biosynthesis genes. *Journal of Bacteriology*, 179(18), pp. 5756–5767.

[Pesci and Iglewski 1997] Pesci, E. C. and Iglewski, B. H. (1997). The chain of command in *Pseudomonas* quorum sensing. *Trends in Microbiology*, 5(4), pp. 132–134.

[Pesci *et al.* 1999] Pesci, E. C., Milbank, J. B., Pearson, J. P., McKnight, S., Kende, A. S., Greenberg, E. P., and Iglewski, B. H. (1999). Quinolone signaling in the cell-to-cell communication system of *Pseudomonas aeruginosa*. *Proceedings of the National Academy of Sciences USA*, 96(20), pp. 11229–11234.

[Pornsunthorntawee *et al.* 2010] Pornsunthorntawee, O., Wongpanit, P., and Rujiravanit, R. (2010). Rhamnolipid biosurfactants: production and their potential in environmental biotechnology. *Advances in Experimental Medicine and Biology*, 672, pp. 211–221.

[Rahim *et al.* 2000] Rahim, R., Burrows, L. L., Monteiro, M. A., Perry, M. B., and Lam, J. S. (2000). Involvement of the *rml* locus in core oligosaccharide and O polysaccharide assembly in *Pseudomonas aeruginosa*. *Microbiology - Society for General Microbiology*, 146, pp. 2803–2814.

[Rahim *et al.* 2001] Rahim, R., Ochsner, U. A., Olvera, C., Graninger, M., Messner, P., Lam, J. S., and Soberon-Chavez, G. (2001). Cloning and functional characterization of the *Pseudomonas aeruginosa rhlC* gene that encodes rhamnosyltransferase 2, an enzyme responsible for dirhamnolipid biosynthesis. *Molecular Microbiology*, 40(3), pp. 708–18.

[Rahman *et al.* 2003] Rahman, K. S. M., Rahman, T. J., Kourkoutas, Y., Petsas, I., Marchant, R., and Banat, I. M. (2003). Enhanced bioremediation of n-alkane in petroleum sludge using bacterial consortium amended with rhamnolipid and micronutrients. *Bioresource Technology*, 90(2), pp. 159–168.

[Rampioni *et al.* 2006] Rampioni, G., Bertani, I., Zennaro, E., Polticelli, F., Venturi, V., and Leoni, L. (2006). The quorum-sensing negative regulator RsaL of *Pseudomonas aeruginosa* binds to the *lasI* promoter. *Journal of Bacteriology*, 188(2), pp. 815–819.

[Rampioni *et al.* 2007] Rampioni, G., Schuster, M., Greenberg, E. P., Bertani, I., Grasso, M., Venturi, V., Zennaro, E., and Leoni, L. (2007). RsaL provides quorum sensing homeostasis and functions as a global regulator of gene expression in *Pseudomonas aeruginosa*. *Molecular Microbiology*, 66(6), pp. 1557–1565.

[Rehm *et al.* 2001] Rehm, B. H. A., Mitsky, T. A., and Steinbüchel, A. (2001). Role of fatty acid de novo biosynthesis in polyhydroxyalkanoic acid (PHA) and rhamnolipid synthesis by *Pseudomonads*: Establishment of the transacylase (PhaG)-mediated pathway for PHA biosynthesis in *Escherichia coli*. *Applied and Environmental Microbiology*, 67(7), pp. 3102–3109.

[Rendell *et al.* 1990] Rendell, N. B., Taylor, G. W., Somerville, M., Todd, H., Wilson, R., and Cole, P. J. (1990). Characterisation of *Pseudomonas* rhamnolipids. *Biochimica et Biophysica Acta*, 1045(2), pp. 189–193.

[Santa Anna *et al.* 2002] Santa Anna, L. M., Sebastian, G. V., Menezes, E. P., Alves, T. L. M., Santos, A. S., Pereira, N., and Freire, D. M. G. (2002). Production of biosurfactants from *Pseudomonas aeruginosa* PA1 isolated in oil environments. *Brazilian Journal of Chemical Engineering*, 19(2), pp. 159–166.

[Scheibel 2004] Scheibel, J. J. (2004). The evolution of anionic surfactant technology to meet the requirements of the laundry detergent industry. *Journal of Surfactants and Detergents*, 7(4), pp. 319–328.

[Schenk *et al.* 1995] Schenk, T., Schuphan, I., and Schmidt, B. (1995). High-performance liquid-chromatographic determination of the rhamnolipids produced by *Pseudomonas aeruginosa*. *Journal of Chromatography A*, 693(1), pp. 7–13.

[Schmidberger *et al.* 2014] Schmidberger, A., Henkel, M., Hausmann, R., and Schwartz, T. (2014). Influence of ferric iron on gene expression and rhamnolipid synthesis during batch cultivation of Pseudomonas aeruginosa PAO1. *Applied Microbiology and Biotechnology*, 98(15), pp. 6725–6737.

[Schuster and Greenberg 2006] Schuster, M. and Greenberg, E. P. (2006). A network of networks: quorum-sensing gene regulation in *Pseudomonas aeruginosa*. *International Journal of Medical Microbiology*, 296(2-3), pp. 73–81.

[Sen 2008] Sen, R. (2008). Biotechnology in petroleum recovery: The microbial EOR. *Progress in Energy and Combustion Science*, 34(6), pp. 714–724.

[Seydlova and Svobodova 2008] Seydlova, G. and Svobodova, J. (2008). Review of surfactin chemical properties and the potential biomedical applications. *Central European Journal of Medicine*, 3(2), pp. 123–133.

[Siegmund and Wagner 1991] Siegmund, I. and Wagner, F. (1991). New method for detecting rhamnolipids excreted by *Pseudomonas* species during growth on mineral agar. *Biotechnology Techniques*, 5(4), pp. 265–268.

[Singh *et al.* 2007] Singh, A., Van Hamme, J. D., and Ward, O. P. (2007). Surfactants in microbiology and biotechnology: Part 2. Application aspects. *Biotechnology Advances*, 25(1), pp. 99–121.

[Sio *et al.* 2006] Sio, C. F., Otten, L. G., Cool, R. H., Diggle, S. P., Braun, P. G., Bos, R., Daykin, M., Camara, M., Williams, P., and Quax, W. J. (2006). Quorum quenching by an *N*-acyl-homoserine lactone acylase from *Pseudomonas aeruginosa* PAO1. *Infection and Immunity*, 74(3), pp. 1673–82.

[Soberón-Chávez *et al.* 2005a] Soberón-Chávez, G., Aguirre-Ramirez, M., and Ordonez, L. (2005a). Is *Pseudomonas aeruginosa* only 'sensing quorum'? *Critical Reviews in Microbiology*, 31(3), pp. 171–182.

[Soberón-Chávez *et al.* 2005b] Soberón-Chávez, G., Lépine, F., and Déziel, E. (2005b). Production of rhamnolipids by *Pseudomonas aeruginosa*. *Applied Microbiology and Biotechnology*, 68(6), pp. 718–725.

[de Sousa *et al.* 2011] de Sousa, J. R., da Costa Correia, J. A., de Almeida, J. G. L., Rodrigues, S., Pessoa, O. D. L., Melo, V. M. M., and Goncalves, L. R. B. (2011). Evaluation of a co-product of biodiesel production as carbon source in the production of biosurfactant by *P. aeruginosa* MSIC02. *Process Biochemistry*, 46(9), pp. 1831–1839.

[Sullivan 1998] Sullivan, E. R. (1998). Molecular genetics of biosurfactant production. *Current Opinion in Biotechnology*, 9(3), pp. 263–269.

[Sumobrain-Solutions 2014] Sumobrain-Solutions (2014). FreePatentsOnline IP research platform for the chemical industry. Available online under http://www.freepatentsonline.com, *accessed 02/2014*.

[Syldatk *et al.* 1985a] Syldatk, C., Lang, S., Matulovic, U., and Wagner, F. (1985a). Production of four interfacial active rhamnolipids from *n*-alkanes or glycerol by resting cells of *Pseudomonas* species DSM 2874. *Zeitschrift für Naturforschung*, 40(1-2), pp. 61–67.

[Syldatk *et al.* 1985b] Syldatk, C., Lang, S., Wagner, F., Wray, V., and Witte, L. (1985b). Chemical and physical characterization of four interfacial-active rhamnolipids from *Pseudomonas* spec. DSM 2874 grown on *n*-alkanes. *Zeitschrift für Naturforschung*, 40(1-2), pp. 51–60.

[Trummler *et al.* 2003] Trummler, K., Effenberger, F., and Syldatk, C. (2003). An integrated microbial/enzymatic process for production of rhamnolipids and L-(+)-rhamnose from rapeseed oil with *Pseudomonas* sp. DSM 2874. *European Journal of Lipid Science and Technology.*, 105(10), pp. 563–571.

[Van Bogaert *et al.* 2007] Van Bogaert, I. N. A., Saerens, K., De Muynck, C., Develter, D., Soetaert, W., and Vandamme, E. J. (2007). Microbial production and application of sophorolipids. *Applied Microbiology and Biotechnology*, 76(1), pp. 23–34.

[Van Delden and Iglewski 1998] Van Delden, C. and Iglewski, B. H. (1998). Cell-to-cell signaling and *Pseudomonas aeruginosa* infections. *Emerging Infectious Diseases*, 4(4), pp. 551–560.

[Van Haesendonck and Vanzeveren 2006] Van Haesendonck, I. P. H. and Vanzeveren, E. C. A. (2006). Rhamnolipids in bakery products. US patent 0233935.

[Van Hamme *et al.* 2003] Van Hamme, J. D., Singh, A., and Ward, O. P. (2003). Recent advances in petroleum microbiology. *Microbiology and Molecular Biology Reviews*, 67(4), pp. 503–549.

[Varnier *et al.* 2009] Varnier, A. L., Sanchez, L., Vatsa, P., Boudesocque, L., Garcia-Brugger, A., Rabenoelina, F., Sorokin, A., Renault, J. H., Kauffmann, S., Pugin, A., Clement, C., Baillieul, F., and Dorey, S. (2009). Bacterial rhamnolipids are novel MAMPs conferring resistance to *Botrytis cinerea* in grapevine. *Plant Cell and Environment*, 32(2), pp. 178–193.

[Velikonja and Kosaric 1993] Velikonja, J. and Kosaric, N. (1993). Biosurfactants in food applications. In: Kosaric, N. (Ed.): *Biosurfactants: production - properties - applications*, Surfactant Science Series, pp. 419–446. New York: Marcel Dekker Inc.

[Wahjudi *et al.* 2011] Wahjudi, M., Papaioannou, E., Hendrawati, O., van Assen, A. H. G., van Merkerk, R., Cool, R. H., Poelarends, G. J., and Ouax, W. J. (2011). PA0305 of *Pseudomonas aeruginosa* is a quorum quenching acylhomoserine lactone acylase belonging to the Ntn hydrolase superfamily. *Microbiology*, 157(7), pp. 2042–2055.

[Walter *et al.* 2010] Walter, V., Syldatk, C., and Hausmann, R. (2010). Microbial production of rhamnolipid biosurfactants. In: Flickinger, M. C. (Ed.): *Encyclopedia of Industrial Biotechnology*. Weinheim: John Wiley & Sons, Inc.

[Winsor *et al.* 2009] Winsor, G. L., Van Rossum, T., Lo, R., Khaira, B., Whiteside, M. D., Hancock, R. E. W., and Brinkman, F. S. L. (2009). *Pseudomonas* Genome Database: facilitating user-friendly, comprehensive comparisons of microbial genomes. *Nucleic Acids Research*, 37, pp. 483–488.

[Yuan and Tam 2008] Yuan, Z. and Tam, V. H. (2008). Polymyxin B: A new strategy for multidrug-resistant gram-negative organisms. *Expert Opinion on Investigational Drugs*, 17(5), pp. 661–668.

[Zhu and Rock 2008] Zhu, K. and Rock, C. O. (2008). RhlA converts β-hydroxyacyl-acyl carrier protein intermediates in fatty acid synthesis to the β-hydroxydecanoyl-β-hydroxydecanoate component of rhamnolipids in *Pseudomonas aeruginosa*. *Journal of Bacteriology*, 190(9), pp. 3147–3154.

[Zhu *et al.* 2007] Zhu, Y., Gan, J. J., Zhang, G. L., Yao, B., Zhu, W. J., and Meng, Q. (2007). Reuse of waste frying oil for production of rhamnolipids using *Pseudomonas aeruginosa* zju.u1M. *Journal of Zhejiang University-Science A*, 8(9), pp. 1514–1520.

4. Kinetic modeling of *N*-butyryl-homoserine lactone levels

This chapter is based on the publication

Kinetic modeling of the time course of *N*-butyryl-homoserine lactone concentration during batch cultivations of *Pseudomonas aeruginosa* PAO1

Marius Henkel[a], *Anke Schmidberger*[b], *Christian Kühnert*[c], *Janina Beuker*[d], *Thomas Bernard*[c], *Thomas Schwartz*[b], *Christoph Syldatk*[a] *and Rudolf Hausmann*[d]

[a]Institute of Process Engineering in Life Sciences, Section II: Technical Biology, Karlsruhe Institute of Technology (KIT), Karlsruhe, Germany [b]Institute of Functional Interfaces, Department Microbiology of Natural and Technical Interfaces, Karlsruhe Institute of Technology (KIT), Eggenstein-Leopoldshafen, Germany [c]Department Systems for Measurement, Control and Diagnosis (MRD), Fraunhofer Institute of Optronics, System Technologies and Image Exploitation, Karlsruhe, Germany [d]Institute of Food Science and Biotechnology, Section Bioprocess Engineering, University of Hohenheim, Stuttgart, Germany

---

The final publication is available at link.springer.com

Bibliographic details

published September 2013, Volume 97, Issue 17, pp 7607-7616
Applied Microbiology and Biotechnology (Springer Berlin Heidelberg)

Print ISSN 0175-7598 - Online ISSN 1432-0614
DOI: 10.1007/s00253-013-5024-5

Authors' contributions to this publication

Marius Henkel designed this study, established the HPLC method for quantifying auto-inducer molecules, developed and fine-tuned the model for *N*-butyryl-homoserine lactone, performed all experiments and collected and evaluated the data and wrote the manuscript.

Anke Schmidberger proof-read the manuscript and performed concomitant experiments to identify genetic expression patterns in the quorum sensing network.

Janina Beuker, Thomas Schwartz, Christian Kühnert and Thomas Bernard contributed to scientific discussions and proof-read the manuscript.

Christoph Syldatk supervised the project, proof-read the manuscript and contributed to scientific discussions.

Rudolf Hausmann supervised the project, proof-read the manuscript and provided input for the design of the study.

4.1 Mathematical description of quorum sensing

Models for quorum sensing regulatory systems have been developed with varying complexities, ranging from a description of the inner regulatory system without external effectors [Chen *et al.* 2004, Viretta and Fussenegger 2004] to a holistic view of the regulatory network, which includes interplay between different regulatory systems and kinetic assumptions on a molecular level, e.g. the formation and degradation of mRNA [Dockery and Keener 2000]. A kinetic model for quorum sensing in C_4-HSL autoinducer null mutant strains ($\Delta rhlI$) of *P. aeruginosa* and the effect on rhamnolipid production was developed in the past [Chen *et al.* 2004]. By using this technique, the authors were able to separate any producing effects from the degradation of C_4-HSL, and focused on the formation and dissociation of the RhlR/C_4-HSL complex, which was shown to act as a transcription factor for the expression of *rhlAB* genes involved in rhamnolipid synthesis in the past [Soberón-Chávez *et al.* 2005a]. The authors assumed only decay of active C_4-HSL over time by cell-associated means, resulting in a first order degradation kinetics. A model which is focused on a system-theoretical investigation of the quorum sensing network in *P. aeruginosa* was developed and investigated in the past [Dockery and Keener 2000]. The authors developed a rigorous model from a genetic perspective, with a focus on simulation of mRNA stability and diffusion rates of autoinducer molecules through the cell membrane. The authors report that the genetic system may indeed act as a biochemical switch of hysteretic character, which allows for two stable steady solutions with low levels of autoinducers and with high levels of autoinducers. Models to describe quorum sensing are either based on stochastic events, such as formation of a transcription factor complex, include kinetic assumptions of formation and degradation of molecules involved in the signaling process, or include a combination of both techniques. Even though most modeling approaches aim at a quantitative description of the regulatory network, qualitative descriptions have also been investigated [Viretta and Fussenegger 2004], which allow for a general systems theoretical view on the interplay of the complex mechanisms. A stochastic model for quorum sensing in *Agrobacterium tumefaciens* was developed and investigated in the past [Goryachev *et al.* 2005]. The authors hypothesized, based on the model, that quorum sensing in *A. tumefaciens* may act as a detector for biofilm formation, since the concentrations to activate the regulatory system can be reached in biofilms, but not during cultivations in a bioreactor, where planctonic cells are subjected to a significantly larger volume. The interactions between the *las* and *rhl* systems and analysis of network dynamics and steady states have been studied in a qualitative model [Viretta and Fussenegger 2004]. The quorum sensing network was furthermore investigated from a systems theoretical point of view in *P. putida* IsoF [Barbarossa *et al.* 2010]. The authors investiga-

ted ranges for stable and instable steady states leading to either hysteretic switch behavior or oscillations. Furthermore, a different study included the simulation of diffusion and uptake of the autoinducer molecules, which is of interest when gradients of autoinducer molecules are present, e.g., due to a local accumulation of cells, such as in biofilms [Anguige *et al.* 2006]. Besides models for cell density dependent mechanisms assuming a homogenous cell population, the interplay between cells producing and affected by autoinducer molecules and cells which are not participating in the signaling process, so-called cheater cells, has also been investigated [Melke *et al.* 2010].

4.1.1 Rhamnolipid production as a model system for studying quorum sensing

P. aeruginosa secretes the autoinducer molecules C_4-HSL (*N*-butyryl-homoserine lactone) and 3o-C_{12}-HSL (3-oxo-dodecanoyl-homoserine lactone). Although C_4-HSL diffuses freely through the membrane, 3o-C_{12}-HSL is reported to require active transport [Pearson *et al.* 1999]. Both C_4-HSL and 3o-C_{12}-HSL influence their own synthesis rate by interaction with their receptor proteins: RhlR for C_4-HSL and LasR for 3o-C_{12}-HSL respectively, which upon binding act as transcription factors. Both systems are interconnected, which is generally believed to be mainly attributed to the *las* system being superordinate to the *rhl* system, since the LasR/3o-C_{12}-HSL complex can also act as a transcription factor for the *rhlR* gene. The interplay of the *rhl* and *las* regulatory network is affected by numerous factors. These factors were identified to act mainly as threshold regulators, which scavenge free autoinducers thereby rendering them inactive [Soberón-Chávez *et al.* 2005a] or as binding partners which then affect ligand binding. Another mechanism for HSL degradation is the specific degradation of autoinducers by acylases or other enzymes acting on HSL molecules. However, this could only be verified for 3o-C_{12}-HSL but not for C_4-HSL [Sio *et al.* 2006]. *P. aeruginosa* also produces another quorum sensing associated signaling molecule, which is known as the *Pseudomonas* quinolone signal (PQS). The molecule was identified as 2-heptyl-3-hydroxy-4-quinolone. Although the PQS system is linked to the *las* and *rhl* systems, the latter have been identified as the core of quorum sensing in *P. aeruginosa* [Williams and Camara 2009]. Therefore, to reduce the complexity of the model, the PQS system was not further investigated in this thesis.

4.1.2 Preliminary considerations and model structure

One of the most important factors for the kinetic understanding of the control mechanisms of the quorum sensing network is whether the *rhl* and *las* systems display

a threshold or a continuous character [Goryachev 2009]. Due to its complex structure with two direct feedback mechanisms and additional activation and quenching mechanisms, modeling of the quorum sensing regulatory network in *P. aeruginosa* usually requires careful consideration of the model structure. To provide a basis for evaluation of quorum sensing during bioreactor cultivations, several simplifications of the model structure have to be included. As the first steps to derive a model for quorum sensing during cultivation in a bioreactor, quantitative data for C_4-HSL and 3o-C_{12}-HSL, a general assumption of the model structure and kinetic data on production and degradation of autoinducers are required. A batch process for the production of rhamnolipids with *P. aeruginosa* PAO1 using sunflower oil as a sole source of carbon and sodium nitrate as a sole source of nitrogen was used for investigation of autoinducer concentration, kinetics and as a reference process for modeling. With *P. aeruginosa* PAO1, a model organism was chosen which is fully sequenced and annotated, and has served as a model organism for quorum sensing in the past [Hentzer *et al.* 2003, Latifi *et al.* 1995]. Additionally, *P. aeruginosa* PAO1 shows comparably high rhamnolipids yields, therefore being a suitable model organism for investigation of processes for enhanced rhamnolipid production. The intention of the work presented in this chapter was to provide a basic understanding of the time course of autoinducers during this reference process, along with production- and degradation kinetics and the effect of autoinducer concentration on rhamnolipid production rates. The obtained data was then used to derive a kinetic model for the time course of C_4-HSL concentration during batch cultivation.

4.2 Materials and Methods

4.2.1 Chemicals and Standards

Standards for high performance liquid chromatography (HPLC) of bacterial autoinducers were obtained from Sigma-Aldrich Laborchemikalien GmbH (Seelze, Germany): *N*-(3-oxododecanoyl)-L-homoserine lactone (3o-C_{12}-HSL) and Cayman Chemical (Ann Arbor, MI, USA): *N*-butyryl-L-homoserine lactone (C_4-HSL). Other chemicals were obtained from Roth GmbH (Karlsruhe, Germany). All chemicals used were of analytical grade, unless indicated otherwise. Food grade sunflower oil was used for all cultivations in a bioreactor. Di-rhamnolipid (Rha-Rha-C_{10}-C_{10}) as a standard for HPLC analysis was a gift from former Hoechst AG (Frankfurt-Hoechst,Germany). Mono-rhamnolipid (Rha-C_{10}-C_{10}) was prepared from di-rhamnolipid as described in the past [Trummler *et al.* 2003]. Chemicals for rhamnolipid derivatization [Schenk *et al.* 1995], triethylamine and 4-bromophenacylbromide were obtained from Sigma-Aldrich Laborchemikalien GmbH (Seelze, Germany).

4.2.2 Microorganism and strain maintenance

Pseudomonas aeruginosa PAO1 (DSM 22644) was obtained from the German Collection of Microorganisms and Cell Cultures (DSMZ, Braunschweig, Germany). All experiments described in this chapter were performed using *P. aeruginosa* PAO1. Strain maintenance was performed routinely as glycerol stocks in lysogeny broth (LB) [Bertani 1951], which were prepared using culture from the exponential growth phase, supplemented with 15% (v/v) glycerol, and stored at -80°C.

4.2.3 Culture conditions

4.2.3.1 Media

Lysogeny broth (LB), containing 10 g/L peptone, 10 g/L tryptone, 20 g/L yeast extract, 5 g/L NaCl was used to inoculate shaking flasks from glycerol stocks. The seed culture for fermentation experiments contained 1.5 g/L $NaNO_3$, 0.05 g/L $MgSO_4 \times 7$ H_2O, 0.1 g/L KCl, 0.1 M sodium phosphate (pH 6.5) with 125 g/L sunflower oil. The production medium contained 0.5 g/L $MgSO_4 \times 7$ H_2O, 1.0 g/L KCl, 0.3 g/L K_2HPO_4 with varying amounts of $NaNO_3$ as a sole source of nitrogen as well as sunflower oil as a sole source of carbon. Trace element solution was added to both seed culture medium as well as production medium at a concentration of 1 mL/L. The trace elements contained 2.0 g/L sodium citrate$\times 2$ H_2O, 0.28 g/L $FeCl_3 \times 6$ H_2O, 1.4 g/L $ZnSO_4 \times 7$ H_2O, 1.2 g/L $CoCl_2 \times 6$ H_2O, 1.2 g/L $CuSO_4 \times 5$ H_2O and 0.8 g/L $MnSO_4 \times H_2O$.

4.2.3.2 Preparation of inoculum cultures

For every fermentation experiment, the inoculum culture was always prepared freshly from glycerol stock, by two liquid cultures in shaking flasks. For the first preculture, 100 µL of glycerol stock was used to inoculate 25 mL LB medium (100 mL baffled flask) and grown for 24 h at 37°C and 120 rpm in a shake incubator (Multitron II, Infors HT, Bottmingen, Switzerland). For the seed culture, 200 mL of seed culture medium with 125 g/L sunflower oil (1 L baffled flask) was inoculated with 5 mL of the LB culture, and grown under the same conditions for 18 - 20 h. The bioreactors were consecutively inoculated with an appropriate amount of seed culture to a final optical density at $\lambda = 580$ nm (OD_{580nm}) of 0.05.

4.2.3.3 Cultivation in a bioreactor

A 42-L stirred tank bioreactor (nominal capacity 30 L) was used for all cultivation experiments (Biostat Cplus, Sartorius Stedim Biotech, Göttingen, Germany). The bioreactor was equipped with standard online measurement and process control for temperature, pH, pO_2 and gasflow as well as a mechanical foam breaker in the

headspace of the bioreactor. Stirrer speed was set to 400 rpm, temperature was set to 37°C, dissolved oxygen was maintained at 5% by gasflow rate (0.1 - 3.3 vvm) and pH was set to 6.50 and controlled by addition of 4 M NaOH and 4 M H_3PO_4. All cultivations were performed with 15 L aqueous phase [Müller *et al.* 2010]. The culture was supplemented with 1 mL/L of trace element solution at $t = 20$ h, $t = 40$ h and $t = 70$ h as described before [Giani *et al.* 1997]. Online parameters were recorded using MFCS/win 2.1 process control software (Sartorius BBI, Göttingen, Germany).

4.2.4 Partition coefficients

The partition coefficients were determined by measuring the concentrations of C_4-HSL and 3o-C_{12}-HSL in the aqueous and hydrophobic medium components in contact in equilibrium. This was investigated in 1 L baffled flasks filled with 200 mL of production medium, preheated to 37°C. The medium was supplemented with C_4-HSL and 3o-C_{12}-HSL standards from a 10 mM stock solution in methanol to a final concentration of 50 µM. The mixture was then incubated at 37°C as described for the seed cultures in section 4.2.3.2. Samples were taken from the flasks after $t = 0$ h, 1 h, 5 h, 6 h, 10 h, 18 h and treated as biological samples as described in section 4.2.6.1. The medium was supplemented with 250 g/L sunflower oil immediately after the sampling at $t = 5$ h, and monitoring was continued to determine the effect C_4-HSL and 3o-C_{12}-HSL distribution between aqueous and hydrophobic phase.

4.2.5 Kinetics of degradation and formation of HSLs

A fractionation in cell-free supernatants and cellular fraction was obtained by centrifugation at 4,600 × g for 30 min at 4°C to allow for separation of cells, aqueous phase and remaining oil in the sample. Cells were washed once in 0.9% NaCl solution and resuspended in 0.9% NaCl solution up to volume equal to the initial volume of the sampling. Each sample was supplemented with C_4-HSL standard from a 10 mM stock solution in methanol to a final concentration of 50 µM. Excess sunflower oil was discarded and cell-free supernatants transferred to a fresh vessel, and supplemented with C_4-HSL as described above (resulting in higher concentrations than 50 µM, due to residual autoinducers). Samples from both cellular fraction and cell-free supernatant were taken after $t = 0$ h, 1.5 h, 3 h and 5 h, and C_4-HSL in the samples was quantified. Production rates for C_4-HSL were calculated by referring to the derivation of the time course of C_4-HSL and the measured total degradation rates. Autodegradation of C_4-HSL was investigated in negative control experiments, treated equally as the samples, in cell-free NaCl solution and spent supernatant-free culture media supplemented with C_4-HSL, respectively.

4.2.6 Analytical techniques

4.2.6.1 Sampling and sample processing

Sampling for offline-measurements was performed as described for the investigated batch process in the past [Müller *et al.* 2010]. Briefly, the culture suspension was mixed vigorously with equal volumes of *n*-hexane and centrifuged at 4,600 × g at 4°C for 30 min to allow for separation of cells, aqueous and *n*-hexane phase. The *n*-hexane phase was used for the gravimetric quantification of sunflower oil and free fatty acids after the evaporation of *n*-hexane. For the gravimetric determination of biomass, the cell pellet was washed once in 0.9% NaCl solution and centrifuged at 4,600 × g at 4°C for 30 min until constant weight was achieved. Rhamnolipids were extracted from the aqueous phase by acidification with 1% (*v*/*v*) H_3PO_4 to precipitate the rhamnolipids. The mixture was then extracted twice with 1.25 volumes of ethylacetate. The aqueous phase was furthermore used for the determination of nitrate, fatty acids, glycerol and lipase activity as described below. The quantification of nitrate was performed with a photometric assay kit (Spectroquant, Merck KGaA, Darmstadt, Germany). Quantification of glycerol was performed with an enzymatic assay kit (Yellow Line, R-Biopharm, Darmstadt, Germany).

4.2.6.2 Quantification of bacterial autoinducers

The extraction of bacterial homoserine lactone (HSL) autoinducers was performed as described previously [Camara *et al.* 1998], with modifications to remove byproducts in the fermentation broth. The broth was centrifuged twice at 4,600 × g for 30 min at 4°C. After each centrifugation step, excess sunflower oil (top phase) was removed, and the supernatant without the cells was transferred to a new centrifugation tube. The supernatant was then acidified with 1% (*v*/*v*) H_3PO_4 to precipitate rhamnolipids and extracellular protein, and consecutively filtered through filter paper. It has been verified that no autoinducers were lost during this process by calculation of recovery rates after extraction of bioreactor samples supplemented with autoinducer molecules. The flow-through was then mixed vigorously with 1.5 volumes of dichloromethane, and kept on ice to allow for separation of the phases. This extraction was repeated once, and the dichloromethane from both extractions was evaporated completely in a vacuum concentrator. To achieve sufficiently high signals during HPLC, a minimum of 20 ml supernatant was processed for each sampling (resulting in a concentration factor of at least 200). The pellets were then stored at -80°C until HPLC analysis for not more than 7 days. For HPLC analysis auf autoinducer molecules, the pellets were resuspended in 100 µL acetonitrile and transfered to HPLC vials. The analysis was performed with a standard HPLC device (Agilent 1100 Series, Agilent, Waldbronn, Germany) equipped with a sample cooling device working at 4°C and a 25.0 × 4.6 cm reversed phase column (Luna 5µ $C_{18\text{-}2}$

100Å, Phenomenex, Aschaffenburg, Germany) at 30°C. Mobile phase solutions were solution A: H_2O and solution B: acetonitrile. For the first 11 min, the separation was performed isocratically at 10% solution B. A gradient of solution B from 10% to 90% was used according to the protocol: from $t = 11$ min to $t = 44$ min increase of solution B from 10% to 70%, followed by an increase from 70% to 90% solution B from $t = 44$ min to $t = 46$ min. Holding 90% solution B up to t = 65 min and decrease to 10% solution B until $t = 72$ min. Holding 90% solution B for 3 more minutes to equilibrate. 3o-C_{12}-HSL and C_4-HSL were prepared as standards in acetonitrile directly before each run in the range of 2.5 - 10 mM. The flow rate was 0.8 mL/min and autoinducers were monitored at 205 nm. Retention times were 10.9 ± 0.1 min for C_4-HSL and 46.2 ± 0.2 min for 3o-C_{12}-HSL.

4.2.6.3 Quantification of rhamnolipids

The quantification of rhamnolipids by HPLC was performed according to a derivatisation protocol with triethylamine and 4-bromophenacylbromide as described previously [Schenk *et al.* 1995]. The analysis was performed with a standard HPLC device (Agilent 1100 Series, Agilent, Waldbronn,Germany) and a 15.0 × 4.6 cm reversed phase column (Supelcosil LC-18, Supelco, Deisenhofen, Germany) at 30°C. Mobile phase solutions were solution A: H_2O with 5% methanol and solution B: methanol with 5% H_2O. A gradient of solution B from 80% to 100% was used according to the protocol: from $t = 0$ to $t = 17$ min increase of solution B from 80% to 100%. Holding 100% solution B up to $t = 25$ min and decrease to 80% solution B until $t = 30$ min. The flow rate was set to 0.8 ml/min and rhamnolipids were monitored at 254 nm. Retention times were 21.5 ± 0.1 min for mono-rhamnolipid (Rha-C_{10}-C_{10}) and 22.2 ± 0.1 min for di-rhamnolipid (Rha-Rha-C_{10}-C_{10}). Mono- and di-rhamnolipid were used as standards in acetonitrile at concentrations between 0.25 - 1.00 g/L [Müller *et al.* 2010].

4.2.6.4 Identification of bacterial autoinducers

The identity of C_4-HSL and 3o-C_{12}-HSL was confirmed using tandem mass spectrometry (MS/MS) with LC fractions collected at the expected retention times ± 0.2 min. The fractions were consecutively evaporated to dryness, and resuspended in acetonitrile with 10 mM NH_4OAc (50:50), and samples were analysed using an API 365 LC/MS/MS System (Perkin Elmer, Waltham, MA, USA). Mass spectrometry of HSL samples was kindly performed by Dr. Gerald Brenner-Weiß and Michael Nusser (Karlsruhe Institute of Technology, Institute of Functional Interfaces).

4.2.7 Modeling platform, regression and analysis of measured data

All modeling was performed in a numerical computing environment (MATLAB, The MathWorks, Natick, MA, USA) by implementing the model as nonlinear differential equations. For simulation of the ordinary differential equations a Runge-Kutta based solver 'ode45s' embedded in the MATLAB environment was used. Nonlinear parameter optimization and fitting was performed using the Nelder-Mead numerical method accomplished by the 'fmincon' and 'fminsearch' functions. For all parameter optimizations, a least-square error function was assumed. For all regression analysis and plotting of measured data, scientific graphing and data analysis software was used (SigmaPlot, Systat Software Inc., San Jose, CA, USA). For calculation of the specific rhamnolipid production rate, a 4-parameter logistic fit was used for both biomass and rhamnolipid concentration. A gaussian curve was used to provide a fit for the time course of C_4-HSL concentration. Data is presented as mean ± standard deviation from 3 independent experiments (biomass concentration, rhamnolipid concentration and C_4-HSL) or a minimum of 2 independent experiments (3o-C_{12}-HSL, C_4-HSL kinetics).

4.3 Results

4.3.1 Time course of extracellular autoinducer molecules C_4-HSL and 3o-C_{12}-HSL during batch fermentation

The time course of biomass, rhamnolipid concentration and specific rhamnolipid production rate (q_{RL}) during a batch process is shown in Fig. 4.1. A maximum biomass concentration of approx. 13 g/L and a maximum total rhamnolipid concentration of approx. 32 g/L was achieved. The production efficiency of rhamnolipids is visualized as the specific rhamnolipid production rate (q_{RL}), which increases during the first 40 hours of cultivation up to a maximum value of approx. 0.08 $g_{\mathrm{RL}}/(g_{\mathrm{BM}}\cdot h)$ at t = 43 h. This maximum production rate was achieved during transition of the bacterial culture to the stationary phase, and declined during the time course of the cultivation to values lower than 0.01 $g_{\mathrm{RL}}/(g_{\mathrm{BM}}\cdot h)$ after approx. t = 80 h. These results are in agreement with previous reports on cultivations of *P. aeruginosa* PAO1 on sunflower oil [Müller *et al.* 2010]. The extracellular concentration of C_4-HSL increases in early stages of the cultivation as the rhamnolipid production rate increases, up to a maximum concentration of 71.6 µmol/L detected at t = 42.5 h. The C_4-HSL concentration then declines over time to a concentration of 12.1 µmol/L at t = 90 h. The concentration of 3o-C_{12}-HSL remains below the detection limit of 0.2 µmol/L over the first 70 h of the cultivation. A concentration of 0.8 µmol/L of 3o-C_{12}-HSL

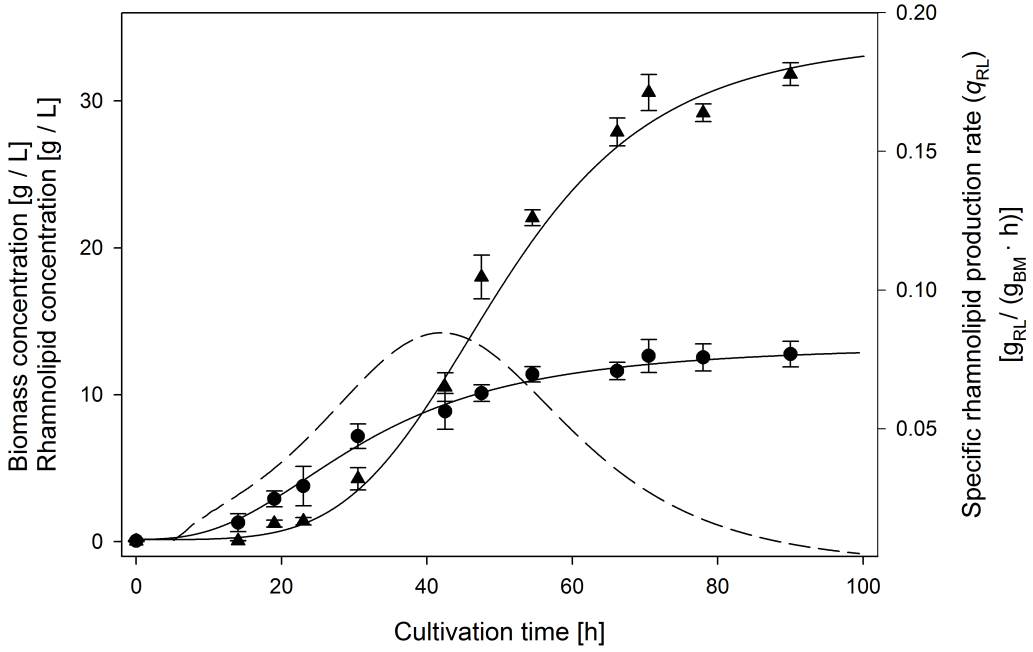

Figure 4.1: Time course of biomass concentration (circle) and total rhamnolipid concentration (triangle) during batch cultivation of *P. aeruginosa* PAO1. A logistic fit is shown for biomass concentration and rhamnolipid concentration (lines). The specific rhamnolipid production rate was calculated (dashed line).

was detected at $t = 70.5$ h, with the highest concentration of 3o-C_{12}-HSL detected after $t = 70$ h of 2.9 µmol/L at $t = 90$ h.

4.3.2 Correlation of extracellular C4-HSL concentration with the rhamnolipid production rate

In Fig. 4.3, the specific rhamnolipid production rate (q_{RL}) is shown in dependence of the C_4-HSL concentration. The cultivation starts with both low C_4-HSL concentrations and low specific production rates ($t = 0$ h) which increases up to highest values for both C_4-HSL and q_{RL} at $t = 43.3$ h, which corresponds to 69.0 µmol/L C_4-HSL and a q_{RL} of 0.0846 $g_{RL}/(g_{BM}{\cdot}h)$ (Fig. 4.1 & 4.2). After reaching the maximum, both C_4-HSL and q_{RL} decline with a linear interrelation to low C_4-HSL concentrations and low specific production rates ($t = 100$ h).

4.3.3 Production and degradation rates of C4-HSL

Production and degradation rates of C_4-HSL were compared in samples from growth phase ($t = 22.5$ h), transition to stationary phase ($t = 48$ h) and stationary phase ($t = 72$ h). Degradation of C_4-HSL was investigated both in spent supernatant of the culture as well as the biomass fraction (Fig. 4.4). Biomass dependent (intracellular) degradation of C_4-HSL was found not to contribute significantly to the

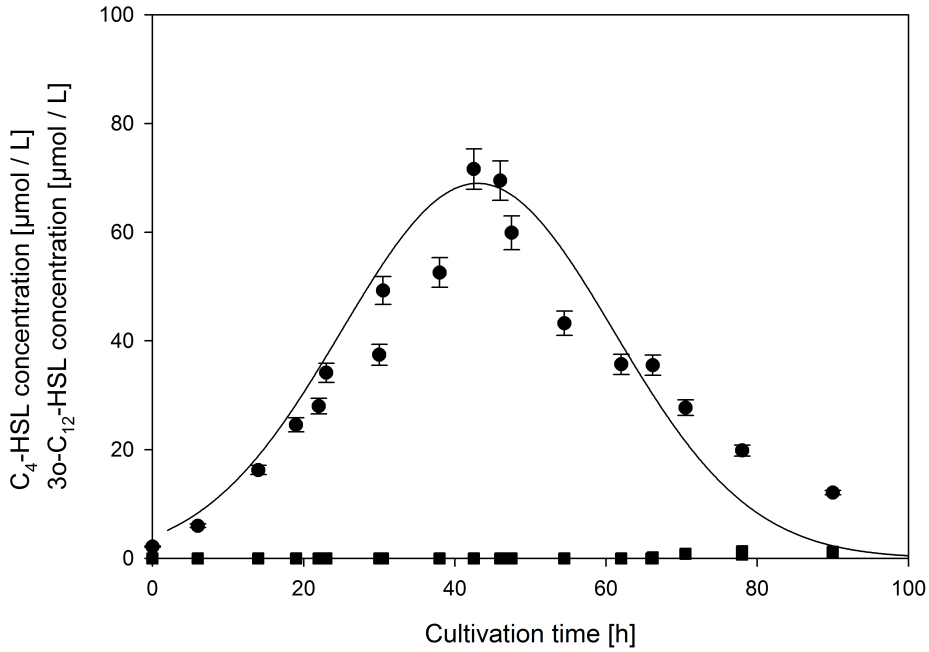

Figure 4.2: Concentration of bacterial autoinducer molecules C_4-HSL (circles) and 3o-C_{12}-HSL (squares) during cultivation of *P. aeruginosa* in a bioreactor with sunflower oil as a sole source of carbon.

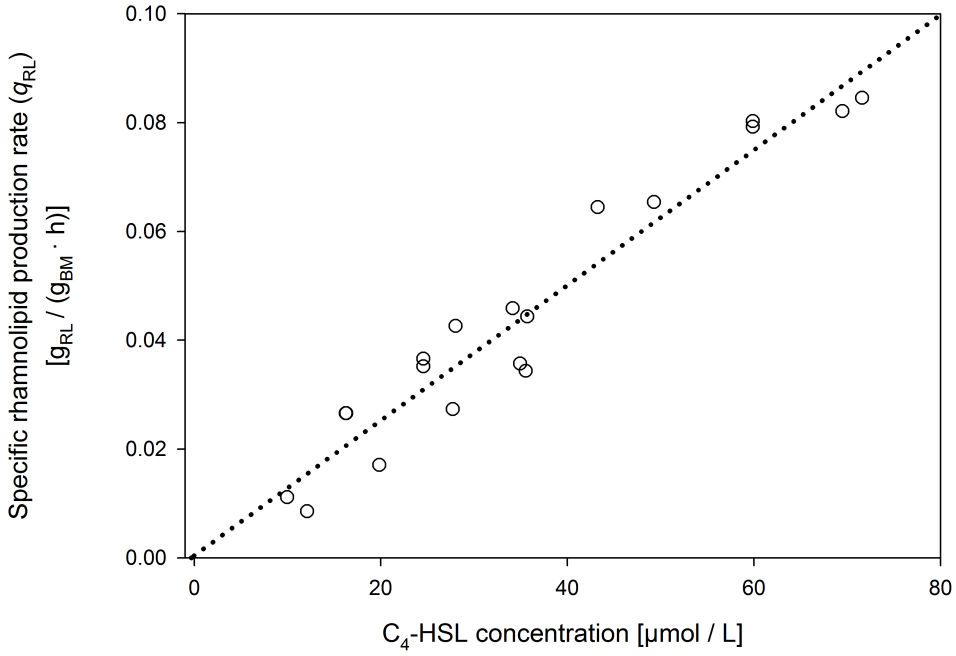

Figure 4.3: Interdependence of rhamnolipid production rates (q_{RL}) and extracellular C_4-HSL concentration during batch cultivation. Data is presented as averages from independent measurements with corresponding specific rhamnolipid production rates (circles) and a linear regression (dotted line) with $r^2 = 0.93$.

observed total degradation rates, and was therefore neglected from the calculations, with measured rates constantly lower than 0.65 µmol/(L·h). It was furthermore verified by the determination of the half-life period of C_4-HSL under fermentation and assay conditions ($t_{1/2\ \text{C4-HSL}}$ = 39 h - 44 h) that autodegradation did not contribute significantly to the observed and calculated decrease in C_4-HSL concentration (decrease in concentration due to autodegradation was consistently below 5% of measured total degradation rates). Monitoring of C_4-HSL concentration in spent supernatant supplemented with C_4-HSL shows considerably higher autoinducer degradation activity than in the biomass fraction. The degradation rate increases from 1.55 µmol/(L·h) to a rate of 11.94 µmol/(L·h) at t = 48 h. In the stationary phase at t = 72 h this rate declined to 5.41 µmol/(L·h). C_4-HSL is produced at a rate of 3.8 µmol/(L·h) at t = 22.5 h which increases until transition to the stationary phase to 10.9 µmol/(L·h). Similar production rates were calculated for the stationary phase with 10.1 µmol/(L·h). The basal production rate q_{basal} for C_4-HSL was calculated from the difference of total C_4-HSL degradation q_{deg} and deviation of the time course of C_4-HSL during cultivation (Fig. 4.4 & B.1) to yield an average value. This average value was 0.763 $\mu\text{mol}_{\text{C4-HSL}}/(g_{\text{BM}}\cdot\text{h})$. It was furthermore found that C_4-HSL autodegradation was insignificant, as no degradation could be detected in control experiments using in the medium at 37°C and pH = 6.5.

4.3.4 Partition coefficient of C_4-HSL and 3o-C_{12}-HSL between aqueous culture broth and hydrophobic carbon source

The partition coefficients of both C_4-HSL as well as 3o-C_{12}-HSL have been found to be in the range of 0.01 to 0.07 for C_4-HSL and $\geq$ 249 for 3o-C_{12}-HSL respectively. C_4-HSL is therefore effectively retained in the aqueous phase, and 3o-C_{12}-HSL in the hydrophobic phase. The calculation of the partition coefficients includes standard deviations of HSL quantification and measurement ranges (minimum detectable concentration of HSLs with the applied method of 0.2 µmol/L).

4.3.5 A model for extracellular C_4-HSL concentration time course

The production rate of C_4-HSL (Eq. 4.1)[1] is assumed to be composed of a basal production rate $q^{\text{basal}}_{\text{C4-HSL}}$ proportional to biomass concentration c_{X} and an autoinductory term proportional to both current biomass c_{X} and C_4-HSL concentration $c_{\text{C4-HSL}}$.

$$q^{\text{prod}}_{\text{C4-HSL}} = \left(q^{\text{basal}}_{\text{C4-HSL}} \cdot c_{\text{X}}(t) + k_{\text{AI}} \cdot c_{\text{C4-HSL}}(t) \cdot c_{\text{X}}(t)\right) \tag{4.1}$$

[1] In-text equation numbering has been changed from the original publication to include the chapter number (Eq. x has been changed to Eq. 4.x)

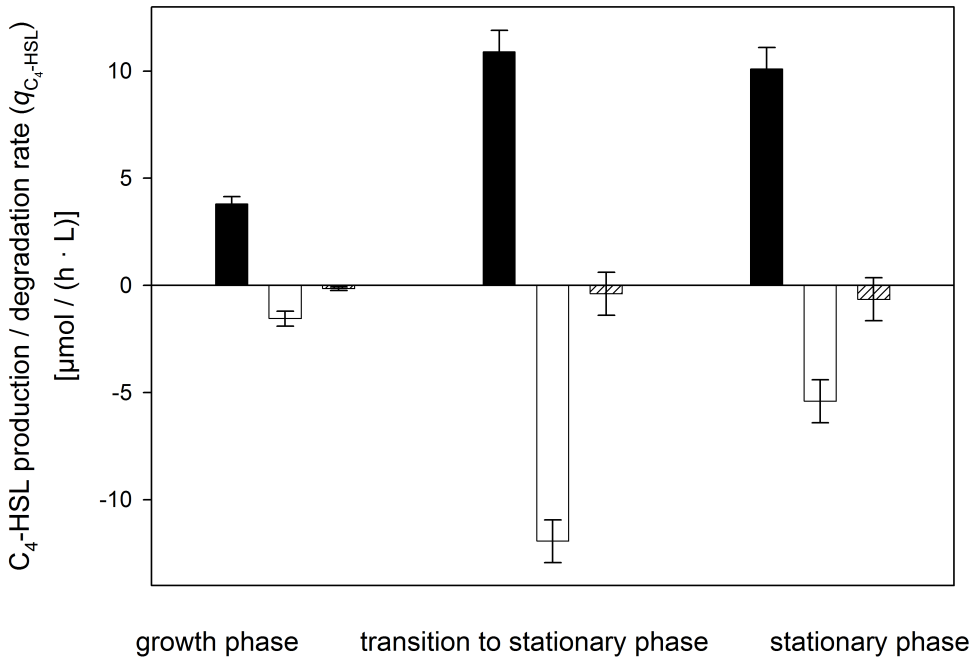

Figure 4.4: Production and degradation rates of C_4-HSL at different stages of the cultivation. C_4-HSL degradation rates and production rates are presented in growth phase (t = 22.5 h), transition to stationary phase (t = 48 h) and stationary phase (t = 72 h) of the cultivation. Degradation of C_4-HSL is presented in spent supernatant (white bar) of and the biomass fraction (dashed bar) along with C_4-HSL production rates (black bars). A more detailed representation of production rates over the course of the cultivation can be found in Fig. B.1.

The degradation rate $q^{\text{deg}}_{\text{C4-HSL}}$ of C_4-HSL (Eq. 4.2) is implemented proportional to the concentration of a putative C_4-HSL specific acylase c_{acyl}, with a Michaelis-Menten model to describe substrate affinity of the acylase.

$$q^{\text{deg}}_{\text{C4-HSL}}(t) = \left(k_{\text{cat}} \cdot c_{\text{acyl}}(t) \cdot \left(\frac{c_{\text{C4-HSL}}(t)}{K_{\text{m}}^{\text{C4-HSL}} + c_{\text{C4-HSL}}(t)} \right) \right) \tag{4.2}$$

Autoinductory mechanisms (proportional to k_{AI}) do not seem to play a major role in the total production rate for C_4-HSL (Eq. 4.1), since production rates were linearly proportional to biomass concentration during the cultivation (Fig. 4.4 & B.1). Therefore, the model for C_4-HSL concentration was simplified by assuming only biomass associated formation. Furthermore, since K_{m} values for HSL-specific acylases are generally reported to be in a milli molar range, e.g. 7.51 mM for 3-hydroxylbutanoyl-L-homoserine lactone [Wang *et al.* 2004], and measured values of C_4-HSL concentration are in a micro molar range, the concentration of C_4-HSL was removed from the denominator. The resulting expression for C_4-HSL is given in equation 4.3.

$$\frac{\mathrm{d}c_{\text{C4-HSL}}}{\mathrm{d}t} = q^{\text{prod}}_{\text{C4-HSL}} - q^{\text{deg}}_{\text{C4-HSL}} \tag{4.3}$$
$$= \left[q^{\text{basal}}_{\text{C4-HSL}} \cdot c_{\text{X}}(t)\right] - \left[\frac{k_{\text{cat}}}{K_{\text{m}}} \cdot c_{\text{acyl}}(t) \cdot c_{\text{C4-HSL}}(t)\right]$$

Production and inactivation of the putative C_4-HSL acylase was simulated by a differential equation (Eq. 4.4), which accounts for biomass-dependent production and auto-degradation of the acylase.

$$\frac{\mathrm{d}c_{\text{acyl}}}{\mathrm{d}t} = k_1 \cdot c_{\text{X}}(t) - k_2 \cdot c_{\text{acyl}}(t) \tag{4.4}$$

For the simulation of the time course of C_4-HSL concentration, 4 parameters are necessary in this simplified model (Tab. 4.1), in addition to the time course of biomass concentration. A useful value for $k_{\text{cat}}/K_{\text{m}}$ was obtained from kinetic studies on *P. aeruginosa* PAO1 gene *pa0305* [Wahjudi *et al.* 2011], a protein which has been reported to show acyl-homoserine lactone acylase activity for shorter chain HSLs. Without quantitative data on the putative acylase, parameters or reference values, which describe formation and degradation of the acylase, are unknown (k_1 and k_2). Therefore, parameters k_1 and k_2 were used as variable fitting parameters. The result of the simulation using the model with optimized parameters (Tab. 4.1), along with measured data on C_4-HSL concentrations time course is shown in Fig. 4.5. The solid line indicates the best simulation as determined by least square error function. The range of different simulation results is presented as dotted curves with the highest deviation from the optimized results, which allow for 20% margin of error in each individual parameter (both measured and fitting parameters). In order to achieve a contimious and steady function for $c_{\text{X}}(t)$ in Fig. 4.5, a logistic fit of the biomass concentration was applied in the modeling of the extracellular C_4-HSL concentration.

4.4 Discussion

Extracellular autoinducer molecules C_4-HSL and 3o-C_{12}-HSL are among the main quorum sensing based signaling molecules in *P. aeruginosa*.

The production of rhamnolipids is believed to be under direct control of the *rhl* system, since the complex of RhlR and C_4-HSL acts as a transcription factor for the *rhlAB* operon, which is involved in rhamnolipid synthesis [Pesci and Iglewski 1997, Soberón-Chávez *et al.* 2005b]. Even though rhamnolipids have been in the focus of research on biosurfactants for decades,

Table 4.1: Parameter values used for the simulation of the time course of C_4-HSL concentration (Fig. 4.5), obtained after optimization of parameters k_1 and k_2.

Parameter	**Value**	**Unit**	**Source**
$q^{\text{basal}}_{\text{C4-HSL}}$	0.763	$\mu\text{mol}_{\text{C4-HSL}}/(g_{\text{BM}}\cdot\text{h})$	This study, calculated (Fig. B.1)
$k_{\text{cat}}/K_{\text{m}}$	5.04	$\text{L}/(\mu\text{mol}_{\text{acyl}}\cdot\text{h})$	[Wahjudi *et al.* 2011], HSL-spec. acylase
k_1	$1.43 \cdot 10^{-4}$	$\mu\text{mol}_{\text{acyl}}/(g_{\text{BM}}\cdot\text{h})$	Fitting parameter
k_2	$0.73 \cdot 10^{-2}$	1/h	Fitting parameter

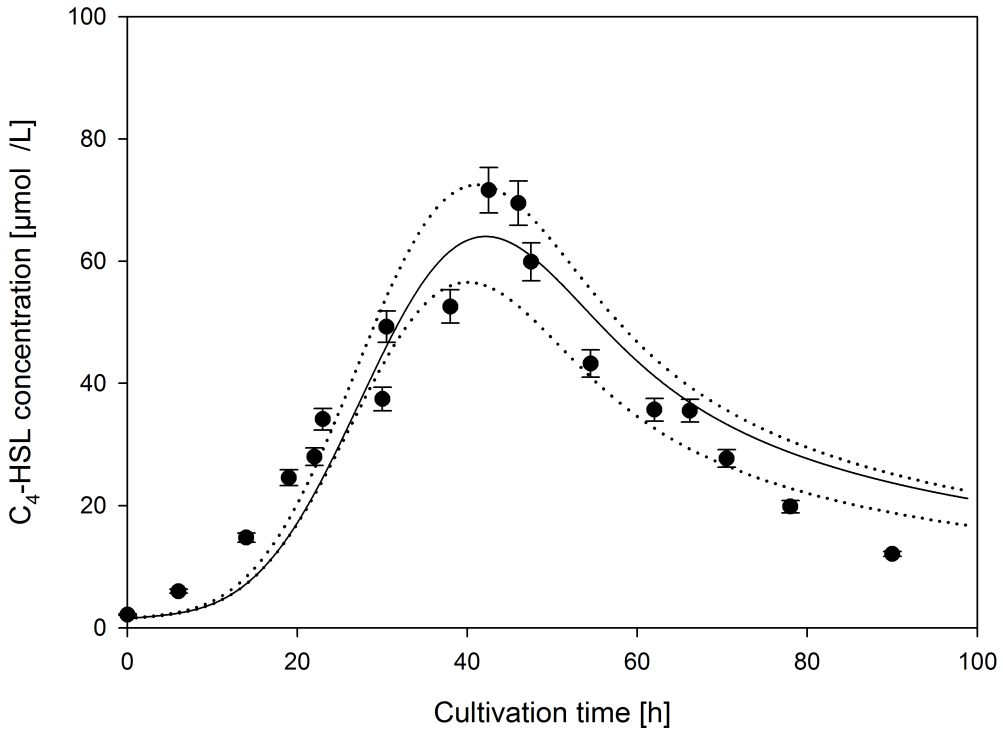

Figure 4.5: Concentration of C_4-HSL (circles) is described by a model (Eq. 4.3 & 4.4). The solid line represents the simulation with optimized parameters (Tab. 4.1), dotted lines are obtained by allowing 20% margin of error for simulations of all parameters, and plots are displayed for two cases with the highest deviation from the optimized curve.

a quantitative determination of autoinducers and correlation to rhamnolipid production rates in a bioreactor has not been addressed before. During cultivation of *P. aeruginosa* on sunflower oil, C_4-HSL levels increased to a maximum at $t = 43$ h, and decreased subsequently. In general, decreasing levels of C_4-HSL during later stages of the cultivation may have several explanations, e.g. active degradation by the cells or strong autodegradation. Autodegradation alone could explain the time course, since the culture reached the stationary phase, and synthesis of C_4-HSL decreased, e.g. due to metabolic limitations. Both a strong autodegradation of C_4-HSL or active biomass dependent degrading mechanisms seem unlikely as depicted by the results from this study, since C_4-HSL was stable under the applied cultivation conditions, and the major part of the C_4-HSL degrading activity was detected in the culture supernatant (Fig. 4.4). Degradation of C_4-HSL has been shown to be due to an extracellular process. This suggests the presence of an extracellular, C_4-HSL specific acylase, lactonase or mechanism of similar function. However, *P. aeruginosa* possesses several HSL-acylases, and their interplay and relevance for the quorum sensing signaling and regulation is not yet understood. A C_4-HSL specific acylase in *P. aeruginosa* PAO1 has not been reported at present, however, an acylase which cleaves HSLs with acyl side chains ranging from 6 to 14 carbons, has recently been discovered in the genome of *P. aeruginosa* PAO1 [Wahjudi *et al.* 2011]. However, it should be noted that even though an extracellular enzyme involved in degradation of C_4-HSL is likely, observed decreasing levels of C_4-HSL may furthermore also be influenced by metabolic events, which causes cells to enter the stationary phase. The facts that 3o-C_{12}-HSL is highly hydrophobic and the partition coefficient strongly favors its absorption into the vegetable oil phase explain why concentrations of 3o-C_{12}-HSL did not exceed of 1 µM in the aqueous phase during cultivation. In contrast to this situation, C_4-HSL is mostly present in the aqueous phase where it accumulates during the cultivation. The presence of a hydrophobic phase distorts the autoinducer 3o-C_{12}-HSL to C_4-HSL ratio in the aqueous phase. This effect may contribute to regulatory events, as it may be assumed that only the aqueous phase is relevant for the environmental sensing of the cells.

This hypothesis is furthermore supported by the results of gene expression during batch cultivation [Schmidberger *et al.* 2013], which focused on the investigation of gene expression during the same cultivation of *P. aeruginosa* on sunflower oil. It could be shown that during cultivation, expression of genes of the *las* system (*lasR* and *lasI*), which is affected by 3o-C_{12}-HSL, remains fairly constant during the entire cultivation. In contrast, expression of genes of the *rhl* system (*rhlR* and *rhlI*) are 15-20 fold upregulated after $t = 10$ h. It should be noted that it was not investigated to what extent 3o-C_{12}-HSL may still act on the cells, even though it is present in the hydrophobic sunflower oil phase. This effect may pro-

vide an explanation for the general assumption that hydrophobic carbon sources display a different effect on rhamnolipid formation as non-hydrophobic substrates [Abdel-Mawgoud *et al.* 2011, Henkel *et al.* 2012]. It is evident that this mechanism may contribute to the molecular sensing of extracellular hydrophobic substances. Rhamnolipid production rates were shown to have a linear interrelation with concentrations of C_4-HSL (Fig. 4.3). At first glance, since the RhlR/C_4-HSL dimer acts as a transcription factor for *rhlAB*, higher concentrations of C_4-HSL possibly result in higher rhamnolipid production rates. Evidently in this scenario the decrease in C_4-HSL concentration led to the reduced rhamnolipid productivity in the second part of the cultivation. Another explanation for declining rhamnolipid production rates is a decrease of metabolic activity of the cells, which is represented by decreasing growth rates upon transition to the stationary phase. This effect could both account for reduced production of C_4-HSL as wells as reduced formation of rhamnolipids. However, the C_4-HSL acylase activity alone is sufficient for the description of the observed decline in C_4-HSL concentration and hence in rhamnolipid productivity. By using data on the time course of C_4-HSL concentration, effective production rates could be calculated. The fact that C_4-HSL is degraded mainly in the supernatant confirms the assumption of quorum quenching mechanisms (e.g. acylases, lactonases) for C_4-HSL, which have been reported for 3o-C_{12}-HSL and other HSLs in the past [Sio *et al.* 2006, Waters and Bassler 2005]. Formation rates of C_4-HSL were found to be proportional to available biomass (Fig. 4.3 & B.1), and no major auto-induction could be confirmed. This is in agreement with a different study which challenged the concept of feedback loops in the *rhl* and *las* systems [Goryachev 2009]. It has been suggested that, depending on the genes investigated, the relation between stimulus (e.g. C_4-HSL) and response (e.g. *rhlAB* expression, rhamnolipid production) shows a continuous and dose-dependent behavior, instead of a hysteretic behavior (switch). The dose-response behavior is in agreement with the data on C_4-HSL concentration and rhamnolipid production rate as presented in this chapter. Since the production rate of C_4-HSL remained proportional to biomass concentration over the whole process, even in the stationary phase, it can be assumed that the formation of C_4-HSL is actively regulated rather than influenced by metabolic events.

The simulation of C_4-HSL concentrations shown in Fig. 4.5 gives a good approximation of the experimental results. In the first 20 h of the cultivation, the simulated values are slightly lower as compared to measured data. This is mainly attributed to the simplifications implemented in the model in terms of production rate. Since mechanisms of autoinduction were found not to contribute significantly to the buildup of C_4-HSL concentration during the cultivation, the term proportional to biomass and C_4-HSL concentration was removed from the model for production rate to sim-

plify the model and reduce the amount of unknown fitting parameters. However, due to this reason, the acceleration of the production rate is too low to accurately represent the data in the first 10 h of the cultivation. This may be corrected by conducting further studies on how auto-induction contributes to formation of C_4-HSL in early stages of the cultivation. At a later stage of the cultivation, after $t = 70$ h, the simulation results in higher C_4-HSL concentrations than the measurements. This may be attributed to the fact that, for reasons of simplicity, only one acylase-like mechanism was implemented in the model, which counteracts formation of C_4-HSL. It is possible however, that more than one mechanism (e.g. different acylases) exist that either actively or passively facilitate or interfere with C_4-HSL degradation. However, it should be noted that data on an acylase was used, which is not known to act on C_4-HSL, and therefore, $k_{\mathrm{cat}}/K_{\mathrm{m}}$ values may be different for the C_4-HSL acylase in question. Therefore, more data is required on the assumption of a C_4-HSL specific acylase. The model should be carefully reviewed and validated, before it is applied to a different process, since the presence of 3o-C_{12}-HSL in the absence of a hydrophobic source of carbon may have an effect on both C_4-HSL concentration and rhamnolipid production rates. So far, both an appropriate model system with known time course of autoinducers, as well as kinetic data on formation and degradation of autoinducers were not available. In this chapter, insights are gained into a practical approach for modeling of C_4-HSL concentration, relevant kinetic behavior and parameters. The model is used in the following chapters to describe quorum sensing mechanisms and rhamnolipid formation during cultivation in a bioreactor.

References for Chapter 4

[Abdel-Mawgoud *et al.* 2011] Abdel-Mawgoud, A. M., Hausmann, R., Lepine, F., Müller, M. M., and Deziel, E. (2011). Rhamnolipids: detection, analysis, biosynthesis, genetic regulation, and bioengineering of production. In: Soberon-Chavez, G. (Ed.): *Biosurfactants*, Microbiology Monographs, pp. 13–55. Berlin Heidelberg: Springer.

[Anguige *et al.* 2006] Anguige, K., King, J. R., and Ward, J. P. (2006). A multi-phase mathematical model of quorum sensing in a maturing *Pseudomonas aeruginosa* biofilm. *Mathematical Biosciences*, 203(2), pp. 240–276.

[Barbarossa *et al.* 2010] Barbarossa, M. V., Kuttler, C., Fekete, A., and Rothballer, M. (2010). A delay model for quorum sensing of *Pseudomonas putida*. *Biosystems*, 102(2-3), pp. 148–156.

[Bertani 1951] Bertani, G. (1951). Studies on lysogenesis I.: The mode of phage liberation by lysogenic *Escherichia coli*. *Journal of Bacteriology*, 62(3), pp. 293–300.

[Camara *et al.* 1998] Camara, M., Daykin, M., and Chhabra, S. R. (1998). Detection, purification, and synthesis of *N*-acylhomoserine lactone quorum sensing signal molecules. *Methods in Microbiology*, 27, pp. 319–330.

[Chen *et al.* 2004] Chen, F., Chen, C. C., Riadi, L., and Ju, L. K. (2004). Modeling *rhl* quorum sensing regulation on rhamnolipid production by *Pseudomonas aeruginosa*. *Biotechnology Progress*, 20(5), pp. 1325–1331.

[Dockery and Keener 2000] Dockery, J. D. and Keener, J. P. (2000). A mathematical model for quorum sensing in *Pseudomonas aeruginosa*. *Bulletin of Mathematical Biology*, 00, pp. 1–22.

[Giani *et al.* 1997] Giani, C., Wullbrandt, D., Rothert, R., and Meiwes, J. (1997). *Pseudomonas aeruginosa* and its use in a process for the biotechnological preparation of L-Rhamnose. US patent 5658793, Hoechst Aktiengesellschaft, Frankfurt am Main, Germany.

[Goryachev 2009] Goryachev, A. B. (2009). Design principles of the bacterial quorum sensing gene networks. *Wiley Interdisciplinary Reviews: Systems Biology and Medicine*, 1(1), pp. 45–60.

[Goryachev *et al.* 2005] Goryachev, A. B., Toh, D. J., Wee, K. B., Lee, T., Zhang, H. B., and Zhang, L. H. (2005). Transition to quorum sensing in an *Agrobacterium* population: A stochastic model. *PLoS Computational Biology*, 1(4), pp. 265–275.

[Henkel *et al.* 2012] Henkel, M., Müller, M. M., Kügler, J. H., Lovaglio, R. B., Contiero, J., Syldatk, C., and Hausmann, R. (2012). Rhamnolipids as biosurfactants from renewable resources: Concepts for next-generation rhamnolipid production. *Process Biochemistry*, 47(8), pp. 1207–1219.

[Hentzer *et al.* 2003] Hentzer, M., Wu, H., Andersen, J. B., Riedel, K., Rasmussen, T. B., Bagge, N., Kumar, N., Schembri, M. A., Song, Z. J., Kristoffersen, P., Manefield, M., Costerton, J. W., Molin, S., Eberl, L., Steinberg, P., Kjelleberg, S., Hoiby, N., and Givskov, M. (2003). Attenuation of *Pseudomonas aeruginosa* virulence by quorum sensing inhibitors. *EMBO Journal*, 22(15), pp. 3803–3815.

[Latifi *et al.* 1995] Latifi, A., Winson, M. K., Foglino, M., Bycroft, B. W., Stewart, G. S. A. B., Lazdunski, A., and Williams, P. (1995). Multiple homologs of Luxr and Luxl control expression of virulence determinants and secondary metabolites through quorum sensing in *Pseudomonas aeruginosa* PAO1. *Molecular Microbiology*, 17(2), pp. 333–343.

[Melke *et al.* 2010] Melke, P., Sahlin, P., Levchenko, A., and Jonsson, H. (2010). A cell-based model for quorum sensing in heterogeneous bacterial colonies. *PLoS Computational Biology*, 6(6).

[Müller *et al.* 2010] Müller, M., Hörmann, B., Syldatk, C., and Hausmann, R. (2010). *Pseudomonas aeruginosa* PAO1 as a model for rhamnolipid production in bioreactor systems. *Applied Microbiology and Biotechnology*, 87(1), pp. 167–174.

[Pearson *et al.* 1999] Pearson, J. P., Van Delden, C., and Iglewski, B. H. (1999). Active efflux and diffusion are involved in transport of *Pseudomonas aeruginosa* cell-to-cell signals. *Journal of Bacteriology*, 181(4), pp. 1203–1210.

[Pesci and Iglewski 1997] Pesci, E. C. and Iglewski, B. H. (1997). The chain of command in *Pseudomonas* quorum sensing. *Trends in Microbiology*, 5(4), pp. 132–134.

[Schenk *et al.* 1995] Schenk, T., Schuphan, I., and Schmidt, B. (1995). High-performance liquid-chromatographic determination of the rhamnolipids produced by *Pseudomonas aeruginosa*. *Journal of Chromatography A*, 693(1), pp. 7–13.

[Schmidberger *et al.* 2013] Schmidberger, A., Henkel, M., Hausmann, R., and Schwartz, T. (2013). Expression of genes involved in rhamnolipid synthesis in *Pseudomonas aeruginosa* PAO1 in a bioreactor cultivation. *Applied Microbiology and Biotechnology*, 97(13), pp. 5779–5791.

[Sio *et al.* 2006] Sio, C. F., Otten, L. G., Cool, R. H., Diggle, S. P., Braun, P. G., Bos, R., Daykin, M., Camara, M., Williams, P., and Quax, W. J. (2006). Quorum quenching by an *N*-acyl-homoserine lactone acylase from *Pseudomonas aeruginosa* PAO1. *Infection and Immunity*, 74(3), pp. 1673–1682.

[Soberón-Chávez *et al.* 2005a] Soberón-Chávez, G., Aguirre-Ramirez, M., and Ordonez, L. (2005a). Is *Pseudomonas aeruginosa* only 'sensing quorum'? *Critical Reviews in Microbiology*, 31(3), pp. 171–182.

[Soberón-Chávez *et al.* 2005b] Soberón-Chávez, G., Lépine, F., and Déziel, E. (2005b). Production of rhamnolipids by *Pseudomonas aeruginosa*. *Applied Microbiology and Biotechnology*, 68(6), pp. 718–725.

[Trummler *et al.* 2003] Trummler, K., Effenberger, F., and Syldatk, C. (2003). An integrated microbial/enzymatic process for production of rhamnolipids and L-(+)-rhamnose from rapeseed oil with *Pseudomonas* sp. DSM 2874. *European Journal of Lipid Science and Technology*, 105(10), pp. 563–571.

[Viretta and Fussenegger 2004] Viretta, A. and Fussenegger, M. (2004). Modeling the quorum sensing regulatory network of human-pathogenic *Pseudomonas aeruginosa*. *Biotechnology Progress*, 20, pp. 670–678.

[Wahjudi *et al.* 2011] Wahjudi, M., Papaioannou, E., Hendrawati, O., van Assen, A. H. G., van Merkerk, R., Cool, R. H., Poelarends, G. J., and Ouax, W. J. (2011). PA0305 of *Pseudomonas aeruginosa* is a quorum quenching acylhomoserine lactone acylase belonging to the Ntn hydrolase superfamily. *Microbiology*, 157(7), pp. 2042–2055.

[Wang *et al.* 2004] Wang, L. H., Weng, L. X., Dong, Y. H., and Zhang, L. H. (2004). Specificity and enzyme kinetics of the quorum quenching *N*-acyl homoserine lactone lactonase (AHL-lactonase). *Journal of Biological Chemistry*, 279(14), pp. 13645–13651.

[Waters and Bassler 2005] Waters, C. M. and Bassler, B. L. (2005). Quorum sensing: Cell-to-cell communication in bacteria. *Annual Review of Cell and Developmental Biology*, 21, pp. 319–346.

[Williams and Camara 2009] Williams, P. and Camara, M. (2009). Quorum sensing and environmental adaptation in *Pseudomonas aeruginosa*: A tale of regulatory networks and multifunctional signal molecules. *Current Opinion in Microbiology*, 12(2), pp. 182–191.

5. Modeling the production of rhamnolipids in a bioreactor

This chapter is based on the publication

Kinetic modeling of rhamnolipid production by *Pseudomonas aeruginosa* PAO1 including cell-density dependent regulation

Marius Henkel[a], *Anke Schmidberger*[b], *Markus Vogelbacher*[c], *Christian Kühnert*[c], *Janina Beuker*[d], *Thomas Bernard*[c], *Thomas Schwartz*[b], *Christoph Syldatk*[a] *and Rudolf Hausmann*[d]

[a]Institute of Process Engineering in Life Sciences, Section II: Technical Biology, Karlsruhe Institute of Technology (KIT), Karlsruhe, Germany [b]Institute of Functional Interfaces, Department Microbiology of Natural and Technical Interfaces, Karlsruhe Institute of Technology (KIT), Eggenstein-Leopoldshafen, Germany [c]Department Systems for Measurement, Control and Diagnosis (MRD), Fraunhofer Institute of Optronics, System Technologies and Image Exploitation, Karlsruhe, Germany [d]Institute of Food Science and Biotechnology, Section Bioprocess Engineering, University of Hohenheim, Stuttgart, Germany

---

The final publication is available at link.springer.com

Bibliographic details

published August 2014, Volume 98, Issue 16, pp 7013-7025
Applied Microbiology and Biotechnology (Springer Berlin Heidelberg)

Print ISSN 0175-7598 - Online ISSN 1432-0614
DOI: 10.1007/s00253-014-5750-3

Authors' contributions to this publication

Marius Henkel performed all cultivation and parameterization experiments, collected and evaluated the data, wrote the manuscript, designed the model structure, implemented and parameterized growth and enzyme kinetics and fine-tuned the model parameters.

Anke Schmidberger provided the data on the time-course of *rhlA* gene expression (shown in Figure 5.4) and proof-read the manuscript.

Markus Vogelbacher, Christian Kühnert and Thomas Bernard implemented the dynamic simulation model in MATLAB and contributed to parameter fitting.

Janina Beuker and Thomas Schwartz contributed to scientific discussions and proof-read the manuscript.

Christoph Syldatk supervised the project, proof-read the manuscript and contributed to scientific discussions.

Rudolf Hausmann supervised the project, proof-read the manuscript and provided input for the design of the study.

5.1 Towards a process model for rhamnolipid production

Existing processes and strategies for rhamnolipid production are mainly based on heuristic approaches. Today, current work is focused on finding and developing alternative non-pathogenic strains [Henkel *et al.* 2012], and methods of optimization of existing processes are mainly restricted to optimization of growth medium components by employing techniques such as response surface methodology [Eswari *et al.* 2013, Luo *et al.* 2013]. Current alternative strains can by far not compete with rhamnolipid levels observed in several wild type strains of *P. aeruginosa*. In *P. putida*, heterologous production of rhamnolipids could be achieved up to a concentration of 7.2 g/L [Cha *et al.* 2008]. In heterologous approaches in non-Pseudomonas strains however, maximum rhamnolipid levels below 100 mg/L are reported [Ochsner *et al.* 1995]. Wild type high-producing strains of *P. aeruginosa* provide a solid basis for optimization of rhamnolipid production, due to the ability to produce rhamnolipids in comparably high yields. By exploiting the full potential of these strains, these levels may be further enhanced. For the knowledge-based development of an optimized process, further quantitative understanding of the process and interrelation of process variables are a prerequisite.

An expression for rhamnolipid production rate from a regulatory point of view has been developed in the past [Chen *et al.* 2004], by modeling the formation and dissociation of the C_4-HSL/RhlR complex in *P. aeruginosa* PAO1. However, no connection to process variables was established during their work. Furthermore, a model was proposed for substrate consumption and rhamnolipid formation in a bioreactor proportional to the cell concentration, by assuming a logistic model for biomass growth [de Lima *et al.* 2009]. The authors included a response surface method to optimize aeration and agitation rate, resulting in a final rhamnolipid concentration of 3.3 g/L rhamnose. In a different study, a model of a thin film was established, which combines hydrodynamical and regulatory mechanisms to simulate swarming behavior [Du *et al.* 2011]. Artificial neural networks (ANN) have also been applied to describe rhamnolipid formation in the past. Rhamnolipid production has been addressed by a response surface approach to the developed ANN, which led to the identification of an optimized composition of growth medium for *P. aeruginosa* strain AT10 [Eswari *et al.* 2013]. The model was fairly successful in predicting a rhamnolipid concentration of 18.07 g/L, while experimentally 16.50 g/L could be detected. A model for rhamnolipid production by *P. aeruginosa* ATCC 9027 in systems with water immiscible carbon sources has been developed in the past [Medina-Moreno *et al.* 2011]. The data on biomass growth was implemented as a logistic curve, predetermined by experimental results. Substrate consumption was

simulated depending on the size and surface of hydrophobic droplets and the presence of rhamnolipids. Rhamnolipid formation in turn was expressed as a function of droplet size. The model included physical parameters such as the critical micellar concentration (CMC) and surface tension.

5.1.1 Choosing the model system

To establish a conclusive approach to account for regulation of rhamnolipid formation, kinetic data on cell-density dependent quorum sensing needs to be included in the process model. By using the strain *P. aeruginosa* PAO1, a model organism was chosen with broad application in the scientific community. *P. aeruginosa* PAO1 is fully sequenced and annotated [Stover *et al.* 2000], and has served as a model organism for quorum sensing in the past [Hentzer *et al.* 2003, Latifi *et al.* 1995]. Additionally, *P. aeruginosa* PAO1 show comparably high rhamnolipids yields [Müller *et al.* 2010], therefore being a suitable model organism for rhamnolipid production experiments. With the complexity of the model, it may also be applied as a tool to research and refine knowledge on the correlation of quorum sensing, growth and gene expression on a process level. Furthermore, the model should provide a first step in developing model-based optimized process control strategies, which may result in higher rhamnolipid production.

5.2 Materials and Methods

5.2.1 Chemicals and standards

Standards for high performance liquid chromatography (HPLC) of bacterial autoinducer *N*-(3-oxododecanoyl)-L-homoserine lactone (3o-C_{12}-HSL) was obtained from Sigma-Aldrich Laborchemikalien GmbH (Seelze, Germany) and *N*-butyryl-L-homoserine lactone (C_4-HSL) was obtained from Cayman Chemical (Ann Arbor, MI, USA). Food grade sunflower oil was obtained from Aldi Sued (Rastatt, Germany). Lipase from *Pseudomonas sp.* used as a control in activity assays was obtained from Sigma-Aldrich Laborchemikalien GmbH (Seelze, Germany). The di-rhamnolipid (Rha-Rha-C_{10}-C_{10}) standard for HPLC analysis was a gift from former Hoechst AG (Frankfurt-Hoechst, Germany). The mono-rhamnolipid (Rha-C_{10}-C_{10}) standard was prepared as described in the past [Trummler *et al.* 2003]. Rhamnolipid derivatization was performed using 4-bromophenacylbromide and triethylamine [Schenk *et al.* 1995], which was obtained from Sigma-Aldrich Laborchemikalien GmbH (Seelze, Germany). All other chemicals were obtained from Carl Roth GmbH (Karlsruhe, Germany). All chemicals used were of analytical grade, unless indicated otherwise.

5.2.2 Culture conditions

All details on cultivation, media as well as analytical techniques for rhamnolipids and autoinducers are provided in the Materials and methods section of Chapter 4 [Henkel *et al.* 2013].

5.2.3 Analytical techniques

5.2.3.1 Enzymatic and photometric kits

The quantification of nitrate was performed with a spectrophotometric assay kit (Spectroquant, Merck KGaA, Darmstadt, Germany). Glycerol was quantified with an enzymatic assay kit (Enztech yellow line, r-biopharm, Darmstadt, Germany). Lipase activity was determined with a fluorescence assay kit (MarkerGene Long Wavelength Fluorescent Lipase Assay Kit, Marker Gene Technologies, Eugene, OR).

5.2.3.2 Quantification of free fatty acids

The colorimetric quantification of free fatty acids was performed with an aqueous solution of cupric acetate [Ayers 1956, Baker 1964]. Briefly, 2 mL of culture supernatant were mixed with 2 mL 2% (w/v) copper(II) acetate solution. Green/blue copper salts of free fatty acids were then extracted with 2 mL chloroform, quantified at 675 nm and compared to standards of oleic acid prepared in the range of 0.1 - 2.0 g/L. In addition to deprotonated fatty acids present in the aqueous phase, evaporated n-hexane extracts were resuspended in 2 mL chloroform and treated with 2 mL copper(II) acetate solution to quantify protonated fatty acids which may have been extracted by n-hexane.

5.2.3.3 Extracellular polymeric substances

Extracellular polymeric substances were determined gravimetrically in culture supernatants extracted with n-hexane to remove contaminations of residual oil and glycerides. The supernatants were dried completely until constant weight was achieved for approx. 48 - 72 h. The obtained cell-free total dry weight was used to calculate extracellular byproduct formation by subtracting measurement data of nitrate-, fatty acid-, mono-rhamnolipid and di-rhamnolipid concentration as well as inorganic components of the medium.

5.2.4 Determination of parameters

5.2.4.1 Growth kinetics and yields

Experiments for the determination of growth parameters (μ_{gly}, μ_{FA}, Eq. 1.2 & 1.3), kinetics (k_{d}, ${K_{\mathrm{i}}}^{\mathrm{FA}}$, n, Eq. 1.1 & 1.2) and yields ($Y_{\mathrm{X|gly}}$, $Y_{\mathrm{X|FA}}$, Eq. 2.2a & 2.2b)

were performed in shaking flasks prepared as described for bioreactor seed cultures [Müller *et al.* 2010, Henkel *et al.* 2013] with the appropriate amount of oleic acid or glycerol. The shaking flasks were inoculated with 1% (v/v) of seed cultures grown with 10 g/L oleic acid or glycerol, respectively. Each shaking flask experiment was performed as triplicates, and samples were drawn every 1.5 h and analyzed routinely for fatty acids, glycerol and biomass concentration. Growth rates as a function of fatty acids and glycerol as well as maximum growth rates were determined using 3 parameter logistic fits for biomass concentration from shaking flasks with 10 - 70 g/L fatty acids and 10 - 150 g/L glycerol, respectively. Biomass yields were determined only in the first 16 h of cultivation to reduce the influence of byproduct formation. Decay of biomass concentration was investigated in seed culture medium without nitrogen and carbon sources cultivated for 1 week at the same conditions as applied for seed cultures.

5.2.4.2 Fatty acid and glycerol released by the cleavage of triglycerides

Release of fatty acids and glycerol from triglycerides by lipase activity in the culture supernatant was investigated using sunflower oil and triolein as substrates in bioreactor samples taken at the stationary phase (t = 52 h). The samples were treated as described previously for culture supernatants [Henkel *et al.* 2013] and released fatty acids and glycerol were quantified as described above. Total volumes of 5 mL supernatant were used for each experiment supplemented with 50 g/L sunflower oil, and incubated at 37°C and 120 rpm in a shake incubator (Multitron II, Infors HT, Bottmingen, Switzerland). Samples were taken for up to 4 h and analyzed for glycerol and fatty acid content. A conversion factor of 8.3 was determined experimentally for the release of 1 µmol oleic acid from resorufin-oleate as compared to the release of 1 µmol oleic acid from triolein, which was used to calculate lipase activity in bioreactor samples, meaning that resorufin-oleate is cleaved more efficiently than triglycerides. In addition, triolein was used for reference experiments with a maximum deviation below 10% of determined fatty acids, glycerol and activity as compared to the results for sunflower oil.

5.2.4.3 Effect of free fatty acids on lipase activity

Effects of free fatty acids and residual triglyceride on lipase activity were investigated in culture supernatants of bioreactor samples taken at the stationary phase (t = 52 h). The samples were treated as described for culture supernatants, and each experiment was performed with 5 mL supernatant supplemented with varying amounts of oleic acid (10 g / L, 25 g / L and 40 g / L) and sunflower oil (50 g / L and 250 g / L). Increase in fatty acid concentration due to cleavage of triglycerides was quantified and used to calculate the relative activity based on the activity in control

samples without the addition of oleic acid and normalized to the activity of purified LipA from *P. aeruginosa* PAO1 from literature [Madan and Mishra 2010]. The reaction was allowed to proceed for at least 2 h.

5.2.5 Modeling and parameter optimization

5.2.5.1 Modeling platform

Modeling was performed in a mathematical/numerical computing environment (MATLAB, The MathWorks, Natick, MA, USA). For the simulation of the ordinary differential equations, the Runge-Kutta-based numeric solver 'ode45s', which is embedded in the MATLAB environment, was used. Parameter optimization was performed with the Nelder-Mead numerical algorithm implemented in the MATLAB embedded functions 'fmincon' and 'fminsearch'. All parameter optimizations (Tab. 1) were performed by minimizing the error of simulation data and measured data according to a least-square error function.

5.2.5.2 Graphing, regression analysis and measurement errors

Regression analysis of measured data, if applicable, was performed using scientific graphing and data analysis software (SigmaPlot, Systat Software Inc., San Jose, CA). Specific rhamnolipid production rates were calculated using a four-parameter logistic fit for biomass and rhamnolipid concentration [Müller *et al.* 2010]. All data and measurement results are presented as mean ± standard deviation from at least 5 independent experiments (biomass, rhamnolipid, nitrate, glycerol) or a minimum of 3 independent experiments (C_4-HSL, fatty acids, extracellular polymeric substances).

5.3 Results

5.3.1 Model set-up

The general model set-up is depicted in Fig. 5.1, which illustrates the consumption of substrates, product formation and regulation of product formation. The parameters, fitting ranges and initial conditions used in the optimized model are provided in Tab. 5.1 & 5.2.

5.3.1.1 Biomass growth

Growth of biomass concentration (c_X, Eq. 5.1)[1] was simulated as an autocatalytic process proportional to existing biomass concentration and the specific growth rate (μ_X). Biomass decay was assumed to follow a first-order degradation kinetic (k_d).

$$\frac{\mathrm{d}c_\mathrm{X}}{\mathrm{d}t} = \mu_\mathrm{X} \cdot c_\mathrm{X} - k_\mathrm{d} \cdot c_X \tag{5.1}$$

[1] In-text equation numbering has been changed from the original publication to include the chapter number (Eq. x has been changed to Eq. 5.x)

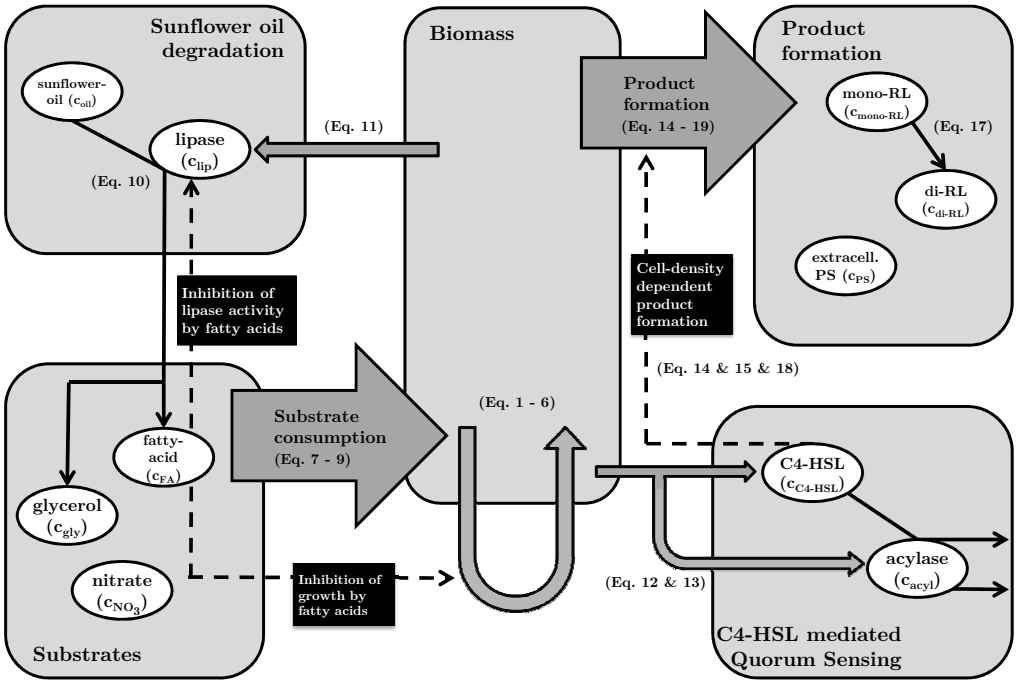

Figure 5.1: Overview of the model structure and interrelations of process variables. Corresponding equation numbers are displayed in brackets. Black arrows indicate reaction/conversion, black dashed arrows indicate influencing effects. Grey planar arrows indicate substrate uptake and conversion (rates). For reasons of simplicity, any substrate limitations (enzymatic or growth) in the dependencies are omitted. Substrates, products and intermediate species are represented by ellipses. Abbreviations: C_4-HSL – *N*-butyryl-homoserine lactone, RL – rhamnolipid, PS – (extracellular) polysaccharide. In-text equation numbering has been changed from the original publication to include the chapter number (Eq. x has been changed to Eq. 5.x)

The specific growth rate μ_X (Eq. 5.2) during cultivation on sunflower oil as a sole source of carbon and consequently the simultaneous consumption of both glycerol and fatty acids was implemented as the maximum of each individual specific growth rate on either glycerol or fatty acids, as if the other source of carbon were absent or depleted (see [Bader 1978] for an investigation on combining growth kinetics in a dual-substrate model). The concentration of fatty acids in the culture broth was found to have a significant effect on the growth rate up to a total inhibition of growth at levels above approx. 58 g/L (Fig. B.2). The growth kinetic of *P. aeruginosa* on fatty acids as a sole source of carbon showed good approximation (Fig. B.2) by an approach first described by Luong et al., which includes an inhibitory constant (K_i) – the concentration of substrate at which the culture ceases to grow – and a shape factor (n) which determines how strongly the effect of inhibition increases with increasing substrate concentration [Luong 1987].

$$\mu_X = \max\left\{\mu^{\mathrm{gly}}; \mu^{\mathrm{FA}}\right\} \cdot \left[1 - \left(\frac{c_{\mathrm{FA}}}{K_{\mathrm{i}}^{\mathrm{FA}}}\right)^{n}\right] \tag{5.2}$$

The specific growth rates for glycerol and fatty acids μ_{gly} and μ_{FA} (Eq. 5.3 & 5.4) were represented by the maximum specific growth rates on each substrate, affected by the strongest, relevant limitation expressed by a MONOD kinetic [Monod 1949].

$$\mu^{\mathrm{gly}} = \mu^{\mathrm{gly}}_{\mathrm{max}} \cdot \min\left\{ \frac{c_{\mathrm{gly}}}{c_{\mathrm{gly}} + K^{\mathrm{gly}}_{\mathrm{S}}}; \frac{c_{\mathrm{NO3}}}{c_{\mathrm{NO3}} + K^{\mathrm{NO3}}_{\mathrm{S}}} \right\} \tag{5.3}$$

$$\mu^{\mathrm{FA}} = \mu^{\mathrm{FA}}_{\mathrm{max}} \cdot \min\left\{ \frac{c_{\mathrm{FA}}}{c_{\mathrm{FA}} + K^{\mathrm{FA}}_{\mathrm{S}}}; \frac{c_{\mathrm{NO3}}}{c_{\mathrm{NO3}} + K^{\mathrm{NO3}}_{\mathrm{S}}} \right\} \tag{5.4}$$

5.3.1.2 Substrate consumption

To account for the simultaneous availability and consumption of both glycerol and fatty acids, the metabolic weights w_{gly} and w_{FA} (Eq. 5.5 & 5.6) were introduced, which were used to determine to what extent substrate consumed from each pool, by comparing growth rates (Eq. 5.3 & 5.4) of each individual substrate.

$$w_{\mathrm{gly}} = \frac{\mu^{\mathrm{gly}}}{\mu^{\mathrm{gly}} + \mu^{\mathrm{FA}}} \tag{5.5}$$

$$w_{\mathrm{FA}} = \frac{\mu^{\mathrm{FA}}}{\mu^{\mathrm{gly}} + \mu^{\mathrm{FA}}} = (1 - w^{\mathrm{gly}}) \tag{5.6}$$

The concentrations of the carbon sources c_{gly} and c_{FA} (Eq. 5.7 & 5.8) were calculated proportional to the reduction in oil concentration and the stoichiometric yields ($Y_{\mathrm{gly|oil}}$ and $Y_{\mathrm{FA|oil}}$) for glycerol and fatty acids, respectively, assuming an average molecular weight of sunflower oil (3 molecules of oleic acid + 1 molecule of glycerol) of 885.4 g/mol. Substrate consumption was simulated according to the production rates for biomass, rhamnolipids, extracellular polymeric substances and lipase and their respective experimental and theoretical yields allocated by the metabolic yields (w_{gly} and w_{FA}). To account for maintenance metabolism independent of cellular growth, substrate consumption proportional to current biomass concentration and maintenance coefficients ($m^{\mathrm{gly}}_{\mathrm{X}}$ and $m^{\mathrm{FA}}_{\mathrm{X}}$) were implemented.

$$\begin{aligned} \frac{\mathrm{d}c_{\mathrm{gly}}}{\mathrm{d}t} = &- Y_{\mathrm{gly|oil}} \cdot \frac{\mathrm{d}c_{\mathrm{oil}}}{\mathrm{d}t} - w_{\mathrm{gly}} \cdot (Y^{-1}_{\mathrm{X|gly}} \cdot \frac{\mathrm{d}c_{\mathrm{X}}}{\mathrm{d}t} + Y^{-1}_{\mathrm{Rl,m|gly}} \cdot \frac{\mathrm{d}c_{\mathrm{RL,m}}}{\mathrm{d}t} \\ &+ Y^{-1}_{\mathrm{RL,m\rightarrow RL,di|gly}} \cdot \frac{\mathrm{d}c_{\mathrm{RL,d}}}{\mathrm{d}t} + Y^{-1}_{\mathrm{PS|gly}} \cdot \frac{\mathrm{d}c_{\mathrm{PS}}}{\mathrm{d}t} + m^{\mathrm{gly}}_{\mathrm{X}} \cdot c_{\mathrm{X}}) \end{aligned} \tag{5.7}$$

$$\frac{\mathrm{d}c_{\mathrm{FA}}}{\mathrm{d}t} = -Y_{\mathrm{FA|oil}} \cdot \frac{\mathrm{d}c_{\mathrm{oil}}}{\mathrm{d}t} - w_{\mathrm{FA}} \cdot (Y^{-1}_{\mathrm{X|FA}} \cdot \frac{\mathrm{d}c_{\mathrm{X}}}{\mathrm{d}t} + Y^{-1}_{\mathrm{Rl,m|FA}} \cdot \frac{\mathrm{d}c_{\mathrm{RL,m}}}{\mathrm{d}t} + Y^{-1}_{\mathrm{RL,m\rightarrow RL,di|FA}} \cdot \frac{\mathrm{d}c_{\mathrm{RL,d}}}{\mathrm{d}t} + Y^{-1}_{\mathrm{PS|FA}} \cdot \frac{\mathrm{d}c_{\mathrm{PS}}}{\mathrm{d}t} + m^{\mathrm{FA}}_{\mathrm{X}} \cdot c_X) \tag{5.8}$$

The concentration of nitrate, c_{NO3} (Eq. 5.9), the sole source of nitrogen during cultivation, was assumed to be consumed only for biomass formation and production of extracellular protein, which was simplified and assumed to solely consist of lipase.

$$\frac{\mathrm{d}c_{\mathrm{NO3}}}{\mathrm{d}t} = -Y^{-1}_{\mathrm{X|NO3}} \cdot \frac{\mathrm{d}c_{\mathrm{X}}}{\mathrm{d}t} - Y^{-1}_{\mathrm{lip|NO3}} \cdot \frac{\mathrm{d}c_{\mathrm{lip}}}{\mathrm{d}t} \tag{5.9}$$

5.3.1.3 Volumetric lipase activity and oil degradation

Degradation of sunflower oil, c_{oil} (Eq. 5.10) was calculated proportional to the volumetric activity of extracellular lipases. Free fatty acids are assumed to have a negative effect on lipase activity [Smith and Alford 1966], and therefore a Michaelis-Menten model for reversible, competitive inhibition was assumed, which raises the half-saturation constant depending on the concentration of inhibitor.

$$\frac{\mathrm{d}c_{\mathrm{oil}}}{\mathrm{d}t} = -a^{\mathrm{lip}}_{\mathrm{sp}} \cdot c_{\mathrm{lip}} \cdot \frac{c_{\mathrm{oil}}}{c_{\mathrm{oil}} + K^{\mathrm{oil}}_{\mathrm{m}} \cdot (1 + \frac{c_{\mathrm{FA}}}{K^{\mathrm{oil}}_{\mathrm{i}}})} \tag{5.10}$$

Production of lipase, c_{lip} (Eq. 5.11), was expressed as the sum of a growth-associated rate (k_{growth}) and a basal production rate (k_{basal}). Due to excess sunflower oil, and consequently a continuous stimulus of hydrophobicity, lipase was assumed to be produced with maximum capacity proportional to newly formed biomass and protein. The basal production rate of lipase was implemented to allow for initial growth on hydrophobic substrates.

$$\frac{\mathrm{d}c_{\mathrm{lip}}}{\mathrm{d}t} = \left[k^{lip}_{\mathrm{growth}} \cdot \frac{\mathrm{d}c_{\mathrm{X}}}{\mathrm{d}t}\right] + \left[k^{\mathrm{lip}}_{\mathrm{basal}} \cdot c_{\mathrm{X}} \cdot \min\left\{\max\left\{\frac{c_{\mathrm{gly}}}{c_{\mathrm{gly}} + K^{\mathrm{gly}}_{\mathrm{S}}}; \frac{c_{\mathrm{FA}}}{c_{\mathrm{gly}} + K^{\mathrm{FA}}_{\mathrm{S}}}\right\}; \frac{c_{\mathrm{NO3}}}{c_{\mathrm{NO3}} + K^{\mathrm{NO3}}_{\mathrm{S}}}\right\}\right] \tag{5.11}$$

5.3.1.4 Quorum sensing dependent product formation

The concentration of *N*-butyryl-homoserine-lactone $c_{\mathrm{C4\text{-}HSL}}$ in the culture broth was simulated as described previously [Henkel *et al.* 2013] (Eq. 5.12 & 5.13), by calculation of a biomass specific C_4-HSL production rate ($q^{\mathrm{basal}}_{\mathrm{C4\text{-}HSL}}$) and degradation

dependent on the concentration of a putative extracellular C_4-HSL specific acylase c_{acyl}.

$$\frac{\mathrm{d}c_{\text{C4-HSL}}}{\mathrm{d}t} = \left[q^{\text{basal}}_{\text{C4-HSL}} \cdot c_{\text{X}}\right] - \left[\frac{k_{\text{cat}}}{K_{\text{m}}} \cdot c_{\text{acyl}} \cdot c_{\text{C4-HSL}}\right] \tag{5.12}$$

$$\frac{\mathrm{d}c_{\text{acyl}}}{\mathrm{d}t} = k_1^{\text{acyl}} \cdot c_{\text{X}} - k_2^{\text{acyl}} \cdot c_{\text{acyl}} \tag{5.13}$$

The simulated concentration of C_4-HSL according to Eq. 5.12 & 5.13 was then used to calculate the specific rhamnolipid production rate $q_{\text{mono-RL}}$ (Eq. 5.14), which was shown to correlate well with observed and simulated autoinducer levels (Chapter 4, [Henkel *et al.* 2013]). The coefficient $q^{\text{C4-HSL}}_{\text{mono-RL}}$ represents a C_4-HSL dependent positive effect on the rhamnolipid biosynthesis genes *rhlAB*, which are under control of the C_4-HSL/*rhl*-quorum sensing system [Soberón-Chávez *et al.* 2005a]. The specific conversion rate of mono-rhamnolipid to di-rhamnolipid $q_{\text{mono}\rightarrow\text{di}}$ (Eq. 5.15) was modeled in a similar manner, so that the coefficient $q^{\text{C4-HSL}}_{\text{mono}\rightarrow\text{di}}$ represents a C_4-HSL dependent positive effect on *rhlC*, the gene encoding for another rhamnosyltransferase, which facilitates the linkage of a second rhamnosyl group to a mono-rhamnolipid, thus resulting in the formation of a di-rhamnolipid. Expression of *rhlC* was furthermore found to be under control of the same promoter than *rhlAB*, and was therefore assumed to be affected by the concentration of C_4-HSL as well [Rahim *et al.* 2001]. Monod-kinetics for either glycerol or fatty acids were added to the equations to account for substrate limitation.

$$q_{\text{mono-RL}} = c_{\text{C4-HSL}} \cdot q^{\text{C4-HSL}}_{\text{mono-RL}} \cdot \max\left\{\frac{c_{\text{gly}}}{c_{\text{gly}} + K_{\text{S}}^{\text{gly}}}; \frac{c_{\text{FA}}}{c_{\text{gly}} + K_{\text{S}}^{\text{FA}}}\right\} \tag{5.14}$$

$$q_{\text{mono}\rightarrow\text{di}} = c_{\text{C4-HSL}} \cdot q^{\text{C4-HSL}}_{\text{mono}\rightarrow\text{di}} \cdot \max\left\{\frac{c_{\text{gly}}}{c_{\text{gly}} + K_{\text{S}}^{\text{gly}}}; \frac{c_{\text{FA}}}{c_{\text{gly}} + K_{\text{S}}^{\text{FA}}}\right\} \tag{5.15}$$

The formation of rhamnolipids $c_{\text{RL,mono}}$ and $c_{\text{RL,di}}$ (Eq. 5.16 & 5.17) was simulated using the specific rates and the biomass concentration (Eq. 5.14 & 5.15). Mono-rhamnolipid, which is converted to di-rhamnolipid, is removed from the pool of mono-rhamnolipids at a rate proportional to di-rhamnolipid formation and the respective stoichiometric yield ($Y_{\text{mono-RL|di-RL}}$). The conversion kinetic of mono-rhamnolipid to di-rhamnolipid was described with a Michaelis-Menten approach to account for substrate (mono-rhamnolipid) limitation.

$$\frac{\mathrm{d}c_{\text{RL,mono}}}{\mathrm{d}t} = q_{\text{mono-RL}} \cdot c_{\text{X}} - Y^{-1}_{\text{RL,d|RL,m}} \cdot \frac{\mathrm{d}c_{\text{RL,di}}}{\mathrm{d}t} \tag{5.16}$$

$$\frac{\mathrm{d}c_{\mathrm{RL,di}}}{\mathrm{d}t} = q_{\mathrm{mono\rightarrow di}} \cdot c_{\mathrm{X}} \cdot \frac{c_{\mathrm{RL,m}}}{c_{\mathrm{RL,m}} + K_{\mathrm{m}}^{\mathrm{mono\rightarrow di}}} \tag{5.17}$$

Since formation of extracellular polysaccharides is linked to the pathways of rhamnolipid precursor synthesis [Lindhout *et al.* 2009, Rahim *et al.* 2000], it was implemented in a similar manner, by calculating specific production rates q_{PS} (Eq. 5.18) and biomass-dependent product formation c_{PS} (Eq. 5.19).

$$q_{\mathrm{PS}} = c_{\mathrm{C4\text{-}HSL}} \cdot q_{\mathrm{PS}}^{\mathrm{C4\text{-}HSL}} \cdot \max\left\{ \frac{c_{\mathrm{gly}}}{c_{\mathrm{gly}} + K_{\mathrm{S}}^{\mathrm{gly}}}; \frac{c_{\mathrm{FA}}}{c_{\mathrm{gly}} + K_{\mathrm{S}}^{\mathrm{FA}}} \right\} \tag{5.18}$$

$$\frac{\mathrm{d}c_{\mathrm{PS}}}{\mathrm{d}t} = q_{\mathrm{PS}} \cdot c_{\mathrm{X}} \tag{5.19}$$

5.3.2 Model structure, parameter fitting and optimization

The model comprises a total of 36 parameters (Tab. 5.1), 12 of which are yield coefficients and 7 of which are substrate affinity and inhibition constants. Of all 36 parameters, 14 were derived from literature and databases, 8 were set fixed or derived from stoichiometry, 8 were determined experimentally and 6 were used as fitting parameters. As the first step, parameters for growth were determined experimentally, including maximum growth rates for both glycerol and fatty acids as well as the kinetic of growth inhibition by fatty acids. These parameters $\mathrm{K_i}^{\mathrm{FA}}$ and n according to Luong et al. [Luong 1987] were determined by fitting them to the experimental observations (see Fig. B.2). Degradation of oil was assumed to be affected by competitive product inhibition by fatty acids. Substrate affinity and activity of a *P. aeruginosa* lipase were taken from literature [Madan and Mishra 2010], while the inhibition constant for reversible competitive product inhibition $K_{\mathrm{i}}^{\mathrm{lip}}$ was used as a fitting parameter in the model. Time-course of C_4-HSL has been calculated as described previously [Henkel *et al.* 2013], and the biomass and C_4-HSL specific product formation rates for mono-rhamnolipid, di-rhamnolipid and extracellular polysaccharides were used as fitting parameters in the model. The simulation results for the applied reference batch process (250 g/L sunflower oil and 15 g/L sodium nitrate) with the set of optimized parameters (Tab. 5.1) are shown along with measurement data in Fig. 5.2. The simulations were performed with initial values of concentrations shown in Tab. 5.2, and displayed along with measurement data. Simulations were furthermore performed using the above mentioned model and parameter set to obtain predictions for a batch process with a 50% lower initial nitrate concentration (Fig. 5.3a) and a concentration of sunflower oil leading to substrate limitation of 60 g/L (Fig. 5.3b) by using different initial conditions for the simulations (Tab. 5.1).

Table 5.1: Parameters and fitting ranges used in the model

Parameter	Value	Unit	Range	Comment/source
Biomass and growth kinetics				
$\mu_{\max}^{\text{gly}}$	0.33	1/h	0.25-0.35	Experimental results
$\mu_{\max}^{\text{FA}}$	0.16	1/h	0.15-0.20	Experimental results
K_{i}^{FA}	58	g/L	55-60	Experimental results, Fig. B.2
n	0.44	-	0.40-0.60	Experimental results, Fig. B.2
$K_{\text{S}}^{\text{gly}}$	0.005	g/L	-	Fixed substrate affinity
K_{S}^{FA}	0.005	g/L	-	Fixed substrate affinity
$K_{\text{S}}^{\text{NO3}}$	0.005	g/L	-	Fixed substrate affinity
k_{d}	0.0022	1/h	-	Experimental results
Substrate consumption				
$Y_{\text{gly\|oil}}$	0.1049	g/g	–	Stoichiometry
$Y_{\text{FA\|oil}}$	0.9567	g/g	–	Stoichiometry
$Y_{\text{X\|gly}}$	0.23	g/g	0.2–0.5	Experimental results
$Y_{\text{X\|FA}}$	0.74	g/g	0.5–1.0	Experimental results
$Y_{\text{RL,m\|gly}}$	0.56	g/g	–	Calc., [Henkel *et al.* 2012]
$Y_{\text{RL,m\|FA}}$	1.17	g/g	–	Calc., [Henkel *et al.* 2012]
$Y_{\text{RL,m}\rightarrow\text{RL,di\|gly}}$	3.302	g/g	–	Calc., [Henkel *et al.* 2012]
$Y_{\text{RL,m}\rightarrow\text{RL,di\|FA}}$	6.96	g/g	–	Calc., [Henkel *et al.* 2012]
$Y_{\text{PS\|gly}}$	0.86	g/g	–	Calc., [Borgos *et al.* 2013]
$Y_{\text{PS\|FA}}$	0.82	g/g	0.5–1.0	Fitting parameter
$m_{\text{X}}^{\text{gly}}$	0.093	g/(g·h)	–	[Verstraete and Voets 1978]
m_{X}^{FA}	0.048	g/(g·h)	–	[Verstraete and Voets 1978]
$Y_{\text{X\|NO3}}$	1.41	g/g	–	Calc., [Müller *et al.* 2010]
$Y_{\text{lip\|NO3}}$	1.33	g/g	–	Stoichiometry
Lipase activity and oil degradation				
$K_{\text{m}}^{\text{lip}}$	0.133	g/L	–	[Madan and Mishra 2010]
$a_{\text{sp}}^{\text{lip}}$	1.377	$g_{\text{oil}}/(mg_{\text{lip}}\cdot h)$	–	[Madan and Mishra 2010]
$k_{\text{growth}}^{\text{lip}}$	0.267	$mg_{\text{lip}}/g_{\text{BM}}$	0.1–5.0	Fitting parameter, Fig. B.4
$k_{\text{basal}}^{\text{lip}}$	$1 \cdot 10^{-4}$	$mg_{\text{lip}}/(g_{\text{BM}}\cdot h)$	–	Fixed
$K_{\text{i}}^{\text{lip}}$	0.021	g/L	0.001–1.0	Fitting parameter, Fig. B.4
Quorum sensing-dependent product formation				
$q_{\text{C4-HSL}}^{\text{basal}}$	0.763	$\mu mol_{\text{C4-HSL}}/(g_{\text{BM}}\cdot h)$	–	[Henkel *et al.* 2013]
$k_{\text{cat}}/K_{\text{m}}$	5.04	$L/(\mu mol_{\text{acyl}}\cdot h)$	–	[Henkel *et al.* 2013]
k_1^{acyl}	$1.43 \cdot 10^{-4}$	$\mu mol_{\text{acyl}}/(g_{\text{BM}}\cdot h)$	–	[Henkel *et al.* 2013]
k_2^{acyl}	$0.73 \cdot 10^{-2}$	h^{-1}	–	[Henkel *et al.* 2013]
$q_{\text{mono-RL}}^{\text{C4-HSL}}$	$8.27 \cdot 10^{-4}$	$g_{\text{RL}}\cdot L/(\mu mol_{\text{C4-HSL}}\cdot g_{\text{BM}}\cdot h)$	$10^{-4} - 10^{-3}$	Fitting parameter
$q_{\text{mono-RL}\rightarrow\text{di-RL}}^{C4-HSL}$	$6.52 \cdot 10^{-4}$	$g_{\text{RL}}\cdot L/(\mu mol_{\text{C4-HSL}}\cdot g_{\text{BM}}\cdot h)$	$10^{-4} - 10^{-3}$	Fitting parameter
$q_{\text{PS}}^{\text{C4-HSL}}$	$9.11 \cdot 10^{-4}$	$g_{\text{RL}}\cdot L/(\mu mol_{\text{C4-HSL}}\cdot g_{\text{BM}}\cdot h)$	$10^{-4} - 10^{-3}$	Fitting parameter
$K_{\text{m}}^{\text{mono}\rightarrow\text{di}}$	0.001	g/L	-	Fixed
$Y_{\text{RL,di\|RL,mono}}$	1.29	g/g	-	Stoichiometry

Table 5.2: Initial conditions used for the simulation of the reference batch process. Values for simulations of validation experiments are given in brackets

Condition	Value	Unit
c^0_{BM}	0.05	g/L
$c^0_{\text{mono-RL}}$	$8 \cdot 10^{-3}$	g/L
$c^0_{\text{di-RL}}$	$8 \cdot 10^{-3}$	g/L
c^0_{PS}	0.01	g/L
c^0_{oil}	250 (60)	g/L
c^0_{gly}	$1 \cdot 10^{-3}$	g/L
c^0_{FA}	1.46	g/L
c^0_{lip}	0.043	mg/L
c^0_{NO3}	10.94 (5.47)	g/L
c^0_{acyl}	$6 \cdot 10^{-7}$	µmol/L
$c^0_{\text{C4-HSL}}$	$1 \cdot 10^{-3}$	µmol/L

Fig. 5.3 shows the simulations for both validations scenarios along with measurement data provided for all simulations.

5.3.3 Partial model for biomass growth

One of the main challenges related to the development of the model was the description of a dual-substrate growth behavior. While dual-substrate growth models have been addressed in the past [Bader 1978], there is still no convincing approach for dealing with multiple substrate systems. As the basis of biomass growth, an exponential growth model (Eq. 5.1) with biomass production proportional to existing biomass and biomass decay was assumed. This is in much better agreement with the biological background than currently widely employed mathematical descriptions, which assume a logistic growth curve. The growth rate was implemented as a function of both substrate concentrations, glycerol and fatty acids, combined with experimental observations on growth at high levels of fatty acids, which was found to be represented well by an inhibition kinetic according to Luong et al. (see also Fig. B.2). Glycerol was successfully assumed not to have a significant negative effect on growth rate up to concentrations of 50 g/L (Fig. B.3). Since these concentrations are by far not reached in the examined process, an inhibition kinetic for glycerol was omitted.

While both individual specific growth rates on glycerol and fatty acids are calculated separately (Eq. 5.3 and 5.4), a biologically viable method for combining both rates to an effective growth rate was required. Combining both individual growth rates by multiplicative means results in effective growth rates which are too low at non-substrate saturated concentrations, as compared to biological observations,

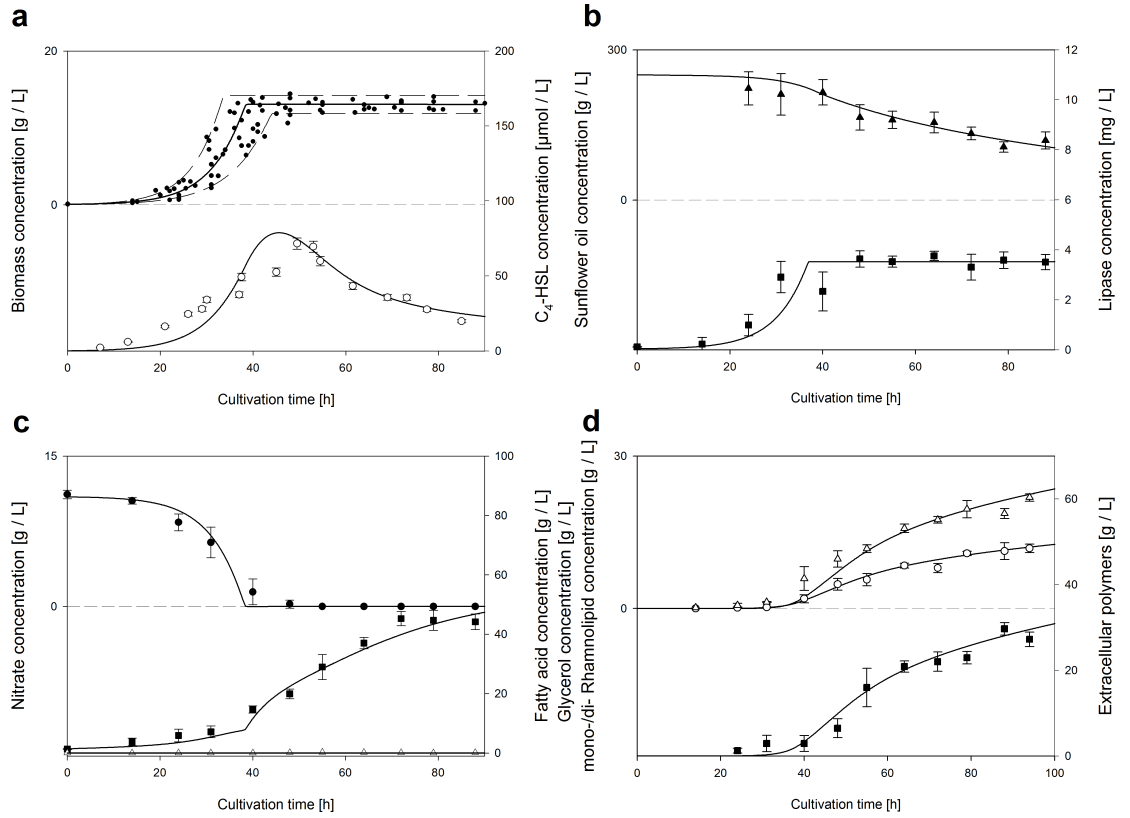

Figure 5.2: Simulation results (solid lines) and measurements of the batch process using optimized parameters as shown in Tab. 5.1. (a) Biomass, top graph and C_4-HSL concentration (as described previously by [Henkel *et al.* 2013]), bottom graph. Dashed lines indicate simulation allowing a maximum error of 10% for maximum growth rate (μmax), initial biomass concentration and nitrate-to-biomass yield ($Y_{X|NO3}$) (b) Sunflower oil, top graph and lipase concentration, bottom graph (c) Nitrate, top graph and fatty acid concentration, bottom graph (d) Mono-/di-rhamnolipid, top graph and extracellular polysaccharide, bottom graph

since both limiting effects are amplified [Bader 1978]. In comparison, an additive combination of both individual growth rates is not viable from a biological point of view, since the presence of a second substrate does not necessarily lead to enhanced growth, since intracellular pathways involved in anabolism may already be saturated and therefore adding another substrate may lead to no or only a partial enhancement of growth.

To circumvent the known shortcomings of both approaches, minimum and maximum operators were applied in the calculation of the effective growth rate. Substrate limitations were assumed to follow standard Monod-kinetics, and were implemented in the calculation of the individual growth rates for glycerol and fatty acids, respectively (Eq. 5.3 & 5.4), and combined with nitrate limitation using a minimum operator, so that only the strongest limitation is affecting growth. Both rates are then joined together using a maximum operator, so that growth occurs with a highest rate bio-

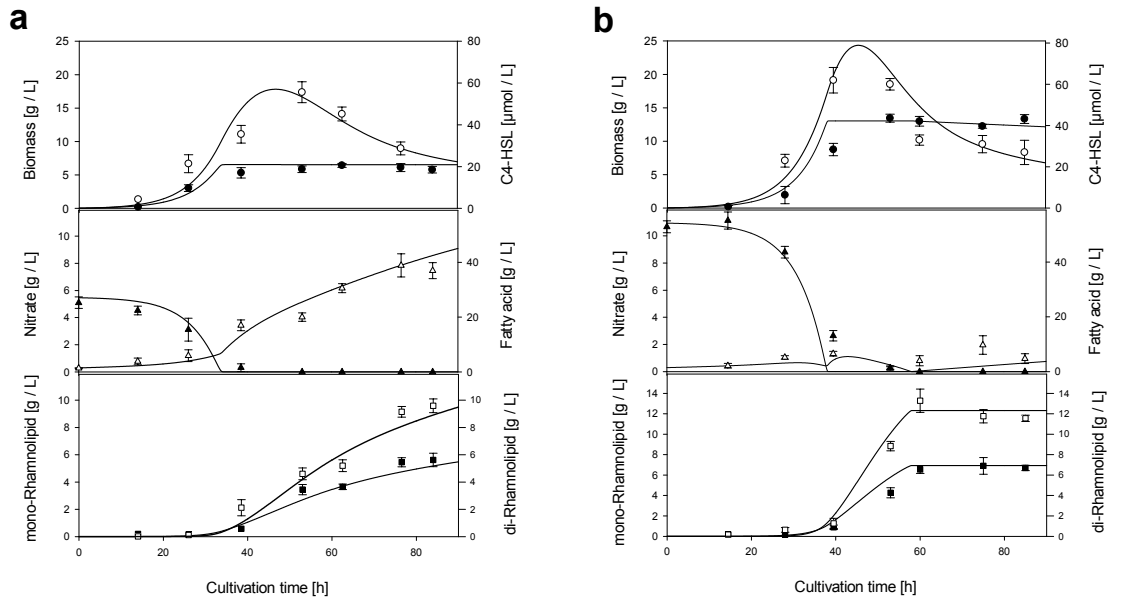

Figure 5.3: Experimental validation experiments and corresponding simulations obtained from the model simulations. Simulations (solid lines) and measured data are provided for scenarios with different initial conditions. Filled circles: biomass, empty circles: C_4-HSL, filled triangles: nitrate, empty triangles: fatty acid, filled squares: mono-rhamnolipid, empty squares: di-rhamnolipid. (a) Process with a nitrate concentration reduced to 50% of the initial value. (b) Process with sunflower oil reduced from a concentration in excess of 250 g/L to 60 g/L

logically possible. While other effects, e.g. phosphate concentration, may also play a role in affecting growth, the model in this simplified form was found to sufficiently describe the experimental data. The model shows good correlation with the measured data (Fig. 5.2a, top graph, solid line), however, the system is highly sensitive resulting from either measurements errors or a prolonged lag-phase, which becomes evident when assuming 10% higher (respectively 10% lower) maximum growth rates, initial biomass concentration and nitrogen-to-biomass yields (Fig. 5.2a, top graph, dashed lines). The measured data suggests that by allowing for these deviations, the experimental scenario can be represented well. These effects of potential lag-phases and measurement errors during the inoculation process are also the reason for generally higher relative standard deviations during the time at which the biggest changes in total biomass concentration occur, from approximately t = 20 - 40 h.

5.3.4 Partial model for substrate consumption

Another major challenge in modeling bioprocesses with two substrates which are consumed simultaneously is the allocation of the total consumption rate to both pools of substrates. The consumption of glycerol and fatty acids is implemented as separate equations (Eq. 5.7 & 5.8). Since yields and growth kinetics are different for both substrates, no further simplification to this was applied. The ratio of consu-

med glycerol and fatty acids is represented by calculating metabolic weights from the individual growth rates (Eq. 5.5 & 5.6). The weights are used to allocate the amount of each substrate consumed for growth, product formation and maintenance according to the yield coefficients, which were determined experimentally, calculated theoretically or derived from stoichiometry (Tab. 5.1).

5.3.5 Partial model for oil degradation by lipase activity

There are several different lipases known to be secreted by *P. aeruginosa*, among them the most prominent members LipA and LipC [Gilbert 1993, Martinez *et al.* 1999]. These individual lipases also exhibit different substrate specificity for mono-/di-/tri-gylcerides as well as different activities, and they are believed to produce different products with different specificity (e.g. 1,2-diacylglyceride vs. 1,3-diacylglyceride). Even though lipases from *Pseudomonas* sp. have been the target of investigation in several studies, only very few kinetic parameters are known, which would be required to characterize the degradation of oil in this system. To develop a basis for modeling oil degradation, this system was simplified by assuming only one pool of total lipase activity, which contains the concerted action of all secreted lipases. This lipase activity was assumed to act on pure triacylglyceride of an averaged composition and molar mass. To further reduce the complexity of the model, substrate specificity of lipases along with all intermediate products (mono-/di-/tri-glycerides) were eliminated from the model, resulting in the simultaneous release of glycerol and fatty acids proportional to the decrease in the triglyceride pool. Lipase activity is generally reported to be reduced in presence of free fatty acids, by blocking of the binding sites for the carbon chains of triglycerides [Smith and Alford 1966]. A Michaelis-Menten model with competitive reversible product inhibition was therefore assumed to describe lipase activity (Eq. 5.10). This dramatically simplified model showed good correlation with measured data in the reference process (Fig. 5.2b & 5.2c) as well as the validation scenarios (Fig. 5.3a & 5.3b). Interestingly it also provides a good approximation for glycerol released during cultivation (Fig. B.4), which could not be described by a multi-step kinetic model for degradation of glycerides. The assumption of a multi-step kinetic model would result in the accumulation of digylycerides before monoglycerides, and fatty acids would predominantly be formed rather than glycerol due to a vast excess of triglyceride substrate. One reason for this could be the concerted action of different lipases, which show different specificity for the individual glycerides. This effect may further be enhanced by different expression rates or enzymatic activities, which may also further be affected by steric effects of the substrate-enzyme complex. The inhibitory effect of fatty acids on lipase activity was furthermore investigated experimentally (Fig. B.5), and the qualitative relationship could be confirmed by the

measured data. However, experimentally determined activities are constantly lower than the simulated kinetic with optimized parameters. This may be due to different reaction conditions in the assay when compared to the bioreactor, where excessive emulsification promotes the formation of a much larger total interface which may benefit the catalyzing action of lipase.

5.3.6 Implementing Quorum sensing dependent product formation

C_4-HSL autoinducer concentration was estimated using the time-course of biomass concentration, combined with degradation by a putative acylase as described previously [Henkel *et al.* 2013]. The specific rhamnolipid production rate was then calculated proportional to C_4-HSL levels in the culture broth. With a total of only 6 fitting parameters out of 36 total parameters, the model is highly correlated with experimental data and based on experimental observations, which played a major part in the development.

5.4 Discussion

The model-based simulation of q_{RL} as calculated from the model shows a similar time-course as compared to the logistic fit (Fig. 5.4). Both curves suggest a maximum specific production rate of approx. 0.06 $g_{RL}/(g_{BM}{\cdot}h)$ at $t \approx 45$ h. However, during the first half of the cultivation until approx. $t = 40$ h, q_{RL} from the model deviates from the experimental fit. This can be explained by the mathematical origin of the time-course of q_{RL} calculated from logistic fits, which displays a steep slope in the first 45 hours up until the inflection point at $t \approx 45$ h, while q_{RL} from the model suggests a different time-course. Since the biomass concentration is comparably low in the first hours of cultivation, this does not play a major role when calculating the rhamnolipid concentration from q_{RL} origination from the logistic fits. The simulation of q_{RL} however seems to be in better agreement with the biological assumption of an induced rhamnolipid synthesis after a sufficient cell-density has been reached. This is also supported by gene expression data of *rhlA* (Fig. 5.4), as described previously for this process [Schmidberger *et al.* 2013], which precedes the time-course of q_{RL} as simulated by the model.

Besides the coupling to quorum sensing mechanisms, nitrogen limitation was shown to affect rhamnolipid formation via the sigma factor RpoN [Rahim *et al.* 2001]. However, it was suggested that during the investigated process, the effect of nitrogen limitation on rhamnolipid production rate is not among the main influencing mechanisms, since highest specific rhamnolipid production rates were observed at non-limiting concentrations of nitrogen in the culture broth [Müller *et al.* 2010]. It was

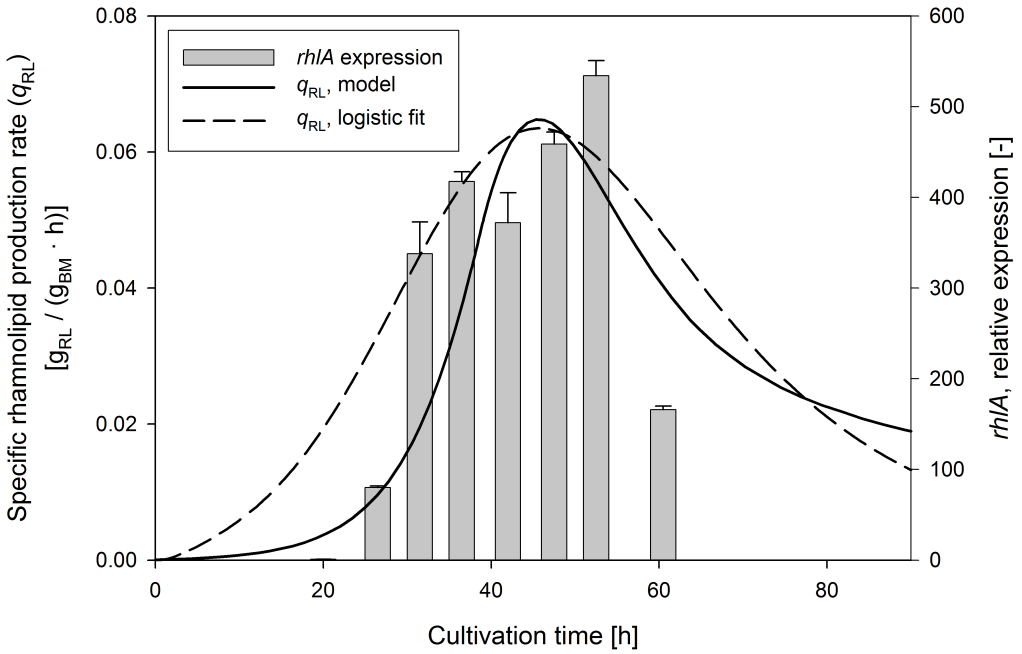

Figure 5.4: Specific rhamnolipid production rate (q_{RL}) as simulated by the modeling (solid line) and calculated by logistic fits of experimental data on rhamnolipid and biomass concentration [Müller *et al.* 2010] over the time-course of *rhlA* gene expression, as described previously for this process [Schmidberger *et al.* 2013]

furthermore shown that gene expression levels during this process could confirm this observations, since expression of sigma factor N was almost unaffected by nitrogen limitation during cultivation [Schmidberger *et al.* 2013]. Due to these observations, the direct effect of nitrogen starvation on rhamnolipid formation was omitted from the model, and nitrogen limitation contributes only indirectly to rhamnolipid formation rates by limiting growth and therefore autoinducer levels (Eq. 5.3 & 5.4). De Lima et al. [de Lima *et al.* 2009] developed a model of rhamnolipid production in the past by using an expression proportional to biomass growth. This has the major advantage of the model being comparably simple, since only 1 parameter is required for every simulate product or substrate, respectively. However, this approach is usually accompanied by a major disadvantage of the inaccuracy and inability to describe certain biological phenomena. This can be overcome for example by introducing enzyme kinetics, which require at least 2 parameters to describe a limitation (e.g. maximum rate and substrate affinity of the Michaelis-Menten model). Another advantage of the simple model assuming proportionalities is that one does not need to differentiate between yields (e.g. substrate required for biomass formation versus substrate required for product formation), since every variable is coupled to biomass. In a complex process model however, as described in this study, yields for each pair of susbtrate and product are required. Since some yields are generally difficult to

determine experimentally, approximations or theoretical assumptions are required. Existing models for rhamnolipid production are not based on experimental observations and biological assumptions. In this study, a model is described which takes 30 out of 36 parameters from experimental or theoretical measurements or calculations, while solely the other 6 parameters are used as fitting parameters. Current models are also based on a predetermined time-course for biomass concentration, e.g., [DE LIMA *et al.* 2009]. In this study, a model is discussed, which does not rely on the representation of biomass by measured data and a logistic fit. This allows for the simulation and investigation of biological interrelations, interactions or feedback loops. The model presented in this study is a first mathematical description of rhamnolipid formation in a bioreactor as a process model, which accounts for interrelation of variables. It also calculates and utilizes cell-density dependent regulatory mechanisms to describe rhamnolipid formation rate during the process.
In this chapter, experimental observations on lipases from *P. aeruginosa* have been used to derive a simplified model for triglyceride hydrolysis in the culture broth to describe formation of glycerol and fatty acids. As a result, a negative feedback of fatty acid concentration on growth and lipase activity has been implemented. Using the example of rhamnolipid from *P. aeruginosa*, it was demonstrated that knowledge-based modeling using tailored experiments led to a better understanding of complex biological process. This understanding is a crucial component for the development of knowledge-based, optimized process control strategies, which are discussed in Chapter 6.

References for Chapter 5

[Ayers 1956] Ayers, C. W. (1956). Estimation of the Higher Fatty Acids C7-C18. *Analytica Chimica Acta*, 15(1), pp. 77–83.

[Bader 1978] Bader, F. G. (1978). Analysis of double-substrate limited growth. *Biotechnology and Bioengineering*, 20(2), pp. 183–202.

[Baker 1964] Baker, D. (1964). Colorimetric method for determining free fatty acids in vegetable oils. *Journal of the American Oil Chemists Society*, 41(1), pp. 21–22.

[Borgos *et al.* 2013] Borgos, S. E. F., Bordel, S., Sletta, H., Ertesvag, H., Jakobsen, O., Bruheim, P., Ellingsen, T. E., Nielsen, J., and Valla, S. (2013). Mapping global effects of the anti-sigma factor MucA in *Pseudomonas fluorescens* SBW25 through genome-scale metabolic modeling. *BMC Systems Biology*, 7(19).

[Cha *et al.* 2008] Cha, M., Lee, N., Kim, M., and Lee, S. (2008). Heterologous production of *Pseudomonas aeruginosa* EMS1 biosurfactant in *Pseudomonas putida*. *Bioresource Technology*, 99(7), pp. 2192–2199.

[Chen *et al.* 2004] Chen, F., Chen, C. C., Riadi, L., and Ju, L. K. (2004). Modeling rhl quorum sensing regulation on rhamnolipid production by *Pseudomonas aeruginosa*. *Biotechnology Progress*, 20(5), pp. 1325–1331.

[Du *et al.* 2011] Du, H. J., Xu, Z. L., Shrout, J. D., and Alber, M. (2011). Multiscale modeling of *Pseudomonas aeruginosa* swarming. *Mathematical Models & Methods in Applied Sciences*, 21(1), pp. 939–954.

[Eswari *et al.* 2013] Eswari, J. S., Anand, M., and Venkateswarlu, C. (2013). Optimum culture medium composition for rhamnolipid production by *Pseudomonas aeruginosa* AT10 using a novel multi-objective optimization method. *Journal of Chemical Technology and Biotechnology*, 88(2), pp. 271–279.

[Gilbert 1993] Gilbert, E. J. (1993). *Pseudomonas* lipases - biochemical-properties and molecular-coning. *Enzyme and Microbial Technology*, 15(8), pp. 634–645.

[Henkel *et al.* 2012] Henkel, M., Müller, M. M., Kügler, J. H., Lovaglio, R. B., Contiero, J., Syldatk, C., and Hausmann, R. (2012). Rhamnolipids as biosurfactants from renewable resources: Concepts for next-generation rhamnolipid production. *Process Biochemistry*, 47(8), pp. 1207–1219.

[Henkel *et al.* 2013] Henkel, M., Schmidberger, A., Kühnert, C., Beuker, J., Bernard, T., Schwartz, T., Syldatk, C., and Hausmann, R. (2013). Kinetic modeling of the time course of *N*-butyryl-homoserine lactone concentration during batch cultivations of *Pseudomonas aeruginosa* PAO1. *Applied Microbiology and Biotechnology*, 97(17), pp. 7607–16.

[Hentzer *et al.* 2003] Hentzer, M., Wu, H., Andersen, J. B., Riedel, K., Rasmussen, T. B., Bagge, N., Kumar, N., Schembri, M. A., Song, Z. J., Kristoffersen, P., Manefield, M., Costerton, J. W., Molin, S., Eberl, L., Steinberg, P., Kjelleberg, S., Hoiby, N., and Givskov, M. (2003). Attenuation of *Pseudomonas aeruginosa* virulence by quorum sensing inhibitors. *EMBO Journal*, 22(15), pp. 3803–3815.

[Latifi *et al.* 1995] Latifi, A., Winson, M. K., Foglino, M., Bycroft, B. W., Stewart, G. S. A. B., Lazdunski, A., and Williams, P. (1995). Multiple homologs of Luxr and Luxl control expression of virulence determinants and secondary metabolites through quorum sensing in *Pseudomonas aeruginosa* PAO1. *Molecular Microbiology*, 17(2), pp. 333–343.

[de Lima *et al.* 2009] de Lima, C. J. B., Ribeiro, E. J., Servulo, E. F. C., Resende, M. M., and Cardoso, V. L. (2009). Biosurfactant production by *Pseudomonas aeruginosa* grown in residual soybean oil. *Applied Biochemistry and Biotechnology*, 152(1), pp. 156–168.

[Lindhout *et al.* 2009] Lindhout, T., Lau, P. C. Y., Brewer, D., and Lam, J. S. (2009). Truncation in the core oligosaccharide of lipopolysaccharide affects flagella-mediated motility in *Pseudomonas aeruginosa* PAO1 via modulation of cell surface attachment. *Microbiology*, 155(1), pp. 3449–3460.

[Luo *et al.* 2013] Luo, Z., Yuan, X. Z., Zhong, H., Zeng, G. M., Liu, Z. F., Ma, X. L., and Zhu, Y. . (2013). Optimizing rhamnolipid production by *Pseudomonas aeruginosa* ATCC 9027 grown on waste frying oil using response surface method and batch-fed fermentation. *Journal of Central South University*, 20(4), pp. 1015–1021.

[Luong 1987] Luong, J. H. T. (1987). Generalization of Monod kinetics for analysis of growth data with substrate-inhibition. *Biotechnology and Bioengineering*, 29(2), pp. 242–248.

[Madan and Mishra 2010] Madan, B. and Mishra, P. (2010). Co-expression of the lipase and foldase of *Pseudomonas aeruginosa* to a functional lipase in *Escherichia coli*. *Applied Microbiology and Biotechnology*, 85(3), pp. 597–604.

[Martinez *et al.* 1999] Martinez, A., Ostrovsky, P., and Nunn, D. N. (1999). LipC, a second lipase of *Pseudomonas aeruginosa*, is LipB and Xcp dependent and is transcriptionally regulated by pilus biogenesis components. *Molecular Microbiology*, 34(2), pp. 317–326.

[Medina-Moreno *et al.* 2011] Medina-Moreno, S. A., Jimenez-Islas, D., Gracida-Rodriguez, J. N., Gutierrez-Rojas, M., and Diaz-Ramirez, I. J. (2011). Modeling rhamnolipids production by *Pseudomonas aeruginosa* from immiscible carbon source in a batch system. *International journal of environmental science and technology*, 8(3), pp. 471–482.

[Müller *et al.* 2010] Müller, M., Hörmann, B., Syldatk, C., and Hausmann, R. (2010). *Pseudomonas aeruginosa* PAO1 as a model for rhamnolipid production in bioreactor systems. *Applied Microbiology and Biotechnology*, 87(1), pp. 167–174.

[Monod 1949] Monod, J. (1949). The growth of bacterial cultures. *Annual Review of Microbiology*, 3(1), pp. 371–394.

[Ochsner *et al.* 1995] Ochsner, U. A., Reiser, J., Fiechter, A., and Witholt, B. (1995). Production of *Pseudomonas aeruginosa* rhamnolipid biosurfactants in heterologous hosts. *Applied and Environmental Microbiology*, 61(9), pp. 3503–3506.

[Rahim *et al.* 2000] Rahim, R., Burrows, L. L., Monteiro, M. A., Perry, M. B., and Lam, J. S. (2000). Involvement of the *rml* locus in core oligosaccharide and O polysaccharide assembly in *Pseudomonas aeruginosa*. *Microbiology - Society for General Microbiology*, 146, pp. 2803–2814.

[Rahim *et al.* 2001] Rahim, R., Ochsner, U. A., Olvera, C., Graninger, M., Messner, P., Lam, J. S., and Soberón-Chávez, G. (2001). Cloning and functional characterization of the *Pseudomonas aeruginosa rhlC* gene that encodes rhamnosyltransferase 2, an enzyme responsible for di-rhamnolipid biosynthesis. *Molecular Microbiology*, 40(3), pp. 708–718.

[Schenk *et al.* 1995] Schenk, T., Schuphan, I., and Schmidt, B. (1995). High-performance liquid-chromatographic determination of the rhamnolipids produced by *Pseudomonas aeruginosa*. *Journal of Chromatography A*, 693(1), pp. 7–13.

[Schmidberger *et al.* 2013] Schmidberger, A., Henkel, M., Hausmann, R., and Schwartz, T. (2013). Expression of genes involved in rhamnolipid synthesis in *Pseudomonas aeruginosa* PAO1 in a bioreactor cultivation. *Applied Microbiology and Biotechnology*, 97(13), pp. 5779–5791.

[Smith and Alford 1966] Smith, J. L. and Alford, J. A. (1966). Inhibition of microbial lipases by fatty acids. *Journal of Applied Microbiology*, 14(5), pp. 699–700.

[Soberón-Chávez *et al.* 2005] Soberón-Chávez, G., Aguirre-Ramirez, M., and Ordonez, L. (2005). Is *Pseudomonas aeruginosa* only 'sensing quorum'? *Critical Reviews in Microbiology*, 31(3), pp. 171–182.

[Stover *et al.* 2000] Stover, C. K., Pham, X. Q., Erwin, A. L., Mizoguchi, S. D., Warrener, P., Hickey, M. J., Brinkman, F. S., Hufnagle, W. O., Kowalik, D. J., Lagrou, M., Garber, R. L., Goltry, L., Tolentino, E., Westbrock-Wadman, S., Yuan, Y., Brody, L. L., Coulter, S. N., Folger, K. R., Kas, A., Larbig, K., Lim, R., Smith, K., Spencer, D., Wong, G. K., Wu, Z., Paulsen, I. T., Reizer, J., Saier, M. H., Hancock, R. E., Lory, S., and Olson, M. V. (2000). Complete genome sequence of *Pseudomonas aeruginosa* PAO1, an opportunistic pathogen. *Nature*, 406(6799), pp. 959–964.

[Trummler *et al.* 2003] Trummler, K., Effenberger, F., and Syldatk, C. (2003). An integrated microbial/enzymatic process for production of rhamnolipids and L-(+)-rhamnose from rapeseed oil with *Pseudomonas sp.* DSM 2874. *European Journal of Lipid Science and Technology.*, 105(10), pp. 563–571.

[Verstraete and Voets 1978] Verstraete, W. and Voets, J. P. (1978). Evaluation of yield and maintenance coefficients, expressed in carbon units, for *Pseudomonas fluorescens* and *Pseudomonas aeruginosa*. *Zeitschrift für Allgemeine Mikrobiologie*, 18(2), pp. 135–141.

6. Application of the model: an optimized fed-batch process

In this chapter, it is described how a feeding strategy leading to optimized rhamnolipid formation was developed using the kinetic model for the batch process ([Henkel *et al.* 2014], Chapter 5), the mathematical description of cell-density-dependent rhamnolipid formation ([Henkel *et al.* 2013], Chapter 4) and theoretical yields obtained from metabolic balancing ([Henkel *et al.* 2012], Chapter 3).

6.1 Development of a feeding strategy

One of the main factors influencing growth in the investigated batch process is the accumulation of fatty acids in the culture broth due to an excess of sunflower oil [Müller *et al.* 2010, Henkel *et al.* 2014]. This negative effect on the growth rate was attributed an indirect connection to the rhamnolipid production rate via the formation of biomass and the biomass-specific build-up of C_4-HSL signaling molecules, which induce rhamnolipid formation (Fig. 6.1 and Chapter 5, Eq. 5.12 - 5.17). The model for the batch process, which includes a description of triglyceride hydrolysis by simulating lipase activity in the culture broth, was used to calculate a sunflower oil feeding strategy leading to a significantly lower fatty acid concentration in simulations (Fig. 6.2). The sunflower oil feed rate was obtained using a simulated proportional controller for the oil concentration. The output of the controller was the sunflower oil feed rate, proportional to the deviation between a chosen setpoint of 5 g/L and the current simulated oil concentration. The proportional gain K_p was set to 50 h^{-1}. While the simulation of the batch process (Fig. 6.2, dashed line) predicts free fatty acids reaching levels above 40 g/L after approx. 80 h of cultivation, the simulated fed-batch process using the calculated sunflower oil feed predicts concentrations of free fatty acids constantly below 5 g/L (Fig. 6.2, dotted line).

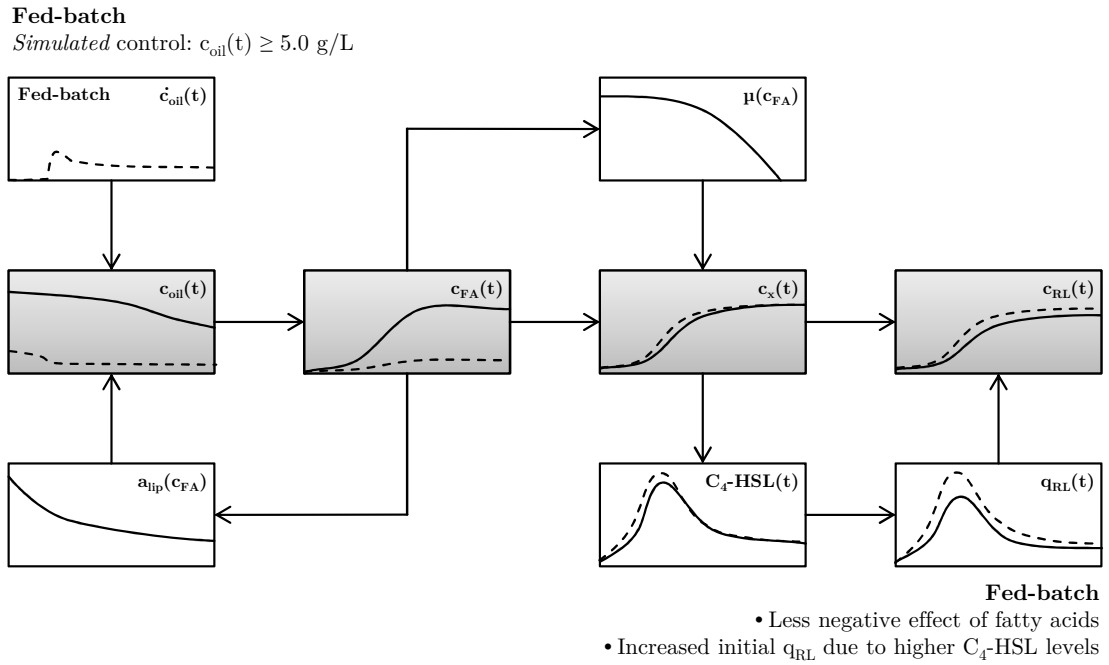

Figure 6.1: Overview of the concept of a fed-batch process (dashed lines) with controlled addition of sunflower oil compared to the batch process (solid lines) to minimize the inhibitory effect of fatty acids.

The process was designed to start with a significantly lower inital concentration of sunflower oil of less than 1/10th of the concentration used in the batch process (20 g/L versus 250 g/L). The simulated control strategy was obtained from the model

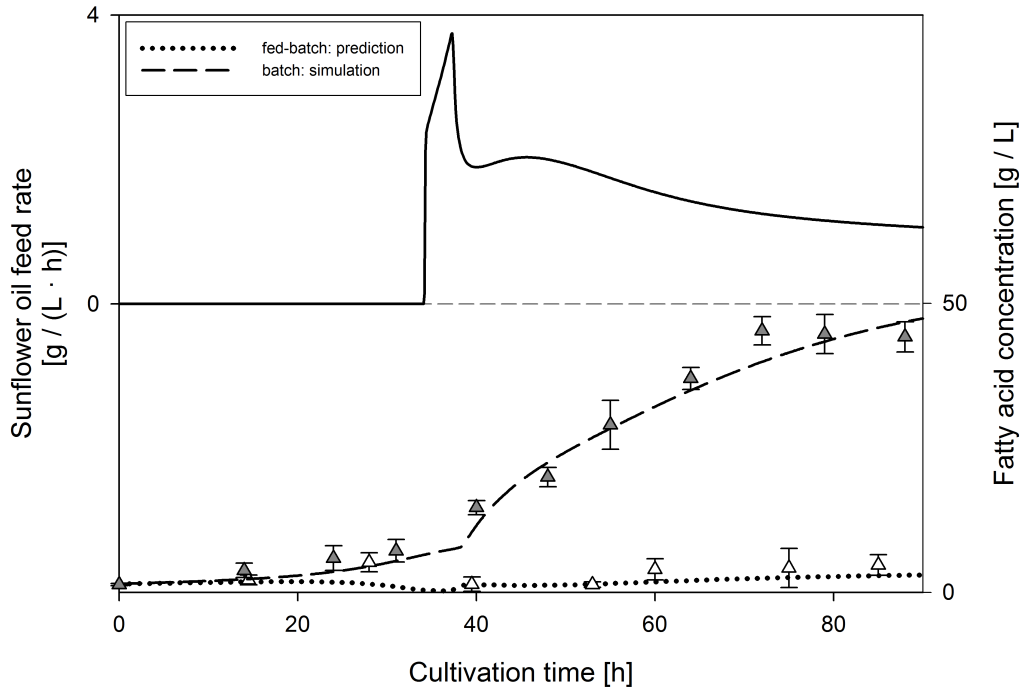

Figure 6.2: Sunflower oil feed rate obtained by simulated control using the process model (Chapter 5) aimed at keeping free sunflower oil constant at 5 g/L (top graph). A proportional controller ($K_p = 50$ h^{-1}) was used to calculate the feeding profile using the simulated sunflower oil concentration. Experimentally determined concentrations of fatty acids are presented along with simulation data obtained using the process model for the reference batch process (filled triangles, dashed line) and the fed-batch process (empty triangles, dotted line).

so that once the concentration of oil is reduced due to cleaving by lipase below a threshold, substrate is added to maintain a triglyceride level of 5 g/L. To perform this task, sunflower oil needs to be fed at rates between approx. 1 - 4 $g_{oil}/(g_{BM} \cdot h)$ starting at $t = 34$ h (Fig. 6.2)[1]. The feeding strategy and its experimental outcome are evaluated in the following sections.

6.2 Evaluation of an oil feeding strategy

The calculated feeding profile was applied to the reference batch process as described in the previous section. Experimental data on fatty acid concentration could confirm that the intended goal of reduced fatty acid formation could be achieved, and that measured data correlated well with the predictions (Fig. 6.2). Measurement data of biomass concentration and rhamnolipid concentration are presented in Fig. 6.3 along with the simulations of the batch and the fed-batch strategy presented in the previous section.

[1]Dr. Thomas Bernard (Fraunhofer Institute of Optronics, System Technologies and Image Exploitation, Karlsruhe) contributed to the calculation of the sunflower oil feed

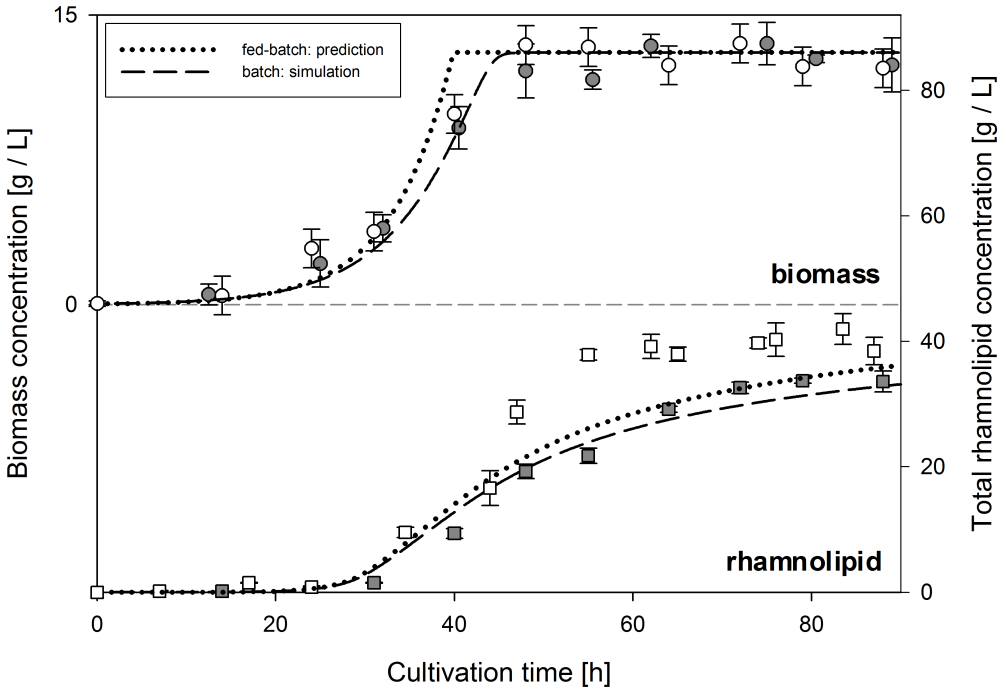

Figure 6.3: Experimental data on biomass concentration (top graph) and total rhamnolipid concentration (bottom graph) for the reference batch process (filled symbols) and the fed-batch process (empty symbols). Both datasets are presented along with simulations obtained using the process model (Chapter 5) for the batch scenario (dashed lines) and the fed-batch scenario (dotted lines).

The time course of biomass concentration in the batch process and in the fed-batch process with oil feeding are similar due to biomass being limited by the availability of nitrogen, reaching biomass concentrations of approx. 12 g/L. The model is able to predict this time-course of experimental data on biomass concentration (Fig. 6.3, top graph). Maximum rhamnolipid concentration, specific rhamnolipid production rate and product yields for the reference batch process and the fed-batch process are shown in Fig. 6.4. The time-course of rhamnolipids produced reached concentrations of over 40 g/L in the fed-batch after 90h, which constitutes an increase of approx. 20% compared to rhamnolipid concentrations of below 35 g/L in the batch process (Fig. 6.4). Consequently, the specific rhamnolipid production rate which was calculated from the data increased to 0.096 $g_{RL}/(g_{BM} \cdot h)$ in the fed-batch process from a value of 0.08 $g_{RL}/(g_{BM} \cdot h)$ in the batch process. In addition, due to the controlled feeding of sunflower oil, as opposed to an initial concentration of sunflower oil in excess, the product yield was increased from 0.14 g_{RL}/g_{oil} to 0.25 g_{RL}/g_{oil}.

While the model was able to predict the time-course of rhamnolipid concentration in the batch process (Fig. 6.3, bottom graph, dashed line and filled squares, [Henkel *et al.* 2014]), the prediction of the outcome of the fed-batch process with oil feeding does not match the obtained experimental data (Fig. 6.3, bottom graph,

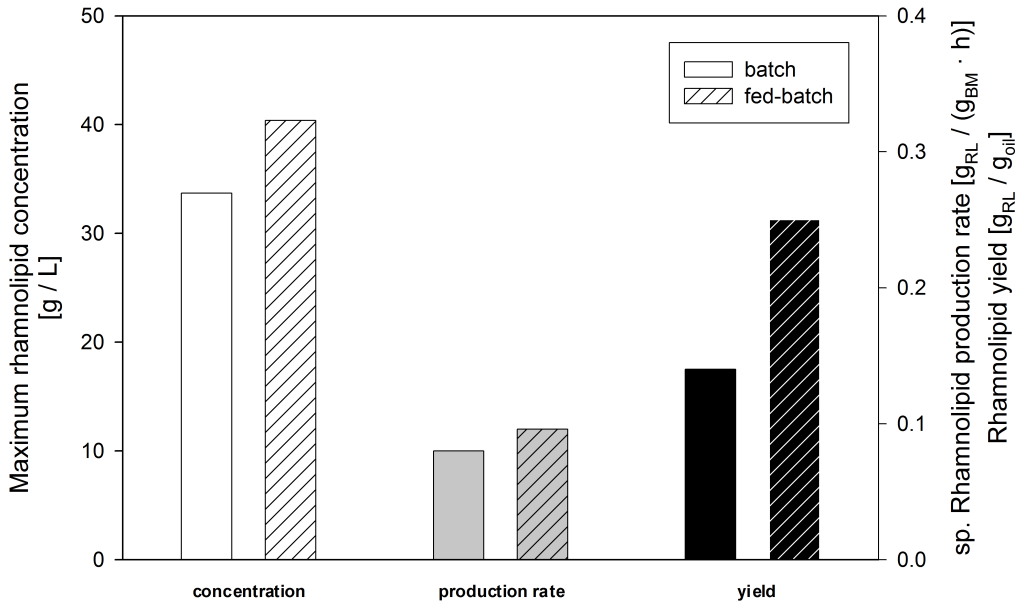

Figure 6.4: Maximum rhamnolipid concentration, specific rhamnolipid production rate and product yields for the reference batch process (filled bars) and the fed-batch process (dashed bars).

dotted line and empty squares). While the prediction is qualitatively correct, the simulation suggest a lower increase in rhamnolipid concentration up to final concentrations of 37 g/L after 90h, which is approx. 10% less than shown by experimental data.

6.3 Adjusting the model to reflect fed-batch data

The high concentration of fatty acids in the investigated batch process, which exhibits a strong inhibitory effect on bacterial growth, overshadowed other metabolic effects on rhamnolipid production, and the reduction of rhamnolipid formation rate was attributed indirectly to the negative effect of fatty acids on growth, which are linked to rhamnolipid production via the formation of biomass and the biomass-specific build-up of C_4-HSL signaling molecules (Fig. 6.1). Therefore, since the model for the batch process was able to describe data on rhamnolipid formation under the investigated conditions, further direct effects of the metabolic state/activity of the cells on rhamnolipid synthesis were not considered in the model [Henkel *et al.* 2014]. For reasons of simplicity and to reduce the number of unknown parameters in the model, a kinetic based on fatty acids directly effecting rhamnolipid formation was omitted, and instead, the simulated product formation rate was adjusted using fitting parameters for biomass- and C_4-HSL-specific production rates (Chapter 5, Tab. 5.1).

Using experimental data from the fed-batch process, the description of growth and

rhamnolipid formation in the model was refined. To allow for a differentiation between growth associated and basal production, the effective specific rhamnolipid production rate was split into a C_4-HSL associated production rate ($q^*_{\text{mono-RL}}$), taken from the model for the batch process (Chapter 5, Eq. 5.14) and influenced by a metabolic, growth dependent kinetic ($f^{\text{metabol.}}$), and a growth independent production rate (q^*_{basal}) (Eq. 6.1).

$$q_{mono-RL} = \overbrace{\underbrace{q^*_{\text{mono-RL}} \cdot f^{\text{metabol.}}}_{C_4\text{-HSL associated}} + \underbrace{q^*_{\text{basal}}}_{\text{growth-independent}}}^{\text{total mono-rhamnolipid production rate}} \tag{6.1}$$

In the following sections, this refined and more complex description of rhamnolipid production rate was used as a basis to modify and reparameterize the model to account for new experimental data from the fed-batch process.

6.3.1 Adjusting the model: inhibition by fatty acids

In addition to fatty acids affecting growth, the model can be modified according to experimental data obtained from fed-batch experiments to include a presumed direct inhibitory effect of fatty acids on rhamnolipid production rate. This approach may be justified biologically by a putative negative effect of fatty acids on enzymes involved in rhamnolipid synthesis, in particular RhlA and RhlB, which catalyze the formation of the rhamnolipid precursor HAA and assembly of a mono-rhamnolipid molecule. A negative effect of long alkyl chains of fatty acids has recently been reported for the RhlA mediated synthesis of rhamnolipid precursors [Gutierrez *et al.* 2013]. Due to their function, these enzymes interact with hydrophobic carbon chains, which allows them to perform their biological function. The negative effect of fatty acids on growth described by the kinetic according to Luong *et al.*, as implented in the process model (Chapter 5, Eq. 5.2) [Luong 1987], was shown to be able to also describe rhamnolipid production in the investigated batch and fed-batch processes (Fig. 6.5). Therefore, this approach was adapted as a fatty acid dependent kinetic (Eq. 6.2).

$$f_1^{\text{metabol.}} = f(c_{\text{FA}}) = \left[1 - \left(\frac{c_{\text{FA}}}{K_{\text{i}}^{\text{FA}}}\right)^n\right] \tag{6.2}$$

Therefore, by using this kinetic, no additional parameters are required for the model, and only the product formation rates for mono-rhamnolipid and di-rhamnolipid were adjusted (Tab. 6.1). Parameter fitting for best description of the experimental data from the fed-batch by the model showed that using this inhibition kinetics, experimental data is described best without a basal production rate. Therefore,

Table 6.1: Optimized and modified parameters for the model of the fed-batch process using C_4-HSL associated rhamnolipid production inhibited in presence of fatty acids with a metabolic factor $f_1^{\text{metabol.}} = f(c_{\text{FA}})$ (Eq. 6.2), disregarding basal production. Parameter optimization was performed using a least square error function as described previously [Henkel *et al.* 2014] using experimental data of the fed-batch process depicted in Fig. 6.3.

Parameter	**Value**	**Unit**	**Comment/source**
$q_{\text{mono-RL}}^{\text{C4-HSL}}$	$9.95 \cdot 10^{-4}$	$g_{RL} \cdot L/(\mu mol_{\text{C4-HSL}} \cdot g_{BM} \cdot h)$	Fitting parameter
$q_{\text{mono-RL}\rightarrow\text{di-RL}}^{\text{C4-HSL}}$	$7.88 \cdot 10^{-4}$	$g_{RL} \cdot L/(\mu mol_{\text{C4-HSL}} \cdot g_{BM} \cdot h)$	Fitting parameter
q_{basal}^{*}	0	$g_{RL}/(g_{BM} \cdot h)$	fixed

q_{basal}^{*} was set to 0 in this approach. Parameters which needed to be changed, newly introduced or optimized for this model are shown in Tab. 6.1.

Alternatively, an enzyme kinetic for RhlA/B with competitive reversible inhibition by fatty acids could be included in the model, as it was successfully implemented in the model for the batch process regarding triglyceride hydrolysis by lipase (Chapter 5, Eq. 5.10). However, to quantify the effect of fatty acids on RhlA/B activity, further experiments are required. Besides the approach presented in this section, a direct effect of growth rate and metabolism on rhamnolipid formation may be applied instead. This approch using an expression for growth rate-dependent kinetics for rhamnolipid production rate is discussed in the following section.

6.3.2 Adjusting the model: growth-dependent kinetic

Negative effects on rhamnolipid synthesis rate due to slower metabolism may be explained due to reduced formation of precursors in metabolically less active cells, e.g. cells in a stationary phase. This is attributable to reduced turnover of cellular protein and enzymes required for the conversion of substrate in both anabolic and catabolic processes. The possibility of increasing the metabolic rate by genetic optimization of the bacterial strains on rhamnolipid formation has been discussed in the past, and enhancing the metabolic rate was suggested as a general target for optimization [Henkel *et al.* 2012].
The description of the kinetic behavior of rhamnolipid synthesis due to the metabolic state $f_2^{\text{metabol.}}$ was achieved by a basic MONOD kinetic (Eq. 6.3). Therefore, at lower growth rates, an increment in $f_2^{\text{metabol.}}$ may be interpreted as a representation of increasing metabolic activity and protein turnover. At higher growth rates, the increasing metabolic activity has a weaker effect on rhamnolipid formation rate, which is described by the saturation behaviour of $f_2^{\text{metabol.}}$ approaching a theoretical maximum product formation rate. This effect accounts for single metabolic pathways possibly already being saturated at non-maximal growth rates, and, when

Table 6.2: Specific rhamnolipid production rates determined for resting cell cultivations of different *Pseudomonads* (Fig. B.6).

Production rate [$\mathbf{mg_{RL}/(g_{BM}{\cdot}h)}$]	**Carbon Source**	**Strain**	**Source**
22	n-alkanes	*P. aeruginosa* DSM2874	[Syldatk *et al.* 1985a]
12	glycerol	*P. aeruginosa* DSM2874	[Syldatk *et al.* 1985a]
18	glucose	*P. putida* KT42C1	[Wittgens *et al.* 2011]
8	glycerol	*P. aeruginosa* PAO1	This thesis
14	fatty acids	*P. aeruginosa* PAO1	This thesis

the growth rate increases further, additional pathways reach saturation, so that the effect on rhamnolipid formation is less prominent the higher the growth rate is.

$$f_2^{\text{metabol.}} = f(\mu_X) = \frac{\mu_X}{\mu_X + K_\mu^{\text{mono-RL}}} \tag{6.3}$$

While in the batch process, the growth rate was experimentally determined to decrease down to the point where growth ceases, the biomass-specific rhamnolipid production rate approaches a fixed value after transition to the stationary phase, which is held if enough carbon source is present [Müller *et al.* 2010, Henkel *et al.* 2014]. This basal production rate was investigated in the past, and it was shown that using resting cells of *P. aeruginosa* in buffered media supplied with different carbon sources, this specific production rate can be held over several days [Syldatk *et al.* 1985a]. The same mechanism was described for the reference batch process in the past [Müller *et al.* 2010], where an excess of sunflower oil caused the specific rhamnolipid production rate to approach a constant value and continue several days in the stationary phase. This specific, growth independent rhamnolipid formation rate $q_{\text{mono-RL}}^{\text{basal}}$ was determined to be between 0.01 - 0.02 $g_{RL}/(g_{BM}{\cdot}h)$ for a strain of *P. aeruginosa* and a process for recombinant production of rhamnolipids in the past (Tab. 6.2). Experimental data for *P. aeruginosa* PAO1 suggests basal production rates for the investigated system are of the same order of magnitude (Tab. 6.2). Consequently, basal production was implemented in the model as a fitting parameter (with a value of 0.01 and a fitting range of ±50%) including substrate limitations for glycerol and fatty acids, to account for substrate depletion (Eq. 6.4). Tab. 6.3 shows optimized and newly introduced parameters utilized for this model.

$$q_{\text{basal}}^{*} = q_{\text{mono-RL}}^{\text{basal}} \cdot \max\left\{ \frac{c_{\text{gly}}}{c_{\text{gly}} + K_S^{\text{gly}}}; \frac{c_{\text{FA}}}{c_{\text{gly}} + K_S^{\text{FA}}} \right\} \tag{6.4}$$

Table 6.3: Optimized and modified parameters for the model of the fed-batch process using C_4-HSL associated rhamnolipid production dependent on the specific growth rate with a metabolic factor $f_2^{\text{metabol.}} = f(\mu_X)$ (Eq. 6.3) combined with a growth independent basal rate (Eq. 6.4). Parameter optimization was performed using a least square error function as described previously [Henkel *et al.* 2014] using experimental data of the fed-batch process depicted in Fig. 6.3.

Parameter	**Value**	**Unit**	**Comment/source**
$q_{\text{mono-RL}}^{\text{C4-HSL}}$	$7.94 \cdot 10^{-3}$	$g_{RL}{\cdot}L/(\mu mol_{\text{C4-HSL}}{\cdot}g_{BM}{\cdot}h)$	Fitting parameter
$q_{\text{mono-RL}\rightarrow\text{di-RL}}^{\text{C4-HSL}}$	$6.26 \cdot 10^{-3}$	$g_{RL}{\cdot}L/(\mu mol_{\text{C4-HSL}}{\cdot}g_{BM}{\cdot}h)$	Fitting parameter
$K_{\mu}^{\text{mono-RL}}$	0.042	(1/h)	Fitting parameter
q_{basal}^{*}	0.009	$g_{RL}/(g_{BM}{\cdot}h)$	Fitting parameter

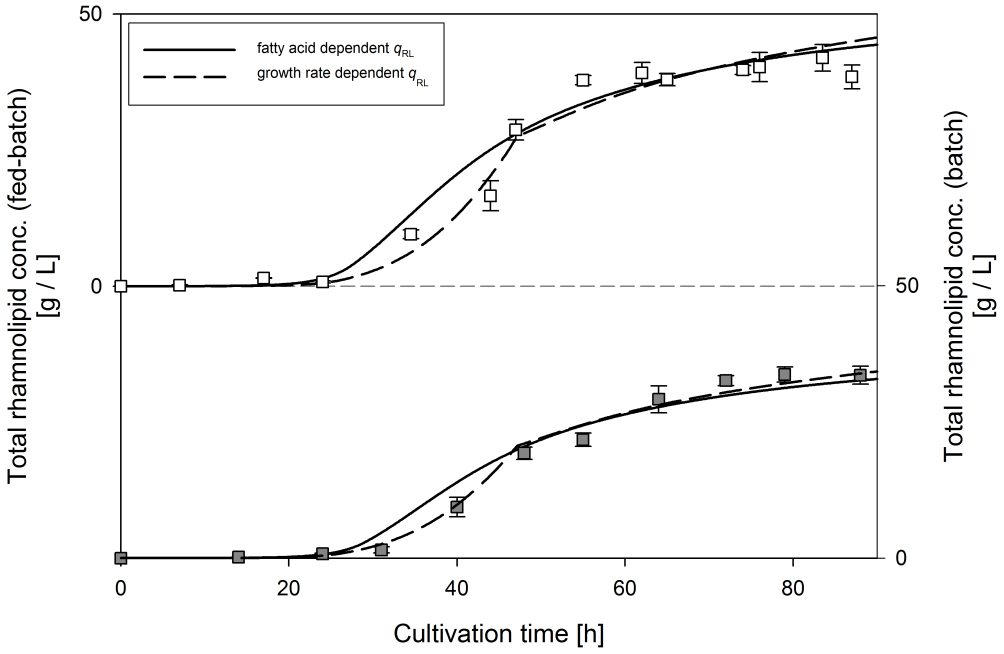

Figure 6.5: Total rhamnolipid concentration in the fed-batch process (top graph, empty squares) and batch process (bottom graph, filled squares) as presented in Fig. 6.3. Simulations are shown for C_4-HSL associated rhamnolipid production (Eq. 6.2, $f^{\text{metabol.}} = f(c_{FA})$) inhibited in presence of fatty acids and C_4-HSL associated rhamnolipid production (Eq. 6.3, $f^{\text{metabol.}} = f(\mu_X)$) dependent on the specific growth rate combined with growth independent mechanisms (Eq. 6.4).

6.4 Experimental design and predictive character of the model

The initial model for the batch process (Chapter 5) describes experimental data on the batch process and validation scenarios with modified initial conditions (Fig. 5.3). The model was then used to develop an optimized sunflower oil feeding strategy for increased rhamnolipid production, which was confirmed by experiments presented in this chapter. The model, however, failed to quantitatively predict the results of the investigated fed-batch scenario using a sunflower oil feed.

To further enable the model to describe experimental data beyond the point of previously known experimental outcome, a broader experimental space is required. This way, the predictive capabilities of the model may be expanded to cover an area of multi-dimensional experimental space (e.g. multiple experiments may be used to create an experimental area generated by 2 different feeds). The model may then be used to predict the best experimental design, as defined by the desired outcome (e.g. optimized productivity or space-time yield).

References for Chapter 6

[Gutierrez *et al.* 2013] Gutierrez, M., Choi, M. H., Tian, B., Xu, J., Rho, J. K., Kim, M. O., Cho, Y.-H., and Yoon, S. C. (2013). Simultaneous inhibition of rhamnolipid and polyhydroxyalkanoic acid synthesis and biofilm formation in *Pseudomonas aeruginosa* by 2-bromoalkanoic acids: effect of inhibitor alkyl-chain-length. *PLoS One*, 8(9).

[Henkel *et al.* 2012] Henkel, M., Müller, M. M., Kügler, J. H., Lovaglio, R. B., Contiero, J., Syldatk, C., and Hausmann, R. (2012). Rhamnolipids as biosurfactants from renewable resources: Concepts for next-generation rhamnolipid production. *Process Biochemistry*, 47(8), pp. 1207–1219.

[Henkel *et al.* 2013] Henkel, M., Schmidberger, A., Kühnert, C., Beuker, J., Bernard, T., Schwartz, T., Syldatk, C., and Hausmann, R. (2013). Kinetic modeling of the time course of *N*-butyryl-homoserine lactone concentration during batch cultivations of *Pseudomonas aeruginosa* PAO1. *Applied Microbiology and Biotechnology*, 97(17), pp. 7607–16.

[Henkel *et al.* 2014] Henkel, M., Schmidberger, A., Vogelbacher, M., Kühnert, C., Beuker, J., Bernard, T., Schwartz, T., Syldatk, C., and Hausmann, R. (2014). Kinetic modeling of rhamnolipid production by *Pseudomonas aeruginosa* PAO1 including cell density-dependent regulation. *Applied Microbiology and Biotechnology*, 98(16), pp. 7013–7025.

[Luong 1987] Luong, J. H. T. (1987). Generalization of Monod kinetics for analysis of growth data with substrate-inhibition. *Biotechnology and Bioengineering*, 29(2), pp. 242–248.

[Müller *et al.* 2010] Müller, M., Hörmann, B., Syldatk, C., and Hausmann, R. (2010). *Pseudomonas aeruginosa* PAO1 as a model for rhamnolipid production in bioreactor systems. *Applied Microbiology and Biotechnology*, 87(1), pp. 167–174.

[Syldatk *et al.* 1985] Syldatk, C., Lang, S., Matulovic, U., and Wagner, F. (1985). Production of four interfacial active rhamnolipids from *n*-alkanes or glycerol by resting cells of *Pseudomonas* species DSM 2874. *Zeitschrift für Naturforschung*, 40(1-2), pp. 61–67.

[Wittgens *et al.* 2011] Wittgens, A., Tiso, T., Arndt, T. T., Wenk, P., Hemmerich, J., Muller, C., Wichmann, R., Kupper, B., Zwick, M., Wilhelm, S., Hausmann, R., Syldatk, C., Rosenau, F., and Blank, L. M. (2011). Growth independent rhamnolipid production from glucose using the non-pathogenic *Pseudomonas putida* KT2440. *Microbial Cell Factories*, 10(1).

7. Concluding remarks

Biological systems generally consist of several subunits which are interconnected by complex mechanisms. The behavior of the system is often difficult to assess by basic observations, mostly due to the presence of nonlinear elements such as feedback or feedforward cascades of biochemical reactions or regulatory networks. Modeling approaches required to describe a complex process in a bioreactor can be assigned to three layers, each representing a different perspective and level of detail: the process layer, the metabolic layer and the genetic layer. For many bioprocesses, modeling approaches include only part of the knowledge available on the process, even though combining information from all layers could benefit the overall understanding of the system. In this thesis, one example for such a complex bioprocess, the biotechnological production of rhamnolipid biosurfactants was used to successfully combine information from different layers of modeling. The result is a process model on a bioreactor scale with information obtained from metabolism and regulation on a genetic scale. One of the main factors influencing growth in the investigated batch process is the accumulation of fatty acids in the culture broth due to an excess of sunflower oil. Consequently, the process model was used to calculate a sunflower oil feeding strategy leading to significantly lower fatty acid concentrations in simulations. Indirectly, this negative effect of fatty acids on the growth rate is linked to rhamnolipid production via the formation of biomass and the biomass-specific build-up of C_4-HSL signaling molecules. The proposed feeding strategy was investigated experimentally. An increase in final rhamnolipid concentration of approx. 20% with approx. 80% increased yield as compared to the previous process in batch mode of operation was determined. As the first study to reach this level of complexity related to modeling of a process for rhamnolipid production, this thesis provides a major piece in a puzzle for knowledge-based strategies for enhanced rhamnolipid formation.

Future work intended to enhance rhamnolipid production may be either focused on developing a more elaborate process using model-based predictions, further investigation of the molecular mechanisms of quorum quenching connected to the C_4-HSL specific degradation activity (putative C_4-HSL acylase) or the development of novel strains for rhamnolipid production. To obtain a further optimized feeding strategy for rhamnolipid production, it may be required to expand the experimental space of fed-batch processes. For this, the addition of other feeds, e.g. the nitrogen source or trace elements such as ferric iron, might be required. The data obtained could then be used to refine the model and derive strategies leading to a further enhancement of rhamnolipid formation. The investigations of quorum sensing in this thesis raised additional questions about the mechanisms of quorum quenching, in particular the putative C_4-HSL specific acylase or related enzyme. The identification of the putative acylase or related mechanism could be the target of further studies, which could then be altered, e.g. by creating a deletion mutant. This could then potentially lead to influenced or prolonged accumulation of C_4-HSL in the culture supernatant. Furthermore, the possibilities of optimized strains for rhamnolipid production might be investigated, which could be focused on metabolic pathways, quorum sensing or the efficiency of rhamnolipid formation itself. This may require further metabolic investigations, especially metabolic flux analysis if the formation and efficiency of precursor availabilty were to be adressed by strain engineering. By combining the approach of this thesis using modeling and simulation with techniques of strain-engineering, substrate costs may be lowered and productivities may be enhanced to an extent that ultimately a point may be reached where large-scale production of rhamnolipids becomes economically feasible.

In this thesis, a process for the production of rhamnolipids in a bioreactor was successfully modeled by combining a process model with information obtained from metabolism and regulation on a genetic scale. It was furthermore shown that a multi-layer modeling approach may also benefit the understanding of the process, e.g. as it was shown for the description of a putative C_4-HSL specific acylase or the quantification of the negative effect of fatty acids on rhamnolipid formation. The developed methods may provide a framework for the model-based optimization of complex bioprocesses in the future.

List of all References

[Abalos *et al.* 2001] Abalos, A., Pinazo, A., Infante, M. R., Casals, M., Garcia, F., and Manresa, A. (2001). Physicochemical and antimicrobial properties of new rhamnolipids produced by *Pseudomonas aeruginosa* AT10 from soybean oil refinery wastes. *Langmuir*, 17(5), pp. 1367–1371.

[Abdel-Mawgoud *et al.* 2011] Abdel-Mawgoud, A. M., Hausmann, R., Lepine, F., Müller, M. M., and Deziel, E. (2011). Rhamnolipids: detection, analysis, biosynthesis, genetic regulation, and bioengineering of production. In: Soberon-Chavez, G. (Ed.): *Biosurfactants*, Microbiology Monographs, pp. 13–55. Berlin Heidelberg: Springer.

[Abdel-Mawgoud *et al.* 2010] Abdel-Mawgoud, A. M., Lépine, F., and Déziel, E. (2010). Rhamnolipids: Diversity of structures, microbial origins, and roles. *Applied Microbiology and Biotechnology,*, 86(5), pp. 1323–1336.

[Alibaba Group 2014] Alibaba Group (2014). Alibaba global retail and wholesale trading platform. Available online under http://www.alibaba.com/, *accessed 02/2014*.

[Andrä *et al.* 2006] Andrä, J., Rademann, J., Howe, J., Koch, M. H. J., Heine, H., Zähringer, U., and Brandenburg, K. (2006). Endotoxin-like properties of a rhamnolipid exotoxin from *Burkholderia* (*Pseudomonas*) *plantarii*: Immune cell stimulation and biophysical characterization. *Biological Chemistry*, 387(3), pp. 301–310.

[Andrews 1989] Andrews, G. (1989). Estimating cell and product yields. *Biotechnology and Bioengineering*, 33(3), pp. 256–265.

[Andrews 1968] Andrews, J. F. (1968). A mathematical model for the continuous culture of microorganisms utilizing inhibitory substrate. *Biotechnology and Bioengineering*, 10(6), pp. 707–724.

[Anguige *et al.* 2006] Anguige, K., King, J. R., and Ward, J. P. (2006). A multi-phase mathematical model of quorum sensing in a maturing *Pseudomonas aeruginosa* biofilm. *Mathematical Biosciences*, 203(2), pp. 240–276.

[de Assis and Filho 2000] de Assis, A. J. and Filho, R. M. (2000). Soft sensors development for on-line bioreactor state estimation. *Computers & Chemical Engineering*, 24(2), pp. 1099–1103.

[Ayers 1956] Ayers, C. W. (1956). Estimation of the Higher Fatty Acids C7-C18. *Analytica Chimica Acta*, 15(1), pp. 77–83.

[Bader 1978] Bader, F. G. (1978). Analysis of double-substrate limited growth. *Biotechnology and Bioengineering*, 20(2), pp. 183–202.

[Bailey 1998] Bailey, J. E. (1998). Mathematical modeling and analysis in biochemical engineering: past accomplishments and future opportunities. *Biotechnology Progress*, 14(1), pp. 8–20.

[Baker *et al.* 2012] Baker, C., Jia, T., and Kulkarni, R. V. (2012). Stochastic modeling of regulation of gene expression by multiple small RNAs. *Physical review E, statistical, nonlinear, and soft matter physics*, 85(6).

[Baker 1964] Baker, D. (1964). Colorimetric method for determining free fatty acids in vegetable oils. *Journal of the American Oil Chemists Society*, 41(1), pp. 21–22.

[Baltz *et al.* 2005] Baltz, R. H., Miao, V., and Wrigley, S. K. (2005). Natural products to drugs: Daptomycin and related lipopeptide antibiotics. *Natural Product Reports*, 22(6), pp. 717–741.

[Banat 1995] Banat, I. M. (1995). Biosurfactants production and possible uses in microbial enhanced oil-recovery and oil pollution remediation - a review. *Bioresource Technology*, 51(1), pp. 1–12.

[Banat *et al.* 2000] Banat, I. M., Makkar, R. S., and Cameotra, S. S. (2000). Potential commercial applications of microbial surfactants. *Applied Microbiology and Biotechnology*, 53(5), pp. 495–508.

[Barbarossa *et al.* 2010] Barbarossa, M. V., Kuttler, C., Fekete, A., and Rothballer, M. (2010). A delay model for quorum sensing of *Pseudomonas putida*. *Biosystems*, 102(2-3), pp. 148–156.

[Bassler *et al.* 1994] Bassler, B. L., Wright, M., and Silverman, M. (1994). Multiple signalling systems controlling expression of luminescence in *Vibrio harveyi*: sequence and function of genes encoding a second sensory pathway. *Molecular Microbiology*, 13(2), pp. 273–286.

[Benincasa *et al.* 2002] Benincasa, M., Contiero, J., Manresa, M. A., and Moraes, I. O. (2002). Rhamnolipid production by *Pseudomonas aeruginosa* LBI growing on soapstock as the sole carbon source. *Journal of Food Engineering*, 54(4), pp. 283–288.

[Bergström *et al.* 1946] Bergström, S., Theorell, H., and Davide, H. (1946). On a metabolic product of *Ps. pyocyanea*, pyolipic acid, active against *Mycobact. tuberculosis*. *Arkiv för Kemi, Mineralogi och Geologi*, 23 A(13), pp. 1–12.

[Bertani 1951] Bertani, G. (1951). Studies on lysogenesis I.: The mode of phage liberation by lysogenic *Escherichia coli*. *Journal of Bacteriology*, 62(3), pp. 293–300.

[Borgos *et al.* 2013] Borgos, S. E. F., Bordel, S., Sletta, H., Ertesvag, H., Jakobsen, O., Bruheim, P., Ellingsen, T. E., Nielsen, J., and Valla, S. (2013). Mapping global effects of the anti-sigma factor MucA in *Pseudomonas fluorescens* SBW25 through genome-scale metabolic modeling. *BMC Systems Biology*, 7(19).

[Brown 1991] Brown, M. J. (1991). Biosurfactants for cosmetic applications. *International Journal of Cosmetic Science*, 13(2), pp. 61–64.

[Burger *et al.* 1963] Burger, M., Glaser, L., and Burton, R. M. (1963). Enzymatic synthesis of a rhamnolipid by extracts of *Pseudomonas aeruginosa*. *Federation Proceedings*, 21(2), pp. 82–83.

[Buziol *et al.* 2002] Buziol, S., Becker, J., Baumeister, A., Jung, S., Mauch, K., Reuss, M., and Boles, E. (2002). Determination of in-vivo kinetics of the starvation-induced Hxt5 glucose transporter of *Saccharomyces cerevisiae*. *FEMS Yeast Research*, 2(1), pp. 283–291.

[Cabrera-Valladares *et al.* 2006] Cabrera-Valladares, N., Richardson, A. P., Olvera, C., Trevino, L. G., Déziel, E., Lépine, F., and Soberón-Chávez, G. (2006). Monorhamnolipids and 3-(3-hydroxyalkanoyloxy)alkanoic acids (HAAs) production using *Escherichia coli* as a heterologous host. *Applied Microbiology and Biotechnology*, 73(1), pp. 187–194.

[Camara *et al.* 1998] Camara, M., Daykin, M., and Chhabra, S. R. (1998). Detection, purification, and synthesis of *N*-acylhomoserine lactone quorum sensing signal molecules. *Methods in Microbiology*, 27, pp. 319–330.

[Cha *et al.* 2008] Cha, M., Lee, N., Kim, M., and Lee, S. (2008). Heterologous production of *Pseudomonas aeruginosa* EMS1 biosurfactant in *Pseudomonas putida*. *Bioresource Technology*, 99(7), pp. 2192–2199.

[Chen *et al.* 2004] Chen, F., Chen, C. C., Riadi, L., and Ju, L. K. (2004). Modeling *rhl* quorum sensing regulation on rhamnolipid production by *Pseudomonas aeruginosa*. *Biotechnology Progress*, 20(5), pp. 1325–1331.

[Chen *et al.* 2007a] Chen, S. Y., Lu, W. B., Wei, Y. H., Chen, W. M., and Chang, J. S. (2007a). Improved production of biosurfactant with newly isolated *Pseudomonas aeruginosa* S2. *Biotechnology Progress*, 23(3), pp. 661–666.

[Chen *et al.* 2007b] Chen, S. Y., Wei, Y. H., and Chang, J. S. (2007b). Repeated pH-stat fed-batch fermentation for rhamnolipid production with indigenous *Pseudomonas aeruginosa* S2. *Applied Microbiology and Biotechnology*, 76(1), pp. 67–74.

[Chéruy 1997] Chéruy, A. (1997). Software sensors in bioprocess engineering. *Journal of Biotechnology*, 52(3), pp. 193–199.

[Contois 1959] Contois, D. E. (1959). Kinetics of bacterial growth: relationship between population density and specific growth rate of continuous cultures. *Journal of General Microbiology*, 21, pp. 40–50.

[Covert and Palsson 2002] Covert, M. W. and Palsson, B. O. (2002). Transcriptional regulation in constraints-based metabolic models of *Escherichia coli*. *Journal of Biological Chemistry*, 277(1), pp. 28058–28064.

[De Lima *et al.* 2007] De Lima, C. J. B., Franca, F. P., Servulo, E. F. C., Resende, A. A., and Cardoso, V. L. (2007). Enhancement of rhamnolipid production in residual soybean oil by an isolated strain of *Pseudomonas aeruginosa*. *Applied Biochemistry and Biotechnology*, 137, pp. 463–470.

[Desai and Banat 1997] Desai, J. D. and Banat, I. M. (1997). Microbial production of surfactants and their commercial potential. *Microbiology and Molecular Biology Reviews*, 61(1), pp. 47–64.

[Develter *et al.* 2007] Develter, D., Walcarius, B., and Fleurackers, S. (2007). Biosurfactants in cleaning and cosmetics. Third International Conference on Renewable Resources & Biorefineries (RRB), June 4 - 6, 2007, Ghent, Belgium. Available online under http://www.rrbconference.com/rrb3-2007.

[Déziel *et al.* 2000] Déziel, E., Lépine, F., Milot, S., and Villemur, R. (2000). Mass spectrometry monitoring of rhamnolipids from a growing culture of *Pseudomonas aeruginosa* strain 57RP. *Biochimica et Biophysica Acta - Molecular and Cell Biology of Lipids*, 1485(2-3), pp. 145–152.

[Déziel *et al.* 2003] Déziel, E., Lépine, F., Milot, S., and Villemur, R. (2003). RhlA is required for the production of a novel biosurfactant promoting swarming motility in *Pseudomonas aeruginosa*: 3-(3-hydroxyalkanoyloxy)alkanoic acids (HAAs), the precursors of rhamnolipids. *Microbiology*, 149, pp. 2005–2013.

[Dockery and Keener 2000] Dockery, J. D. and Keener, J. P. (2000). A mathematical model for quorum sensing in *Pseudomonas aeruginosa*. *Bulletin of Mathematical Biology*, 00, pp. 1–22.

[Du *et al.* 2011] Du, H. J., Xu, Z. L., Shrout, J. D., and Alber, M. (2011). Multiscale modeling of *Pseudomonas aeruginosa* swarming. *Mathematical Models & Methods in Applied Sciences*, 21(1), pp. 939–954.

[Dubeau *et al.* 2009] Dubeau, D., Déziel, E., Woods, D. E., and Lépine, F. (2009). *Burkholderia thailandensis* harbors two identical *rhl* gene clusters responsible for the biosynthesis of rhamnolipids. *BMC Microbiology*, 9(263).

[Dubey and Juwarkar 2001] Dubey, K. and Juwarkar, A. (2001). Distillery and curd whey wastes as viable alternative sources for biosurfactant production. *World Journal of Microbiology & Biotechnology*, 17(1), pp. 61–69.

[Edwards and Hayashi 1965] Edwards, J. R. and Hayashi, J. A. (1965). Structure of a rhamnolipid from *Pseudomonas aeruginosa*. *Archives of Biochemistry and Biophysics*, 111(2), pp. 415–421.

[Eisenstein 2004] Eisenstein, B. I. (2004). Lipopeptides, focusing on daptomycin, for the treatment of gram-positive infections. *Expert Opinion on Investigational Drugs*, 13(9), pp. 1159–1169.

[Erickson 1981] Erickson, L. E. (1981). Energetic yields associated with hydrocarbon fermentations. *Biotechnology and Bioengineering*, 23(4), pp. 793–803.

[Eswari *et al.* 2013] Eswari, J. S., Anand, M., and Venkateswarlu, C. (2013). Optimum culture medium composition for rhamnolipid production by *Pseudomonas aeruginosa* AT10 using a novel multi-objective optimization method. *Journal of Chemical Technology and Biotechnology*, 88(2), pp. 271–279.

[Gartshore *et al.* 2000] Gartshore, J., Lim, Y. C., and Cooper, D. G. (2000). Quantitative analysis of biosurfactants using Fourier Transform Infrared (FT-IR) spectroscopy. *Biotechnology Letters*, 22(2), pp. 169–172.

[Giani *et al.* 1997] Giani, C., Wullbrandt, D., Rothert, R., and Meiwes, J. (1997). *Pseudomonas aeruginosa* and its use in a process for the biotechnological preparation of L-Rhamnose. US patent 5658793, Hoechst Aktiengesellschaft, Frankfurt am Main, Germany.

[Gilbert 1993] Gilbert, E. J. (1993). *Pseudomonas* lipases - biochemical-properties and molecular-coning. *Enzyme and Microbial Technology*, 15(8), pp. 634–645.

[Goryachev 2009] Goryachev, A. B. (2009). Design principles of the bacterial quorum sensing gene networks. *Wiley Interdisciplinary Reviews: Systems Biology and Medicine*, 1(1), pp. 45–60.

[Goryachev *et al.* 2005] Goryachev, A. B., Toh, D. J., Wee, K. B., Lee, T., Zhang, H. B., and Zhang, L. H. (2005). Transition to quorum sensing in an *Agrobacterium* population: A stochastic model. *PLoS Computational Biology*, 1(4), pp. 265–275.

[Gunther *et al.* 2009] Gunther, J. C., Baclaski, J., Seborg, D. E., and Conner, J. S. (2009). Pattern matching in batch bioprocesses - Comparisons across multiple products and operating conditions. *Computers and Chemical Engineering*, 33(1), pp. 88–96.

[Gutierrez *et al.* 2013] Gutierrez, M., Choi, M. H., Tian, B., Xu, J., Rho, J. K., Kim, M. O., Cho, Y.-H., and Yoon, S. C. (2013). Simultaneous inhibition of rhamnolipid and polyhydroxyalkanoic acid synthesis and biofilm formation in *Pseudomonas aeruginosa* by 2-bromoalkanoic acids: effect of inhibitor alkyl-chain-length. *PLoS One*, 8(9).

[Haba *et al.* 2000] Haba, E., Espuny, M. J., Busquets, M., and Manresa, A. (2000). Screening and production of rhamnolipids by *Pseudomonas aeruginosa* 47T2 NCIB 40044 from waste frying oils. *Journal of Applied Microbiology*, 88, pp. 379–387.

[Hauser and Karnovsky 1954] Hauser, G. and Karnovsky, M. L. (1954). Studies on the production of glycolipide by *Pseudomonas aeruginosa*. *Journal of Bacteriology*, 68(6), pp. 645–654.

[Hauser and Karnovsky 1957] Hauser, G. and Karnovsky, M. L. (1957). Rhamnose and rhamnolipide biosynthesis by *Pseudomonas aeruginosa*. *Journal of Biological Chemistry*, 224(1), pp. 91–105.

[Hauser and Karnovsky 1958] Hauser, G. and Karnovsky, M. L. (1958). Studies on the biosynthesis of L-rhamnose. *Journal of Biological Chemistry*, 233(2), pp. 287–291.

[Henkel *et al.* 2012] Henkel, M., Müller, M. M., Kügler, J. H., Lovaglio, R. B., Contiero, J., Syldatk, C., and Hausmann, R. (2012). Rhamnolipids as biosurfactants from renewable resources: Concepts for next-generation rhamnolipid production. *Process Biochemistry*, 47(8), pp. 1207–1219.

[Henkel *et al.* 2013] Henkel, M., Schmidberger, A., Kühnert, C., Beuker, J., Bernard, T., Schwartz, T., Syldatk, C., and Hausmann, R. (2013). Kinetic modeling of the time course of *N*-butyryl-homoserine lactone concentration during batch cultivations of *Pseudomonas aeruginosa* PAO1. *Applied Microbiology and Biotechnology*, 97(17), pp. 7607–16.

[Henkel *et al.* 2014] Henkel, M., Schmidberger, A., Vogelbacher, M., Kühnert, C., Beuker, J., Bernard, T., Schwartz, T., Syldatk, C., and Hausmann, R. (2014). Kinetic modeling of rhamnolipid production by *Pseudomonas aeruginosa* PAO1 including cell density-dependent regulation. *Applied Microbiology and Biotechnology*, 98(16), pp. 7013–7025.

[Hentzer *et al.* 2003] Hentzer, M., Wu, H., Andersen, J. B., Riedel, K., Rasmussen, T. B., Bagge, N., Kumar, N., Schembri, M. A., Song, Z. J., Kristoffersen, P., Manefield, M., Costerton, J. W., Molin, S., Eberl, L., Steinberg, P., Kjelleberg, S., Hoiby, N., and Givskov, M. (2003). Attenuation of *Pseudomonas aeruginosa* virulence by quorum sensing inhibitors. *EMBO Journal*, 22(15), pp. 3803–3815.

[Heurlier *et al.* 2004] Heurlier, K., Williams, F., Heeb, S., Dormond, C., Pessi, G., Singer, D., Camara, M., Williams, P., and Haas, D. (2004). Positive control of swarming, rhamnolipid synthesis, and lipase production by the posttranscriptional RsmA/RsmZ system in *Pseudomonas aeruginosa* PAO1. *Journal of Bacteriology*, 186(10), pp. 2936–45.

[Heyd *et al.* 2008] Heyd, M., Kohnert, A., Tan, T. H., Nusser, M., Kirschhofer, F., Brenner-Weiss, G., Franzreb, M., and Berensmeier, S. (2008). Development and trends of biosurfactant analysis and purification using rhamnolipids as an example. *Analytical and Bioanalytical Chemistry*, 391(5), pp. 1579–1590.

[Hinz 2006] Hinz, D. C. (2006). Process analytical technologies in the pharmaceutical industry: the FDA's PAT initiative. *Analytical and Bioanalytical Chemistry*, 384(5), pp. 1036–1042.

[Hong *et al.* 2012] Hong, K. W., Koh, C. L., Sam, C. K., Yin, W. F., and Chan, K. G. (2012). Quorum quenching revisited - from signal decays to signalling confusion. *Sensors*, 12(4), pp. 4661–96.

[Hörmann *et al.* 2010] Hörmann, B., Müller, M. M., Syldatk, C., and Hausmann, R. (2010). Rhamnolipid production by *Burkholderia plantarii* DSM 9509(T). *European Journal of Lipid Science and Technology*, 112(6), pp. 674–680.

[IndexMundi Portal 2014] IndexMundi Portal (2014). Trade Statistics and Commodities Data. Available online under http://www.indexmundi.com/, *accessed 02/2014*.

[Jarvis and Johnson 1949] Jarvis, F. G. and Johnson, M. J. (1949). A glyco-lipide produced by *Pseudomonas aeruginosa*. *Journal of the American Chemical Society*, 71, pp. 4124–4126.

[Kanehisa and Goto 2000] Kanehisa, M. and Goto, S. (2000). KEGG: Kyoto Encyclopedia of Genes and Genomes. *Nucleic Acids Research*, 28(1), pp. 27–30.

[Karim *et al.* 2003] Karim, M. N., Hodge, D., and Simon, L. (2003). Data-based modeling and analysis of bioprocesses: some real experiences. *Biotechnology Progress*, 9(5), pp. 1591–1605.

[de Kievit and Iglewski 2000] de Kievit, T. R. and Iglewski, B. H. (2000). Bacterial quorum sensing in pathogenic relationships. *Infection and Immunity*, 68(9), pp. 4839–49.

[Kitamoto *et al.* 2002] Kitamoto, D., Isoda, H., and Nakahara, T. (2002). Functions and potential applications of glycolipid biosurfactants - from energy-saving materials to gene delivery carriers. *Journal of Bioscience and Bioengineering*, 94(3), pp. 187–201.

[Klamt 2006] Klamt, S. (2006). A methodology for the structural and functional analysis of signaling and regulatory networks. *BMC Bioinformatics*, 7(56).

[Klekner and Kosaric 1993] Klekner, V. and Kosaric, N. (1993). Biosurfactants for cosmetics. In: Kosaric, N. (Ed.): *Biosurfactants: production - properties - applications*, Surfactant Science Series, pp. 373–390. New York: Marcel Dekker Inc.

[Kosaric 1992] Kosaric, N. (1992). Biosurfactants in industry. *Pure And Applied Chemistry*, 64(11), pp. 1731–1737.

[Lamont and Martin 2003] Lamont, I. L. and Martin, L. W. (2003). Identification and characterization of novel pyoverdine synthesis genes in *Pseudomonas aeruginosa*. *Microbiology*, 149(Pt 4), pp. 833–42.

[Landman *et al.* 2008] Landman, D., Georgescu, C., Martin, D. A., and Quale, J. (2008). Polymyxins revisited. *Clinical Microbiology Reviews*, 21(3), pp. 449–465.

[Lang 2002] Lang, S. (2002). Biological amphiphiles (microbial biosurfactants). *Current Opinion in Colloid & Interface Science*, 7(1-2), pp. 12–20.

[Lang and Trowitzsch-Kienast 2002] Lang, S. and Trowitzsch-Kienast, W. (2002). *Biotenside*. Stuttgart, Leipzig, Wiesbaden: Teubner.

[Lang and Wullbrandt 1999] Lang, S. and Wullbrandt, D. (1999). Rhamnose lipids - biosynthesis, microbial production and application potential. *Applied Microbiology and Biotechnology*, 51(1), pp. 22–32.

[Latifi *et al.* 1995] Latifi, A., Winson, M. K., Foglino, M., Bycroft, B. W., Stewart, G. S. A. B., Lazdunski, A., and Williams, P. (1995). Multiple homologs of Luxr and Luxl control expression of virulence determinants and secondary metabolites through quorum sensing in *Pseudomonas aeruginosa* PAO1. *Molecular Microbiology*, 17(2), pp. 333–343.

[de Lima *et al.* 2009] de Lima, C. J. B., Ribeiro, E. J., Servulo, E. F. C., Resende, M. M., and Cardoso, V. L. (2009). Biosurfactant production by *Pseudomonas aeruginosa* grown in residual soybean oil. *Applied Biochemistry and Biotechnology*, 152(1), pp. 156–168.

[Lin *et al.* 2003] Lin, Y. H., Xu, J. L., Hu, J., Wang, L. H., Ong, S. L., Leadbetter, J. R., and Zhang, L. H. (2003). Acyl-homoserine lactone acylase from *Ralstonia* strain XJ12B represents a novel and potent class of quorum-quenching enzymes. *Molecular Microbiology*, 47(3), pp. 849–60.

[Lindhout *et al.* 2009] Lindhout, T., Lau, P. C. Y., Brewer, D., and Lam, J. S. (2009). Truncation in the core oligosaccharide of lipopolysaccharide affects flagella-mediated motility in *Pseudomonas aeruginosa* PAO1 via modulation of cell surface attachment. *Microbiology*, 155(1), pp. 3449–3460.

[Linhardt *et al.* 1989] Linhardt, R., Bakhit, R., Daniels, L., Mayerl, F., and Pickenhagen, W. (1989). Microbially produced rhamnolipid as a source of rhamnose. *Biotechnology and Bioengineering*, 33, pp. 365–368.

[Luo *et al.* 2013] Luo, Z., Yuan, X. Z., Zhong, H., Zeng, G. M., Liu, Z. F., Ma, X. L., and Zhu, Y. . (2013). Optimizing rhamnolipid production by *Pseudomonas aeruginosa* ATCC 9027 grown on waste frying oil using response surface method and batch-fed fermentation. *Journal of Central South University*, 20(4), pp. 1015–1021.

[Luong 1987] Luong, J. H. T. (1987). Generalization of Monod kinetics for analysis of growth data with substrate-inhibition. *Biotechnology and Bioengineering*, 29(2), pp. 242–248.

[Luttmann *et al.* 2012] Luttmann, R., Bracewell, D. G., Cornelissen, G., Gernaey, K. V., Glassey, J., Hass, V. C., Kaiser, C., Preusse, C., Striedner, G., and Mandenius, C. F. (2012). Soft sensors in bioprocessing: a status report and recommendations. *Biotechnology Journal*, 7(8), pp. 1040–1048.

[Madan and Mishra 2010] Madan, B. and Mishra, P. (2010). Co-expression of the lipase and foldase of *Pseudomonas aeruginosa* to a functional lipase in *Escherichia coli*. *Applied Microbiology and Biotechnology*, 85(3), pp. 597–604.

[Mahadevan *et al.* 2002] Mahadevan, E., Edwards, J. S., and Doyle, F. J. (2002). Dynamic flux balance analysis of diauxic growth in *Escherichia coli*. *Biophysical Journal*, 83(3), pp. 1331–1340.

[Makkar and Cameotra 1997] Makkar, R. S. and Cameotra, S. S. (1997). Utilization of molasses for biosurfactant production by two *Bacillus* strains at thermophilic conditions. *Journal Of The American Oil Chemists Society*, 74(7), pp. 887–889.

[Makkar and Cameotra 2002] Makkar, R. S. and Cameotra, S. S. (2002). An update on the use of unconventional substrates for biosurfactant production and their new applications. *Applied Microbiology and Biotechnology*, 58(4), pp. 428–434.

[Makkar *et al.* 2011] Makkar, R. S., Cameotra, S. S., and Banat, I. M. (2011). Advances in utilization of renewable substrates for biosurfactant production. *AMB Express*, 1(5).

[Martinez *et al.* 1999] Martinez, A., Ostrovsky, P., and Nunn, D. N. (1999). LipC, a second lipase of *Pseudomonas aeruginosa*, is LipB and Xcp dependent and is transcriptionally regulated by pilus biogenesis components. *Molecular Microbiology*, 34(2), pp. 317–326.

[Mata-Sandoval *et al.* 1999] Mata-Sandoval, J., Karns, J., and Torrents, A. (1999). High-performance liquid chromatography method for the characterization of rhamnolipid mixtures produced by *Pseudomonas aeruginosa* UG2 on corn oil. *Journal of Chromatography A*, 864, pp. 211 – 220.

[Medina *et al.* 2003a] Medina, G., Juarez, K., Diaz, R., and Soberon-Chavez, G. (2003a). Transcriptional regulation of *Pseudomonas aeruginosa* rhlR, encoding a quorum-sensing regulatory protein. *Microbiology*, 149(11), pp. 3073–81.

[Medina *et al.* 2003b] Medina, G., Juarez, K., and Soberon-Chavez, G. (2003b). The *Pseudomonas aeruginosa rhlAB* operon is not expressed during the logarithmic phase of growth even in the presence of its activator RhlR and the autoinducer *N*-butyryl-homoserine lactone. *Journal of Bacteriology*, 185(1), pp. 377–80.

[Medina *et al.* 2003c] Medina, G., Juarez, K., Valderrama, B., and Soberon-Chavez, G. (2003c). Mechanism of *Pseudomonas aeruginosa* RhlR transcriptional regulation of the *rhlAB* promoter. *Journal of Bacteriology*, 185(20), pp. 5976–83.

[Medina-Moreno *et al.* 2011] Medina-Moreno, S. A., Jimenez-Islas, D., Gracida-Rodriguez, J. N., Gutierrez-Rojas, M., and Diaz-Ramirez, I. J. (2011). Modeling rhamnolipids production by *Pseudomonas aeruginosa* from immiscible carbon source in a batch system. *International journal of environmental science and technology*, 8(3), pp. 471–482.

[Melke *et al.* 2010] Melke, P., Sahlin, P., Levchenko, A., and Jonsson, H. (2010). A cell-based model for quorum sensing in heterogeneous bacterial colonies. *PLoS Computational Biology*, 6(6).

[Mercade *et al.* 1993] Mercade, M. E., Manresa, M. A., Robert, M., Espuny, M. J., Deandres, C., and Guinea, J. (1993). Olive oil mill effluent (OOME) - New substrate for biosurfactant production. *Bioresource Technology*, 43(1), pp. 1–6.

[Michaelis and Menten 1913] Michaelis, L. and Menten, M. L. (1913). Die Kinetik der Invertinwirkung. *Biochemische Zeitschrift*, 49(1), pp. 333–369.

[Miller and Bassler 2001] Miller, M. B. and Bassler, B. L. (2001). Quorum sensing in bacteria. *Annual Review of Microbiology*, 55, pp. 165–199.

[Müller *et al.* 2011] Müller, M., Hörmann, B., Kugel, M., Syldatk, C., and Hausmann, R. (2011). Evaluation of rhamnolipid production capacity of *Pseudomonas aeruginosa* PAO1 in comparison to the rhamnolipid over-producer strains DSM 7108 and DSM 2874. *Applied Microbiology and Biotechnology*, 89, pp. 585–592.

[Müller *et al.* 2010] Müller, M., Hörmann, B., Syldatk, C., and Hausmann, R. (2010). *Pseudomonas aeruginosa* PAO1 as a model for rhamnolipid production in bioreactor systems. *Applied Microbiology and Biotechnology*, 87(1), pp. 167–174.

[Monod 1949] Monod, J. (1949). The growth of bacterial cultures. *Annual Review of Microbiology*, 3(1), pp. 371–394.

[Moser 1957] Moser, H. (1957). Structure and dynamics of bacterial populations maintained in the chemostat. *Cold Spring Harbor Symposia on Quantitative Biology*, 22, pp. 121–137.

[Mulligan 2005] Mulligan, C. N. (2005). Environmental applications for biosurfactants. *Environmental Pollution*, 133(2), pp. 183–198.

[Mulligan and Gibbs 1993] Mulligan, C. N. and Gibbs, B. F. (1993). Factors influencing the economics of biosurfactants. In: Kosaric, N. (Ed.): *Biosurfactants: production - properties - applications*, Surfactant Science Series, pp. 329 – 371. New York: Marcel Dekker Inc.

[Nealson and Hastings 1979] Nealson, K. H. and Hastings, J. W. (1979). Bacterial bioluminescence: its control and ecological significance. *Microbiological Reviews*, 43(4), pp. 496–518.

[Nitschke and Costa 2007] Nitschke, M. and Costa, S. G. V. A. O. (2007). Biosurfactants in food industry. *Trends in Food Science & Technology*, 18(5), pp. 252–259.

[Nitschke *et al.* 2010] Nitschke, M., Costa, S. G. V. A. O., and Contiero, J. (2010). Structure and applications of a rhamnolipid surfactant produced in soybean oil waste. *Applied Biochemistry and Biotechnology*, 160(7), pp. 2066–2074.

[Nitschke *et al.* 2005] Nitschke, M., Costa, S. G. V. A. O., Haddad, R., Goncalves, L. A. G., Eberlin, M. N., and Contiero, J. (2005). Oil wastes as unconventional substrates for rhamnolipid biosurfactant production by *Pseudomonas aeruginosa* LBI. *Biotechnology Progress*, 21(5), pp. 1562–1566.

[Ochsner *et al.* 1994] Ochsner, U. A., Fiechter, A., and Reiser, J. (1994). Isolation, characterization, and expression in Escherichia coli of the *Pseudomonas aeruginosa rhlAB* genes encoding a rhamnosyltransferase involved in rhamnolipid biosurfactant synthesis. *The Journal of Biological Chemistry*, 269, pp. 1–9.

[Ochsner and Reiser 1995] Ochsner, U. A. and Reiser, J. (1995). Autoinducer-mediated regulation of rhamnolipid biosurfactant synthesis in *Pseudomonas aeruginosa*. *Proceedings of the National Academy of Sciences USA*, 92, pp. 6424–6428.

[Ochsner *et al.* 1995] Ochsner, U. A., Reiser, J., Fiechter, A., and Witholt, B. (1995). Production of *Pseudomonas aeruginosa* rhamnolipid biosurfactants in heterologous hosts. *Applied and Environmental Microbiology*, 61(9), pp. 3503–3506.

[Ochsner *et al.* 2002] Ochsner, U. A., Wilderman, P. J., Vasil, A. I., and Vasil, M. L. (2002). GeneChip expression analysis of the iron starvation response in *Pseudomonas aeruginosa*: identification of novel pyoverdine biosynthesis genes. *Molecular Microbiology*, 45(5), pp. 1277–87.

[Oinuma and Greenberg 2011] Oinuma, K. and Greenberg, E. P. (2011). Acyl-homoserine lactone binding to and stability of the orphan *Pseudomonas aeruginosa* quorum-sensing signal receptor QscR. *Journal of Bacteriology*, 193(2), pp. 421–428.

[Oliveira *et al.* 2008] Oliveira, F. J. S., Vazquez, L., de Campos, N. P., and Franca, F. P. (2008). Production of rhamnolipids by a *Pseudomonas alcaligenes* strain. *Process Biochemistry*, 44(4), pp. 383–389.

[Paria 2008] Paria, S. (2008). Surfactant-enhanced remediation of organic contaminated soil and water. *Advances in Colloid and Interface Science*, 138(1), pp. 24–58.

[Pearson *et al.* 1999] Pearson, J. P., Van Delden, C., and Iglewski, B. H. (1999). Active efflux and diffusion are involved in transport of *Pseudomonas aeruginosa* cell-to-cell signals. *Journal of Bacteriology*, 181(4), pp. 1203–1210.

[Pearson *et al.* 1997] Pearson, J. P., Pesci, E. C., and Iglewski, B. H. (1997). Roles of *Pseudomonas aeruginosa las* and *rhl* quorum-sensing systems in control of elastase and rhamnolipid biosynthesis genes. *Journal of Bacteriology*, 179(18), pp. 5756–5767.

[Pesci and Iglewski 1997] Pesci, E. C. and Iglewski, B. H. (1997). The chain of command in *Pseudomonas* quorum sensing. *Trends in Microbiology*, 5(4), pp. 132–134.

[Pesci *et al.* 1999] Pesci, E. C., Milbank, J. B., Pearson, J. P., McKnight, S., Kende, A. S., Greenberg, E. P., and Iglewski, B. H. (1999). Quinolone signaling in the cell-to-cell communication system of *Pseudomonas aeruginosa*. *Proceedings of the National Academy of Sciences USA*, 96(20), pp. 11229–11234.

[Pornsunthorntawee *et al.* 2010] Pornsunthorntawee, O., Wongpanit, P., and Rujiravanit, R. (2010). Rhamnolipid biosurfactants: production and their potential in environmental biotechnology. *Advances in Experimental Medicine and Biology*, 672, pp. 211–221.

[Rahim *et al.* 2000] Rahim, R., Burrows, L. L., Monteiro, M. A., Perry, M. B., and Lam, J. S. (2000). Involvement of the *rml* locus in core oligosaccharide and O polysaccharide assembly in *Pseudomonas aeruginosa*. *Microbiology - Society for General Microbiology*, 146, pp. 2803–2814.

[Rahim *et al.* 2001] Rahim, R., Ochsner, U. A., Olvera, C., Graninger, M., Messner, P., Lam, J. S., and Soberón-Chávez, G. (2001). Cloning and functional characterization of the *Pseudomonas aeruginosa rhlC* gene that encodes rhamnosyltransferase 2, an enzyme responsible for di-rhamnolipid biosynthesis. *Molecular Microbiology*, 40(3), pp. 708–718.

[Rahman *et al.* 2002] Rahman, K. S. M., Banat, I. M., Thahira, J., Thayumanavan, T., and Lakshmanaperumalsamy, P. (2002). Bioremediation of gasoline contaminated soil by a bacterial consortium amended with poultry litter, coir pith and rhamnolipid biosurfactant. *Bioresource Technology*, 81(1), pp. 25–32.

[Rahman *et al.* 2003] Rahman, K. S. M., Rahman, T. J., Kourkoutas, Y., Petsas, I., Marchant, R., and Banat, I. M. (2003). Enhanced bioremediation of n-alkane in petroleum sludge using bacterial consortium amended with rhamnolipid and micronutrients. *Bioresource Technology*, 90(2), pp. 159–168.

[Rampioni *et al.* 2006] Rampioni, G., Bertani, I., Zennaro, E., Polticelli, F., Venturi, V., and Leoni, L. (2006). The quorum-sensing negative regulator RsaL of *Pseudomonas aeruginosa* binds to the *lasI* promoter. *Journal of Bacteriology*, 188(2), pp. 815–819.

[Rampioni *et al.* 2007] Rampioni, G., Schuster, M., Greenberg, E. P., Bertani, I., Grasso, M., Venturi, V., Zennaro, E., and Leoni, L. (2007). RsaL provides quorum sensing homeostasis and functions as a global regulator of gene expression in *Pseudomonas aeruginosa*. *Molecular Microbiology*, 66(6), pp. 1557–1565.

[Rehm *et al.* 2001] Rehm, B. H. A., Mitsky, T. A., and Steinbüchel, A. (2001). Role of fatty acid de novo biosynthesis in polyhydroxyalkanoic acid (PHA) and rhamnolipid synthesis by *Pseudomonads*: Establishment of the transacylase (PhaG)-mediated pathway for PHA biosynthesis in *Escherichia coli*. *Applied and Environmental Microbiology*, 67(7), pp. 3102–3109.

[Rendell *et al.* 1990] Rendell, N. B., Taylor, G. W., Somerville, M., Todd, H., Wilson, R., and Cole, P. J. (1990). Characterisation of *Pseudomonas* rhamnolipids. *Biochimica et Biophysica Acta*, 1045(2), pp. 189–193.

[Santa Anna *et al.* 2002] Santa Anna, L. M., Sebastian, G. V., Menezes, E. P., Alves, T. L. M., Santos, A. S., Pereira, N., and Freire, D. M. G. (2002). Production of biosurfactants from *Pseudomonas aeruginosa* PA1 isolated in oil environments. *Brazilian Journal of Chemical Engineering*, 19(2), pp. 159–166.

[Scheibel 2004] Scheibel, J. J. (2004). The evolution of anionic surfactant technology to meet the requirements of the laundry detergent industry. *Journal of Surfactants and Detergents*, 7(4), pp. 319–328.

[Schenk *et al.* 1995] Schenk, T., Schuphan, I., and Schmidt, B. (1995). High-performance liquid-chromatographic determination of the rhamnolipids produced by *Pseudomonas aeruginosa*. *Journal of Chromatography A*, 693(1), pp. 7–13.

[Schügerl 2001] Schügerl, K. (2001). Progress in monitoring, modeling and control of bioprocesses during the last 20 years. *Journal of Biotechnology*, 85(2), pp. 149–173.

[Schmidberger *et al.* 2013] Schmidberger, A., Henkel, M., Hausmann, R., and Schwartz, T. (2013). Expression of genes involved in rhamnolipid synthesis in *Pseudomonas aeruginosa* PAO1 in a bioreactor cultivation. *Applied Microbiology and Biotechnology*, 97(13), pp. 5779–5791.

[Schmidberger *et al.* 2014] Schmidberger, A., Henkel, M., Hausmann, R., and Schwartz, T. (2014). Influence of ferric iron on gene expression and rhamnolipid synthesis during batch cultivation of Pseudomonas aeruginosa PAO1. *Applied Microbiology and Biotechnology*, 98(15), pp. 6725–6737.

[Schuster and Greenberg 2006] Schuster, M. and Greenberg, E. P. (2006). A network of networks: quorum-sensing gene regulation in *Pseudomonas aeruginosa*. *International Journal of Medical Microbiology*, 296(2-3), pp. 73–81.

[Sen 2008] Sen, R. (2008). Biotechnology in petroleum recovery: The microbial EOR. *Progress in Energy and Combustion Science*, 34(6), pp. 714–724.

[Seo and Bailey 1985] Seo, J. H. and Bailey, J. E. (1985). A segregated model for plasmid content and product synthesis in unstable binary fission recombinant organisms. *Biotechnology and Bioengineering*, 27(2), pp. 156–166.

[Seydlova and Svobodova 2008] Seydlova, G. and Svobodova, J. (2008). Review of surfactin chemical properties and the potential biomedical applications. *Central European Journal of Medicine*, 3(2), pp. 123–133.

[Siegmund and Wagner 1991] Siegmund, I. and Wagner, F. (1991). New method for detecting rhamnolipids excreted by *Pseudomonas* species during growth on mineral agar. *Biotechnology Techniques*, 5(4), pp. 265–268.

[Simakov and Pismen 2013] Simakov, D. S. and Pismen, L. M. (2013). Discrete model of periodic pattern formation through a combined autocrine-juxtacrine cell signaling. *Physical Biology*, 10(4).

[Singh *et al.* 2007] Singh, A., Van Hamme, J. D., and Ward, O. P. (2007). Surfactants in microbiology and biotechnology: Part 2. Application aspects. *Biotechnology Advances*, 25(1), pp. 99–121.

[Sio *et al.* 2006] Sio, C. F., Otten, L. G., Cool, R. H., Diggle, S. P., Braun, P. G., Bos, R., Daykin, M., Camara, M., Williams, P., and Quax, W. J. (2006). Quorum quenching by an *N*-acyl-homoserine lactone acylase from *Pseudomonas aeruginosa* PAO1. *Infection and Immunity*, 74(3), pp. 1673–1682.

[Smith and Alford 1966] Smith, J. L. and Alford, J. A. (1966). Inhibition of microbial lipases by fatty acids. *Journal of Applied Microbiology*, 14(5), pp. 699–700.

[Soberón-Chávez *et al.* 2005a] Soberón-Chávez, G., Aguirre-Ramirez, M., and Ordonez, L. (2005a). Is *Pseudomonas aeruginosa* only 'sensing quorum'? *Critical Reviews in Microbiology*, 31(3), pp. 171–182.

[Soberón-Chávez *et al.* 2005b] Soberón-Chávez, G., Lépine, F., and Déziel, E. (2005b). Production of rhamnolipids by *Pseudomonas aeruginosa*. *Applied Microbiology and Biotechnology*, 68(6), pp. 718–725.

[de Sousa *et al.* 2011] de Sousa, J. R., da Costa Correia, J. A., de Almeida, J. G. L., Rodrigues, S., Pessoa, O. D. L., Melo, V. M. M., and Goncalves, L. R. B. (2011). Evaluation of a co-product of biodiesel production as carbon source in the production of biosurfactant by *P. aeruginosa* MSIC02. *Process Biochemistry*, 46(9), pp. 1831–1839.

[Stephanopoulos and San 1984] Stephanopoulos, G. and San, K. Y. (1984). Studies on on-line bioreactor identification. I. Theory. *Biotechnology and Bioengineering*, 26(10), pp. 1176–1188.

[Stover *et al.* 2000] Stover, C. K., Pham, X. Q., Erwin, A. L., Mizoguchi, S. D., Warrener, P., Hickey, M. J., Brinkman, F. S., Hufnagle, W. O., Kowalik, D. J., Lagrou, M., Garber, R. L., Goltry, L., Tolentino, E., Westbrock-Wadman, S., Yuan, Y., Brody, L. L., Coulter, S. N., Folger, K. R., Kas, A., Larbig, K., Lim, R., Smith, K., Spencer, D., Wong, G. K., Wu, Z., Paulsen, I. T., Reizer, J., Saier, M. H., Hancock, R. E., Lory, S., and Olson, M. V. (2000). Complete genome sequence of *Pseudomonas aeruginosa* PAO1, an opportunistic pathogen. *Nature*, 406(6799), pp. 959–964.

[Sullivan 1998] Sullivan, E. R. (1998). Molecular genetics of biosurfactant production. *Current Opinion in Biotechnology*, 9(3), pp. 263–269.

[Sumobrain-Solutions 2014] Sumobrain-Solutions (2014). FreePatentsOnline IP research platform for the chemical industry. Available online under http://www.freepatentsonline.com, *accessed 02/2014*.

[Syldatk *et al.* 1985a] Syldatk, C., Lang, S., Matulovic, U., and Wagner, F. (1985a). Production of four interfacial active rhamnolipids from *n*-alkanes or glycerol by resting cells of *Pseudomonas* species DSM 2874. *Zeitschrift für Naturforschung*, 40(1-2), pp. 61–67.

[Syldatk *et al.* 1985b] Syldatk, C., Lang, S., Wagner, F., Wray, V., and Witte, L. (1985b). Chemical and physical characterization of four interfacial-active rhamnolipids from *Pseudomonas* spec. DSM 2874 grown on *n*-alkanes. *Zeitschrift für Naturforschung*, 40(1-2), pp. 51–60.

[Teissier 1936] Teissier, G. (1936). Les lois quantitatives de la croissance. *Annales de Physiologie et de Physiochimie Biologique*, 12, pp. 527–573.

[Theobald *et al.* 1997] Theobald, U., Mailinger, W., Baltes, M., Rizzi, M., and Reuss, M. (1997). In-vivo analysis of metabolic dynamics in *Saccharomyces cerevisiae*: I. Experimental observation. *Biotechnology and Bioengineering*, 55(1), pp. 305–316.

[Trummler *et al.* 2003] Trummler, K., Effenberger, F., and Syldatk, C. (2003). An integrated microbial/enzymatic process for production of rhamnolipids and L-(+)-rhamnose from rapeseed oil with *Pseudomonas* sp. DSM 2874. *European Journal of Lipid Science and Technology*, 105(10), pp. 563–571.

[Van Bogaert *et al.* 2007] Van Bogaert, I. N. A., Saerens, K., De Muynck, C., Develter, D., Soetaert, W., and Vandamme, E. J. (2007). Microbial production and application of sophorolipids. *Applied Microbiology and Biotechnology*, 76(1), pp. 23–34.

[Van Delden and Iglewski 1998] Van Delden, C. and Iglewski, B. H. (1998). Cell-to-cell signaling and *Pseudomonas aeruginosa* infections. *Emerging Infectious Diseases*, 4(4), pp. 551–560.

[Van Haesendonck and Vanzeveren 2006] Van Haesendonck, I. P. H. and Vanzeveren, E. C. A. (2006). Rhamnolipids in bakery products. US patent 0233935.

[Van Hamme *et al.* 2003] Van Hamme, J. D., Singh, A., and Ward, O. P. (2003). Recent advances in petroleum microbiology. *Microbiology and Molecular Biology Reviews*, 67(4), pp. 503–549.

[Varnier *et al.* 2009] Varnier, A. L., Sanchez, L., Vatsa, P., Boudesocque, L., Garcia-Brugger, A., Rabenoelina, F., Sorokin, A., Renault, J. H., Kauffmann, S., Pugin, A., Clement, C., Baillieul, F., and Dorey, S. (2009). Bacterial rhamnolipids are novel MAMPs conferring resistance to *Botrytis cinerea* in grapevine. *Plant Cell and Environment*, 32(2), pp. 178–193.

[Velikonja and Kosaric 1993] Velikonja, J. and Kosaric, N. (1993). Biosurfactants in food applications. In: Kosaric, N. (Ed.): *Biosurfactants: production - properties - applications*, Surfactant Science Series, pp. 419–446. New York: Marcel Dekker Inc.

[Verstraete and Voets 1978] Verstraete, W. and Voets, J. P. (1978). Evaluation of yield and maintenance coefficients, expressed in carbon units, for *Pseudomonas fluorescens* and *Pseudomonas aeruginosa*. *Zeitschrift für Allgemeine Mikrobiologie*, 18(2), pp. 135–141.

[Viretta and Fussenegger 2004] Viretta, A. and Fussenegger, M. (2004). Modeling the quorum sensing regulatory network of human-pathogenic *Pseudomonas aeruginosa*. *Biotechnology Progress*, 20, pp. 670–678.

[Wahjudi *et al.* 2011] Wahjudi, M., Papaioannou, E., Hendrawati, O., van Assen, A. H. G., van Merkerk, R., Cool, R. H., Poelarends, G. J., and Ouax, W. J. (2011). PA0305 of *Pseudomonas aeruginosa* is a quorum quenching acylhomoserine lactone acylase belonging to the Ntn hydrolase superfamily. *Microbiology*, 157(7), pp. 2042–2055.

[Walsh *et al.* 2007] Walsh, R., Martin, E., and Darvesh, S. (2007). A versatile equation to describe reversible enzyme inhibition and activation kinetics: modeling β-galactosidase and butyrylcholinesterase. *Biochimica et Biophysica Acta*, 1770(5), pp. 733–746.

[Walter *et al.* 2010] Walter, V., Syldatk, C., and Hausmann, R. (2010). Microbial production of rhamnolipid biosurfactants. In: Flickinger, M. C. (Ed.): *Encyclopedia of Industrial Biotechnology*. Weinheim: John Wiley & Sons, Inc.

[Wang *et al.* 2004] Wang, L. H., Weng, L. X., Dong, Y. H., and Zhang, L. H. (2004). Specificity and enzyme kinetics of the quorum quenching *N*-acyl homoserine lactone lactonase (AHL-lactonase). *Journal of Biological Chemistry*, 279(14), pp. 13645–13651.

[Waters and Bassler 2005] Waters, C. M. and Bassler, B. L. (2005). Quorum sensing: Cell-to-cell communication in bacteria. *Annual Review of Cell and Developmental Biology*, 21, pp. 319–346.

[Wiechert 2002] Wiechert, W. (2002). Modeling and simulation: tools for metabolic engineering. *Journal of Biotechnology*, 94(1), pp. 37–63.

[Williams and Camara 2009] Williams, P. and Camara, M. (2009). Quorum sensing and environmental adaptation in *Pseudomonas aeruginosa*: A tale of regulatory networks and multifunctional signal molecules. *Current Opinion in Microbiology*, 12(2), pp. 182–191.

[Winsor *et al.* 2009] Winsor, G. L., Van Rossum, T., Lo, R., Khaira, B., Whiteside, M. D., Hancock, R. E. W., and Brinkman, F. S. L. (2009). *Pseudomonas* Genome Database: facilitating user-friendly, comprehensive comparisons of microbial genomes. *Nucleic Acids Research*, 37, pp. 483–488.

[Wittgens *et al.* 2011] Wittgens, A., Tiso, T., Arndt, T. T., Wenk, P., Hemmerich, J., Muller, C., Wichmann, R., Kupper, B., Zwick, M., Wilhelm, S., Hausmann, R., Syldatk, C., Rosenau, F., and Blank, L. M. (2011). Growth independent rhamnolipid production from glucose using the non-pathogenic *Pseudomonas putida* KT2440. *Microbial Cell Factories*, 10(1).

[Yuan and Tam 2008] Yuan, Z. and Tam, V. H. (2008). Polymyxin B: A new strategy for multidrug-resistant gram-negative organisms. *Expert Opinion on Investigational Drugs*, 17(5), pp. 661–668.

[Zhu and Rock 2008] Zhu, K. and Rock, C. O. (2008). RhlA converts β-hydroxyacyl-acyl carrier protein intermediates in fatty acid synthesis to the β-hydroxydecanoyl-β-hydroxydecanoate component of rhamnolipids in *Pseudomonas aeruginosa*. *Journal of Bacteriology*, 190(9), pp. 3147–3154.

[Zhu *et al.* 2007] Zhu, Y., Gan, J. J., Zhang, G. L., Yao, B., Zhu, W. J., and Meng, Q. (2007). Reuse of waste frying oil for production of rhamnolipids using *Pseudomonas aeruginosa* zju.u1M. *Journal of Zhejiang University-Science A*, 8(9), pp. 1514–1520.

[Zimmermann 1980] Zimmermann, H. (1980). OSI reference model - the ISO model of architecture for open systems interconnection. *IEEE Transactions on Communications*, 28(4), pp. 425–432.

Abbreviations & Symbols

3o-C_{12}-HSL	*N*-3-oxo-dodecanoyl-homoserine lactone
ACP	acyl carrier protein
AI	autoinducer (molecule)
ANN	Artificial neural network
ara	arabinose
ATP	adenosine triphosphate
APG	alkylpolygylcoside
API	atmospheric pressure ionization
BM	biomass (dry weight)
C_4-HSL	*N*-butyryl-homoserine lactone
CMC	critical micelle concentration
CoA	coenzyme A
C	carbon
CC	citric acid cycle (tricarboxylic acid cycle)
-C_n-	carbon chain of length n
DE	differential equation
DHAP	dihydroxyacetone phosphate (glycerone phophate)
DNA	deoxyribonucleic acid
DSMZ	Deutsche Sammlung von Mikroorganismen und Zellkulturen (German Collection of Microorganisms and Cell Cultures)
dTDP	deoxythymidine 5'-diphosphate
e.g.	lat. exempli gratia (for example)
EC	enzyme commission (number)
EC_{50}	half maximal effective concentration
ED	Entner-Doudoroff pathway
EOR	enhanced oil recovery
EPS	extracellular polysaccharide
Eq	Equation
FA	fatty acid
FAD / $FADH_2$	flavin adenine dinucleotide
FAME	fatty acid methyl ester ('biodiesel')
FB	fed-batch (process)
FDA	(US) Food and Drug Administration
Fig	Figure
fru	fructose
F6P	fructose 6-phosphate
gal	galactose
gap	glyceraldehyde 3-phosphate
GDP	guanosine diphosphate
glu	glucose

GLY	glycolysis
gly	glycerol
HAA	3-(3-hydroxyalkanoyloxy)alkanoate
HPLC	high-performance liquid chromatography
HSL	*N*-acyl-homoserine lactone
KEGG	Kyoto Encyclopaedia of Genes and Genomes
KDPG	2-keto-3-deoxy-6-phosphogluconate
LAS	Linear alkylbenzene sulfonate
LB	lysogeny broth
LC	liquid chromatography
LPS	lipopolysaccharide
MEL	mannosylerythritol lipid
MEOR	microbial enhanced oil recovery
MS	mass spectrometry
MW	molecular weight
N	nitrogen
NADH / NADPH	nicotinamide adenine dinucleotide phosphate
NCBI	National Center for Biotechnology Information (US) National Institutes of Health
NIRS	near infrared spectroscopy
OD	optical density
ODE	ordinary differential equation
ox	oxidation
PAI	*Pseudomonas* autoinducer
PAT	process analytical technology
PBE	population balance equation
pH	- $\log_{10}$ of a(H^+)
PHA	polyhydroxyalkanoate
P_i	inorganic phosphate
pO_2	dissolved oxygen (%)
PPP	pentose phosphate pathway
PQS	*Pseudomonas* quinolone signal
PS	polysaccharide
PTS	phosphotransferase system
pyr	pyruvate
QS	quorum sensing
Rha	L-rhamnose
ribu	ribulose
RL	rhamnolipid
RL-1 / Rha-C_{10}-C_{10}	mono-rhamnolipid (α-L-rhamnopyranosyl-3-hydroxydecanoyl-3-hydroxydecanoate
RL-3 / Rha-Rha-C_{10}-C_{10}	di-rhamnolipid (α-L-rhamnopyranosyl-(1-2)-α-L-rhamnopyranosyl-3-hydroxydecanoyl-3-hydroxydecanoate)
RNA	ribonucleic acid
rpm	revolutions per minute
RQ	respiratory quotient
RSM	response surface methodology
sp. / spec.	species
spp.	species pluralis
σ^N	sigma factor RpoN
σ^s	sigma factor RpoS
Tab	Table

UDP	uridine diphosphate
USD	US Dollar
UV	ultraviolet (light / radiation)
vvm	aeration rate (gas volume flow per liquid volume per minute)
xylu	xylulose
xyl	xylose
$Y_{m\|n}$	yield coefficient m to n

μ	specific growth rate
P_v	volumetric productivity
c_i	concentration of component i
$\times$ g	gravitational acceleration
k_{cat}/K_m	catalytic efficiency
K_p	proportional gain (control thoery)
$q_m^{sp.}$	specific production rate of component m
V / vol.	volume (fraction)
(v/v)	volume per volume (concentration)
(w/v)	weight per volume (concentration)
T	temperature
t	(process- or reaction-) time

List of Figures

List of Tables

Appendix

A. Metabolic pathways and calculation of theoretical yields

The following pages contain data applied for the calculation of theoretical yields which were used for the parameterization of the process model (Chapter 5) as well as the calculation of theoretical substrate costs (Chapter 3, Tab. 3.4). Information on the metabolic pathways (Fig. A.1 and Tab. A.1) were taken from the *Kyoto Encyclopedia of Genes and Genomes* [Kanehisa and Goto 2000] and the *Pseudomonas Genome Database* ([Winsor *et al.* 2009], available online under http://www.pseudomonas.com/). This material has been previously published as online supplemental material for the following article

Rhamnolipids as biosurfactants from renewable resources: Concepts for next-generation rhamnolipid production. *Marius Henkel, Markus M. Müller, Johannes H. Kügler, Roberta B. Lovaglio, Jonas Contiero, Christoph Syldatk and Rudolf Hausmann.* Process Biochemistry (2012), 47(8):1207-1219.

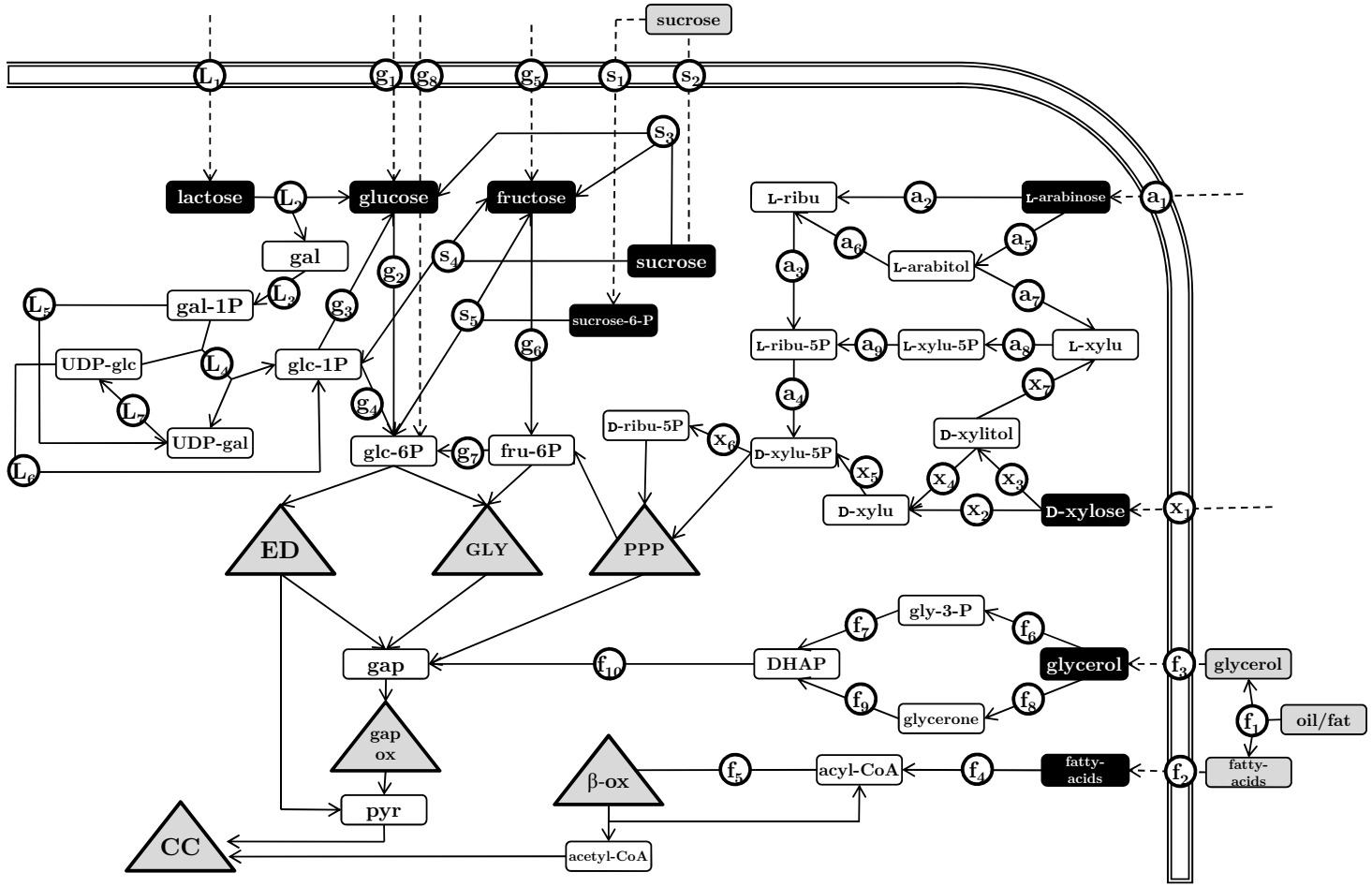

Figure A.1: Overview of metabolic pathways in *P. aeruginosa* related to utilization, conversion and uptake of selected renewable carbohydrates. Dashed lines indicate active or passive uptake/diffusion. Abbreviations: Intermediates/substrates: glucose glc; galactose gal; fructose fru; glycerol gly; dihydroxyacetone phosphate (glycerone phosphate) DHAP; xylulose xylu; Uridine diphosphate UDP; glyceraldehyde 3-phosphate gap; pyruvate pyr; ribulose ribu; pathways: Entner-Doudoroff pathway ED; glycolysis GLY; pentose phosphate pathway PPP; citric acid cycle CC.

Table A.1: Metabolic analysis of utilization, conversion and uptake of selected renewable carbohydrates by *P. aeruginosa* PAO1. Genes are presented by GenBank locus tag (National Center for Biotechnical Information, NCBI), genes absent or currently not known to be present are indicated by 'unknown'. Gene and gene products are provided for the most common path/reaction.

#	Orthology	Gene	Locus tag
Lactose			
L1	β-galactoside permease	*lacY*	unknown
L2	β-galactosidase	*lacZ*	unknown
L3	galactokinase	*galK*	unknown
L4	hexose-1-phosphate uridylyltransferase	*galT*	unknown
L5	galactose-1-phosphate uridylyltransferase	-	unknown
L6	UTP-glucose-1-phosphate uridylyltransferase	*galU*	*galU* (PA2023)
L7	UDP-glucose 4-epimerase	*galE*	*galE* (PA1384)
Fat/oil, fatty acids and glycerol			
f1	triacylglycerol lipase	*lipA*	*lipA* (PA2862)
f2	fatty acid uptake protein OMPP1	*fadL*	PA4589/PA1288
f3	glycerol uptake facilitator protein	*glpF*	*glpF* (PA3581)
f4	long-chain acyl-CoA synthetase	*fadD*	*fadD* (PA3299/3300)
f5	multifunctional fatty acid oxidation complex		
f6	glycerol kinase	*glpK*	PA3582
f7	glycerol-3-phosphate dehydrogenase	*gpsA / glpD*	PA1614/3584
f8	glycerol dehydrogenase	*gldA*	unknown
f9	dihydroxyacetone kinase	*dhaK / dhaL*	unknown
f10	triosephosphate isomerase	*tpiA*	PA4748
Lignocellulose C_5 sugars			
a1	outer membrane protein D1 (Porin B)	*oprB*	PA3186
a2	L-arabinose isomerase	*araA*	unknown
a3	L-ribulokinase	*araB*	unknown
a4	L-ribulose-5-phosphate 4-epimerase	*araD*	unknown
a5	aldehyde reductase	*akr1*	unknown
a6	L-arabinitol 2-dehydrogenase	-	unknown
a7	L-arabinitol 4-dehydrogenase	-	unknown
a8	L-xylulokinase	*lyxK*	unknown
a9	L-xylulose 5-phosphate 3-epimerase	*sgbU*	unknown
x1	outer membrane protein D1 (Porin B)	*oprB*	PA3186
x2	xylose isomerase	*xylA*	unknown
x3	aldehyde reductase	*akr1*	unknown
x4	D-xylulose reductase	-	unknown
x5	xylulose kinase	*mtlY / xylB*	*mtlY* (PA2343)
x6	ribulose-phosphate 3-epimerase	*rpe*	PA0607
x7	D-iditol 2-dehydrogenase		unknown
glucose, fructose, sucrose			
g1	outer membrane protein D1 (Porin B)	*oprB*	PA3186
g2	glucokinase/hexokinase	*glk*	*glk* (PA3193)
g3	glucose-1-phosphate phosphodismutase	*agp*	unknown
g4	phosphoglucomutase	*pgm/algC*	*algC* (PA5322)
g5	outer membrane protein D1 (Porin B)	*oprB*	PA3186
g6	fructokinase	*mtlZ*	PA2344
g7	glucose-6-phosphate isomerase	*pgi*	PA4732
g8	PTS system, glucose-specific IIA component	*crr*	unknown
s1	PTS system, sucrose-specific IIA component	*scrA*	unknown
s2	outer membrane protein D1 (Porin B)	*oprB*	PA3186
s3	α-glucosidase/β-fructofuranosidase	*malZ/sacA/scrB*	unknown
s4	sucrose phosphorylase	-	unknown
s5	sucrose-6-phosphate hydrolase	*sacA*	unknown

Table A.2: Calculation of maximum theoretical rhamnolipid yields for different substrates. Theoretical maximum rhamnolipid yields were estimated assuming energy-limitation, no by-products, no cell-growth and the absence of other limiting factors (e.g. oxygen limitation, carbon limitation, redox-equivalents) and disregarding maintenance metabolism [Erickson 1981, Andrews 1989]. Calculations are based on ATP energy balancing assuming presence of metabolic pathways according to Fig. A.1 [Kanehisa and Goto 2000, Winsor *et al.* 2009]. Conversion of redox-equivalents to ATP was calculated by GTP: 1 ATP; Acetyl-CoA: 12 ATP; NAD(P)H/H^+: 3 ATP; FAD(P)H_2: 2 ATP; pyruvate 15 ATP. Details on calculation of ATP energy balancing can be found on the following pages (Tab. A.3 - A.6). Abbreviations: Entner-Doudoroff-pathway ED; glycolysis GLY; rhamnose Rha; thymidine diphosphate dTDP; acyl carrier protein ACP.

Substrate	**ATP gain** [**mol/mol**]	**MW** [**g/mol**]	**ATP gain** [**mol/g**]	**MW** [**gC/mol**]	**ATP gain** [**mol/gC**]
Glucose (GLY)	38	180	0.211	72	0.528
Glucose (ED)	37	180	0.206	72	0.514
Lactose (GLY)	75	342.3	0.219	144	0.521
Sucrose (GLY)	76	342.3	0.222	144	0.528
L-Arabinose	31	150.1	0.207	60	0.517
D-Xylose	31	150.1	0.207	60	0.517
Glycerol	22	92	0.239	36	0.611
$C_{18:2}$ fatty acid (β-oxidation)	141	280	0.504	216	0.653
Glycerolipid (Gly & 3 $C_{18:2}$)	445	878.24	0.507	681.6	0.653
C_{18} fatty acid (β-oxidation)	146	284.5	0.513	216	0.676
Product	**ATP loss** [**mol/mol**]	**MW** [**g/mol**]	**ATP loss** [**mol/g**]	**MW** [**gC/mol**]	**ATP gain** [**mol/gC**]
dTDP-L-Rhamnose (gluconeogensis)	-47	164	-0.287	72	-0.653
(R)-3-HDA-ACP	-85	188.26	-0.452	120	-0.708
C_{10}-C_{10}	-170	358.52	-0.474	240	-0.708
Rha-C_{10}-C_{10}	-217	504	-0.431	312	-0.696
Rha_2-C_{10}-C_{10}	-264	650	-0.406	384	-0.688

Table A.3: ATP energy balancing: calculation of ATP gain for substrates glycerol and fatty acids. Pathways ('PW') named according to Fig. A.1. Abbreviations: 3-phospho-D-glyceroyl-phosphate 3-PG; 3-phospho-D-glyceroyl-phosphate 2-PG; Phosphoenolpyruvate PEP; pyruvate pyr; Dihydroxyacetone-phosphate DHAP; fatty acid FA; inorganic phosphate P_i.

Glycerol - Pathway (via f6/f7)			PW	Redox equivalent	in ATP
Glycerol + ATP	→	Glycerol-3-phosphate + ADP	f6	-1 ATP	-1
Glycerol-3-phosphate + $NAD(P)^+$	→	DHAP + $NAD(P)H/H^+$	f7	$NAD(P)H/H^+$ ($FADH_2$)	3
DHAP	→	Glyceraldehyd-3-phosphate	f10		
Glyceraldehyd-3-phosphate + NAD+ + P_i	→	3-phospho-D-glyceroyl-phosphate + $NAD(P)H/H^+$	gap ox	$NADH/H^+$	3
3-phospho-D-glyceroyl-phosphate + ADP	→	3-PG + ATP	gap ox	1 ATP	1
3-PG	→	2-PG	gap ox		
2-PG	→	Phosphoenolpyruvate (PEP)	gap ox		
PEP + ADP	→	pyr + ATP	gap ox	ATP + pyr	16
					Total 22
Glycerol - Pathway (via f8/f9)					
Glycerol + NAD^+	→	Glycerone + $NADH/H^+$	f8	$NAD(P)H/H^+$	3
Glycerone + ATP	→	DHAP (Glycerone-P)	f9	-1 ATP	-1
DHAP	→→	Pyr + ATP		$NADH/H^+$ + 2 ATP + Pyr	22
					Total 22
Fatty acid degradation (β-oxidation, activation)					
fatty acid + ATP	→	FA-AMP (Acyl adenylate) + PP_i		-1 ATP	-1
fatty acid + CoA	→	Acyl-CoA	f4	-1 ATP	-1
Fatty acid degradation (β-oxidation)					
Acyl-CoA + FAD^+	→	trans-Δ^2-enoyl-CoA + $FADH_2$	f5	$FADH_2$	2
trans-Δ^2-enoyl-CoA + H_2O	→	L-3-Hydroxyacyl-CoA f5			
L-3-Hydroxyacyl-CoA + NAD^+	→	3-Ketoacyl-CoA + $NADH/H^+$	f5	$NADH/H^+$	3
3-Ketoacyl-CoA + CoA-SH	→	Acyl-CoA + Acetyl-CoA	f5	AcetylCoA	12
					Total (per cycle) 22

Table A.4: ATP energy balancing: calculation of ATP gain for C_5-sugars arabinose and xylose. Pathways ('PW') named according to Fig. A.1. Abbreviations: pentose phosphate pathway PPP; glyceraldehyde 3-phosphate GAP; fructose-6-phosphate F6P.

Pentose-Phosphate-Pathway (L-Arabinose, via a2/a3/a4/x6)			PW	Redox equivalent	in ATP
3 L-Arabinose	→	3 L-Ribulose	a2		
3 L-Ribulose + 3 ATP	→	3 L-Ribulose-5-P + 3 ADP	a3	- 3 ATP	-3
3 L-Ribulose-5-P	→	3 D-Xylulose 5-P	a4		
D-Xylulose 5-P	→	D-Ribulose 5-P	x6		
D-Ribulose 5-P	→	D-Ribose 5-P	PPP		
D-Ribose 5-P + D-Xylulose 5-P	→	Sedoheptulose 7-P + D-Glyceraldehyde 3-P	PPP	+1 GAP	20
Sedoheptulose 7-P + D-Glyceraldehyde 3-P	→	D-Erythrose 4-P + D-Fructose 6-P	PPP	-1 GAP + F6P	18
D-Erythrose 4-P + D-Xylulose 5-P	→	D-Fructose 6-P + D-Glyceraldehyde 3-P	PPP	+1 GAP + F6P	58
					Total 31
Pentose-Phosphate-Pathway (D-Xylose, via x2/x5/x6)					
3 D-Xylose	→	3 D-Xylulose	x2		
3 D-Xylolose + 3 ATP	→	3 D-Xylulose 5-phosphate	x5	- 3 ATP	-3
D-Ribulose 5-phosphate	→→	D-Fructose 6-phosphate + D-Glyceraldehyde 3-phosphate		+1 GAP + 2 F6P	93
					Total 31
Entner - Duodoroff - Pathway (galactose, via L2/L3/L5/L7/L6/G4)					
Lactose + H_2O	→	D-Glucose + D-Galactose	L2		
D-Galactose + ATP	→	α-D-Galactose-1-Phosphate + ADP	L3	- ATP	-1
α-D-Galactose-1-Phosphate + UTP	→	PP_i + UDP-D-Galactose	L5	- UTP	-1
UDP-D-Galactose	→	UDP-D-Glucose	L7		
UDP-D-Glucose + H_2O	→	UMP + D-Glucose-1-Phosphate	L6		
D-Glucose-1-Phosphate	→	α-D-Glucose 6-phosphate	g4		
Glucose-6-phosphate + $NADP^+$	→	6-P-Glucono-δ-Lactone + $NADPH/H^+$	ED	+1 $NADPH/H^+$	3
6-P-Glucono-δ-Lactone + H_2O	→→	Pyr + ATP		2 Pyr + 2 ATP +1 $NADPH/H^+$	35
					Total 36

Table A.5: ATP energy balancing: calculation of ATP gain for C_6-sugars and disaccharides sucrose and galactose. Pathways ('PW') named according to Fig. A.1. Degradation of glucose is considered both via glycolysis and the Entner-Doudoroff-pathway ('ED'). Abbreviations: glyceraldehyde 3-phosphate GAP; fructose-6-phosphate F6P; 2-Keto-3-desoxy-6-phosphogluconate KDPG; 3-phospho-D-glyceroyl-phosphate 3-PG; 3-phospho-D-glyceroyl-phosphate 2-PG; 1,3-biphospho-glycerat 1,3-bPG, pyruvate Pyr.

Entner - Dudoroff - Pathway (glucose)			PW	Redox equivalent	in ATP
Glucose + ATP	$\rightarrow$	Glucose-6-phosphate + ADP	g2	-1 ATP	-1
Glucose-6-phosphate + $NADP^+$	$\rightarrow$	6-P-Glucono-δ-Lactone + $NADPH/H^+$	ED	+1 $NADPH/H^+$	3
6-P-Glucono-δ-Lactone + H_2O	$\rightarrow$	6-P-Gluconate	ED		
6-P-Gluconate	$\rightarrow$	2-Keto-3-desoxy-6-phosphogluconate + H_2O	ED		
KDPG	$\rightarrow$	Pyruvate (Pyr) + Glycerinaldehyde-3-P (GAP)	ED	Pyr	15
GAP + P_i + NAD+	$\rightarrow$	1,3-biphospho-glycerat (1,3-bPG) + $NADH/H^+$	ED	+1 $NADH/H^+$	3
1,3-bPG + ADP	$\rightarrow$	3-phospho-glycerate (3-PG) + ATP	ED	ATP	1
3-PG	$\rightarrow$	2-PG	ED		
2-PG	$\rightarrow$	Phosphoenolpyruvate (PEP) + H_2O	ED		
PEP + ADP	$\rightarrow$	Pyr + ATP	ED	ATP + Pyr	16
					Total 37
					(with glycolysis +1 ATP)
Oxidative decarboxylation (pyruvate)					
Pyruvate + NAD^+ +CoA-SH	$\rightarrow$	Acetyl-CoA + CO_2 + $NADH/H^+$		ACoA + $NADH/H^+$	15
Citric acid cycle (acetyl-CoA)					
AcetylCoA + 3 NAD^+ + FAD^+ + GDP + P_i + 2 H_2O	$\rightarrow$	2 CO_2 + 3 NADH/ H^+ + $FADH_2$ + GTP + CoA		3 $NADH/H^+$ + $FADH_2$ + GTP	12
Entner - Dudoroff - Pathway (sucrose/glucose/fructose)					
D-Fructose + ATP	$\rightarrow$	β-D-Fructose-6-Phosphat + ADP	g6	-1 ATP	-1
β-D-Fructose-6-Phosphate	$\rightarrow$	β-D-Glucose-6-Phosphate	g7		
β-D-Glucose-6-Phosphate	$\rightarrow$	α-D-Glucose-6-Phosphate	ED		
α-D-Glucose-6-Phosphate + NADP+$^+$	$\rightarrow$	6-P-Glucono-δ-Lactone + $NADPH/H^+$	ED	+1 $NADPH/H^+$	3
6-P-Glucono-δ-Lactone + H_2O	$\rightarrow\rightarrow$	Pyr + ATP		2 Pyr + 2 ATP +1 $NADPH/H^+$	35
					total (fructose) 37
					total (sucrose) 74
					(with glycolysis +1 ATP)

Table A.6: ATP energy balancing: calculation of ATP requirements for de novo synthesis of precursors for mono-/di-rhamnolipids.

Gluconeogenesis (dTDP-rhamnose)			Redox equivalent	in ATP
2 Pyruvate + 4 ATP + 2 GTP + 2 $NADH/H^+$ + 6 H_2O	→	Glucose + 4 ADP + 2 GDP + 6 P_i + 2 NAD^+	-4 ATP - 2 GTP - 2 $NADH/H^+$ - 2 Pyr	-42
Glucose + ATP	→	Glucose-1-phosphate (G1P) + ADP	-1 ATP	-1
G1P + TTP	→	dTDP-D-glucose + P_i	- 1 TTP	-1
dTDP-D-glucose	→	dTDP-4-dehydro-6-deoxy-D-glucose		
dTDP-4-dehydro-6-deoxy-D-glucose	→	dTDP-4-dehydro-6-deoxy-L-mannose		
dTDP-4-dehydro-6-deoxy-L-mannose + $NADPH/H^+$	→	dTDP-rhamnose + NAD^+	- 1 $NADPH/H^+$	-3
				total -47
Malonyl-CoA synthesis				
AcetylCoA + ATP + HCO_3^-	→	malonyl-CoA + ADP + H^+ + P_i	-1 ATP - 1 AcetylCoA	-13
malonyl-CoA + ACP	→	malonyl-[ACP] + CoA-SH		
De novo fatty acid synthesis				
Acetyl-CoA + ACP	→	Acetyl-[ACP] + CoA-SH	- 1 AcetylCoA	-12
Acetyl-[ACP] + Malonyl-[ACP]	→	Acetoacyl-[ACP] + CO_2 + ACP	- 1 Malonyl-[ACP]	-13
Acetoacyl-[ACP] + $NADPH/H^+$	→	(R)-3-Hydroxybutanoyl-[ACP] + $NADP^+$	- 1 $NADPH/H^+$	-3
(R)-3-Hydroxybutanoyl-[ACP] + H_2O	→	But-2-enoyl-[ACP]		
But-2-enoyl-[ACP] + NADPH/H+	→	Butyryl-[ACP]	-1 $NADPH/H^+$	-3
Butyryl-[ACP] + Malonyl-[ACP]	→	3-Oxohexanoyl-[ACP] + CO_2 + ACP	- 1 Malonyl-[ACP]	-13
3-Oxohexanoyl-[ACP] + $NADPH/H^+$	→	(R)-3-Hydroxyhexanoyl-[ACP] + $NADP^+$	- 1 $NADPH/H^+$	-3
(R)-3-Hydroxyhexanoyl-[ACP] + H_2O	→	Trans-hex-2-enoyl-[ACP]		
Trans-hex-2-enoyl-[ACP] + $NADPH/H^+$	→	Hexanoyl-[ACP]	-1 $NADPH/H^+$	-3
Hexanoyl-[ACP] + Malonyl-[ACP]	→	3-Oxooctanoyl-[ACP] + CO_2 + ACP	- 1 Malonyl-[ACP]	-13
3-Oxooctanoyl-[ACP] + $NADPH/H^+$	→	(R)-3-Hydroxyoctanoyl-[ACP] + NADP+	- 1 $NADPH/H^+$	-3
(R)-3-Hydroxyoctanoyl-[ACP] + H_2O	→	Trans-oct-2-enoyl-[ACP]		
Trans-oct-2-enoyl-[ACP] + $NADPH/H^+$	→	Octanoyl-[ACP]	-1 $NADPH/H^+$	-3
Octanoyl-[ACP] + Malonyl-[ACP]	→	3-Oxodecanoyl-[ACP] + CO_2 + ACP	- 1 Malonyl-[ACP]	-13
3-Oxodecanoyl-[ACP] + $NADPH/H^+$	→	(R)-3-Hydroxydecanoyl-[ACP] + $NADP^+$	- 1 $NADPH/H^+$	-3
			total (1 β-Hydroxy-decanoyl-[ACP])	**-85**
Rhamnolipid synthesis				
β-hydroxydecanoyl-β-hydroxydecanoate (HAA) + dTDP-rhamnose			Rha-C_{10}-C_{10}	-217
			Rha_2-C_{10}-C_{10}	-264

B. Experiments for parameterization of the model

The following pages contain experimental data applied for the development and parameterization of the cell-density dependent partial model for C_4-HSL (Chapter 4) and the process model on a bioreactor scale (Chapter 5). This material has been previously published as online supplemental material for the following articles

---

Kinetic modeling of the time course of *N*-butyryl-homoserine lactone concentration during batch cultivations of *Pseudomonas aeruginosa* PAO1. *Marius Henkel, Anke Schmidberger, Christian Kühnert, Janina Beuker, Thomas Bernard, Thomas Schwartz, Christoph Syldatk and Rudolf Hausmann*. Applied Microbiology and Biotechnology (2013), 97:7607-7616.

Kinetic modeling of rhamnolipid production by *Pseudomonas aeruginosa* PAO1 including cell-density dependent regulation. *Marius Henkel, Anke Schmidberger, Markus Vogelbacher, Christian Kühnert, Janina Beuker, Thomas Bernard, Thomas Schwartz, Christoph Syldatk and Rudolf Hausmann*. Applied Microbiology and Biotechnology (2014), 98:7013-7025.

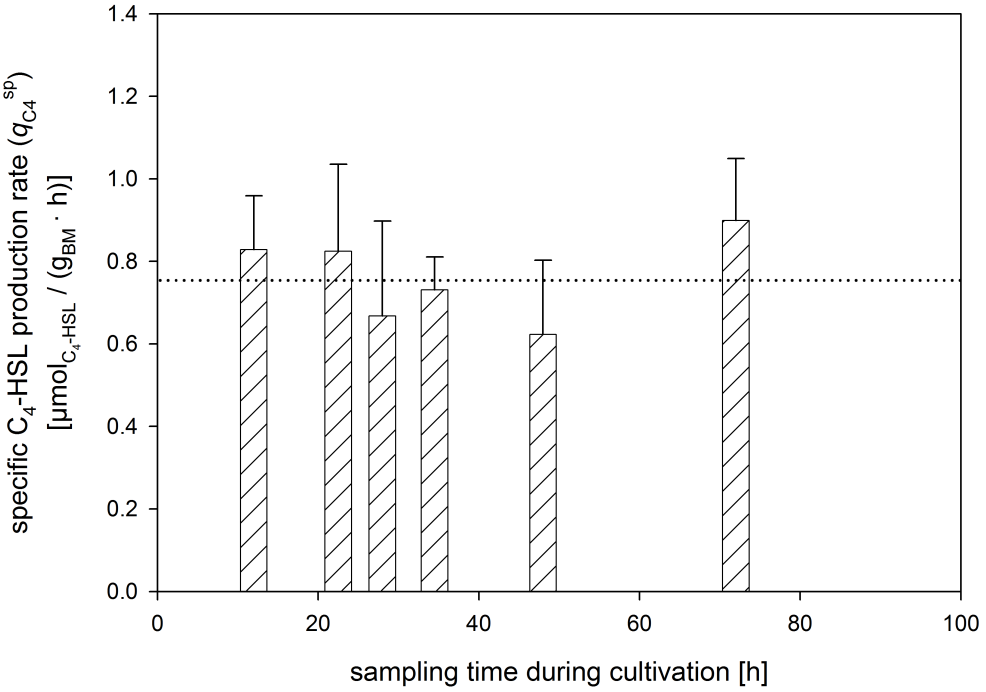

Figure B.1: Calculated specific C_4-HSL production rates over the time course of the cultivation presented in Fig. 4.1, obtained by measuring total degradation rates and time course of C_4-HSL as described for Fig. 4.3.

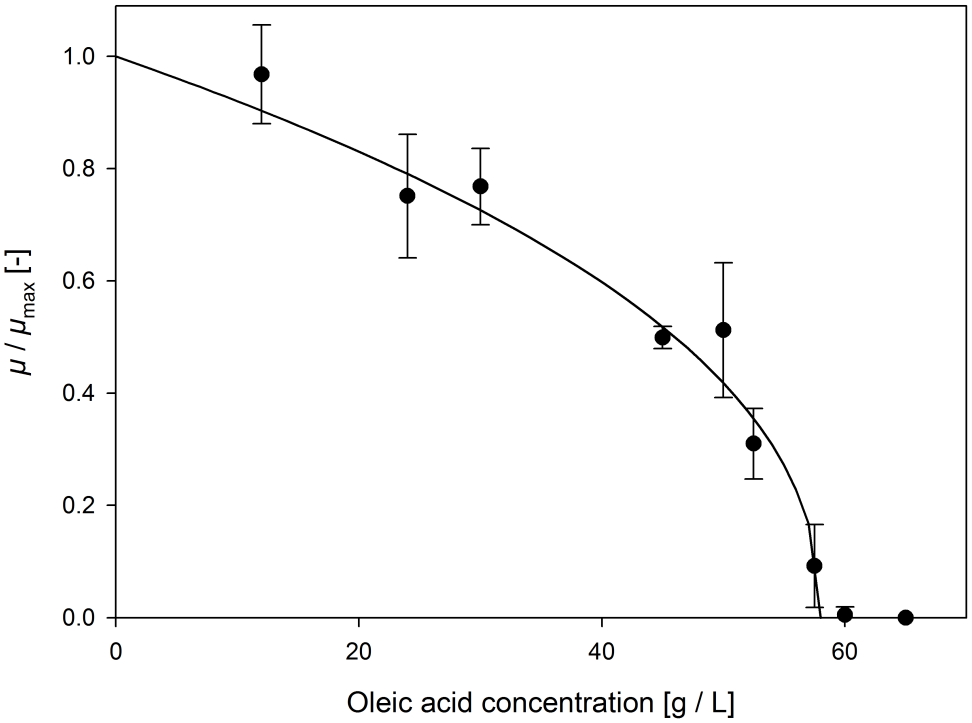

Figure B.2: Specific growth rate of *P. aeruginosa* PAO1 in presence of different concentrations of oleic acid. Measured data (filled circles) is described using the growth kinetic according to [Luong 1987] for substrate inhibition. The curve shown (solid line) represents the best fit with parameters $K_{\mathrm{i}}^{\mathrm{FA}} = 58$ g / L and $n = 0.44$

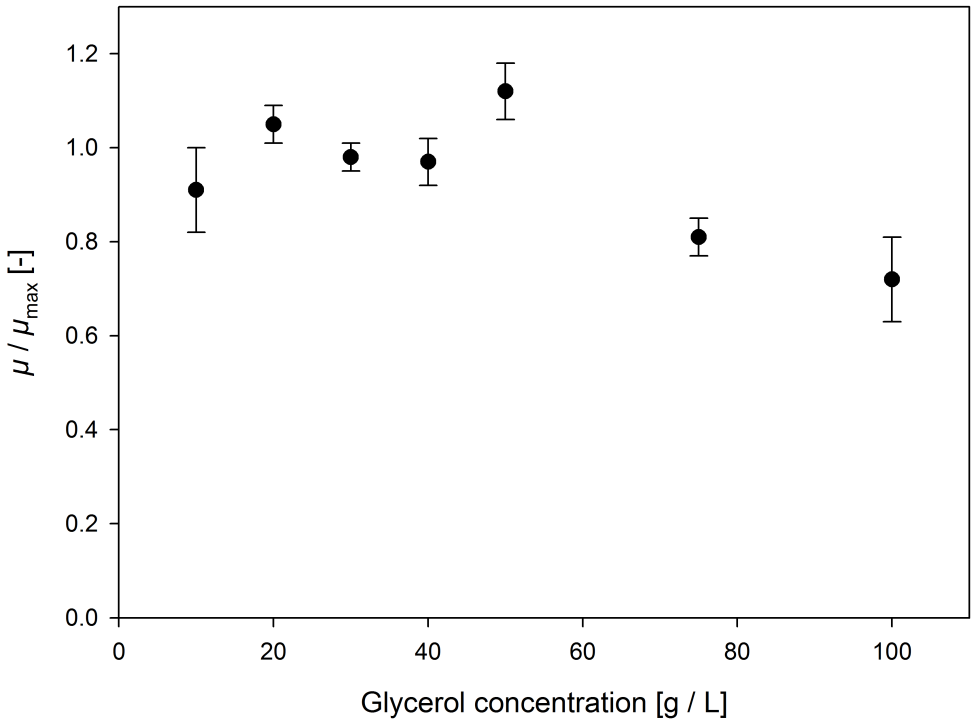

Figure B.3: Specific growth rate of *P. aeruginosa* PAO1 in presence of different concentrations of glycerol

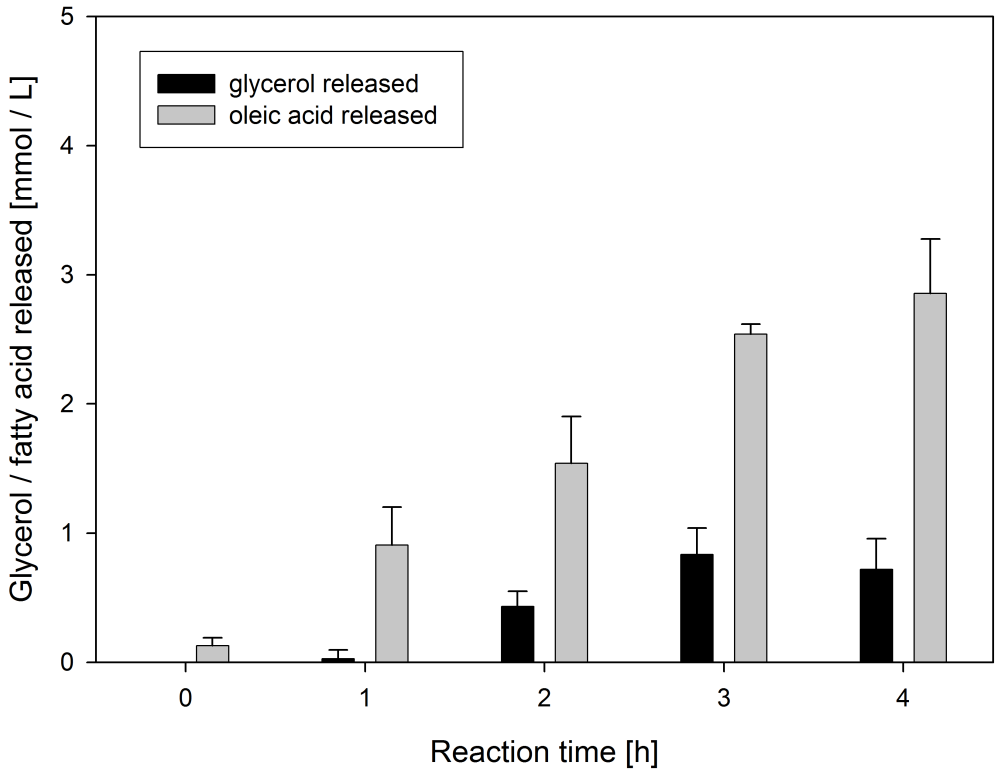

Figure B.4: Accumulation of glycerol and fatty acids due to lipase activity. Glycerol (black bars) and fatty acids (grey bars) were monitored in cell-free culture supernatant supplemented with sunflower oil.

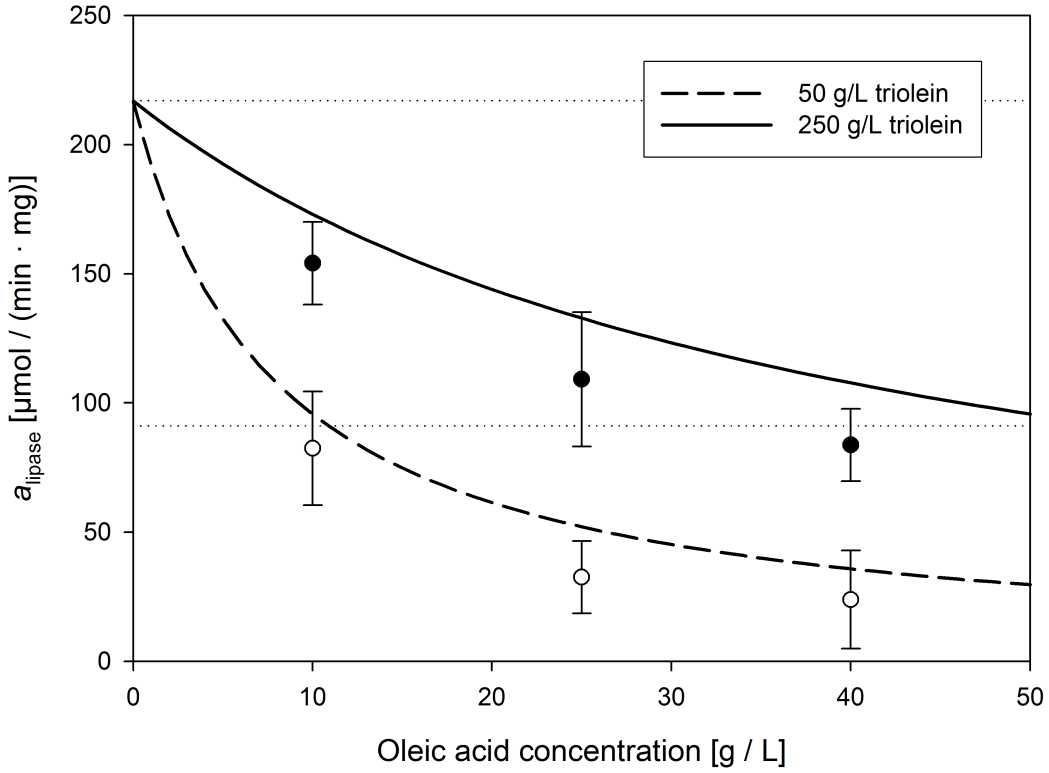

Figure B.5: Simulation and measurement data on specific oil degradation rate by lipase in presence of fatty acids. Horizontal dotted lines indicate maximum specific activity of 217 µmol/(min·mg) as reported by [Madan and Mishra 2010] used for scaling (top line), and calculated specific activity assuming no inhibition by fatty acids, as determined by oil degradation and consumption in the model. The curves represent the kinetics of oil degradation with optimized parameters $K_{\mathrm{m}}^{\mathrm{lip}} = 0.133$ g/L and $K_{\mathrm{i}}^{\mathrm{lip}} = 0.021$ g/L as applied in the model, assuming reversible, competitive inhibition by fatty acids, along with measurement data in the presence of 250 g/L oil (solid line, filled circles) and 50 g/L oil (dashed line, empty circles)

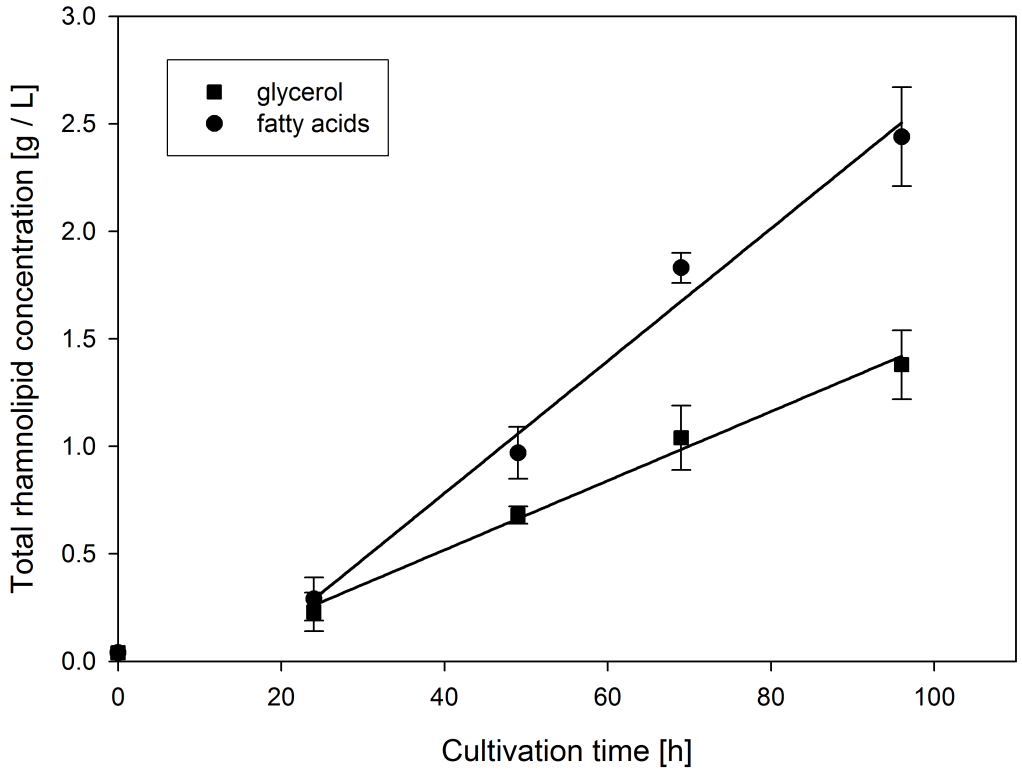

Figure B.6: Rhamnolipid production in resting cell cultivations of *P. aeruginosa* PAO1 with glycerol and oleic acid. Resting cells were prepared as described by [Syldatk *et al.* 1985a], with a biomass concentration of 2.5 g/L.